Finite Element Modelling of Screw Fixation in Augmented and Non-Augmented Cancellous Bone

A thesis submitted for the degree of Doctor of Philosophy at Brunel University

Philippe Bennani Kamane

November 2012

Declaration

I confirm that the intellectual content of this research presented in this thesis is the original work of the author, save for any express acknowledgements, references and / or bibliographies cited in the work. This work or any part thereof has not previously been presented in any form to any institutional body whether for another degree, award or other purposes.

This project was carried out at the School of Engineering and Design, Brunel University, under the supervision of C. J. Brown.

Abstract

This research project presents a study of the fixation of screws in augmented and non-augmented cancellous bone at a microscopic scale. It is estimated that somewhere close to one million screws are failing each year. Therefore, the aim is to identify the key parameters affecting screw pull-out in order to improve screw fixation in cancellous bone, and hence screw design.

The background for this study comes from work by Stryker, comparing screw pull-out from augmented and non-augmented cancellous bone, where a few cases of screw pull-out gave better results without bone augmentation. This is contrary to most evidence and the hypothesis to explain these results is that the screw pull-out from cancellous bone could be strongly affected by the cancellous bone micro architecture.

The effect of the influence of the screw's initial position was first verified with 2D finite element (FE) models of screw pull-out from simplified cancellous bone models. The results showed a force reaction variation up to 28% with small change in position. The hypothesis was then tested with 3D FE models of screw pull-out from more complex cancellous bone models with different volume fractions. Three volume fractions were tested and again the effects were confirmed, but only in models with the lower volume fraction. A variation up to 30% of the force reaction was observed.

The 3D simplified cancellous bone models with 5.3% volume fraction were also used to study the influence of augmentation using calcium phosphate cement. A significant improvement of the screw holding power (almost 2 times) as well as an important diminution of the variability of the pull-out force due to the screw initial position was found. Other augmentation geometries were used to model cement. They all showed an increase of the screw pull-out force reaction with an increase of the cement volume.

Validation of FE results was achieved by comparing screw pull-out from a cadaver cancellous bone and the FE model constructed from the same bone sample. New studies were then carried out from the cadaver cancellous bone

model. The first study examined the screw initial position influence with cancellous and cortical screws and again showed that there is a strong correlation between screw pull-out stiffness and bone volume fraction. The cortical screw showed improved performance over the cancellous screw.

Augmentation cases were explored using three bone samples with a range of volume fractions obtained from different sites within the cadaver bone sample. The cancellous screw was tested with 3 types of augmentation and the cortical screw was tested with one augmentation in these 3 samples. The results showed each time a significant improvement of stiffness with augmentation but when compared with the effect of volume variation inside the bone sample, it appeared that the improvement of stiffness from augmentation might not cover the loss in stiffness from a small change in bone structure.

Finally, screw design parameters were investigated, as cortical screws seemed to give as good or better stiffness results than cancellous screw. The thread pitch, the thread angle and the core diameter were analysed independently and it appeared that the most important parameter was the thread pitch with an improvement of the stiffness of +46% for cancellous screws with a smaller thread pitch. The two other factors studied (core diameter and thread angle) showed somewhat stiffer results but with a relatively small influence (less than 10%). From this study, the best screw for use in cancellous bone could be a cortical screw (diameter and pitch) with thread angles similar to a cancellous screw.

Acknowledgements

I would like to thank my supervisors Chris J. Brown and Philip Procter for giving me the opportunity to carry out this project and for their precious guidance and supervision all along this PhD experience.

I would like to thank Stryker Osteosynthesis for sponsoring this project and sharing their knowledge and data.

I would like to mention some of the people who helped me to survive this PhD and made my London experience memorable with their supports and friendships: Alessandra, Antonio, Anya, Aurore, Carmen, Emil, Erwann, Francesco, Gianpaolo, Hela, Iky, Krzysiek, Linda, Rhona and Vincenzo.

Special thanks for Shavini who, on top of the latest comment, was so helpful while writing this thesis.

I would like to thank my partner Renata, for everything she has brought in my life and for her support and kindness during that time.

At last but not least, I would like to thank my family and mostly my father for his incommensurable support and encouragements.

Contents

Table of Figures

1. Chapter 1 – Introduction

The background of the project is that approximately 100 million bone screws are used each year, with a rate of failure of at least 1%. This means that somewhere close to 1 million screws could be failing, each potentially leading to further surgery (Procter, 2012).

This study focuses on the fixation of screws in cancellous bone and has been carried out in collaboration with Stryker Osteosynthesis. The first objective was to develop the current understanding of the factors affecting screw pull-out from cancellous bone. This was done through the use of finite element modelling in order to propose a better screw design. The second objective was to study the effect of bone augmentation for screw pull-out and to be able to explain results obtained by a study carried out by Stryker, where 2 out of 11 cases of screw pull-out comparisons were giving better results without bone augmentation.

The main outcomes from this study were a classification of the significant factors affecting screw pull-out from cancellous bone, a new screw design for the cancellous bone environment and finally the improvement generated from bone augmentation was confirmed and could explain the results from Stryker's study.

The contribution to the body of knowledge of this study came from the presentation of a novel finite element modelling technique, which enabled the modelling of screw pull-out from cancellous bone generated from medical images with sliding contacts. The models built with this process are described in this thesis and were used to prove that bone augmentation strengthens screw fixation. They were also used to investigate the key factors affecting screw pull-out from cancellous bone. The analysis of these key factors gave evidence of a better screw design for cancellous bone.

A validation of the finite element model was carried out by comparison with experimental data.

This thesis is composed of 9 chapters. Chapter 2 introduces the problem with the presentation of osteosynthesis, cancellous bone, bone screw and the hypothesis concerning the bone screw fixation in cancellous bone.

Chapter 3 shows the preliminary simulations made of 2D models and 3D models with simplified architecture.

Finite element validation processes were investigated and tested in chapter 4 and the selected validation process was applied in chapter 5.

The screw position and type influence study was carried out in chapter 6 leading to the comparison of cancellous screw with cortical screw and the finding of the screw pull-out stiffness dependence on the bone volume fraction.

The bone augmentation study is presented in chapter 7 showing that bone augmentation systematically improves screw fixation and the more cement the stiffer the pull-out.

Chapter 8 is composed of the study of the factors dependent on the screw design and also a comparison of the real bone model with the simplified bone model from chapter 3.

All these studies led to the improvement of screw design and fixations, with a better understanding of the key factors influencing screw fixation, which were summarised in chapter 9 with recommendations for further work.

2. Chapter 2- Background to the problem

2.1. Why are devices needed?

Bone screws are used for the fixation of bone fractures or for stabilising bone transplants (e.g. Gefen, 2002a). Screws can be used alone or with plates to connect the different fragments of a fractured bone. Screws alone are usually used to "fix intracapsular hip fractures, slipped capital femoral epiphysis, distal femoral condyle and tibial fracture plateau fractures, as well as for treating ankle, elbow and shoulder fractures" (Perren *et al.*, 1992). Using such devices to fix bone fractures is a process called osteosynthesis. It was first undertaken in 1894 by William Arbuthnot Lane. The idea of using devices to fix bone fractures was older but impossible to practice successfully due to infections. For example, in 1850 Rigaud was suggesting the use of an ivory implant in the medullary canal to fix together the 2 main parts of the fractured bones but never did it himself. The term osteosynthesis was used initially in 1870 by Béranger Feraud. This history of osteosynthesis was developed by Vichard and Gagneux (1995) where they highlighted that the practice of osteosynthesis grew only when Pasteur discovered micro-organisms in 1862; it was then becoming possible to avoid infection while using first Joseph Lister's antisepsis or later the asepsis technique. The second aspect that gave a boost to osteosynthesis development was the discovery of the X-ray in 1895 by Roentgen. The use of X-rays allowed surgeons to see; prior to this they used sense of touch to feel the nature of the fracture (Vichard, Gagneux, 1995).

Nowadays, it has been suggested that approximately 100 million screws are inserted in the body each year with a rate of failure of about 1%. This means that somewhere close to 1 million screws might be failing, potentially leading to further surgery (Procter, 2012). This project aims to highlight the reasons of those failures and to offer some solutions in order to reduce the number of failing screws.

2.2. Bone

This project focuses firstly on cancellous bone. In order to understand the complexity of this structure, it is important to introduce general knowledge about bone through basic anatomy and physiology. Then, in the second part, an overview of the relevant material properties has been developed in order to outline out the key elements for this study.

2.2.1. Anatomy and physiology

The obvious functions performed by the bone tissue are to support muscles, organs, and soft tissues, to support the effort needed for leverage and movement, to protect vital organs such as the heart or brain, and also to store calcium phosphate. Indirectly, the formation of blood cells is performed in the bone marrow (haematopoiesis). (Martini, 2006)

Bone is composed mainly of a series of cylindrical structures called osteons (part of the Haversian system). Osteons are themselves composed of cylindrical layers of mineralised matrix called lamellae. The centre of the osteon makes a canal that contains blood vessels and nerves called the Haversian canal (Figure 2.1).

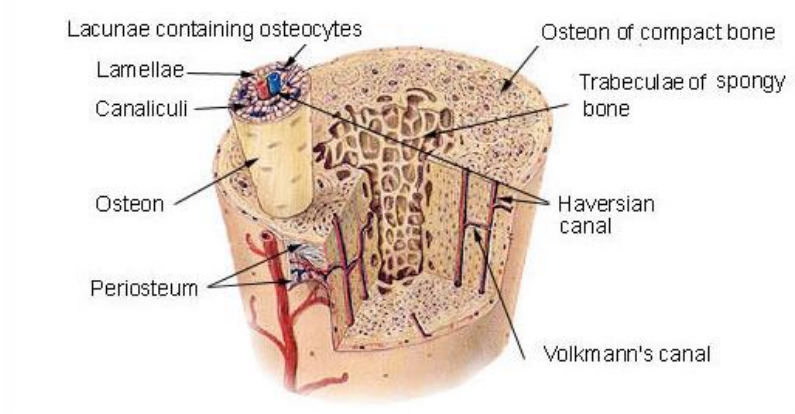

Figure 2.1: Compact and Cancellous bone structure (http://training.seer.cancer.gov/anatomy/skeletal/tissue.html, August 2012)

At the cellular level, four types of cells compose the bone. The osteoblasts, which build the matrix with collagen and inorganic components (calcium, magnesium, and phosphate ions). The osteocytes are mature bone cells that mainly control the mineral and protein content around them and can possibly transform to other cell type in order to repair the bone. The osteoprogenitor cells are stem cells that can create osteoblasts and finally the osteoclasts remove the bone tissues for its renewal. (Martini, 2006)

Each bone in the skeleton is composed of two forms of osseous tissue: the cortical (or compact) bone which is relatively solid and always on the surface of the bones as a protective layer, and the cancellous (or spongy or trabecular) bone which composes the inner part (Figure 2.2). They have a very similar composition but differ in their porosity and the microstructure of their extracellular matrix.

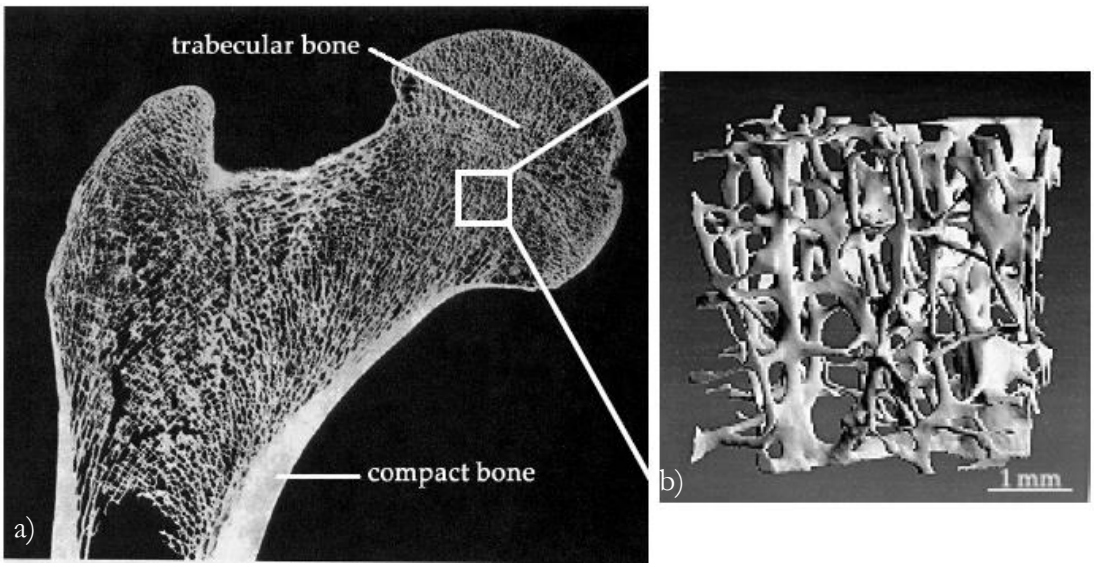

Figure 2.2: a) Macroscopic structure of bones composed of a structural shell (compact bone) and b) a 3D network of rods or plates at the core (trabecular bone). (Rincon Kohli, 2003)

Bone is composed of organic compounds for 33% (mostly collagen). The rest is inorganic components such as calcium (39%), phosphate (17%) and carbonate (9.8%). This is the combination of hard mineral and flexible collagen that creates the hardness and strength of bones.

The overall skeleton is designed in such a way that the compact bone's structure is supporting the daily loads and the cancellous bone's structure can transmit these loads or absorb shocks. Cancellous bone has higher porosity that varies from 60 to 95% compared to compact bone that is in the range from 5 to 10%. This way the weight of the whole structure is optimized. The matrix in spongy bone forms struts and plates called trabeculae and the thin trabeculae branches create an open three-dimensional network (Figure 2.2).

As explained by Martini (2004): "Spongy bone is located where bones are not heavily stressed or where stresses arrive from many directions. The trabeculae are oriented along stress lines, but with extensive cross-bracing. For example, at the proximal epiphysis of the femur, trabeculae transfer forces from the hip to the compact bone of the femoral shaft." (Figure 2.3)

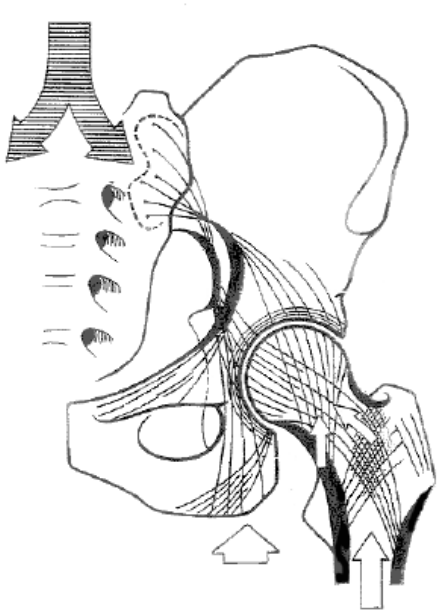

Figure 2.3: Trajectory lines of the trabecular structure, aligned with the direction of the principal stresses result from loading the proximal femur (Kapandji, 1988)

Martini's citation (2004) is explained by the fact that bone is subjected to two different processes: The first one is the development of bone until maturity and the second one is a life-long remodelling process. With these two processes, bone can evolve and adapt itself depending on the activities and the pressures

that it is subjected to through two mechanisms: bone deposition (done by osteoblasts) and bone resorption (done by osteoclasts). Bone as a living tissue is responsive to external stimuli. The modelling process increases the volume and the density of bone tissue and remodelling maintains it as long as the activities of the osteoclasts and osteoblasts are balanced in time and space. Thus, through the remodelling process, this is how the trabecular architecture is constantly evolving depending on the activities: the architecture constitutes columns aligned along the directions of the principal stresses (Figures 2.4 and 2.5). This observation has been made by Meyer, Culmann, Wolff and Roux in 1892 therefore it is called Wolff's trajectory hypothesis (Kapandji, 1988).

The remodelling process can be unbalanced and create a significant loss of bone mass and density. This trouble occurs with increasing age, sex hormone deficiency in women, other hormonal disorders, or calcium and vitamin D deficiency, and can lead to osteoporosis (Figure 2.4).

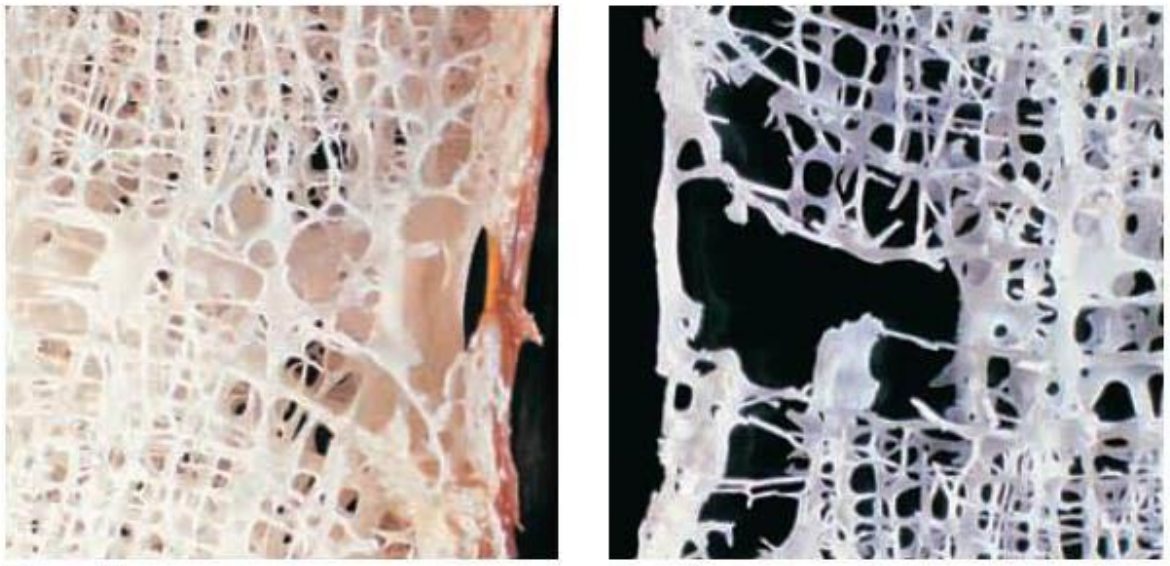

Figure 2.4: Normal (left side) and osteoporotic bone (right side). (http://www.utsouthwestern.edu/education/medical-school/departments/min-metab-center/research.html, August 2012)

"Osteoporosis is a systemic skeletal disease characterised by low bone mass and micro-architectural deterioration of bone tissue, with a consequent increase in bone fragility and susceptibility to fracture." as described by Woolf and St John Dixon (1998). Fractures are more likely to happen after minor or

moderate trauma to people having osteoporosis. This problem which affects mainly the elderly female population, often produces complications which may extend healing.

2.2.2. Material Properties of cancellous bone

The key parameters that characterise cancellous bone from a mechanical point of view are defined below.

The complexity of cancellous bone comes from its unique and specific structure that depends mainly on its environment, as seen previously (stress history, activities, age, sex *etc.*). Thus, its open-cell structure of trabeculae has a relative density that varies from 5% to 70% depending on loads it has experienced and the location within the body (Gibson *et al*., 1999).

2.2.3. Structural properties

Cancellous bone is a cellular porous material made up of connected networks of rods or plates that represent the cell walls (trabeculae). The consistency of the networks - rods or plates, depends on the localisation of the bone and the stresses that it is subjected to. Low stresses lead to rod-like structures and high stresses lead to plate-like structures. According to Wolff's law, the higher the stresses magnitude undergone, the thicker the cell's structure (Kapandji, 1988).

The density of cancellous bone can vary significantly. Various definitions of density exist due to the complexity of the material. The most significant one for the mechanical properties of cancellous bone is the apparent density: the weight of the three-dimensional structure divided by its bulk volume according to Carter and Hayes (1977) or Rice *et al.* (1988) studies. But density is not enough to characterise by itself the structure of bone. From Wolff's trajectory hypothesis, the bone architecture is constituted of columns aligned along the directions of the principal stresses, and since *in situ* the bone is never

loaded equally in all directions; the cells will always show an anisotropic geometry and orientation. It has been proved that the architecture contributes to the inherent mechanical properties in many studies (Keaveny *et al.*, 2001).

Cancellous bone is an organic material composed of water and minerals. Therefore, theoretically and depending on the criteria, there are multiple ways to calculate and define the density (Rincon Kohli, 2003). These include:

- Apparent density (ρ^*)
- Solid-phase density (ρ_s)
- Relative density (ρ^*/ρ_s)
- Volume fraction (BV/TV), which represents the bone volume divided by the total volume of the sample.
- Ash content (ρ_{ash})
- Ash fraction (ρ_{ash}/ρ_s)

Practically, there are many ways to measure the density:

- *In vivo*, most methods are based on sending radiation through tissue:
  - Dual photon absorptiometry (DPA)
  - Dual X-ray absorptiometry (DXA)
  - Quantitative computed tomography (QCT).

Some other techniques have been developed to protect the patient from excessive radiation:

- Quantitative ultrasound (QUS)
- Quantitative magnetic resonance (QMR). (Augat *et al.*, 2002).

- *In vitro*, the method was first based on Stereological analysis but it was time-consuming and destructive (Odgaard, 1997). Other techniques have been developed from computed tomography and magnetic resonance: μCT or μMR. These techniques can produce high-resolution 3D image reconstruction of trabecular bone without causing damage.

From the *in vitro* techniques, it is possible to determine directly structural indices such as bone surface (BS), bone volume (BV), total volume (TV) and

therefore volume fraction (BV/TV). Then it is also possible, indirectly, to measure other indices like trabecular thickness (Tb.Th), trabecular number (Tb.N) and trabecular spacing (Tb.Sp) (Parfitt *et al.*, 1987).

2.2.4. Mechanical properties

The mechanical behaviour of cancellous bone shows 3 different phases in compression: Firstly, there is a linear-elastic regime as the cell walls bend. Secondly, there is the plastic regime as the cells begin to collapse. The curve reaches the point of maximal compressive stress before stabilising at a nearly constant level until the cells collapse and meet the next wall. Then, this final phase is known as densification as a steep rise of the stress is observed. In tension, the reaction is different as the linear-elastic portion of the curve results from the extension of the cell walls until plasticity when they start to crack. Then, the curve starts to fall due to final fracture of the structure (Figure 2.5). This was first suggested as a generic definition for cellular solid such as cancellous bone by Gibson and Ashby (1982).

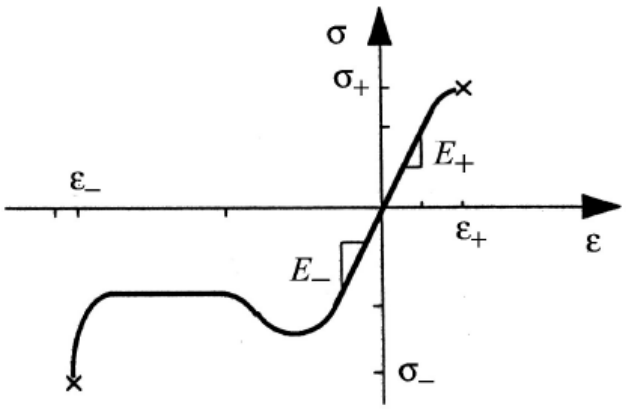

Figure.2.5: Uniaxial stress-strain curve for cellular solids. The linear stress-strain relationship is defined by the Young's elastic modulus ($E_-=E_+$), while the ultimate compressive and tensile stresses are defined by σ_- (ε_-) and σ_+ (ε_+). (Rincon Kohli, 2003)

Another phenomenon that affects the mechanical properties of cancellous bone is the reduction in bone mass with age. Gibson (1985) has estimated that

the relative density of the cancellous bone can reduce by 50% between 20 and 80 years old. This phenomenon is natural but creates complications as the structure gets weaker. If the reduction becomes significant, it becomes then osteoporosis (c.f. definition). The chart (Figure 2.6) shows a first peak of fracture due to young age, and then there is another one more important coming with older age. The second peak is a direct effect of the bone mass reduction. Fractures can happen with insignificant trauma. It has been shown by Weaver (1966) that, in the elderly, fractures occur mostly where cancellous bone is the main supporting structure showing that age effects of bone density reduction affects cancellous bone much more than cortical. Then, fracture fixation gets more complex. From Augat *et al.* (2002) studies, the low relative density of the bone implies that there might be only a small contact surface for the healing process to begin. From Barucci *et al.* studies (1985), in elderly population the fracture is often multiple and therefore the fixation failure is quite high due to its complexity.

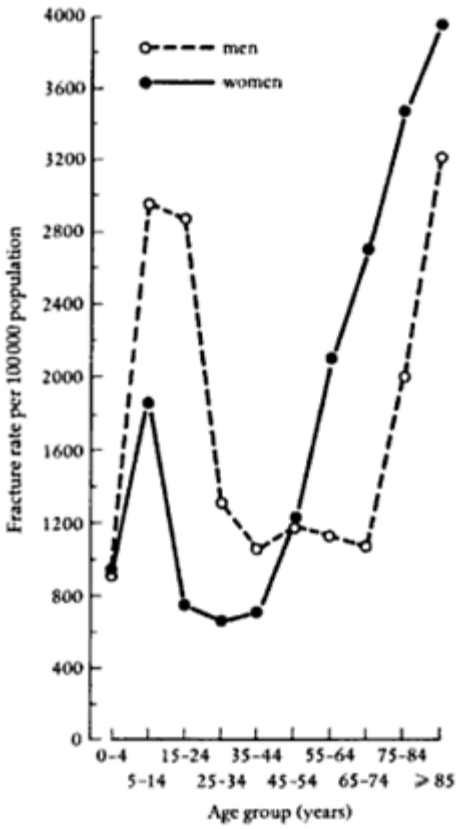

Figure 2.6: Age and sex specific incidence of limb fracture (Woolf, 1998)

It is also possible to reconstruct the cancellous bone in 3D from the images that allow a wide range of possible tests on the bone through Finite Elements Analysis (FEA) software. These include: Yield strength (Bayraktar and Keaveny, 2004), bone quality (Hernandez and Keaveny, 2006), failure mechanisms (Bevill *et al.*, 2006), microstructural properties (Mittra *et al.*, 2005), and bone strength (Bevill and Keaveny, 2009). The main advantage is the repeatability of the FE model experiments – leading to the possibility to work on the same structure through different experiments, which is not possible with real bones as they are all unique. Then, it is also less expensive and allows more accuracy.

2.3. Bone Screws

Metallic implants have been used for the reduction and fixation of human bone since the late eighteenth century as described by Ernberg (1996). At that time, procedures and materials became sufficient for success (non-sterile operating environment, unstable chemical materials in the human body etc.). Nowadays, one of the targets, in order to improve bone's healing, is to understand further the connection between the screw and the cancellous bone. Therefore, it is important to start with a brief review of the design and manufacturing of bone screws to understand the possibilities and limitations of screw design. Then, the second part is showing the state of the art on screws in cancellous bone, and the reasons why bone screws can fail in cancellous bone.

2.3.1. Design and manufacturing process

2.3.1.1. Design

First of all, it is important to be aware of the functions of the orthopaedic screw in order to understand the design needs. Basically, the screw function is to pull two components together (plate and bone in figure 2.7 but it could be two

pieces of bones). In this example, the shaft is going through a sliding hole and the thread through a pilot hole. A torque is applied to the screw resulting in a compressive force joining the two components together.

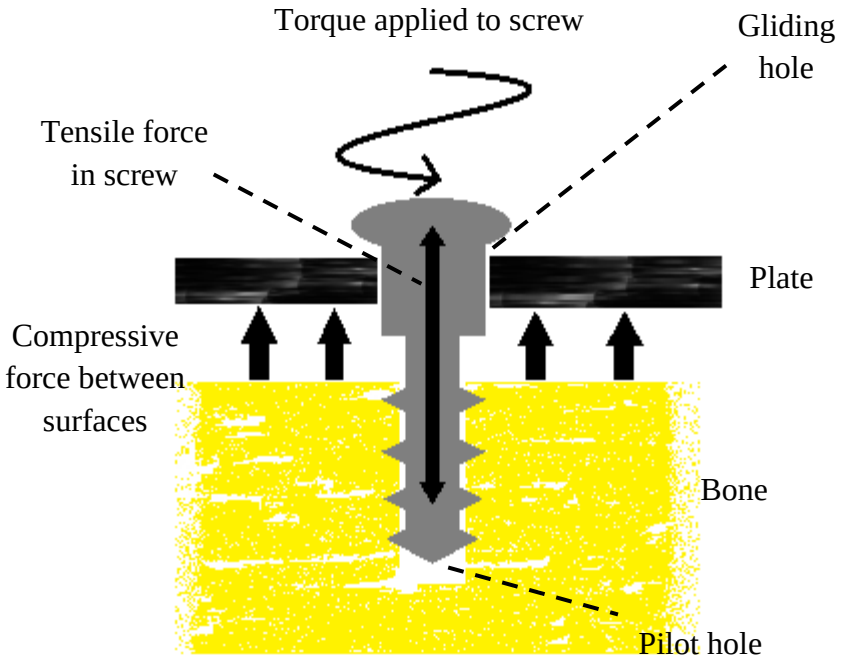

Figure 2.7: Illustration of the function of a screw (after Asnis* et al.*;1996)

The screw is characterised by many different factors, (Figure 2.8). The most significant, which have been studied in this study, are highlighted to be:

- The pitch which represents the distance between threads.
- The root diameter which represents the diameter at the base of the threads
- The major diameter which represents the outside diameter of the screw.

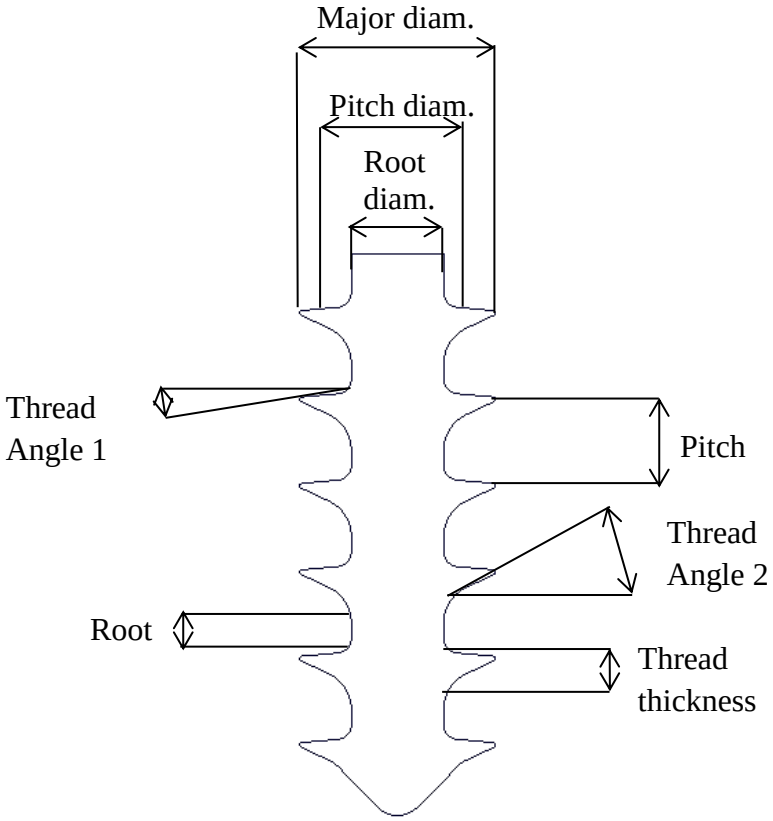

Figure 2.8: Basic nomenclature of a screw

The main factor which characterises a "good" screw is the holding power or the force needed to pull it out of the bone. According to Tencer *et al*. (1996) this resistance to pull-out in porous materials such as cancellous bone is dependent on six factors with three related to the design geometry of the screw:

- Its outer diameter
- Its length of engagement in bone
- The thread geometry: length and pitch (not tooth profile).

The other three factors are related to the bone and its preparation:

- The shear strength of the bone that the threads engage,
- Pilot hole size
- Tapping

Figure 2.9 is illustrating the factors affecting the holding power between the screw geometry and the bone shear strength.

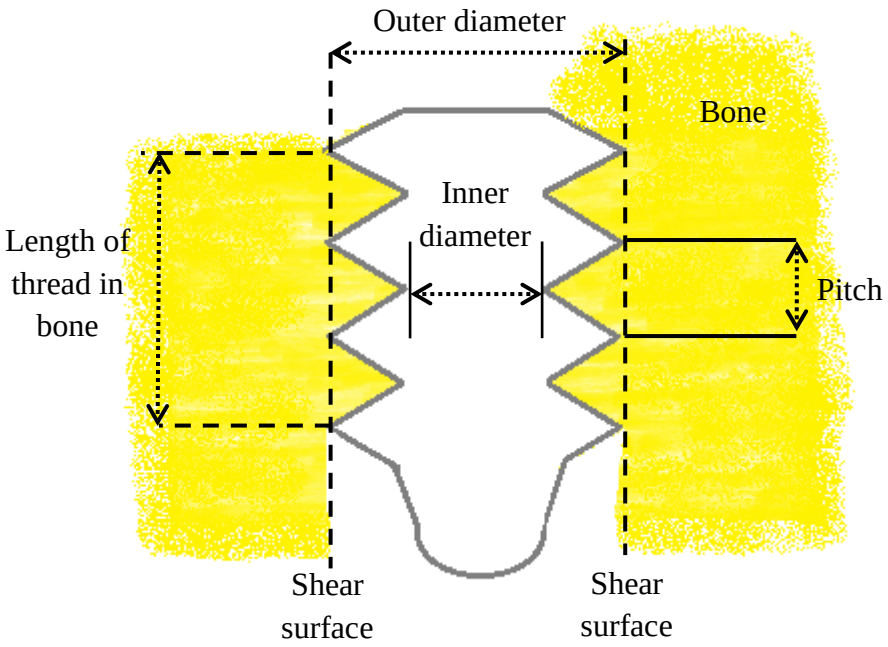

Figure 2.9: Schematic representation of some factors affecting holding power

The following relationship determines the theoretical holding power from four of the above factors. According to Tencer *et al.* (1996) this relationship "explains 97% of the variability in pull-out strength of non-tapped screw placed in porous foam" and at the same time, it has been admitted that it is not that accurate for cancellous bone (Chapman *et al.,* 1996):

$$\mathbf{F_S = S \times A_S = S \times (L \times \pi \times D_{major}) \times TSF}$$

Where:

F_S=predicted shear failure force (N)

S= material ultimate shear stress (MPa)

A_S= thread shear area (mm^2)

L= length (mm)

D_{major}= major diameter (mm)

($L \times \pi \times D_{major}$) = area of cylinder of diameter D_{major} and length L

TSF= thread shape factor (dimensionless)

= (0.5 + 0.57735d/p)

d= thread depth (mm)

= $(D_{major} - D_{minor})/2$

D_{minor}= minor (root) diameter (mm)

P= thread pitch (mm)

The main design factors for orthopaedic screws have been surveyed but there are still some other minor factors that affect the overall performance and these are illustrated in Figure 2.10:

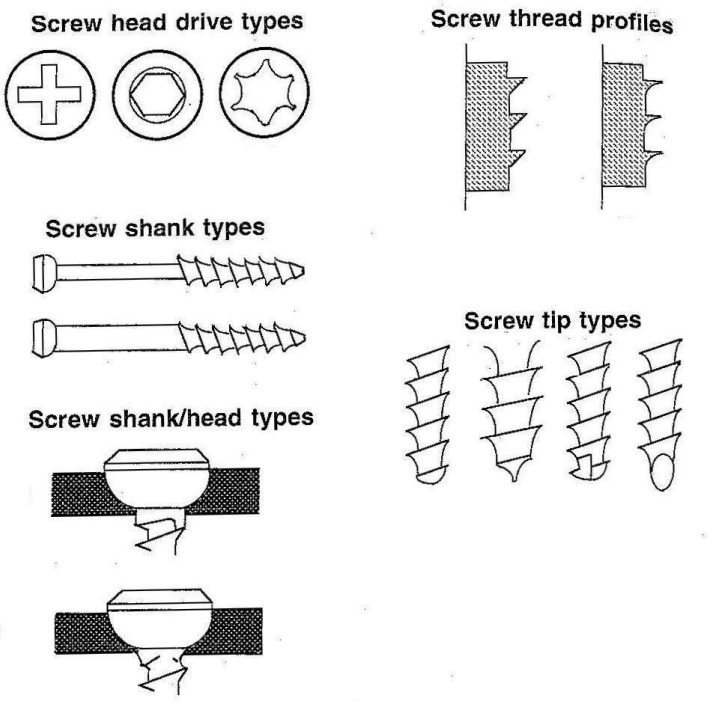

Figure 2.10: Features of bone screw design (taken from Tencer* et al.*, 1996)

2.3.1.2. Manufacturing

As detailed by Ernberg and Asnis (1996), the manufacturing of an orthopaedic screw follows a series of very precise procedures:

- Material selection: Alloys of Titanium and Stainless steel are the most commonly used because they offer good strength characteristics as well as being workable.

- Cutting: The material chosen is cut into bar stock of dimensions close to the largest dimensions of the screw. Usually, the stock material is purchased in cylindrical rod with a diameter close to the biggest diameter of screw.

- Machining 1: the workpiece is then transformed to the profile geometry of the screw with the screw head and the shank with the right dimensions and the future threaded segment with the outer diameter of the screw threads. The workpiece at the end of this stage is commonly called the blank.

- The screw head drive is then produced.

- Drilling: The cannulation is created to the blank with a gun drilling. This stage needs tools with tight tolerances. The drill has to be cooled with a fluid going through a central channel which also removes metallic debris.

- Machining 2: The production of the threads. This stage can be composed of many different steps: first the cutting flutes are milled into the thread cylinder and then the final thread can be produced through different processes like turning, milling, or grinding operations, or by using cutting dies.

- Electropolishing and passivation: this last stage aims is to clean the material and increase the resistance to the corrosion.

The overview on the design and manufacturing processes show the constraints and the limits in the design of orthopaedic screw.

2.3.1.3. Previous testing

The most important factor in fracture fixation using orthopaedic screws is screw holding power or screw pull-out strength (Asnis *et al.,* 1996, Brown *et al.,* 2010, Chapman *et al.,* 1996, DeCoster *et al.,* 1990). Any failure leads to further complications and a significant increase of the healing time. The different

studies are separated here in 3 categories: Real bone studies from cadaver or animals, foam studies, and finite element modelling studies.

Real bone studies are very interesting as they represent reality but have some disadvantages like cost, variability of the specimens and of course ethics but they cannot be avoided in a validation process of any theory. There has been a lot of research in this area using various methods (Seideman and Asnis, 1996, Asnis, 1996, Asnis and Kyle, 1996) which has led to varying conclusions. The main factor that has been regularly emphasised is the bone density effect (Crum *et al.*, 2000, Zanetti *et al.*, 2009 and Yakacki *et al.*, 2010). Indeed, it seems natural that less contact surface leads to less force for the screw pull-out from the bone.

Recently, it has been common to carry out the research with synthetic foam materials that appear to have almost the same characteristics as cancellous bone. One of these experimental investigations has been carried out by Kissel *et al.* (2003). The purpose was to compare the pull-out strength between small diameter cannulated and solid-core screws. Cannulated screws offer a number of advantages in terms of screw placement and insertion procedure. Kissel's study has shown that the results from pull-out test are equal or better with small diameter cannulated screw when compared with conventional solid-core screws. Therefore, the cannulation of these small diameter bone screws does not diminish their mechanical performance. Chapman's investigation (1996) on the factors affecting the pull-out strength of cancellous bone screws confirmed the relationship on TSF (thread shape factor).

Nowadays, as explained by Zhang *et al*. (2004): "compared to the experimental models, mathematical models can offer the ideal opportunity from the point of view of control. They are characterised by absolute repeatability, with the additional advantage that any parameter can be varied in the desired degree", Finite Element (FE) modelling has the potential to create an infinite set of results easily.

Chen *et al.* (2003) used FE modelling to investigate the interface conditions affecting the performance of pedicle screws in vertebrae. In this

study, CT scans of a human lumbar spine have been used to create the vertebrae model in which they include the screw. They compared the stress interface between the two cases: bonded and frictional contacts. The results were different as the screw is subject to significantly higher stresses in a contact interface compared to a bonded interface. Therefore, provision of a binding surface would improve screw fixation into vertebra. This investigation has shown how the stress varies with interface but in this investigation, the interface is clearly truncated as the inner part of the vertebrae is considered as a continuum while in reality it is composed of cancellous bone.

Gefen (2002) has studied a comparison of different screw designs using their dimensionless stress transfer parameter (STP) to analyse the performance of the different screws through FEA, "STP values were calculated as ratios of bone averaged von Mises equivalent stress to screw-averaged stress in designated regions of interest". In this study, the peak stress region appears to be always on the first thread of the screw. Then, the results show that the length of the screws affects the stress concentration as well as the number of threads involved. Therefore, the longer screw with the more threads would reduce stress concentration for the fixation in the cancellous bone. It appears that the trapezoidal or rectangular profile of screw would be the best for STP value. A similar study from Shuib *et al.* (2007) showed similar conclusions. In their study, the screw design parameters that have been varied were the profile shape, thread pitch, thread angle, thread length and major diameter. They considered that the biomechanical compatibility of a fixation screw is directly linked to its stress transfer ability, measured by the STP. From their results, all the different parameters tested affect the STP calculation. It appears that the STP value is not completely accepted as a valuable screw parameter. These results represent an innovative way to see the cement implication in the threads geometry through the STP except the fact that the model used for the bone was again a continuum.

This aspect has been studied by Wirth *et al.* (2010, 2011). Those are the first studies showing the influence of the cancellous bone architecture on the screw pull-out. They actually created models from micro-computed tomography (μCT) with implants using the principle of a direct voxel to element conversion.

This technique creates really computationally heavy models, with models over 20 million elements. In this case the contacts were chosen to be bonded, which simplify the solving matrix substantially, anyway such a tessellated structure does not have to be bonded but the geometry leads certain characteristics similar to bonded. The bonded contacts gave different results than expected as described by Chen *et al*. (2003). On the other hand, this technique is automatic and with access to a powerful computer (1024 cores of a CRAY XT5 tm super-computer) they manage to create and solve each simulation in a few minutes. Despite the bonded contacts, they could manage to show the "clear limitations of the continuum assumptions" for cancellous bone and some screw pull-out differences due to the different bone apparent densities.

2.4. Bone Augmentation

The previous section has shown the importance of the screw holding power for some fractures healing and presents a brief overview of screw design. In this section, another technique is described to improve the overall holding power: augmentation. The bone augmentation principle is to insert cement around the screw in order to strengthen the whole construct. Therefore a lot of research has been done in order to determine the best way to apply the cement in order to get not only the best healing but also to get the best postoperative effects.

Barucci *et al.* (1985) made a study with patients that have been operated for intertrochanteric fractures. Two groups were created: fixation with or without cement augmentation. The results of this study are really positive on the cement effects but with the caution that the cement has to be applied into the exact location as cement filling in the intramedullary canal can block the normal endosteal blood circulation. Therefore, it was important to be sure that no cement was inserted between the cortical fragments at the fracture site in order to avoid non-union of the bone. The results of this experience show that the group with cement augmentation spent an average of 21 days in hospital after

the operation against 31 days for those without. The group with cement augmentation also became mobile quicker. The rate of fixation complication was also significantly lower and the healing rate was higher. The postoperative drawbacks shows also that many of the patients who had a cement augmented fixation had a lower decreased range of motion (hip score) than those without cement augmentation.

Bretton (2008) has studied the effects of the cortical shell in bone augmentation. This study was done with open foam. The results showed that cement augmentation increases the screw pull-out force and also that the pull-out force increases with the quantity of cement.

One important point of research in this area is the cement application method for the bone augmentation. McKoy *et al.* (2000) have created a new cannulated screw design for cancellous osteoporotic bone. This screw has holes along the main axis between the threads in order to get a better distribution of the cement in the bone. The cement injection process is in two phases for this new screw. The first injection is, as usual, in the tapped hole and the second is done through the cannulation when the screw is inserted. This process and design is mainly compared to non-cannulated augmented screws on cadaver vertebrae from 2 kinds of preservations (frozen and embalmed). All the samples had a t-score less than -3.00 which means osteoporotic according to the World Health Organisation, e.g. osteoporotic bones are defined by the World Health Organisation with a t-score less than -2.5 (McKoy *et al.*, 2000, Kanis *et al.*, 2000). The test is an axial pull-out test and the results showed a significant increase (+278%) of the holding power for the newly designed screw compared to the solid one. Two other tests were made between a normal cannulated screw and this new one but showed a decrease of 24%. Unfortunately, no relevant conclusion has been made about this point but some other factors were revealed. The lowest bone mineral density had the largest ultimate load to failure and the bone with highest density had the lowest pull-out strength. It is explained by the fact that the penetration of the cement is depending on the density of the bone. The idea to have the cement spread more radially into the bone is relevant but the design and technique chosen are weakening the screw; moreover it is mainly

compared with a non-cannulated screw. Therefore, it is a theory that could be relevant to develop through FE models as it could be easier to vary only cement injection and not the screw or the bone.

A similar study has been made by Chen *et al.* (2009). In this case the screw is a pedicle screw and 6 different screws have been compared. One screw is non-cannulated and the difference between the others, cannulated, is the number of holes along the axis in the threaded portion (from 0 to 8). It shows again that these holes allow a better dispersion of the cement. This time, the tapped hole has been also tested. It is again a pull-out test with synthetic foam and the results show that the holding power increases with the number of holes as the cement is wider spread into the foam and that hole tapping is decreasing it.

Stoffel *et al.* (2008) have also tried a new technique for the polymethylmethacrylate (PMMA) cement augmentation of the sliding hip screw in proximal femur fractures. The cut-out resistance was assessed in this study. An overview of disadvantages of augmentation for this kind of fracture is shown at the beginning of this study such as problems of accuracy in the quantity and in the dispersion of the PMMA cement but also the fact that the cement can cause osteonecrosis and thermal damage. Therefore, their new technique would avoid this entire problem and it consists to introduce the cement just above the position of the lag screw using a customised jig. The result of this study shows that the cement augmentation improves significantly the cut-out strength of the fixation (average 42%). This study shows that depending on the circumstances the cement could be applied in a different location to strengthen a structure. This kind of test could be done first through FE models before doing any validation with cadaver bone.

Another study has been created on that purpose by Augat *et al.* (2002) using a modified hip screw with low viscosity cement. The study was made on nine pairs of femora, while on one femur standard sliding hip screws were used, on the other one they used their new screw together with the cement. The result from this study shows that the total displacement of the femoral head was

reduced by 39 percent on average using cement augmentation in the modified screw compared with the standard sliding hip screw. The largest improvement in initial fixation stability was found for bones that were more osteoporotic. The accuracy of the localisation of the cement was accentuated.

Concerning osteoporotic bone, Fransen (2007) has been increasing pedicle screw anchoring in osteoporotic spine by injecting cement through the implant. In his study the cement increased the pull-out force by 250% compared to the non- cemented.

Wuisman *et al.* (2000) have studied calcium apatite cement (CAC) in patients with severe progressive osteoporotic spinal deformities. This study shows that CAC cement behaviour was different from PMMA cement as it breaks without taking part of bone whilst PMMA cement remains intact leading to a failure of the surrounding bone.

A FE simulation of cement bone interface micromechanics has been made by Janssen *et al.* (2009) in order to compare with experimental results. The test principle is to replicate with FE software a cycle of fully reversible tension and compression. The results are in the same range of those from experimental test. The model used in this study is relatively small as it is focused only on the interface. The main result from this study is to consider the contact between the cement and the bone as frictional and not bonded. This study reveals that dealing with μCT data is offering great opportunities theoretically but then, nowadays, it can lead easily to excessive computational costs as the resolution of the data increase.

Wirth *et al.* (2011) could manage to model screw pull-out from augmented cancellous bone with different thicknesses of augmentation and with different level of bone loss simulation. The modelling process is again based on the principle of a direct voxel to element conversion. This time they could simulate bone loss effect on the cancellous architecture and also augmentation as well. In this study they showed that the implant stability depends mostly on bone mass and architecture. They showed as well that augmentation improves implant stability meanwhile the augmentation efficiency decreases with bone loss.

2.5. Hypothesis, demonstration process and objectives

The great variance between results from screw pull-out tests could be explained by the fact that each cancellous bone is different but cannot explain the difference when the comparison is made in the same bone sample. The idea explaining these results comes from the cancellous bone structure. If the cancellous bone is simplified as a cubic matrix, as it is illustrated in figure 2.11, it is then possible to consider pull-out force from the position 1 could be different than the one from position 2. Therefore, the augmentation effect could be hidden behind this variability of results.

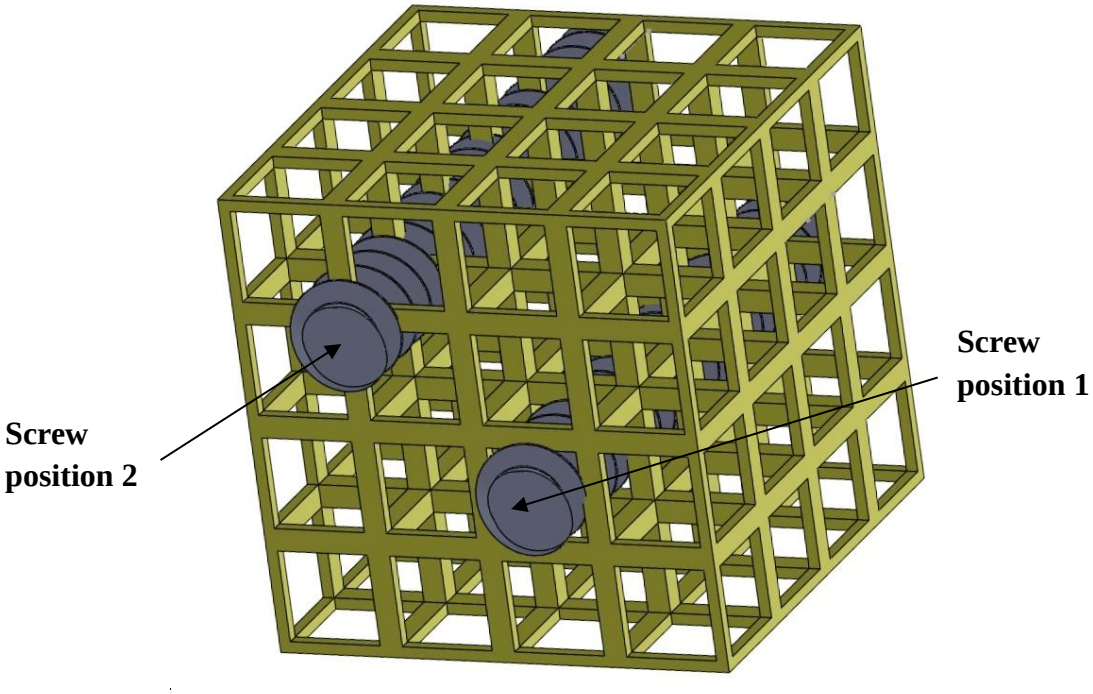

Figure 2.11: Screw position effects theory

As demonstrated by Procter (2008-2012), in the position 1, the screw threads are fitting the cells size without destroying the structure. Moreover, if it is considered that the thread pitch is the same as the trabecular pitch, the result would be to have one thread per unbroken strut. Then, the pull-out force (F) expected would be:

$$F = n \times F_{breaking\ strut}$$

Where,

n = number of threads engaged

$F_{breaking\ strut}$ = Force to break one strut (assuming stiff and brittle struts).

In the position 2, each thread is now in contact with one broken strut. It is known that a brittle stiff strut will fail due to the tensile forces induced by bending, therefore the pull-out force (F) expected would be:

$$F = n \times F_{bending\ strut}$$

Where,

n = number of threads engaged

$F_{bending\ strut}$ = Force to bend one strut

As the cancellous bone architecture is not a perfect cubic matrix, the fixation strength would depend upon a combination of both types of engagements. Also, as the cancellous bone structure has a specific geometry, there is also a distribution function of the trabecular strut number, length and orientation. Therefore, the final pull-out strength can vary with a small difference at the entry point as shown on the following figure.

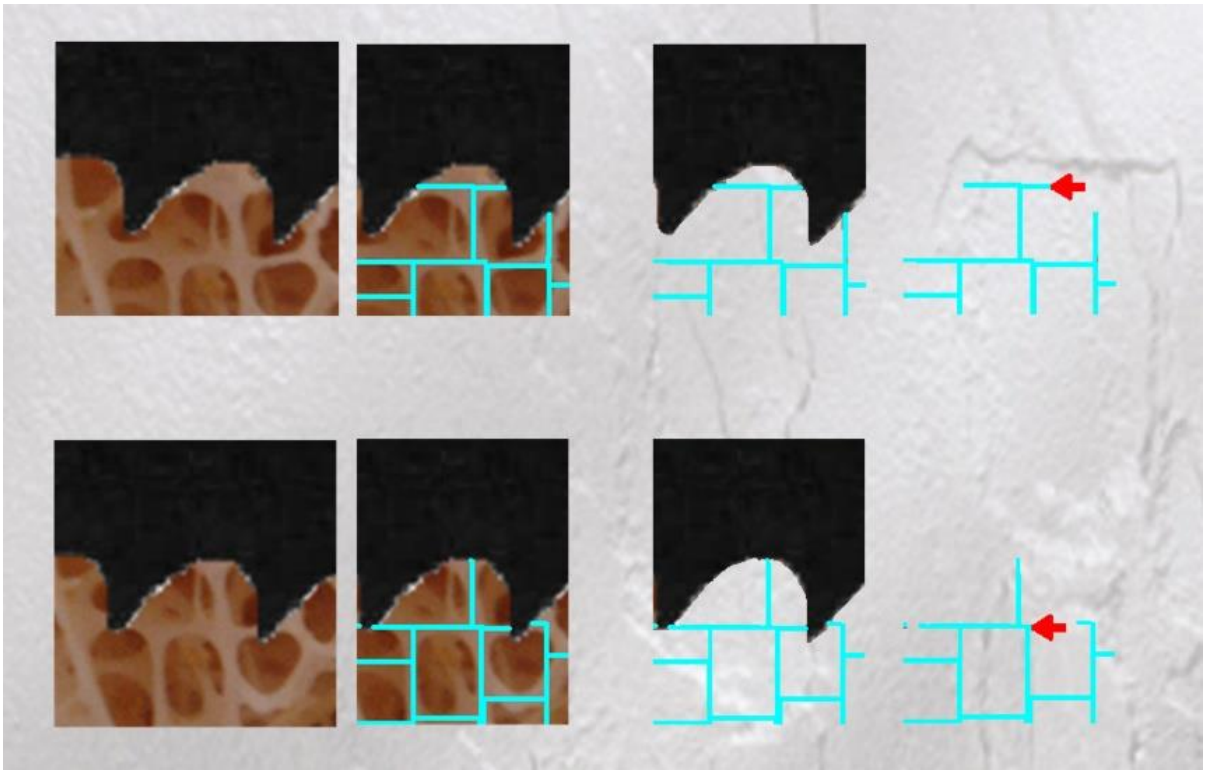

Figure 2.12: examples of small differences that could affect the pull-out force (Philip Procter, Stryker Osteosynthesis)

The Figure 2.12 shows a superposition of a screw over a picture of cancellous bone. This photomontage shows that a slightly different position of the screw thread could result in a different contact as it does in one case where it would be entrapped in a trabecular cell.

It is natural then to speculate on the different options that could improve the holding power of the screw. For example, the size of the threads pitch (Figure 2.13) or also the thread's shape as suggested by some other studies (even if the cancellous bone model was a continuum).

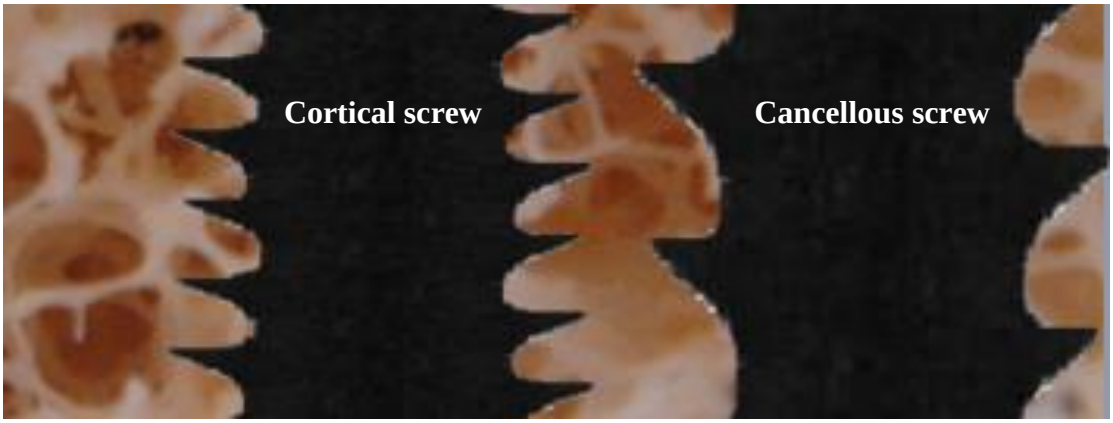

Figure 2.13: Which one would have the best pull-out force? Smaller or bigger threads pitch (Philip Procter, Stryker Osteosynthesis)

In the Figure 2.13 example, it would be natural to think that the one with smaller pitch would have the greater pull-out force as it has more contacts and entrapped more struts. This is typically a test that would be feasible with FE models.

Thus, the first aim of this study is to show the evidence of the screw positions effects through FE models as illustrated by the Figure 2.14.

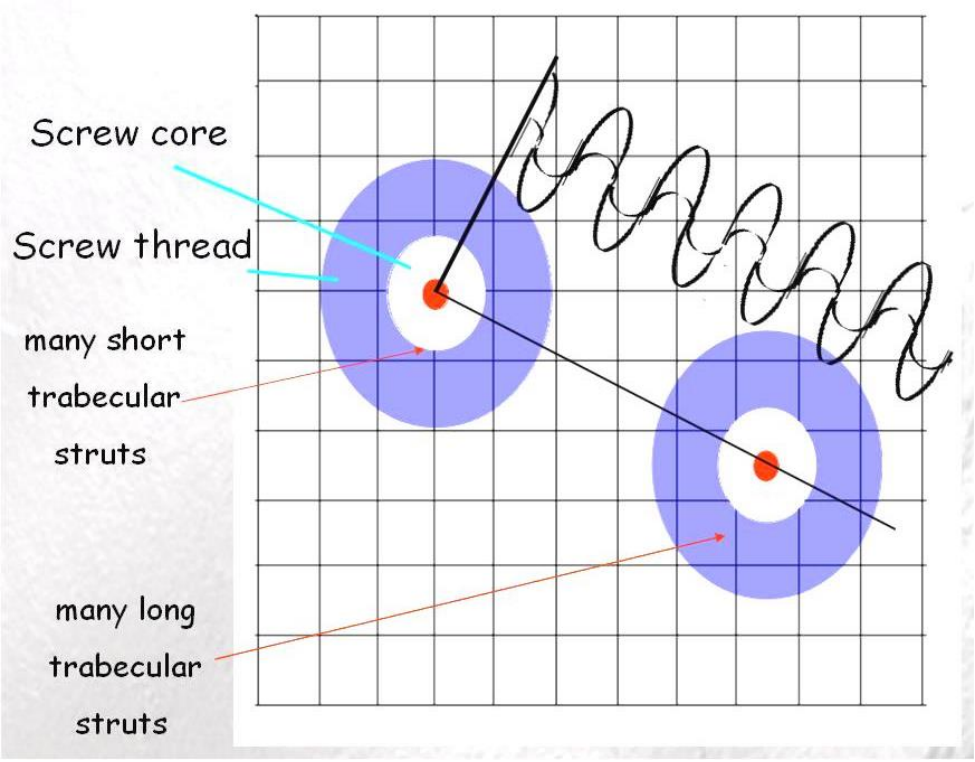

Figure 2.14: Position affecting the pull-out forces (Philip Procter, Stryker Osteosynthesis)

The second stage aim is to show the effect of the bone augmentation on the screw pull-out for comparison with non-augmented.

Finally, the major aim is to understand fundamental phenomena affecting the behaviour of screws in cancellous bone by means of FE models, and hence to predict the influence of key variables.

3. Chapter 3- Simplified bone models

This chapter focuses on simplified bone models that have been developed. These models have been generated in order to test the hypothesis of the influence of the screw initial position outlined in the previous chapter. In this chapter, FE models will progress in complexity. In a first attempt, the FE models are in 2D. Similar 2D models have already shown the augmentation effect by Brown *et al.* (2011). Here, the study is about the screw position's effects on the pull-out force. Then, different models suitable for 3D modelling have been tested and one has been selected in order to test the position theory again and also to study the bone augmentation influence.

3.1. Simplified 2D models

3.1.1. Overall settings:

All the models have been run with Ansys® software. The material properties and boundary conditions have been made following previous studies from Brown *et al.* (2011). Screws are modelled as titanium alloy with isotropic elasticity, as they are much stronger than all the other bodies, with a Young's modulus of 114GPa and a Poisson's ratio of 0.3. Cancellous bone was assumed to be perfectly elasto-plastic, as shown in figure 3.1.

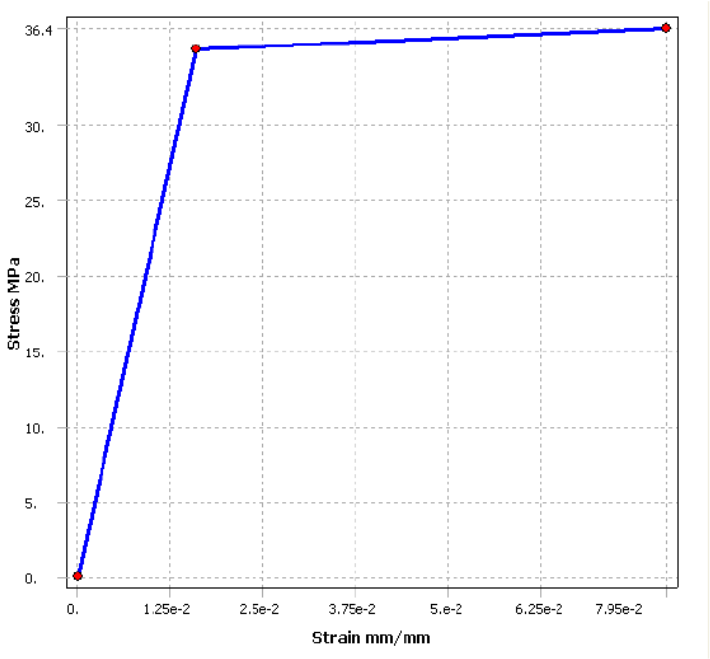

Figure 3.1: Stress-strain Curve for cancellous bone

Elastic behaviour for cancellous bone was defined using a Young's Modulus of 2.2GPa and a Poisson's ratio of 0.3 (Rincon Kohli, 2003). The plastic behaviour was defined as a bilinear hardening model with a yield stress of 35MPa and a tangent modulus of 22MPa (i.e. 1%). The cement was modelled with calcium phosphate cement's properties with Young's modulus of 1.52GPa, a yield stress of 16.3MPa and Poisson's ratio of 0.3 (Ikenaga *et al.*, 1998; Brown *et al*., 2011).

3.1.2. The influence of screw position

3.1.2.1. Principle

The 2D model principle is to change the screw initial position and to analyse the pull-out force needed in each case. The model is set up with an axial symmetry and half a screw is involved in cancellous bone. The screw model is a non-cannulated screw following the cancellous screw model 604010/-100 manufactured by Stryker. It was modelled in Ansys® Workbench with a length

of 10mm, a pitch of 1.75mm, an outer diameter of 4mm, and an inner diameter of 1.9mm. The cancellous bone model was also modelled in Ansys® Workbench following Brown *et al*. (2011) study and here the cancellous cells sizes are square with a 0.8mm size. A vertical displacement is applied on the top of the screw while the side part of the cancellous bone is considered as a fixed support (figure 3.2). It has been chosen to apply a displacement rather than a force in order to obtain similar results as mechanical tests.

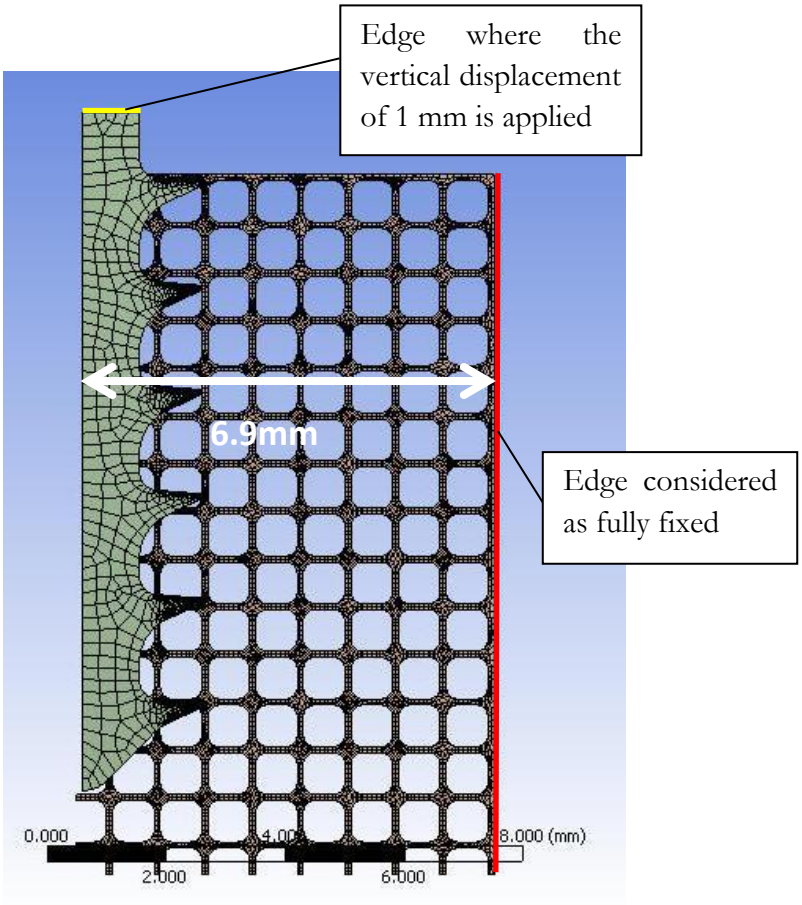

Figure 3.2: General view of the model

Models have been tested with 11 different screw initial positions as illustrated in the figure 3.3. The screw position is moved radially of 0.1mm along a bone made of 8.5 rows of 0.8mm cells as illustrated. An axisymmetric FEA was carried for each case to compute pull-out strength. The elements used were quadratic and linear.

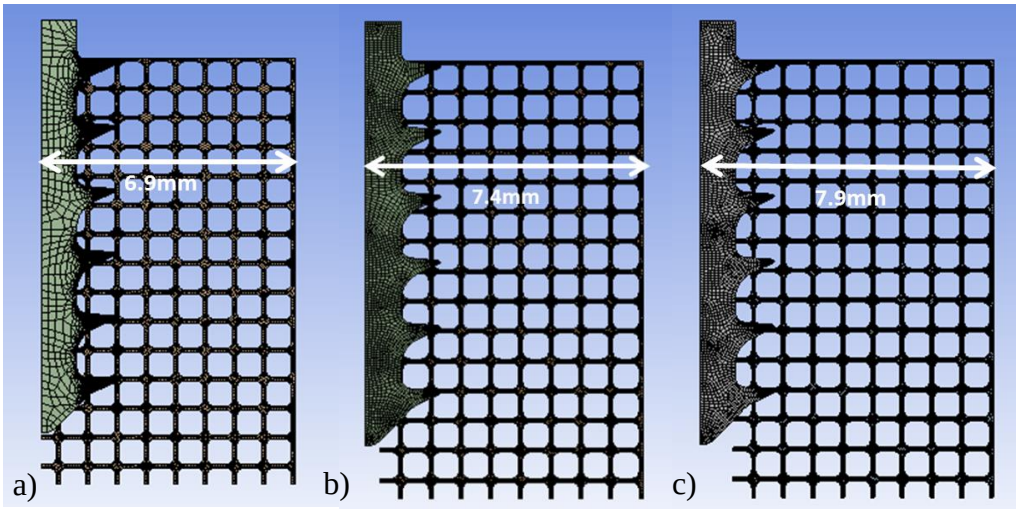

Figure 3.3: The screw is moved to the left every 0.1mm on 1mm from the initial position a) passing though the intermediate position b) until the last one c).

The aim of this study was to highlight the influence of the screw position. The distance between the screw centre and the fixed edge could have a potentially influence on results as it varies from 6.9mm to 7.9mm. One possible option was to chop the bone systematically in order to have the same length but it would be just trabecular tips in most of the cases. Therefore, it was decided to study as well the effect of the distance of the fixed edge by adding or removing cell columns in the initial case.

3.1.2.2. Results

The following image (figure 3.4) is an illustration of the different types of issues that arose during simulations. It shows the total deformation image resulting after 1mm vertical displacement of the screw.

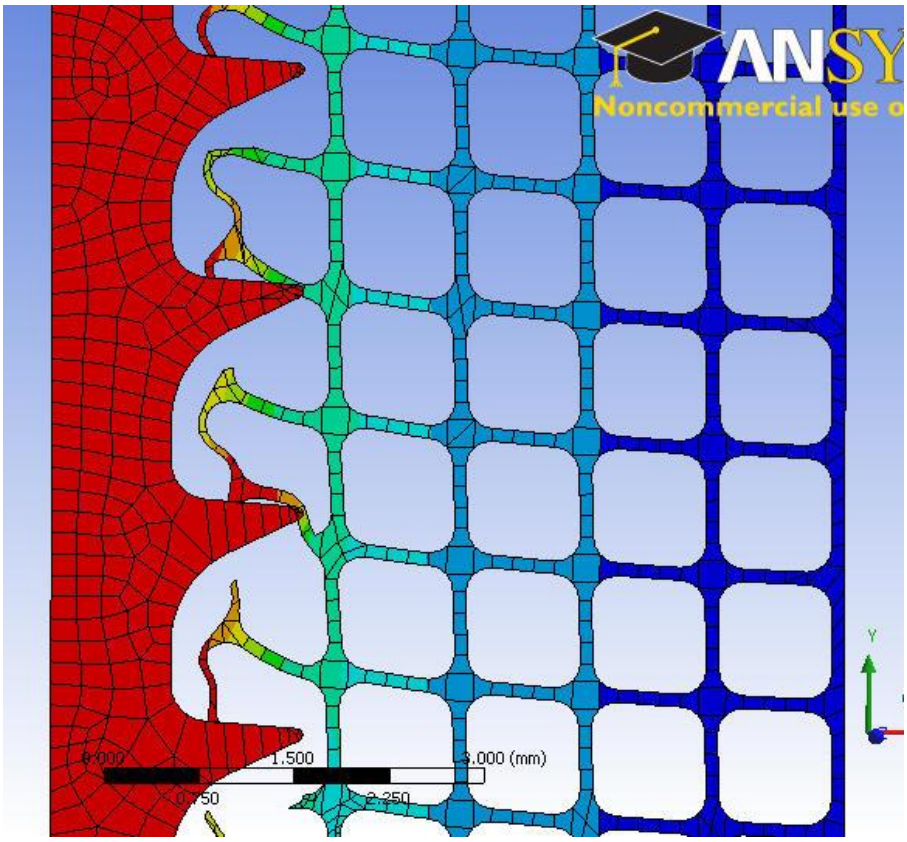

Figure 3.4: example of 2D total deformation results for 1mm vertical upward displacement of screw.

This process was not automatic: For each position, it was necessary to have many runs following a technique of trial and improvement. After each run, the problematic elements had to be found to get remeshed, usually with a denser mesh, for the next run until the solution file could reach values of interest.

The problematic elements were generally elements that were highly distorted due to the fact that it was a hard material against a much softer one. The cancellous bone elements can become extremely distorted as illustrated in figure 3.4. For example: It was necessary to have a finer mesh, i.e. to increase the number of elements for some models, in order to avoid the simulations to stop due to elements reaching too high distortion.

Another aspect that was problematic was the contact regions. The important number of contact areas increases significantly the solving matrix

making the simulation run longer and generate bigger files. As illustrated in figure 3.4, some surfaces were not in contact at the beginning of the simulation before touching each other. It was then necessary to anticipate this phenomenon for each case by selecting manually all the areas that could potentially be involved in the process.

An overview of the contact definition in FE was made by Simpson (2005) which showed that there are negligible differences from the use of different formulations for the penetration prevention. From this result, Lagrange multiplier, Penalty function or Augmented Lagrangian method showed similar results. This study also involved the contact stiffness effect and concluded that if the contact stiffness was between 0.1 and 1 it does not affect the results of the simulation.

A convergence study was undertaken in order to be certain that the number of elements would not influence results is shown in figure 3.5.

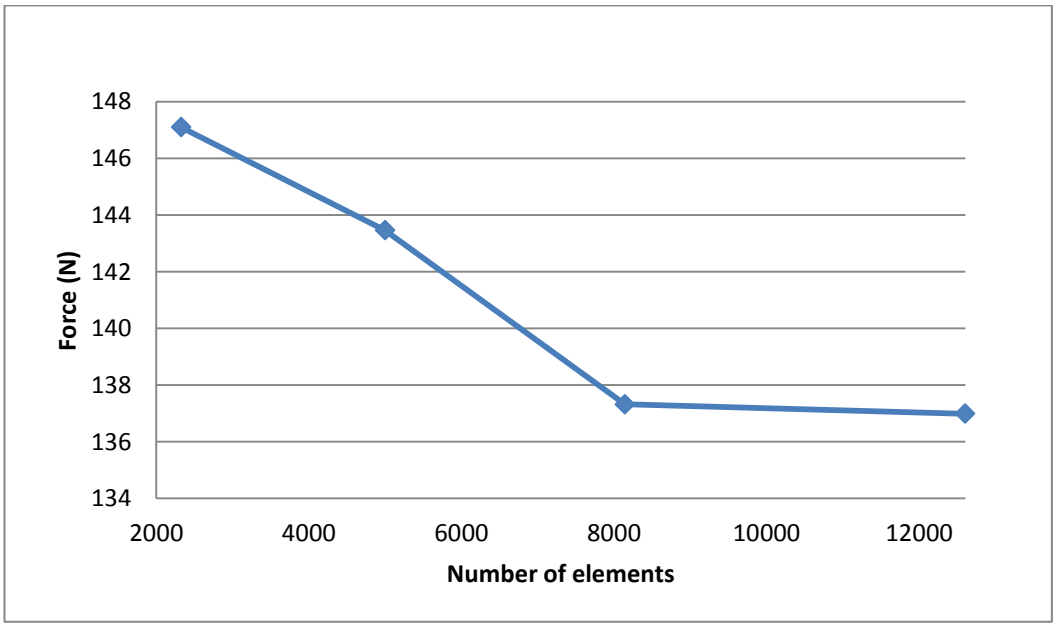

Figure 3.5: Force convergence graph - Force reaction at 0.3mm screw vertical displacement by number of elements.

The results started to converge when models had at least 8,000 elements; therefore all the models presented in this section have been meshed with at least 8,000 elements.

Concerning the influence of the distance between the screw centre and the fixed edge, the results are presented in the graph, figure 3.6.

Figure 3.6: Force reaction at 0.3mm screw vertical displacement by distance to fixed edge

As expected, it appeared that as the distance between the screw centre and the fixed support increased, the resultant force decreased. The maximum difference between 2 rows (0.8mm) was giving a force increase of 9.5%. In the main study the distance between the screw centre and fixed edge change up to 1mm. Then from the study on the distances between the screw centres from the fixed edge, a change of approximately 10% was expected due to this phenomenon of the distance between the screw centre and the fixed edge in the main study.

The influence of screw position results can been seen on figure 3.7 and clearly showed that the pull-out force varies significantly depending on the initial location of screw. A difference of 0.5mm between 2 positions (position 6.9mm and the position 7.4mm are the 2 extreme cases) generates a difference of reaction force of up to 28%.

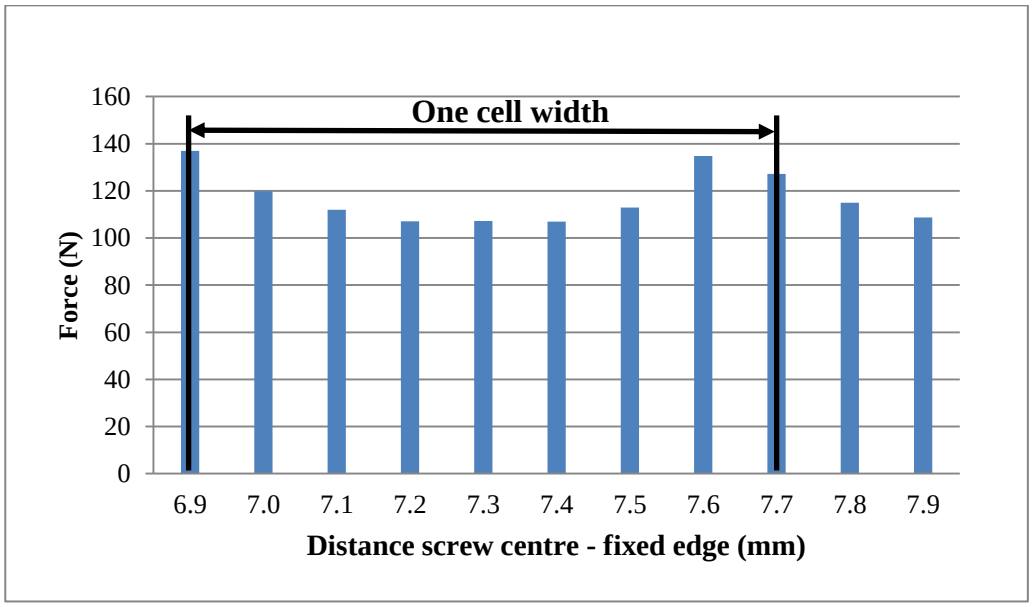

Figure 3.7: Force reaction at 0.3mm screw vertical displacement by distance to fixed edge 2D models

2D models confirmed the hypothesis about the influence of screw initial position for the pull-out force and showed the difficulties that could arise from these simulations (number of elements, contacts and high distortion of bone elements). The next stage was to check this hypothesis about the influence of the screw initial position also with 3D models.

3.2. 3D models

3.2.1. Model selection:

In this study, the cancellous bone model has been selected after tests with models from literature (Appendix A). Due to computational limitations, the cancellous bone model's size was 2.4x9.6x9.6mm. The screw model used for the simulation was again taken from a Stryker 4-mm diameter cancellous screw (Stryker item No. 604010/-100) with a pitch of 1.75mm, therefore only 1.37 pitches were inserted in the cancellous bone model. Even though it has been proved previously that the screw pull-out force is directly

proportional to the length of screw inserted (Brown *et al.*, 2011, Tencer *et al.*, 1996), a comparison test has been made in this study to confirm it. (Appendix B)

3.2.2. 3D model tested

3.2.2.1. Model Principle

The 3D model represented a cancellous bone with a screw inserted in figure 3.8. The principle was to change the screw positions to see the effects on the screw pull out force.

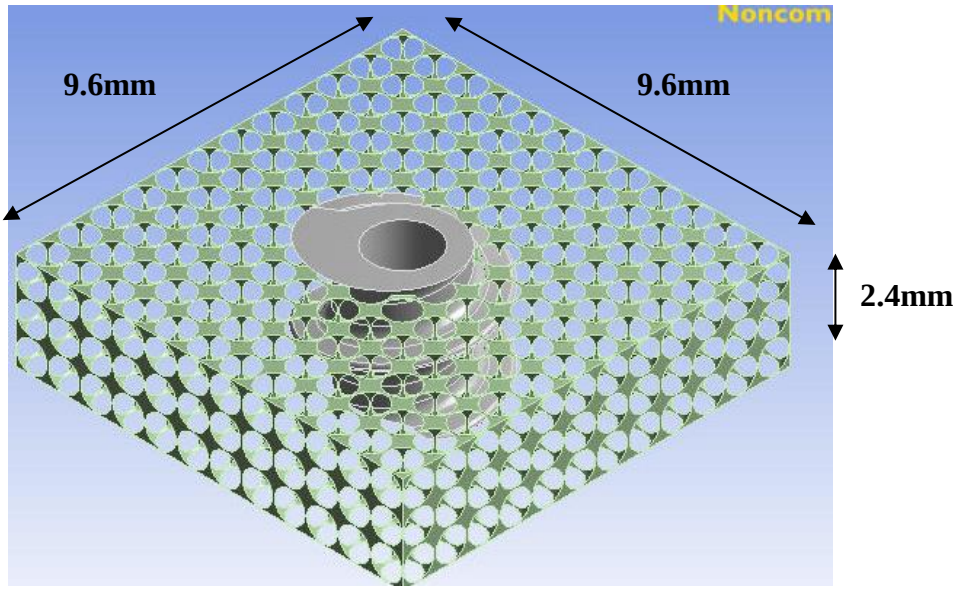

Figure 3.8: Overall view of model selected

The cancellous bone model was based on a series of 0.8mm cubes with a spherical hole of diameter 1 or 1.1mm depending on the volume fraction. These cubes were joined side by side to create a block of cancellous bone model (figure 3.9).

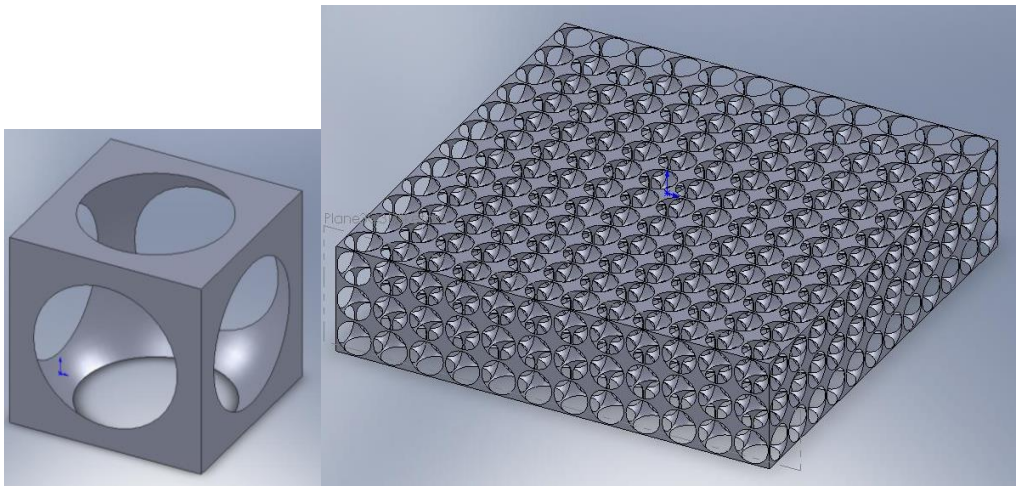

Figure 3.9:: Cubes model on the left and models assembled on the right

Five different strategic positions for the centre of the screw were chosen (figure 3.10). They have been chosen to go along the diagonal and to stop in the middle as it would be symmetrical.

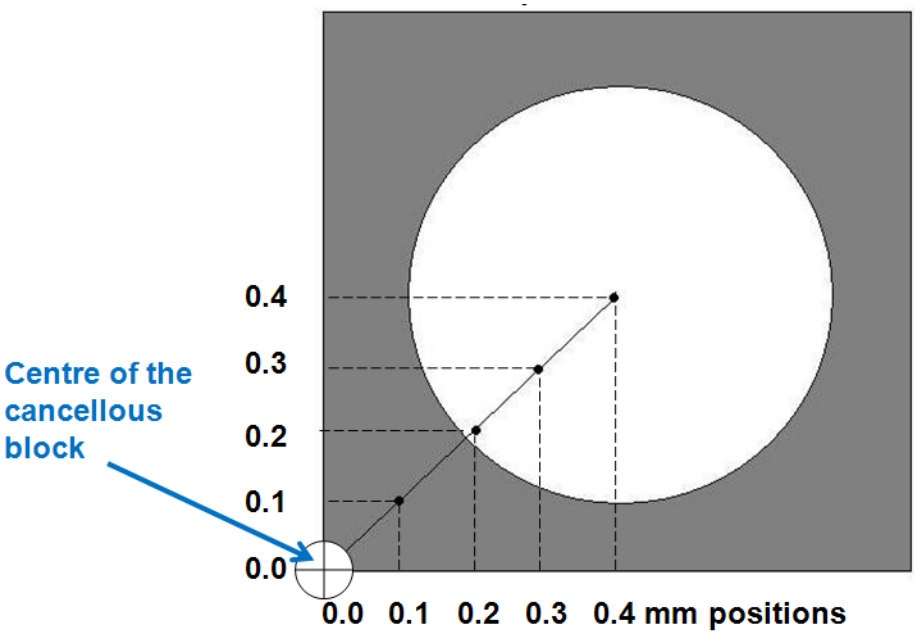

Figure 3.10: different positions for the centre of the screw

The material properties were similar to the 2D study and the sides of the bone models were considered as fully fixed while a vertical displacement of 0.5mm was applied on the top surface of the screw.

3.2.2.2. Screw position influence

The first series has been made with spherical holes of 1.0mm diameter that represented a volume fraction of 15% (figure 3.11).

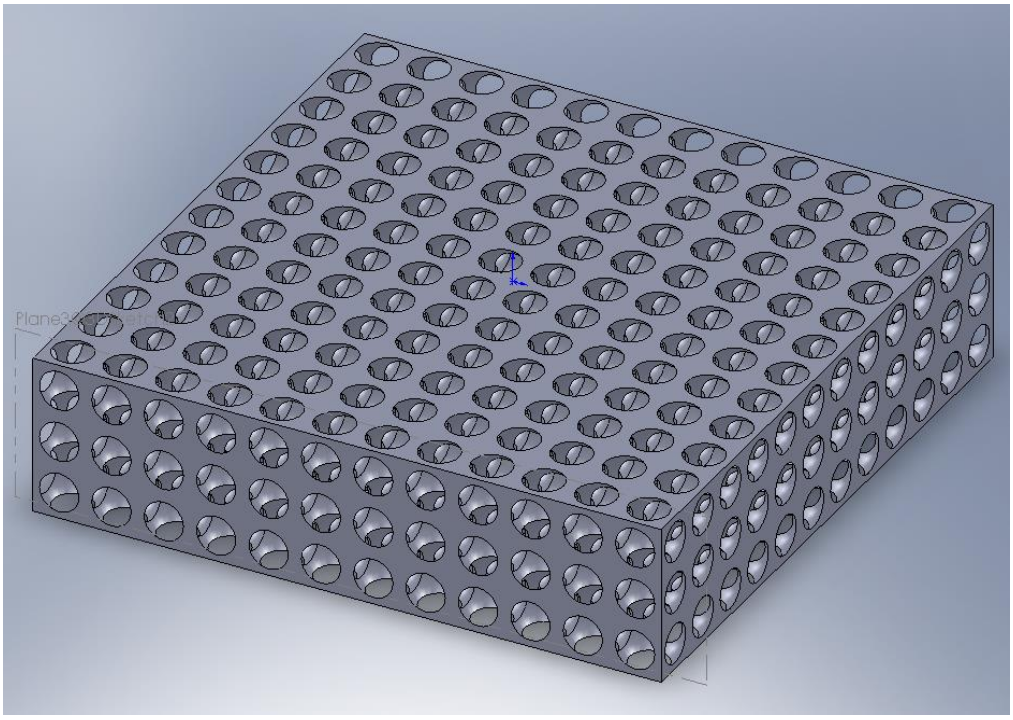

Figure 3.11: Overall view of the 3D models with volume fraction of 15.0%

The total deformation split views are shown in figure 3.12 and figure 3.13 and the graph comparing the pull-out force depending on the position is shown in figure 3.14. Two model results were missing because computer models were failing prematurely and were unable to be compared with the others but this did not affect the analysis from this model.

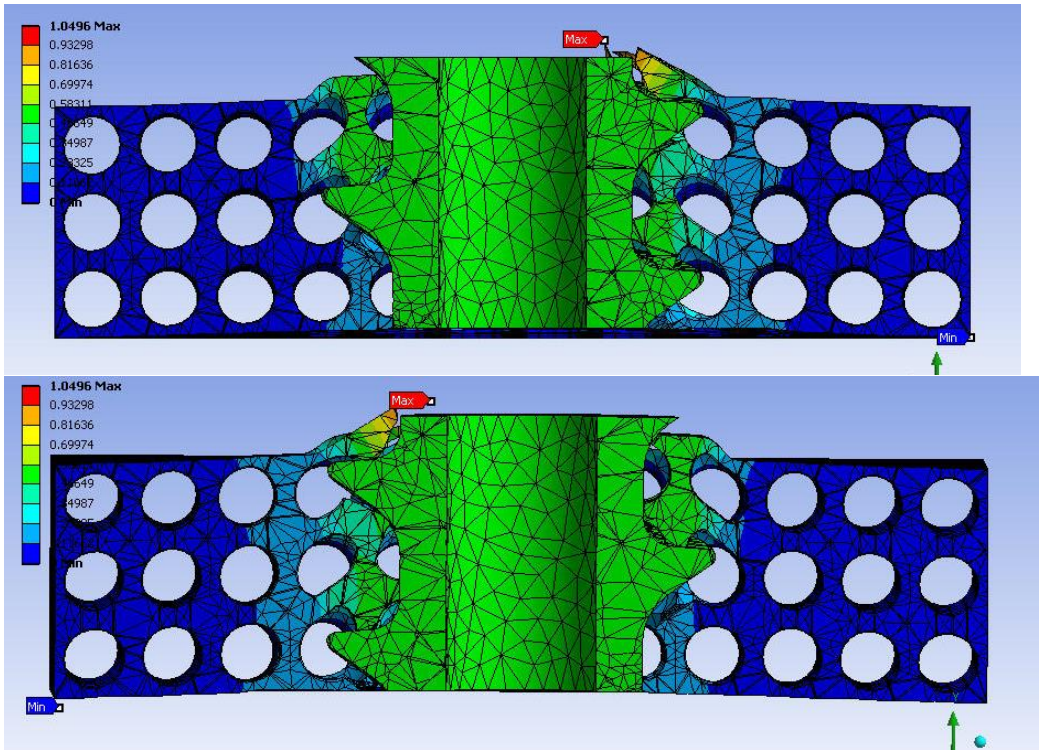

Figure 3.12: Front section view (up) and Back section view (down) of deformation at screw position 0.0 with 3D models with volume fraction of 15.0%

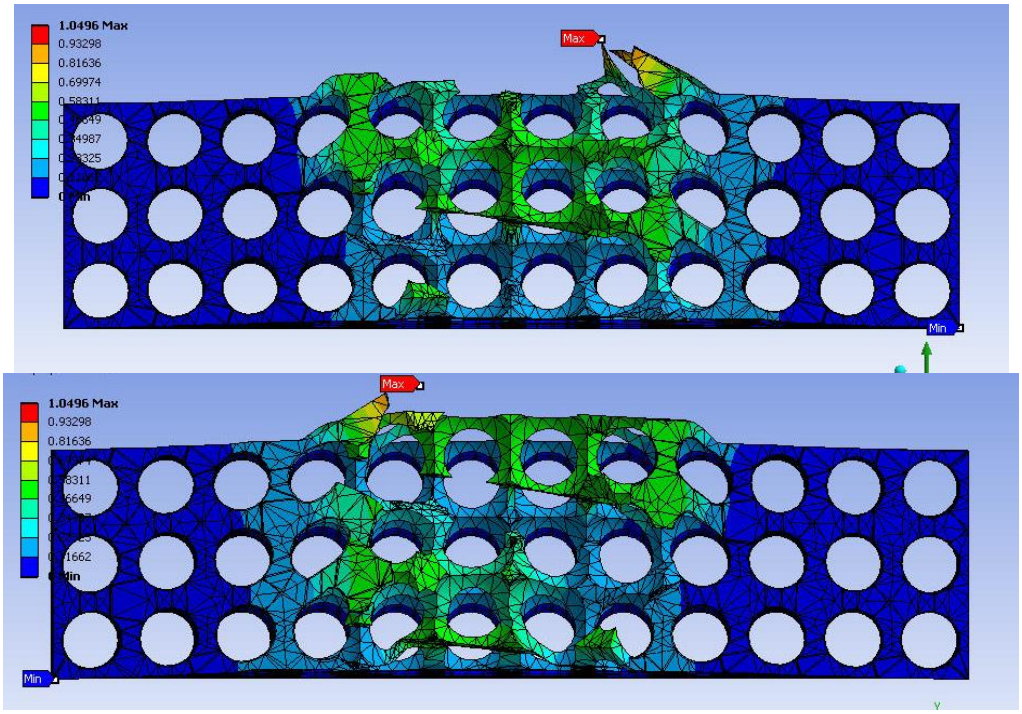

Figure 3.13: Front section view (up) and Back section view (down) of deformation at screw position 0.0 with 3D models with volume fraction of 15.0% with screw hidden

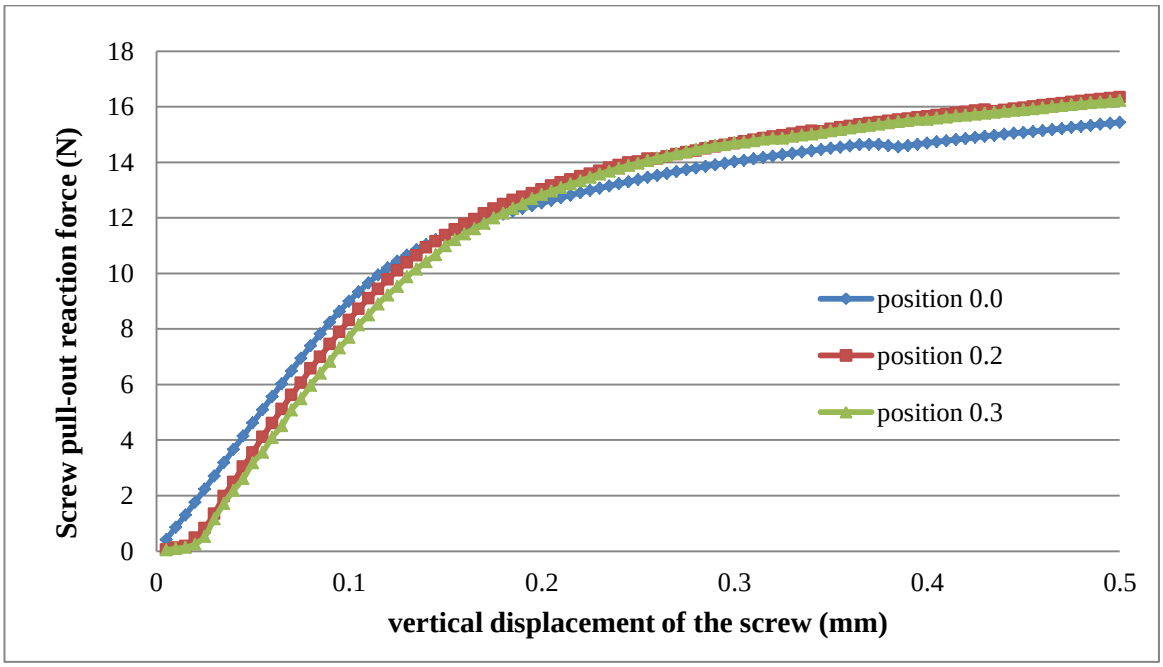

Figure 3.14: Pull-out forces depending on the screw position for 3D models with volume fraction of 15.0%.

Two main results appear from this study:

1. The variation of force reaction is much lower in comparison with 2D models (only 5%). Therefore, another test has been made to validate the idea that it depends on the screw depth inserted in cancellous bone. This model is with double length of screw threads involved in the cancellous bone was tested in Appendix B.
2. The results show a small variability between the different positions (maximum difference 6%) that could be explained by the bone volume fraction of the cancellous bone model created. Therefore, another model with a much lower volume fraction has been tested in the next section.

3.2.2.3. Bone volume fraction influence

Due to the lack of screw pull-out force difference between the different initial positions of the screw, the same simulations were undertaken but this time with spherical holes of 1.1mm diameter that represented a volume fraction of 5.3% (see figure 3.15).

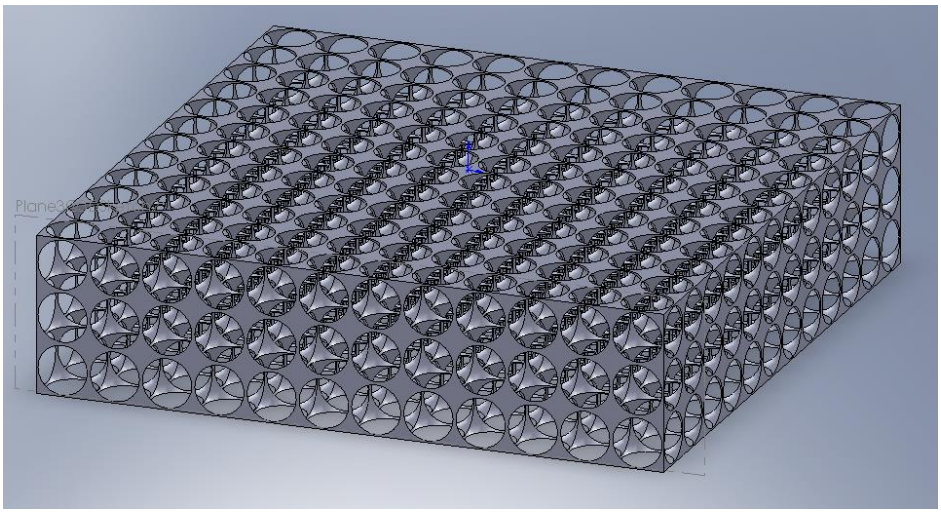

Figure 3.15: Overall view of the 3D models with volume fraction of 5.3%

Figure 3.16 show the results from the pull-out forces depending on the screw position for 3D models with volume fraction of 5.3%.

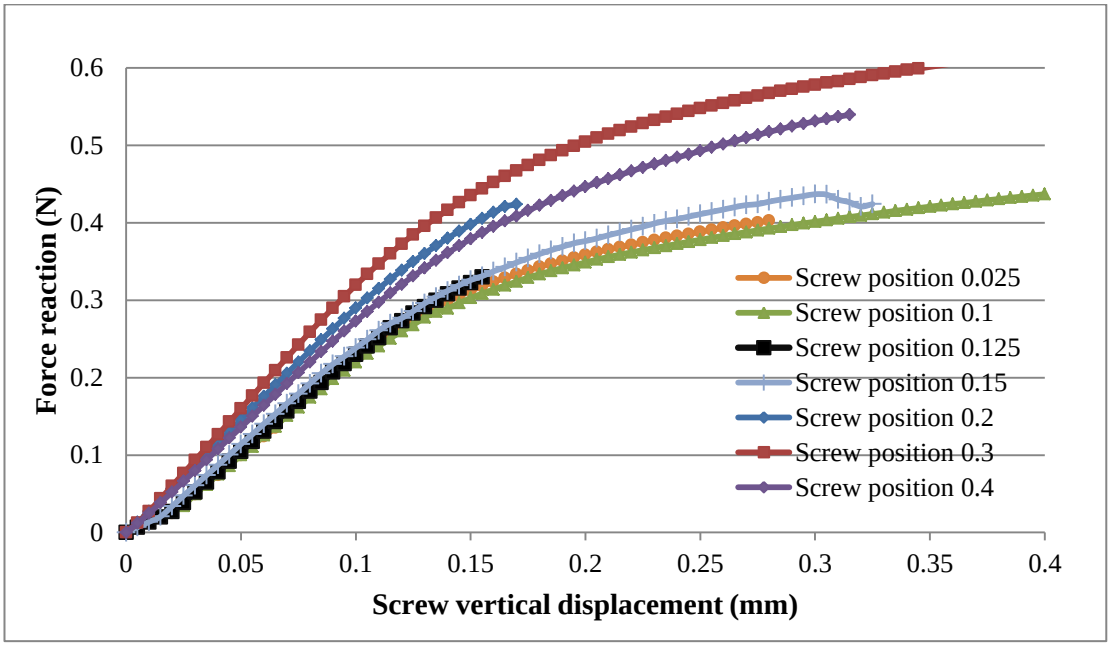

Figure 3.16: Pull-out forces depending on the screw position for 3D models with volume fraction of 5.3%

With this model, the screw pull-out force had a difference up to 30% with a difference of 0.2 mm in the initial screw position, i.e. between screw positions 0.1mm and 0.3mm (figure 3.16).

A potential relation between the volume of cancellous bone removed by inserting the screw and the pull out force was observed by comparing graph 3.17 and 3.18. It appeared that the more cancellous bone was removed by the screw the less difficult it was to pull-out. On figure 3.17, it was possible to see that the positions 0.2mm, 0.3mm and 0.4mm had the highest results for the pull-out force. Figure 3.18 showed also that the volume of bone removed at these positions was the minimum. These results were obtained by subtracting the volume of cancellous bone sliced by the screw insertion from the initial volume of cancellous bone, data provided in Ansys®. It did not seem proportional as the position 0.1mm and 0.025mm showed equivalent results for the pull-out forces while the bone removal was more important for the position 0.025mm.

Concerning the magnitude of force, Appendix B shows that the results are proportional to the screw depth and therefore in this case, the results were also in the same range as 2D models.

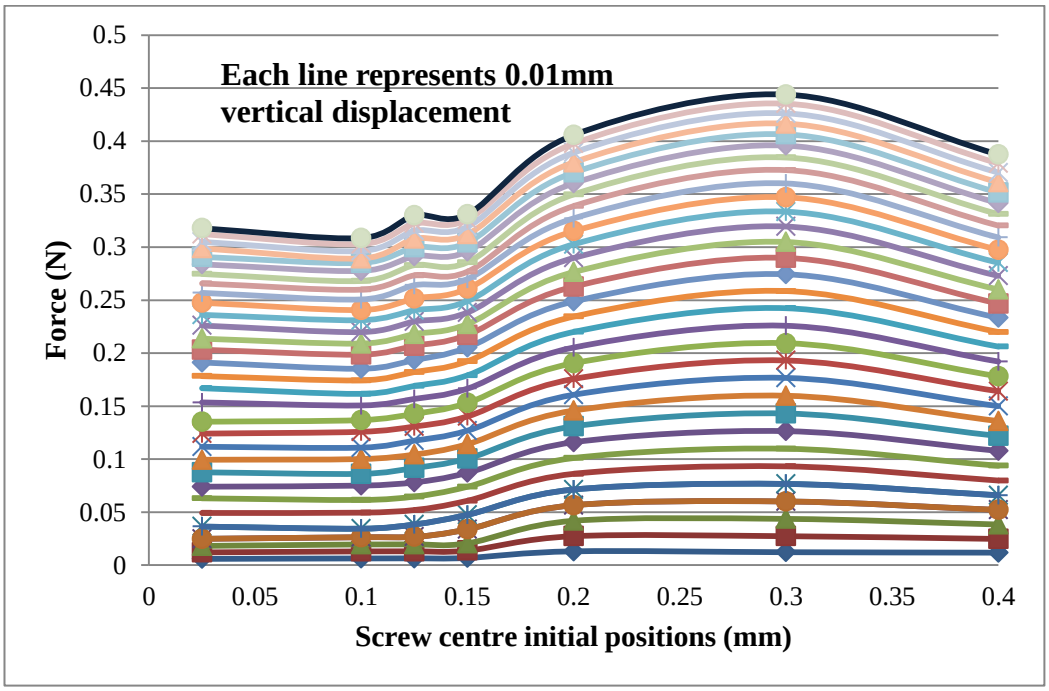

Figure 3.17: Pull-out force required for gradual vertical displacement (up to 0.16mm) of 7 screw positions (3D models with 5.3% apparent density)

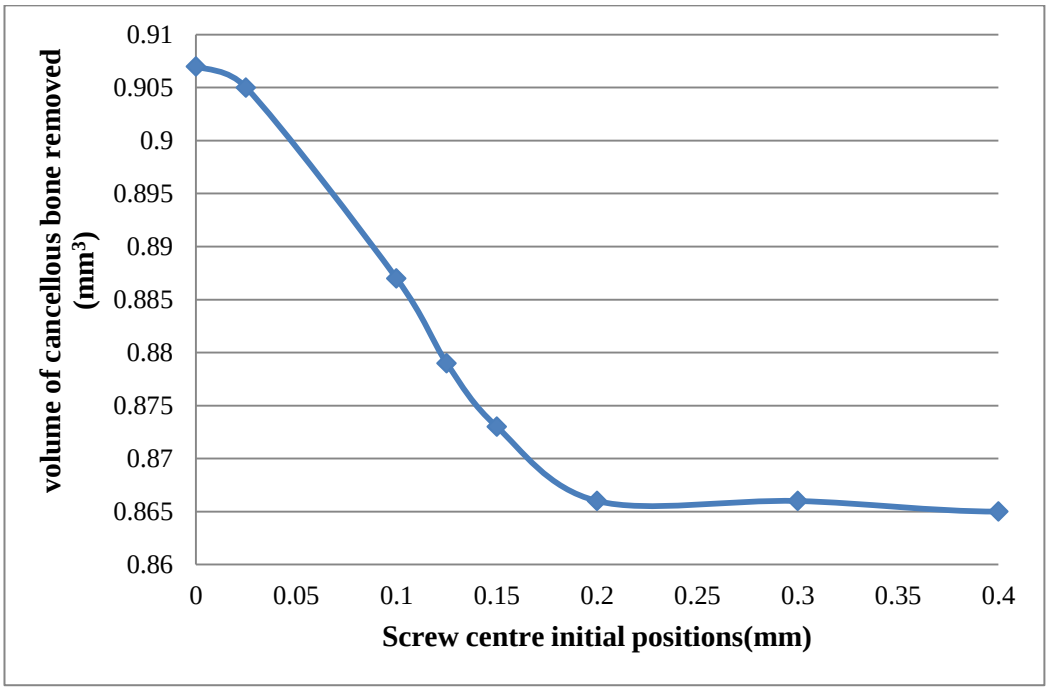

Figure 3.18: Volume of cancellous bone removed by screw positions

The deformation views are shown in figure 3.19. The problem identified with these models came from a large distortion of elements occurring at the edge, where the screw was penetrating the cancellous bone (Figure 3.20).

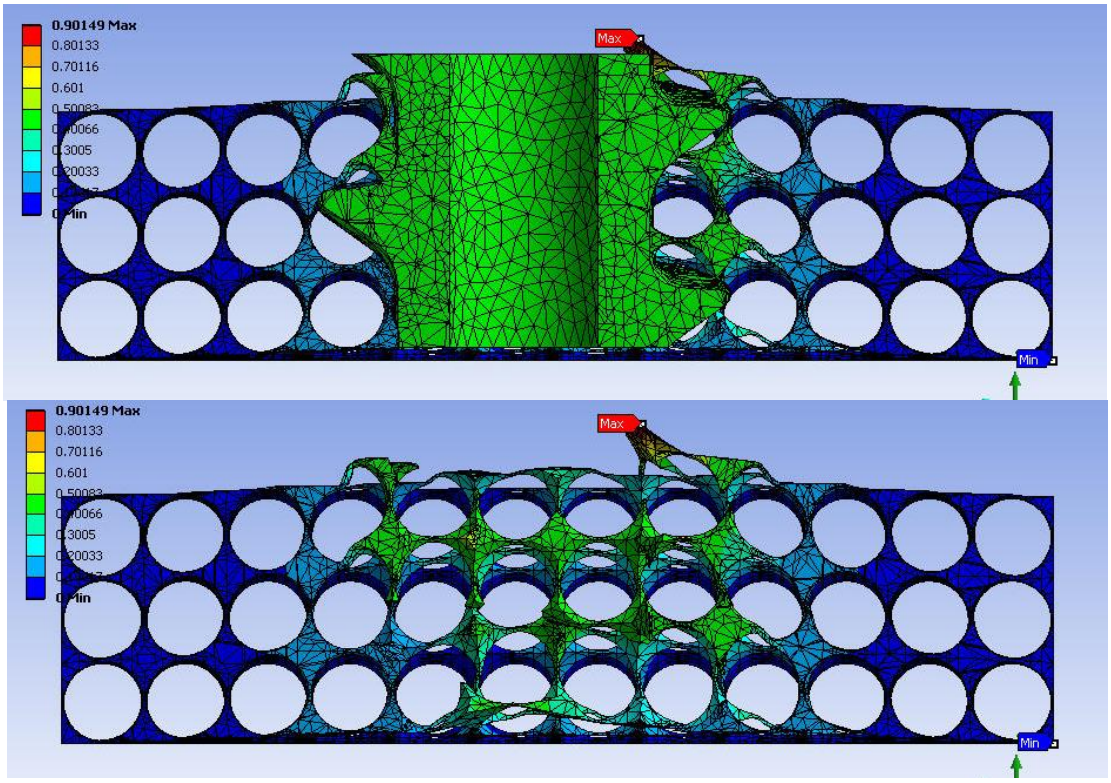

Figure 3.19: Split views of deformation of the 3D models with volume fraction of 5.3% with (top) and without screw (hidden) (bottom)

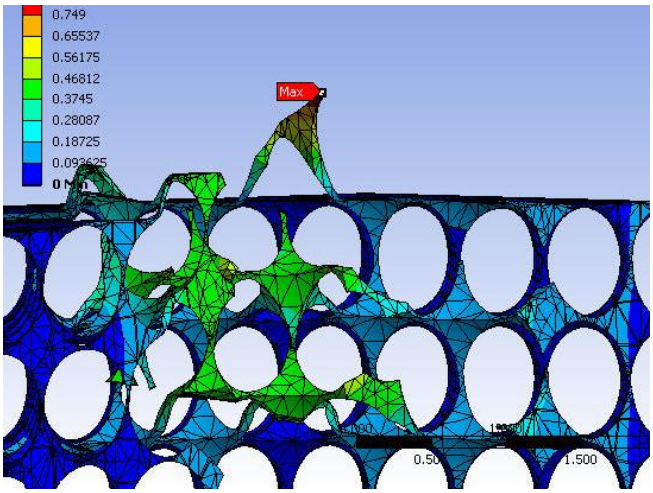

Figure 3.20: Section view of the deformation of the edge where the screw (hidden) is penetrating the bone model

From this observation, it was decided to try to simplify computationally the model by strengthening this weak point with the use of a washer as a very thin layer of bone on the top of the models. (Appendix D) This study showed

that a washer simplified the computational difficulties but also influenced strongly the results so could not be used in this study.

3.2.2.4. Augmentation influence: 3D models augmented with 5.3% apparent density bone

In order to study the effect of augmentation, a series of tests were created with bone augmentation. The principle was still the same, with different initial positions for the screw, except that a cement cylinder of 5mm diameter was added in the models with 5.3% volume fraction. The model was illustrated with total deformation views in figure 3.21.

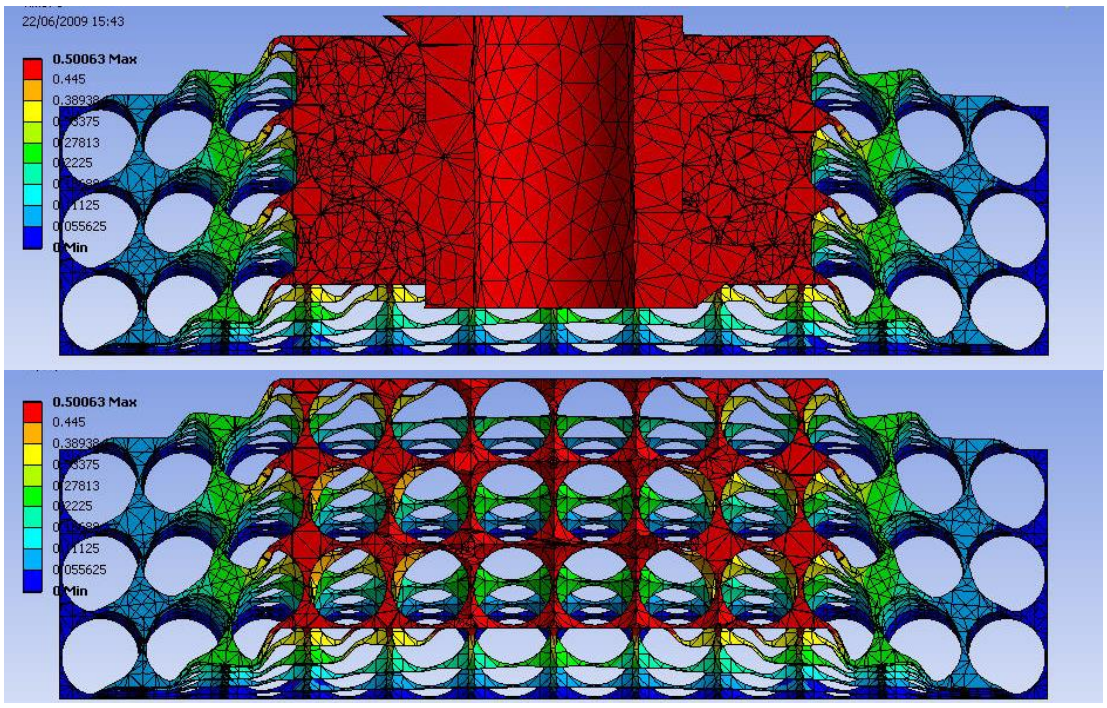

Figure 3.21: Split views of deformation of the 3D models augmented with cement diameter of 5mm with volume fraction of 5.3% with (top) and without screw (hidden) (bottom)

The results obtained showed that the bone augmentation increased the pull-out force up to 170% and the variability got extremely small (less than 1% difference) (figure 3.22).

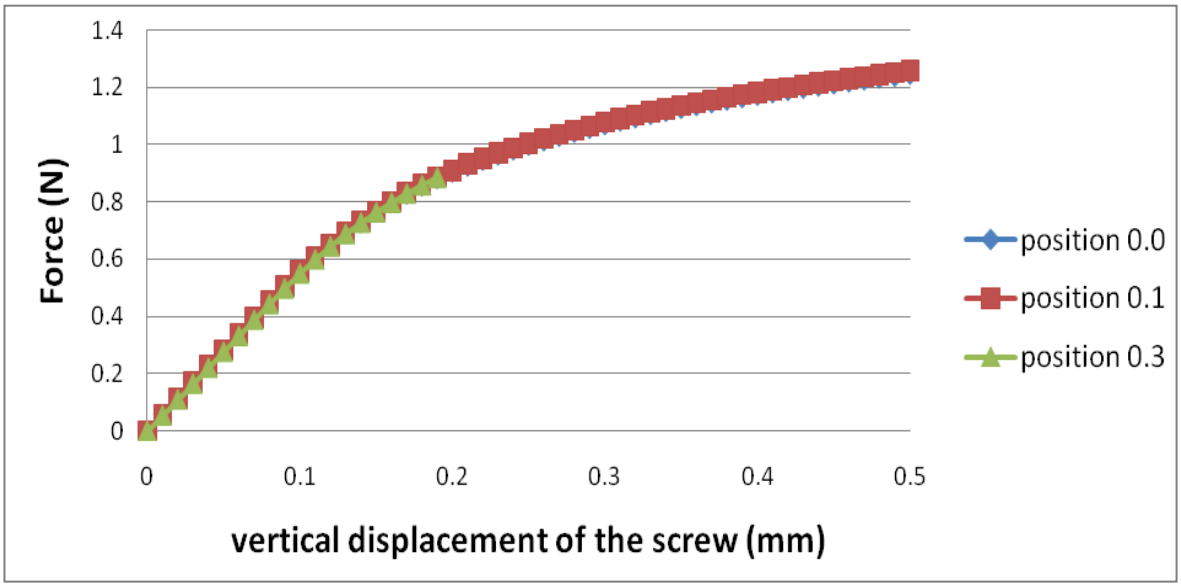

Figure 3.22: Pull-out forces depending on the screw position for 3D models augmented (5mm diameter cement) with 5.3% apparent density

The idea was then to study the influence of the cement diameters. A series of models was created in order to be able to compare the influence of the cement diameter. The diameters tested were: 3.75mm (figure 3.35), 4.5mm, 5mm (figures 3.36), 6mm, 7mm, 8mm and a conical model with the smallest diameter of 4.5mm and the biggest of 6mm at the top (figure 3.23).

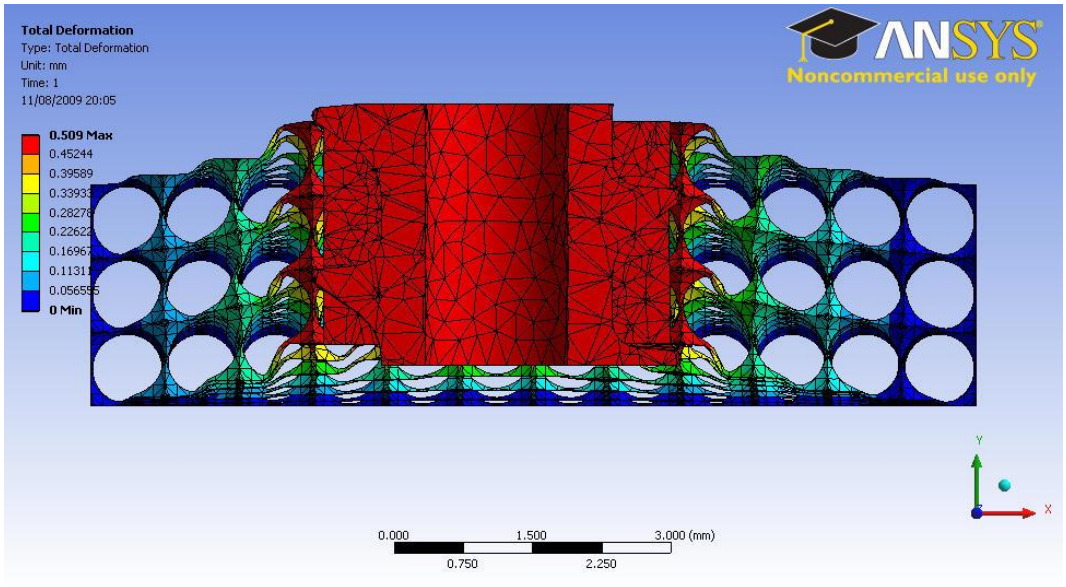

Figure 3.23: Front section view of deformation at screw position 0.4 augmented with cement of 3.75mm diameter with 3D models with 5.3% apparent density

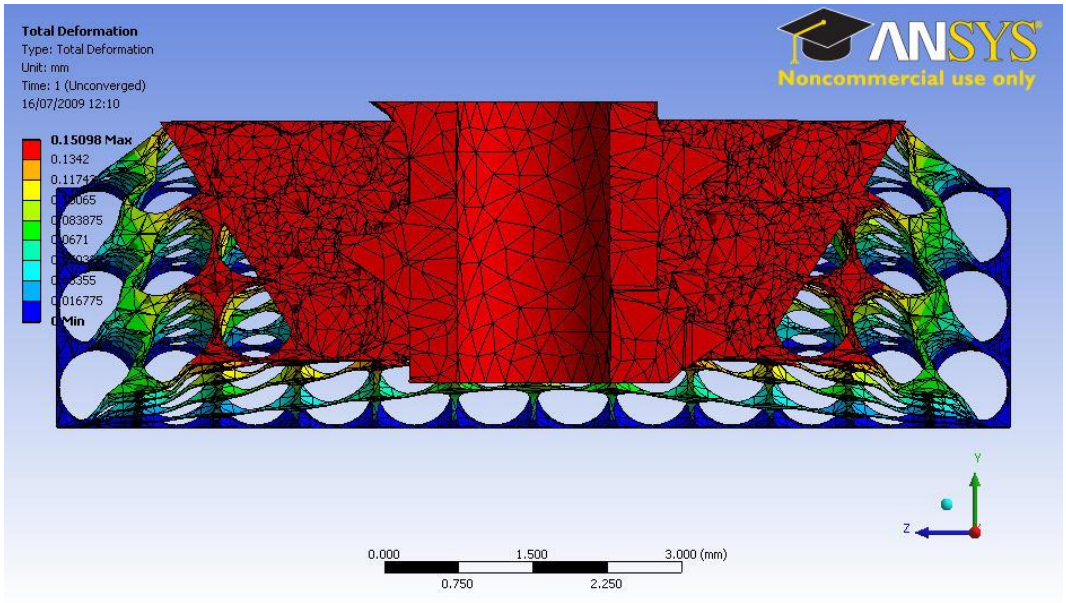

Figure 3.24: Front section view of deformation at screw position 0.4 augmented with conical cement with 3D models with 5.3% apparent density

The results showed that the pull-out force was proportional to the diameter of cement (figure 3.25), except in one case where it appears that the 6mm diameter model was stronger than the 7mm diameter model. The result

from the conical augmentation was unexpected as the pull-out force was stronger than the case of its maximum diameter, i.e. 6mm.

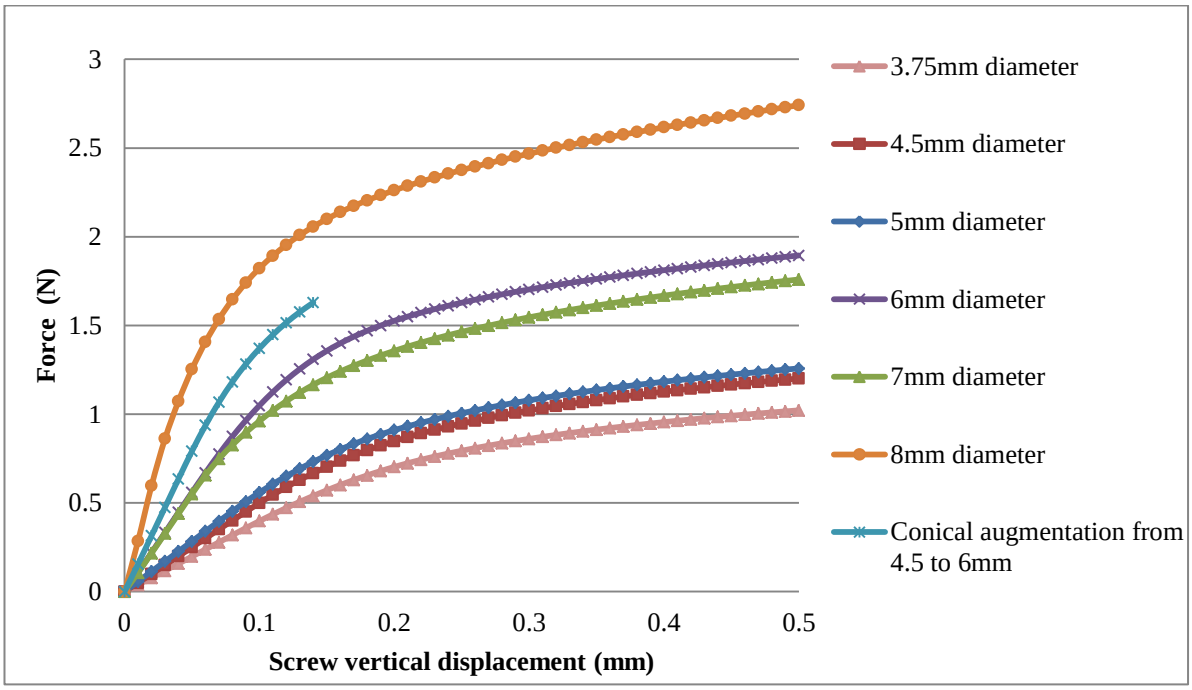

Figure 3.25: Pull-out forces depending on the augmentation volume for 3D models with 5.3% apparent density

After a comparison with the augmentation possibility in real cases, it appeared that a cement diameter larger than 5mm for a 4mm diameter screw was not realistic (figure 3.26).

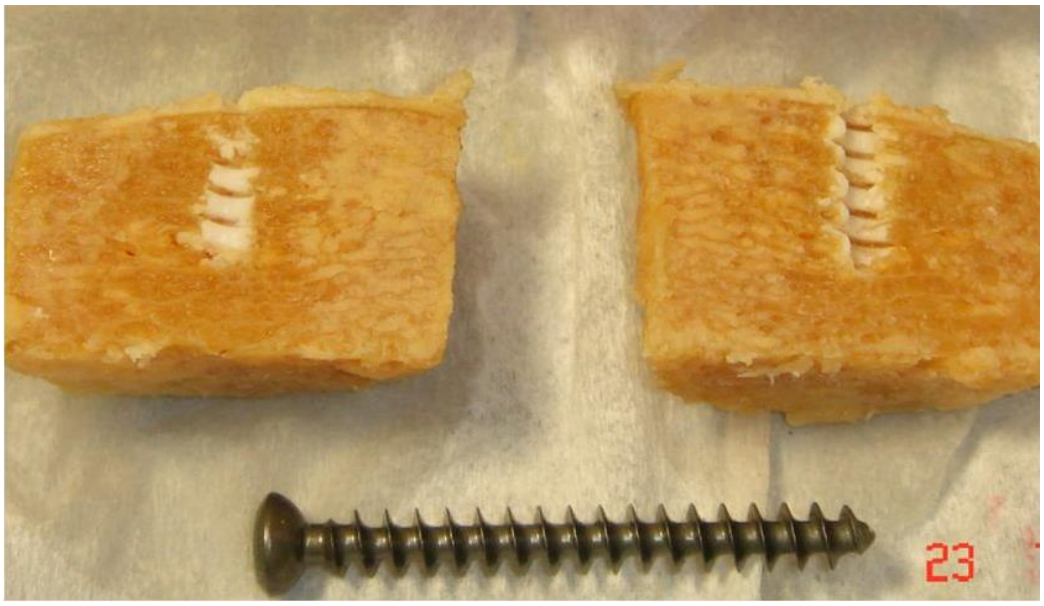

Figure 3.26: Rabbit and Human cadaver study at EPFL: No Pull-out, Example of Augmented Fill around Screw (Stryker Osteosynthesis)

3.2.2.5. Volume fraction influence

The volume fraction of the bone was observed to be significant for the pull out force. In these simulations, the model with a volume fraction of 15.0% cancellous bone was up to 33 times stronger than the one with 5.3% volume fraction (for the same screw initial position). Important factor of strength needed attention and therefore an intermediate apparent density cancellous bone model was created with a volume fraction of 10%.

The stiffness results from the model with 10% volume fraction are presented in figure 3.27 and 3.28.

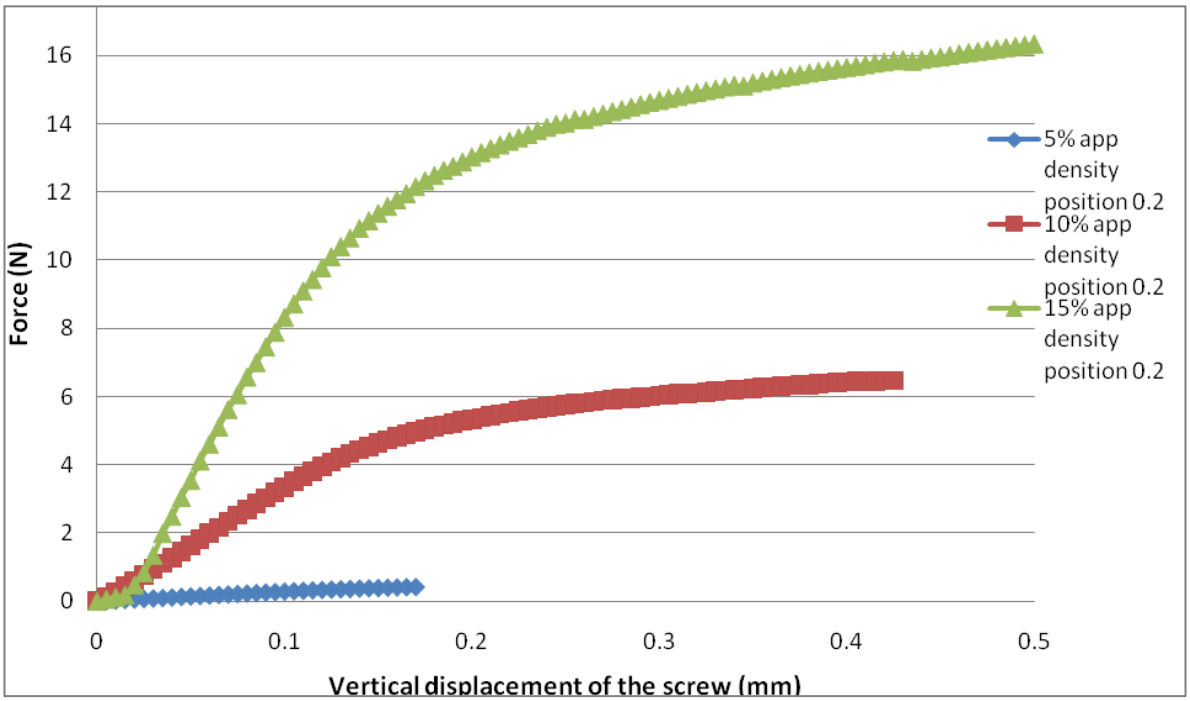

Figure 3.27: Pull-out forces depending on apparent density with 3D models

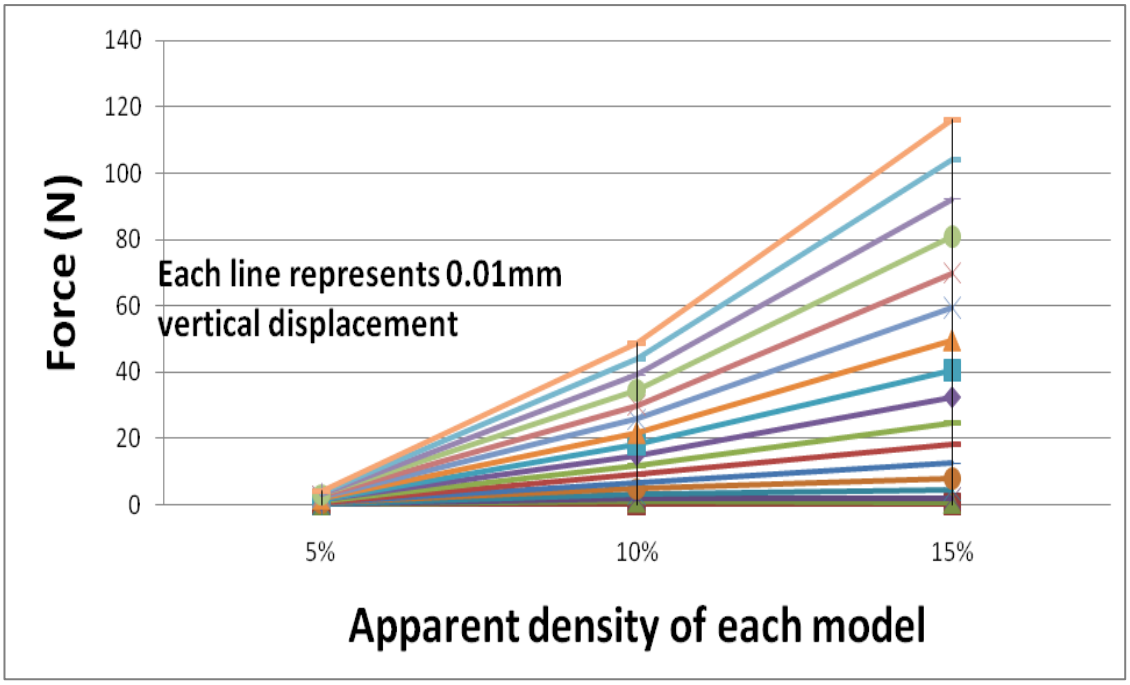

Figure 3.28: Pull-out force required for gradual vertical displacement (up to 0.17mm) of 3 different densities

The results show that bone apparent density is the most important factor affecting the pull-out force reaction. From figure 3.28, the results seemed to represent an exponential or a power relation between the apparent density and the screw pull-out force.

3.3. Conclusion

From these studies, it was possible to conclude that the influence of the screw initial position in cancellous bone was proved with 2D models with difference of results of up to 30% for the screw pull-out.

From the 3D models, it showed again that the screw initial position influences the pull-out force only with the cancellous bone model with 5.3% apparent density. Concurrently, it appeared that the most important factor concerning the pull-out force was the density as the holding power of the screw was 33 times stronger in the model with 15% apparent density compared to the model with 5.3% apparent density. Also, the intermediate model (apparent density10%) showed intermediate results.

The augmented models with 5mm diameter cement showed a significant improvement of the screw holding power (almost 2 times) and also an important diminution of the variability of the pull-out force due to the screw initial position.

All these results confirmed and highlighting the phenomenon in the initial hypothesis, which was about the effect of screw initial position, the augmentation effects and the apparent density influence. As they are only simulations with many simplifications, it was important to validate these results. The next chapter will show a review of the possibilities and the direction selected.

4. Chapter 4 - Processes investigated for validation of FE results

So far, cancellous bone has been represented as a structured model. These models were designed as 0.8mm cubes side by side with spherical holes inside with a diameter bigger than the cube size. The size of the entire model was 9.6mm x 9.6mm x 2.4mm. This diameter has been set in such a way that the volume fraction of the bone varies between 5%, 10% and 15%, with the 5% model only showing variability due to the screw position. Questions that therefore arise with this investigation are: Are the models sufficient for modelling cancellous bone? How accurate are they in the representation? FE models cannot be accepted alone, and they have to be compared with other studies in order to be validated (Dobson *et al*., 2006). Therefore, in this chapter different methods are reported for the investigation of validation of FE results. The first one is to compare FE simulations with screw pull-out from cadaver bone, while the second is to compare FE simulations with mechanical tests from RP models. This chapter represents the investigations undertaken in order to solve the challenges that arose along each process.

4.1. Comparison with mechanical tests

The first option considered was to compare the screw pull-out test from a cadaver bone with FE simulation created from this mechanical test. The ability to scan cancellous bone at different stages and then create models from these scans allowed a comparison to be made. The comparisons of FE simulations from these models with mechanical tests validated the FE results while simultaneously offering the possibility to test other aspects such as screw position, augmentation and screw design in models from real bone.

Numerous cancellous bone samples would be ideal for statistics and also to compare bone architecture effect. This process is schematically shown in Figure 4.1.

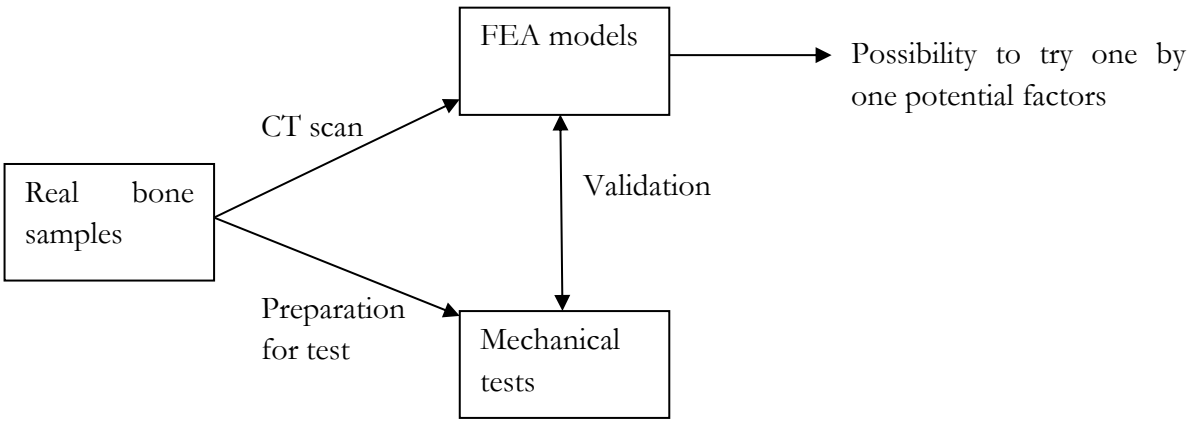

Figure 4.1: Comparison with mechanical test process.

One of the difficulties that arose was the ability to obtain cancellous bone samples that could be tested and scanned in the same place. FE modelling from scans is a challenging process and at the beginning, only one model from real cancellous bone was modelled. As a trial for this process, the first cancellous bone sample was a cube with dimensions 5x5x5mm as STL and it has been treated using Geomagic Studio in order to export it as a solid body to Ansys® Workbench. The process used with Geomagic Studio has been summarised in Figure 4.2. The problems observed with this software were that it was mainly time consuming with most of the stages requiring a significant amount of manual effort. Visualisation of the problematic areas were difficult and would be even more with a larger sample and finally many modifications have been applied to the bone sample (spikes have been removed and the whole structure has been smoothed) so it has been decided to use another software: Mimics.

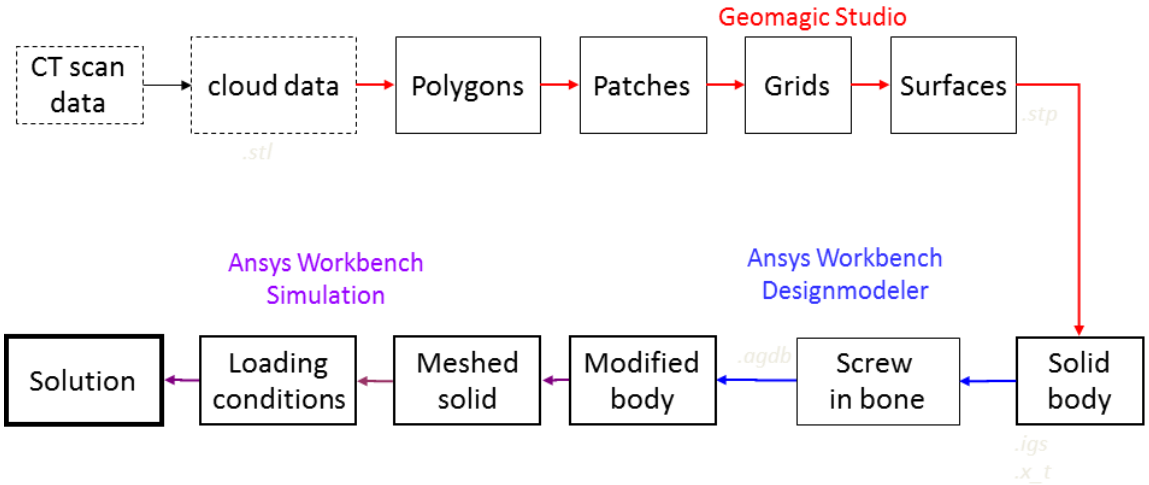

Figure 4.2: from images to FE with Geomagic studio and Ansys® Workbench.

Geomagic Studio is mostly designed for the creation of solid body for CAD purposes. At this stage, it was a trial for the feasibility of the creation of a FE model from a cancellous bone and despite the success, the Mimics package set has been preferred finally and the detailed procedure is explained later on this chapter.

4.2. Rapid Prototyping (RP)

Another option considered was to use Rapid Prototyping (RP). A review of previous studies using RP representing cancellous bone for the validation of mechanical tests or FE analysis is shown later in this section. This validation technique could be used in the project at 2 levels.

The first one could compare and validate screw pull-out test results from scaled real bone FE models, with mechanical tests on scaled RP of real bone models.

The second stage could be for the validation of the screw pull-out test on scaled FE results from simplified bone geometry.

Use of RP representing cancellous bone for validation of results has been studied by numerous researchers (McDonnell *et al*., 2009, Cosmi and Dreossi, 2006, Su *et al*., 2007, Woo *et al*., 2010, Ulrich *et al*., 1980, Dobson *et al*., 2006, Jones and Hench, 2003). In all these cases, the prototypes have been scaled up because of the limitation of the actual RP machine. At the moment, the most accurate RP process can have an accuracy of 0.1mm, which represents an average trabecular strut diameter (Rincon Kohli, 2003).

All these models have been created with solid free form machine: stereolithography (STL) (Dobson *et al*., 2006), selective laser sintering (SLS) (McDonnell *et al*., 2010) or fused deposition modelling (FDM) (Su *et al*., 2007). These machines offer varying degrees of accuracy, according to the technical specifications provided by Materialise for each technique:

- standard STL layer thickness: 0.1 – 0.15mm
- SLS standard accuracy: ±0.3mm with minimal wall thickness: 1mm with living hinges possible at 0.3mm
- FDM layer thickness: 0.13 – 0.25mm

Thus, from these accuracies it is necessary to scale up the models and scaling varies from 10:1 from McDonnell *et al*. (2010) up to 18:1 by Cosmi and Dreossi (2007).

Compared to FE models this process is also limited by the computational power that requires the analysis of the sample of real bone. Therefore, the samples usually used are small and vary from 1.7x1.7x1.7 mm (Su *et al*., 2007) up to 4.5x4.5x25mm (McDonnell *et al*., 2010).

The screw pull-out study from RP cancellous bone would be a novelty as previous studies are mainly concerned with different ways to compress the samples. However, some studies are relevant concerning the validation process and the testing set up.

McDonnell *et al*. have investigated the mechanical interaction of the trabecular core with an external shell using rapid prototype and finite element

models. In their study, they focused on the interaction between the trabecular core and cortex: the stiffening provided by the shell. For that purpose, they created models from SLS from µCT data (using Mimics software) and compared mechanical results in order to find a corrective factor between the real bone's mechanical compression and the RP models created. Therefore, they created new RP models with different shell thickness and analysed its influence. This study compared twenty ovine bones to seven RP models, with focus on the ultimate strength effects. In a second part, the models have been thinned in order to simulate osteoporosis effect (surface erosion), which would be relevant for this study.

Dobson *et al*. (2006) created 3D stereolithography models of cancellous bone structures from µCT data in order to test and validate finite elements results. The models were scaled up from $4mm^3$ samples to $55mm^3$ RP models (13.75 times) with a built resolution of 0.3mm (STL machine used). The samples were from the iliac crest, the femoral head, and two lumbar vertebrae locations (L2 &L4). Compression tests were repeated twenty times and compared to FE results of scaled up bones with STL resin properties in order to compare stiffness. The variance between mechanical tests and FE prediction results was around 6% in this study.

Williams (2000), Jones and Hench (2003) and Quadrani *et al*. (2005) have completed reviews of other existing options for the creation of bone models. However they did not validate any test to include the regeneration of bones. Instead they treated the different processes needed and the different materials available. Both studies ended with the process using a RP mould for the ceramic or bioactive glass. Quadrani *et al*. explained that the porous structure of ceramics can overcome the lack of accuracy of RP machine to create a realistic model. It would have been a relevant option due to the material used but at the time, this process was only theoretical and the porosity of the ceramic was not manageable.

In the Engineering and Design school of Brunel University, there is access to a 3D printer which was using the FDM process. Three versions of the simplified geometry model with an apparent density of 5% (figure 4.3) have

been attempted with the machine: 1:1, 4:1 and 10:1 because the smallest wall thickness for this model is 23µm which represents a challenge for classical RP. Figures 4.4 and 4.5 show the RP obtained for scales 4:1 and 10:1 respectively.

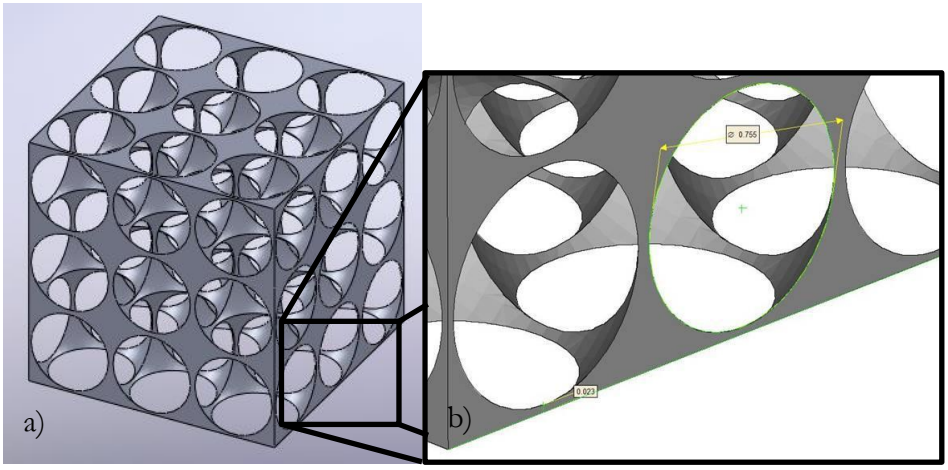

Figure 4.3: a) Simplified geometry model tried in RP machine based on the structure of the simplified cancellous bone that has been modelled with 5% volume fraction and dimensions 2.4x2.4x2.4mm cube. b) Zoom on problematic edges

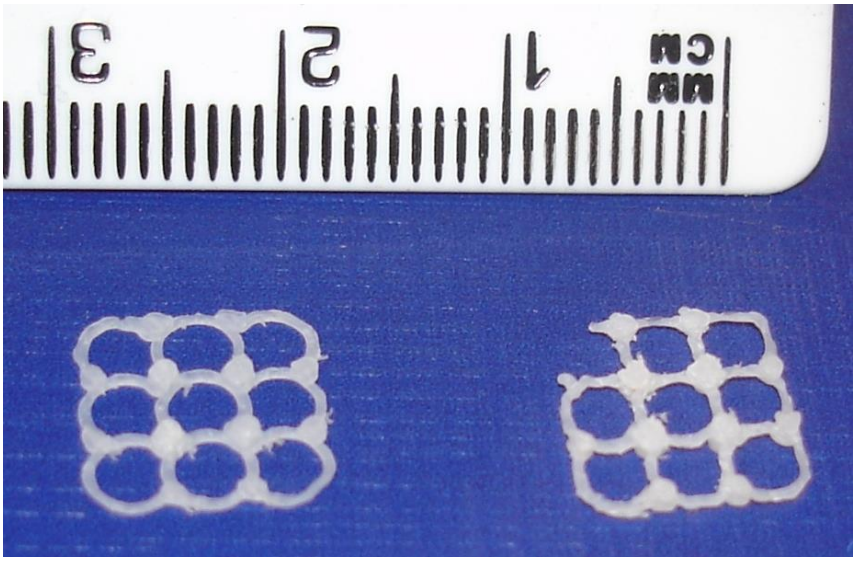

Figure 4.4: RP model at the scale 4:1. The walls are as thin as the minimum layer of the machine: No details of the structure could have been represented and the model is split by layers.

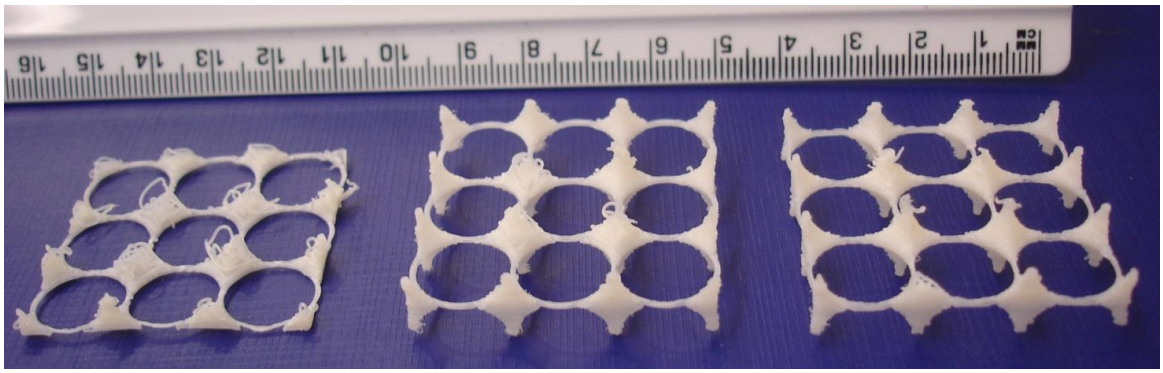

Figure 4.5: RP model at the scale 10:1. The model is still split by layers but more details are noticeable. The model failed where the wall are the thinnest vertically.

Two models have been created, one from a real bone model and the second from a simplified geometry bone model both with an apparent density of 20% and with a scaling ratio of 10:1. These models have been built using Brunel University facilities (figures 4.6, 4.7 and 4.8) in order to compare FE simulations and mechanical tests.

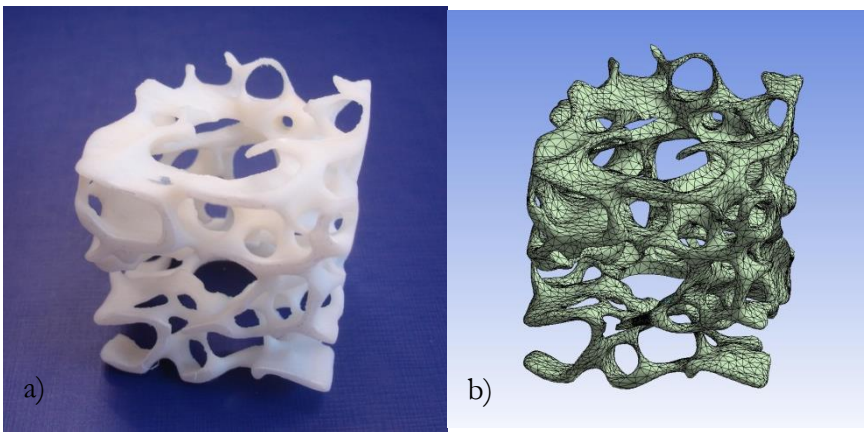

Figure 4.6: a) RP model and b)FE model from real bone. Volume fraction 20%. Scale 10:1.

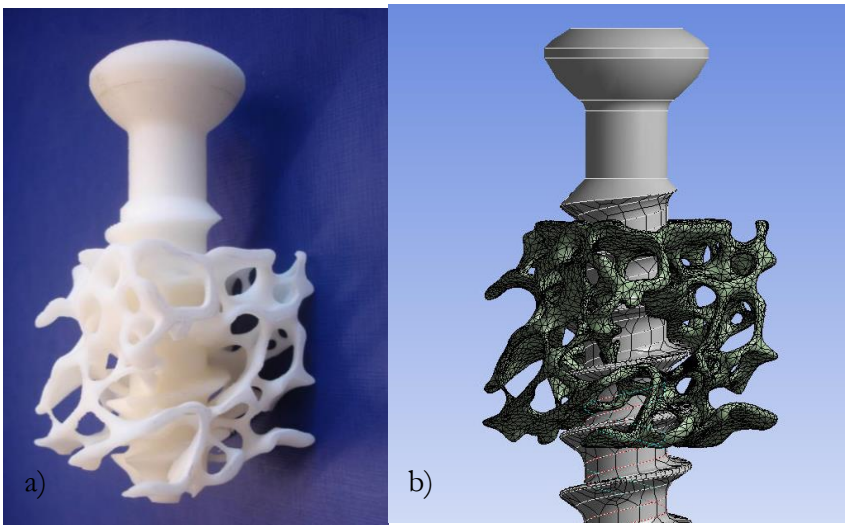

Figure 4.7: a) RP model and b)FE model from real bone with screw. Volume fraction 20%. Scale 10:1.

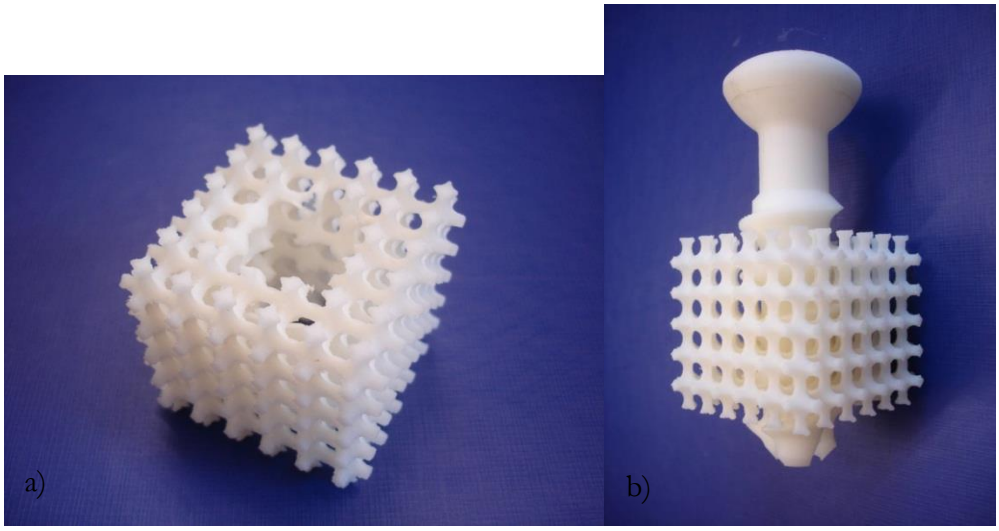

Figure 4.8: Simplified bone model RP. Volume fraction 20%. Scale 10:1.a) without screw. b) with screw inserted.

In order to simplify the different stages, it would be recommended to choose the same scaling for the 2 possibilities of validations in order to create a unique metallic scaled screw for the tests. Therefore on one hand the cancellous bone could be scaled bigger than 10:1, which on the other hand the simplified model could be modified in order to have more realistic trabecular size.

From the different comparisons between FE results and RP mechanical tests met in the literature, the easiest way to avoid the issues from the scaling is

to represent the FE models scaled and with the appropriate materials property (Dobson *et al*., 2006).

None of the referenced studies described the effects of scaling with comparison with real size models. Therefore, a study on how scaling affects results has been made with continuum models.

Compression tests between two parallel plates and screw pull-out tests have been completed on FE simplified bone models with an apparent density of 5% at 3 different scales: 1:1, 4:1 and 10:1. Figure 4.9 shows results of the compression tests.

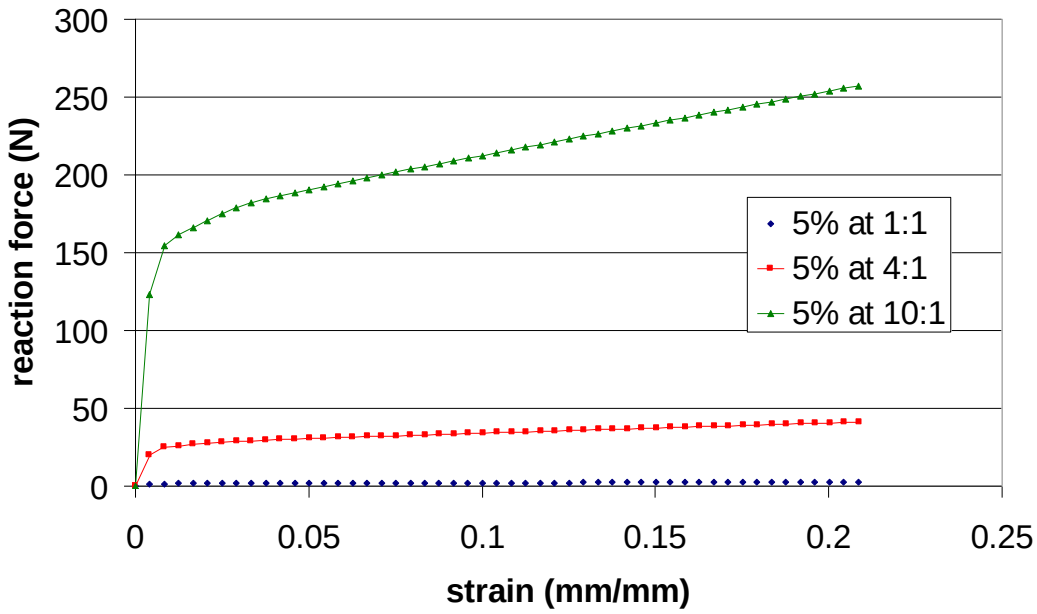

Figure 4.9: Reaction forces from compression with simplified bone models with 5% apparent density at 3 different scales.

The results appear to be directly proportional to the square of the scaling ratio. For example: 4:1 results = 4^2x 1:1 results or 10:1= 10^2 x 1:1 results. Figure 4.10 shows the same results with the correction factor from scaling applied.

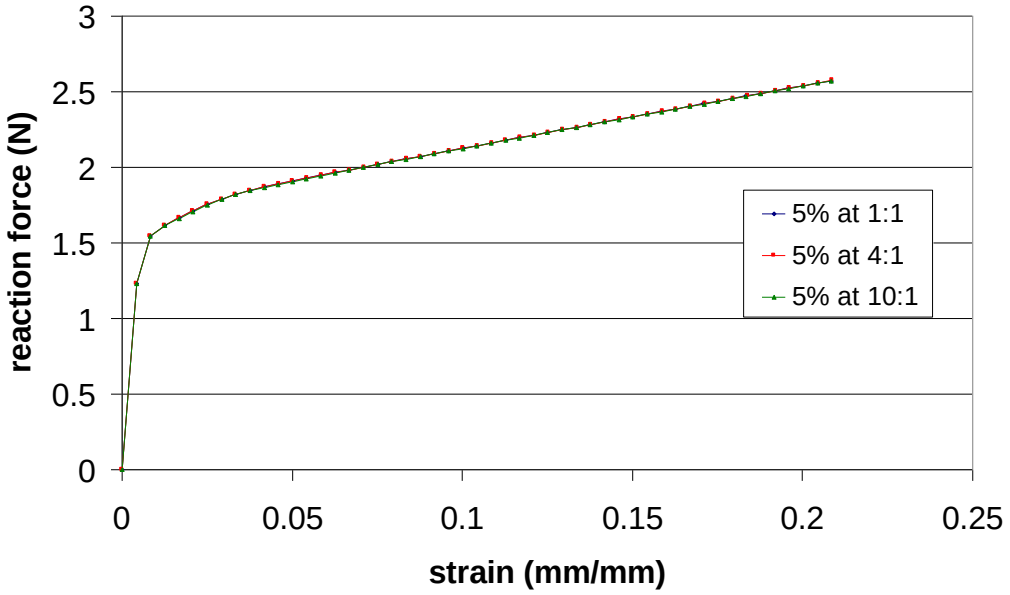

Figure 4.10: Reaction forces from compression with simplified bone models with 5% apparent density at 3 different scales with scaling correction.

.

The graph confirms that the results are directly proportional to the square of the scaling ratio, i.e. the area.

A screw pull-out simulation has been scaled as well and gave similar results, figures 4.11 and 4.12.

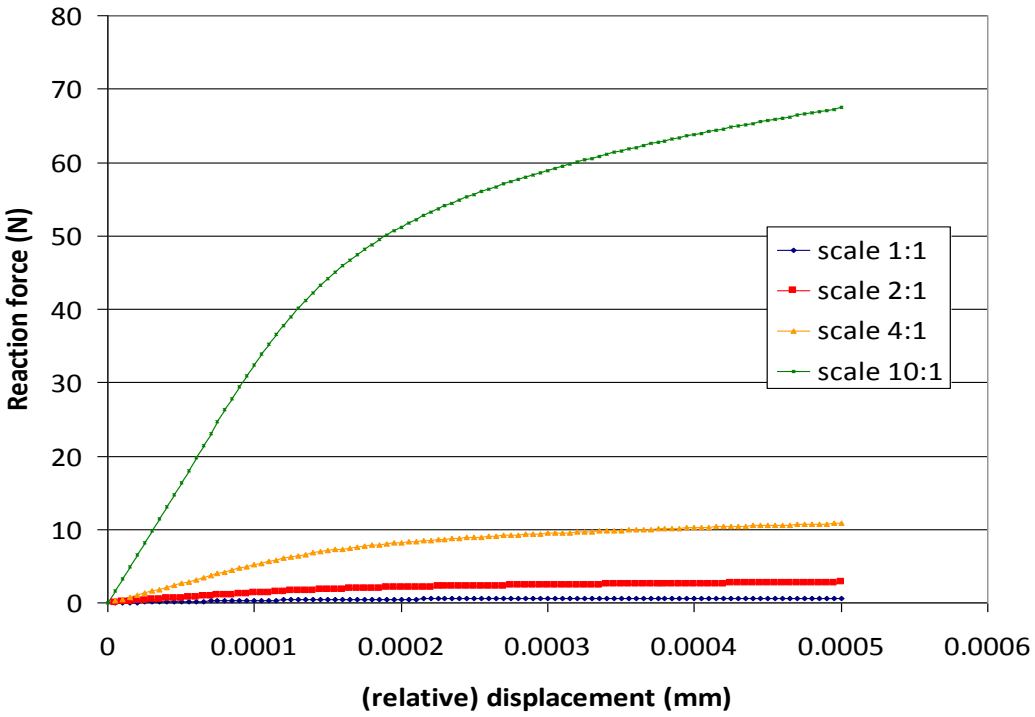

Figure 4.11: Screw pull-out force with simplified bone models with 5% apparent density at 4 different scales.

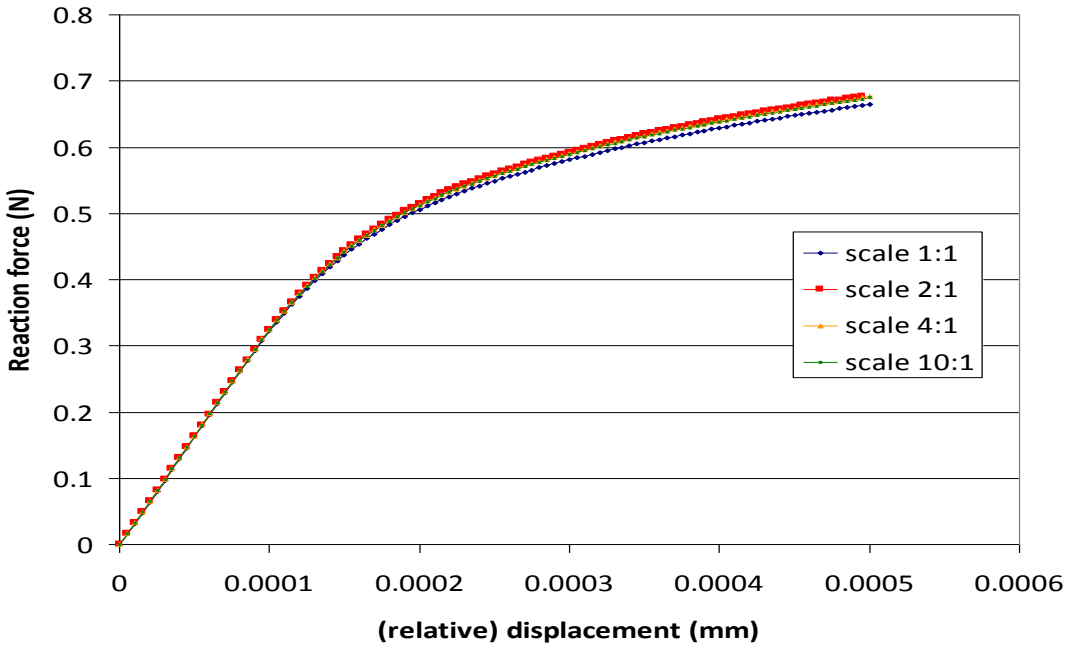

Figure 4.12: Screw pull-out force with simplified bone models with 5% apparent density at 4 different scales with scaling correction.

The study on scaling effect for compression and screw pull-out tests shows that it can be solved with the correction factor which is the square of the scale factor, preventing scaling models from becoming an issue.

The principle of the FDM process is a filament of ABSP400 that is melted and deposed with precision in order to create the prototype wanted as illustrated in figure 4.13.

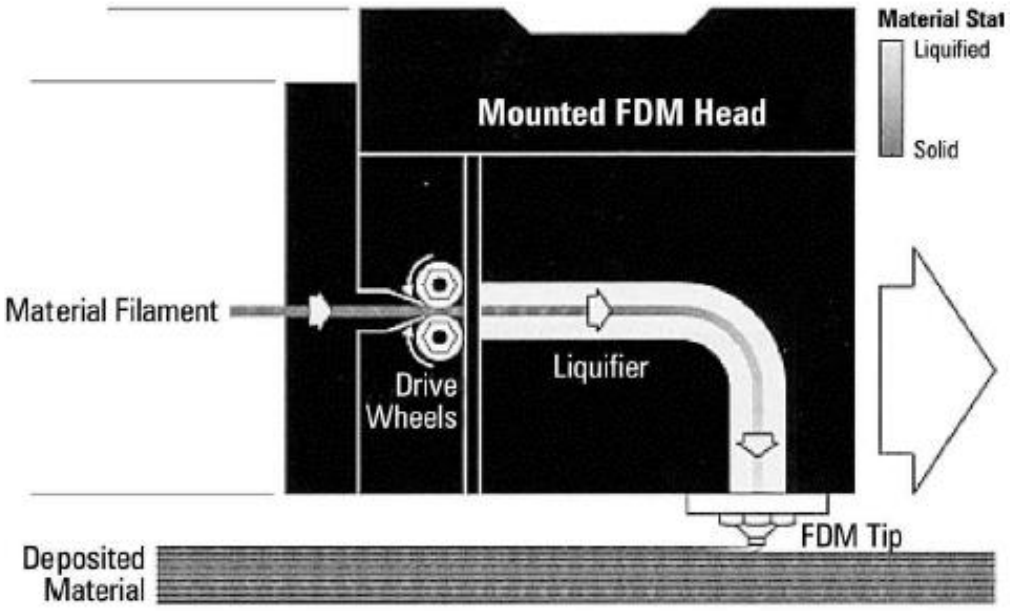

Figure 4.13: FDM process (Ahn et* al.*, 2002)

Ahn *et al.* (2002) looked at the consequences generated from the building process, one of which is the anisotropic material property dependence on the building method. Figure 4.14 are sketches showing how an identical simple structure can be built in two different ways with two microscopic views of the two examples.

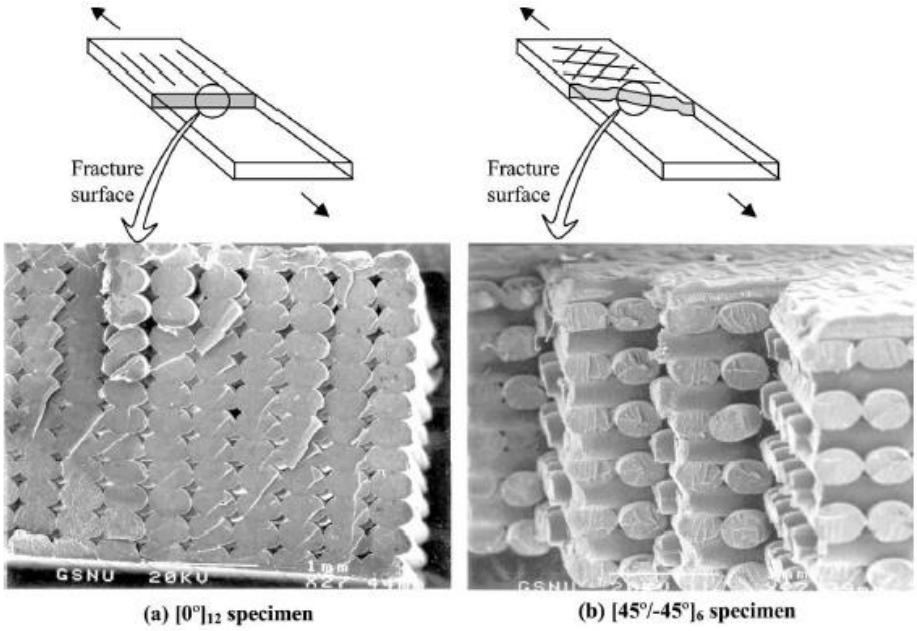

Figure 4.14: microscopic view of 2 FDM building processes (Ahn et* al.*, 2002)

In their study, they built the same sample with different processes and looked at the different results obtained from tension and compression tests. The results showed major differences mainly in tension. The implication from the Ahn *et al*. study is that RP material properties have to be found from samples built by Brunel machine (transverse and axial modulus). Bone models will need to be created using a known orientation for each test. Anisotropy can be modelled in FE, so this part of the validation process is still feasible.

The first step for the use of RP is to find out the material properties of the ABSP400. From the manufacturer data, the tensile strength is 22MPa and the compressive strength is 41MPa. These values are from injection moulded samples and as the samples are from a FDM machine (Ahn *et al*., 2002), it is necessary to create samples from the machine to test. The samples created are two cubes with 2cm sides (figure 4.15).

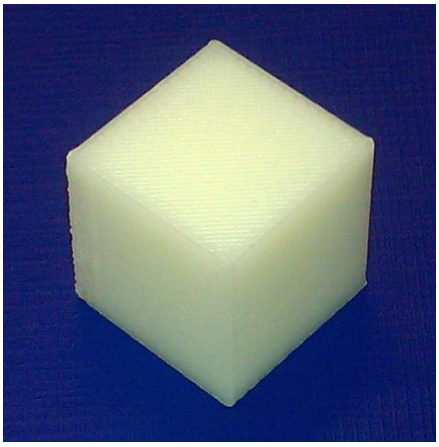

Figure 4.15: Cube sample tested for compression where it was possible to notice the cross section from the building process on the top side and the layers on the sides.

The two cubes were compressed between two parallel plates once, the first on the top side and the second on the sides. The results are shown in the graph on figure 4.16.

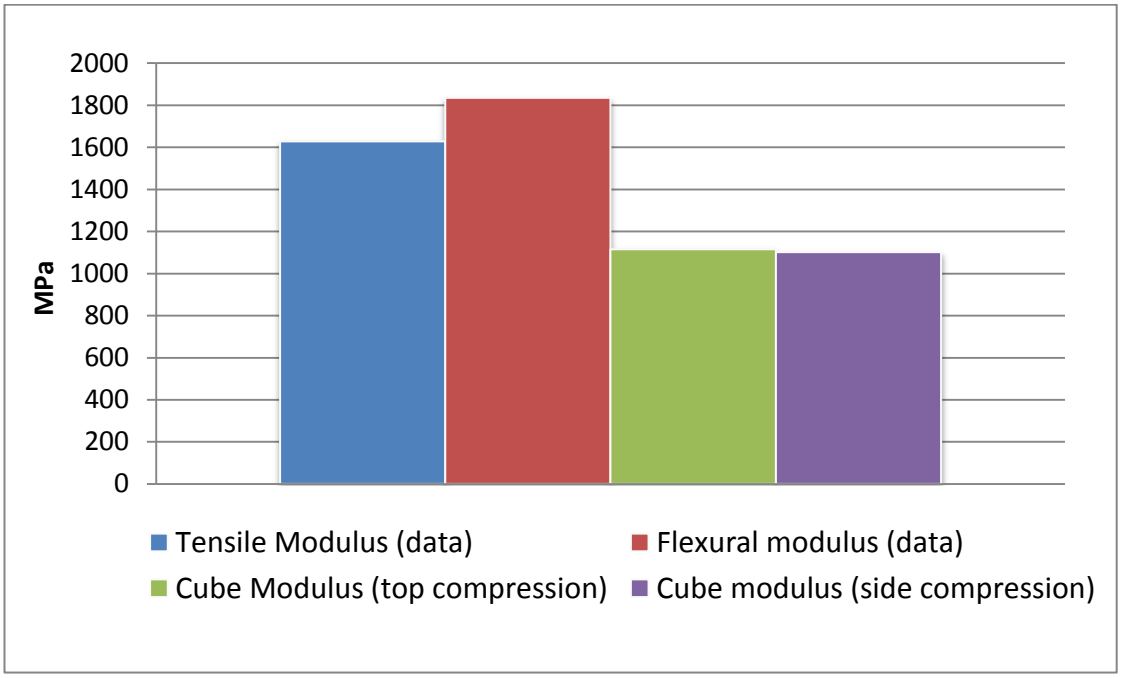

Figure 4.16: Comparison between materials property data and compression tests.

As expected, the results differ from the manufacturer data when compared to injection moulded. Also, as found by Ahn *et al.* (2002), the compression tests show isotropy in compression with no effect from the building direction from the FDM machine.

The next stage in order to test the RP process is to compare compression tests on RP models from FE models. The first model is from a bone sample with a volume fraction of 19.5%. These models have been compressed on the 3 directions as illustrated on figure 4.17.

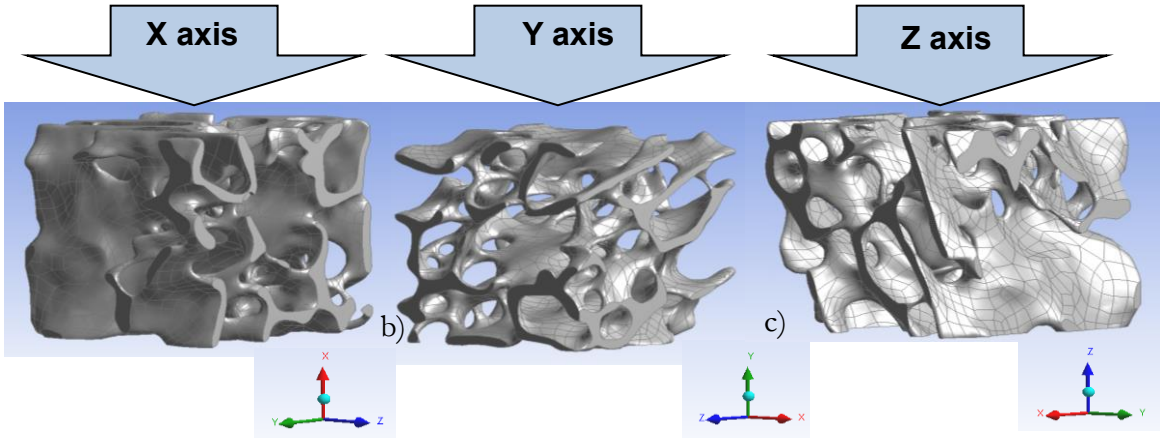

Figure 4.17: Same sample compress on 3 directions. a) compression x axis b) compression on y axis c) compression on z axis.

The FE models were set up with two parallel plates of steel compressing each sample. The plates are modelled as steel with a frictional coefficient of 0.3 with ABS P400. Figure 4.18 shows the results of this comparison.

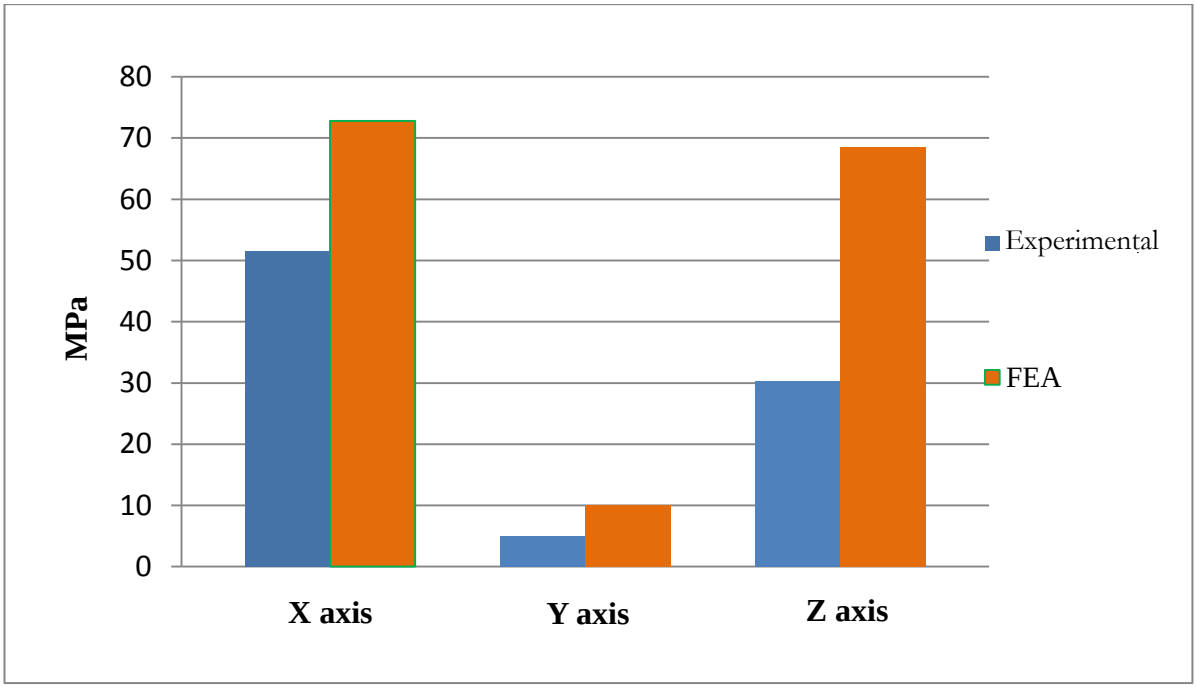

Figure 4.18: Comparison of modulus between FEA and mechanical compression of RP models

The results are showing significant differences between experimental results and FE simulations. These differences could be partially explained by the frictional coefficient between steel and ABS P400. From various engineering websites (www.eng-tips.com and www.royamech.co.uk) the frictional coefficient between steel and ABS P400 varies from 0.002 and 0.5. These variations are explained by the potential lubrication of the surfaces. A coefficient of 0.5 is for dry surfaces (the case here) and 0.02 is for lubricated surfaces. Therefore, the influence of frictional coefficient on the reaction force has been compared. The results are shown in figure 4.19. It appears that FE results could match the mechanical test using a frictional coefficient of lubricated surfaces.

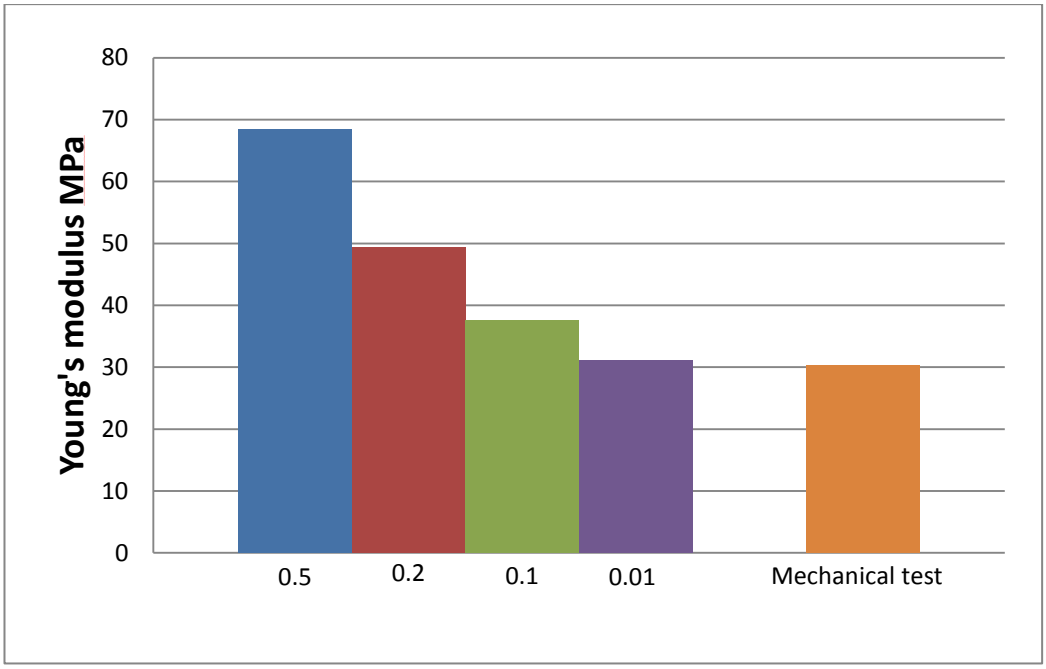

Figure 4.19: Young's modulus by frictional coefficient from FE simulation with compression on Z axis.

A simplified bone made from RP (Figure 4.20) with the same volume fraction of 19.5% has been compressed mechanically in the x, y and z directions and compared with FE results, with also a frictional coefficient of 0.5 for the comparison with the same apparent density cancellous bone model. The results are shown in figure 4.21. In this case, the results are different as FE models show a relative isotropy while mechanical tests are anisotropic.

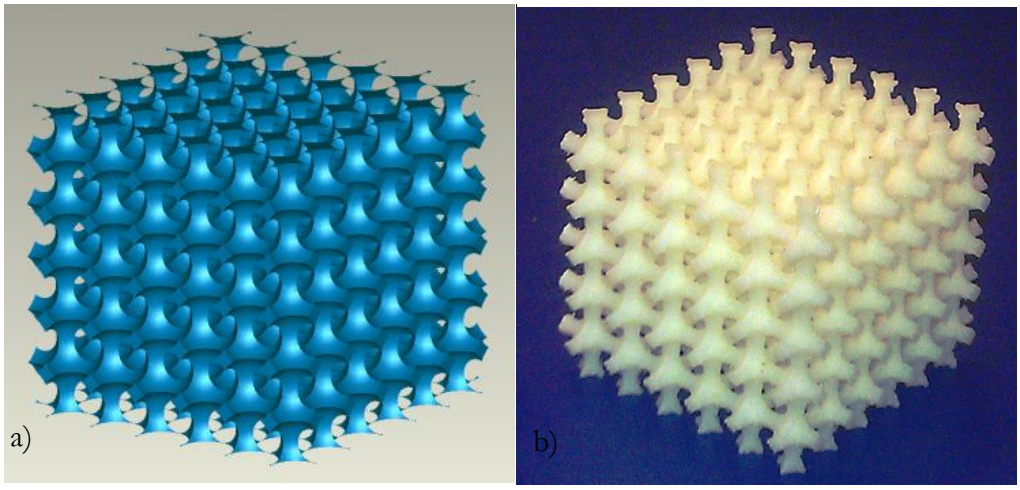

Figure 4.20: Simplified bone model with 19.5% volume fraction. a)FE model b) RP model

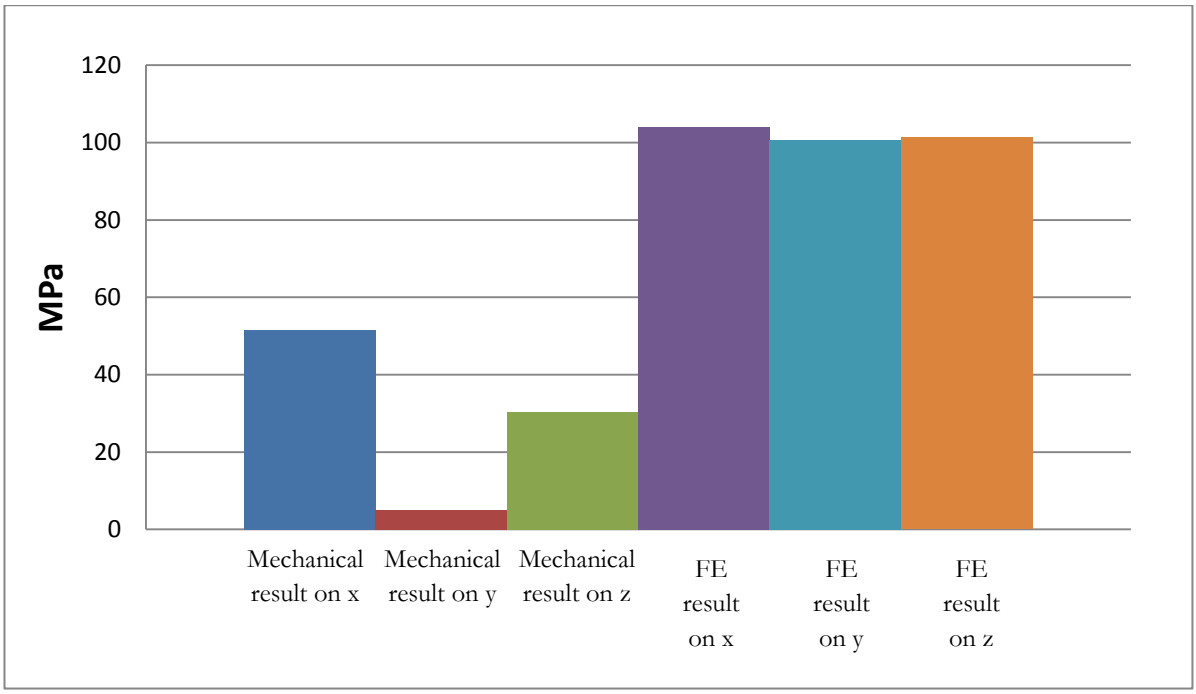

Figure 4.21: Comparison of mechanical and FE compression test with simplified bone model with 19.5% volume fraction

This difference could be explained hypothetically by the building process of the RP models which the FE models do not have, as seen in previous studies (Ahn *et al.*, 2002). Moreover, the study of cubes did not show that the compression is affected by the building orientation as well, except that it is possible that building orientations are compensated by the shape of the cubes in compression, while for small struts in the simplified models it could cause significant bias in the results. This is a hypothesis that could be easily tested by creating similar RP models in different ways. RP has been considered first as a basic way to compare FE results and mechanical tests in order to double check results of screw pull-out from real bones and finally many complications occurred due to building resolution and process. Therefore it has been decided to focus only on the bone mechanical test and the FE comparison.

4.3. Conclusion and procedure selected

For the validation of the FE results, many comparisons were initially suggested between:

- The mechanical test with real bone and FE replication of the test
- Mechanical tests of RP scaled models from real bone and FE replications of the scaled models with RP material property.
- Simplified bone geometry FE models with FE replicating mechanical tests with real bones.
- FE with simplified bone models and mechanical tests of RP models.

All these comparisons are illustrated in figure 4.22.

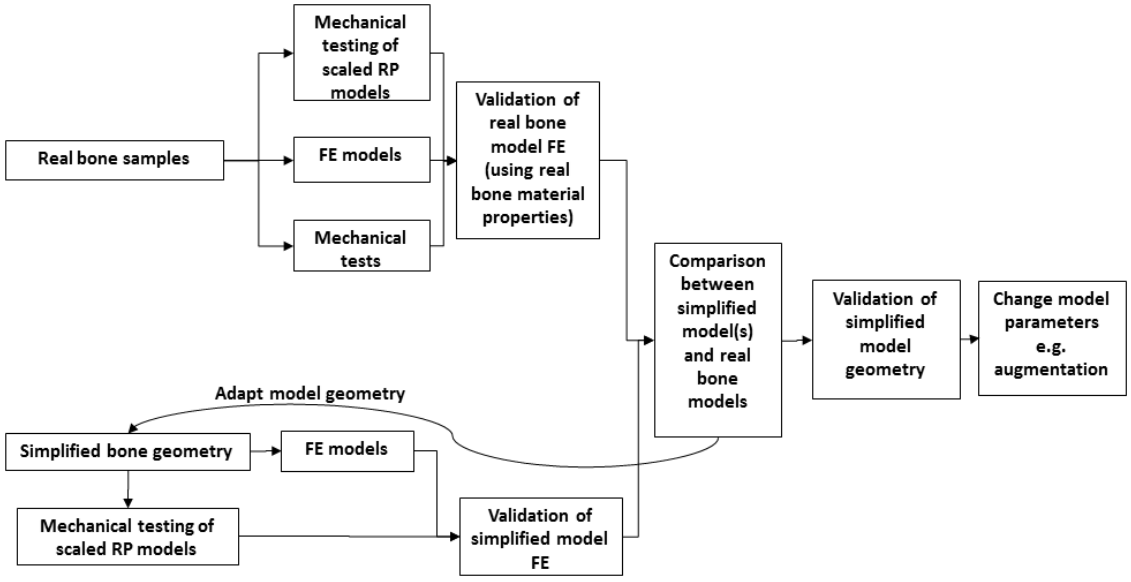

Figure 4.22: Initial validation diagram

RP enabled a method to double check the validation from the mechanical tests of real bones. This program was theoretical and finally the options using RP were not satisfactory due to inaccuracy of results linked with the building process, cost of each model and time for model creations, as seen previously.

Also, one screw pull-out test from human bone was necessary to validate FE results. Finally, the validation procedure consists of a screw pull-out test from human bone. A FE model of this test has been made for comparison and in order to validate the FE. Meanwhile, a model made from simplified bone having similar bone characteristics was made for comparison in order to validate the simplified bone models. This process is illustrated in figure 4.23.

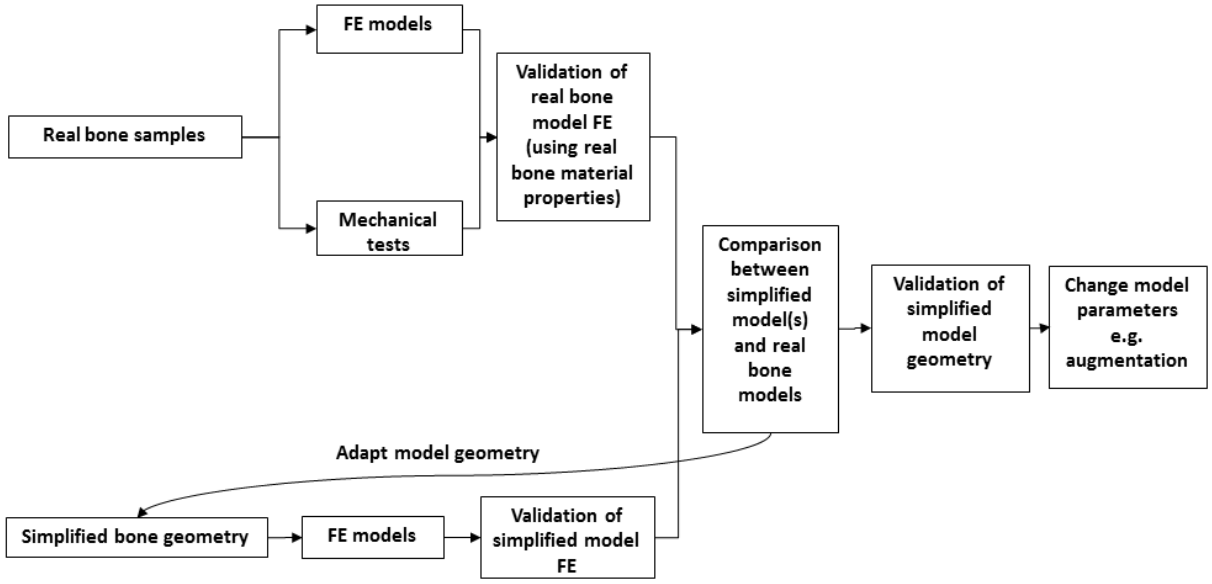

Figure 4.23: Final validation diagram

5. Chapter 5 - Validation of FE results

This chapter describes the step-by-step validation process selected previously. It starts first with the mechanical screw pull-out from a cadaver, followed by the description of the process to create models from images of the cadaver bone. Then it was necessary to simplify the model and the explanations are given in the third part of this chapter. In the final part, the FE model is compared with the results from the screw pull-out from cadaver undertaken in the first part of this chapter.

5.1. Screw pull-out in real bone

The work on human bone samples was achieved with thanks to the collaboration with the Laboratory of Biomechanical Orthopaedics of EPFL, Switzerland and to Professor Dominique Pioletti for his guidance while using the facilities there.

5.1.1. Sample extraction from the bone

The sample is extracted from a frozen femur using a punch of 12mm diameter (figure 5.1). The bone is clamped while the user is inserting the punch on the area of interest (figure 5.2).

Figure 5.1: Punch 12mm diameter

The extremity of the bone cut by the punch is then flattened with a saw using the edges of the punch as reference point. The sample is then extracted from the punch and put back the other way around, in order to chop the cortical layer in a flat way and perpendicular to the other end.

Figure 5.2: Bone with sample extracted

5.1.2. First scan

The sample was put in a test tube along the tube axis (figure 5.3) with tissues (not detectable from the µCT machine) to maintain it and then scanned with a µCT machine (figure 5.4) using an X-ray fan-beam-type tomograph

(µCT40, Scanco Medical AG, Switzerland), also referred to as a desktop µCT (Rüegsegger, 1996) at an energy of 50 kVp and a spatial resolution of 12 µm.

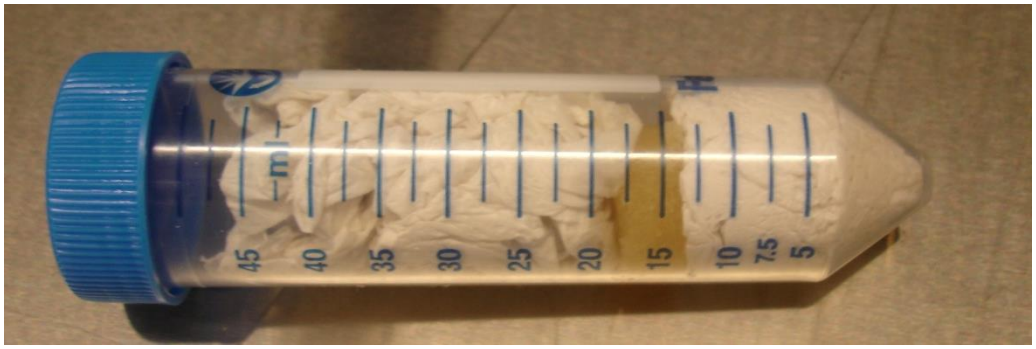

Figure 5.3: Sample positioned along the tube axis with tissues

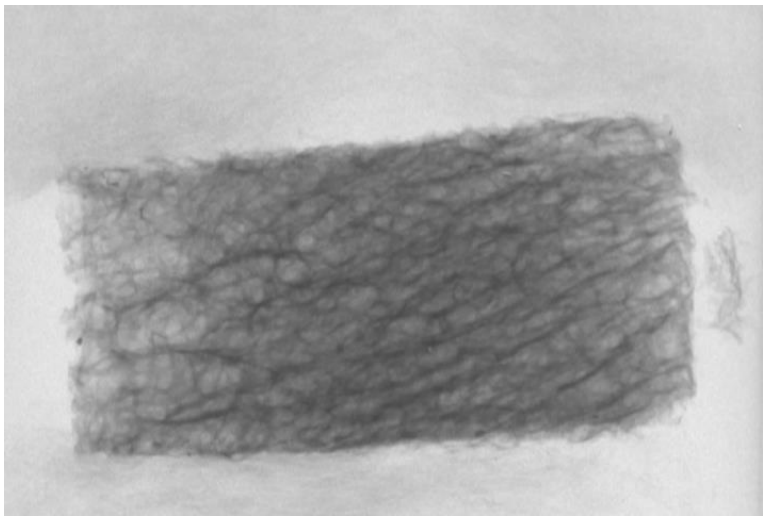

Figure 5.4: Bone sample scanned image

The first scan of the bone is to be used for the bone model creation. It is important to do it in order to have the architecture of the bone sample without any damage for the finite element model creation.

At this stage, a compression in the elastic range of the bone sample was considered in order to obtain the Young's modulus of the bone sample for the screw pull-out simulation. Finally it was decided to prevent the risk of any micro damage. The compression test did not occur. The option to compress an adjacent piece of bone was not considered due to the intra-specimen variation.

5.1.3. Screw insertion

The screw was inserted without any predrill, and positioned centrally and vertically with a screw guide.

5.1.4. Scan

The sample was put in a test tube along the tube axis (figure 5.5) with tissues again to maintain the whole and then scanned with a µCT machine (figure 5.6).

Figure 5.5: Bone sample with screw inserted positioned along the tube axis with tissues

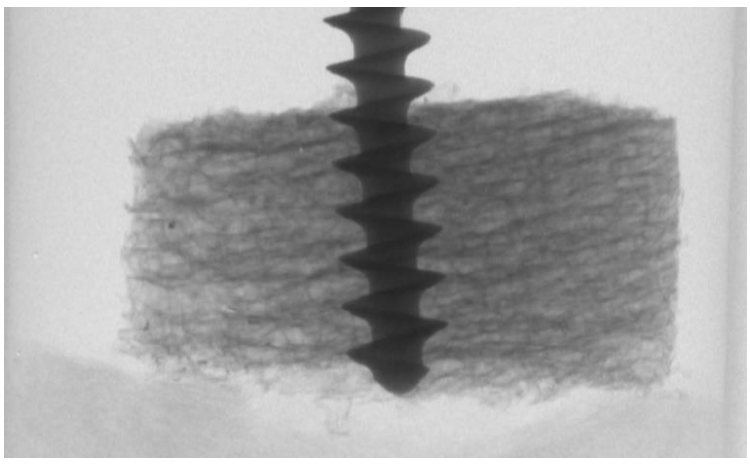

Figure 5.6: Bone sample with screw inserted scanned (front view)

This second scan of the bone with the screw inserted was used for the screw positioning for the FE models.

5.1.5. Screw pull-out

The sample was tested on an Instron Microtester 5848, (Instron, MA, USA). A plate with a hole of 9mm diameter was placed on the bone sample. The whole was placed under a piece that retained the plate and the top of the bone around the screw. This piece was then screwed on the base of the Instron machine. The screw head is clamped to a custom-made system, which is linked to the testing machine's jack (figure 5.7). Figure 5.8 shows the set-up before and in the machine.

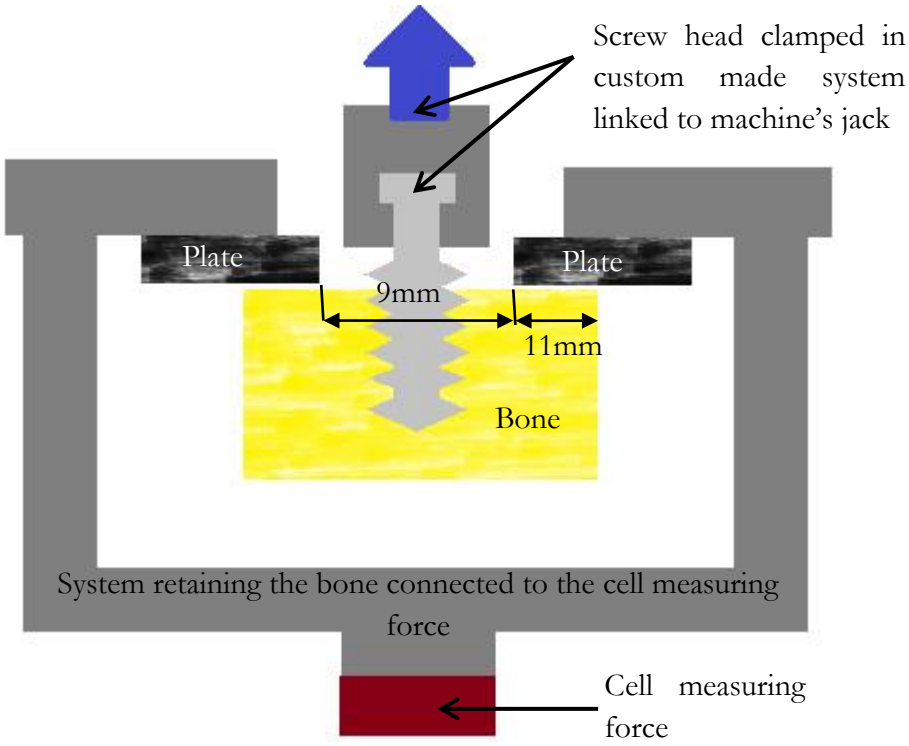

Figure 5.7: Diagram representing the assembly in the Instron machine

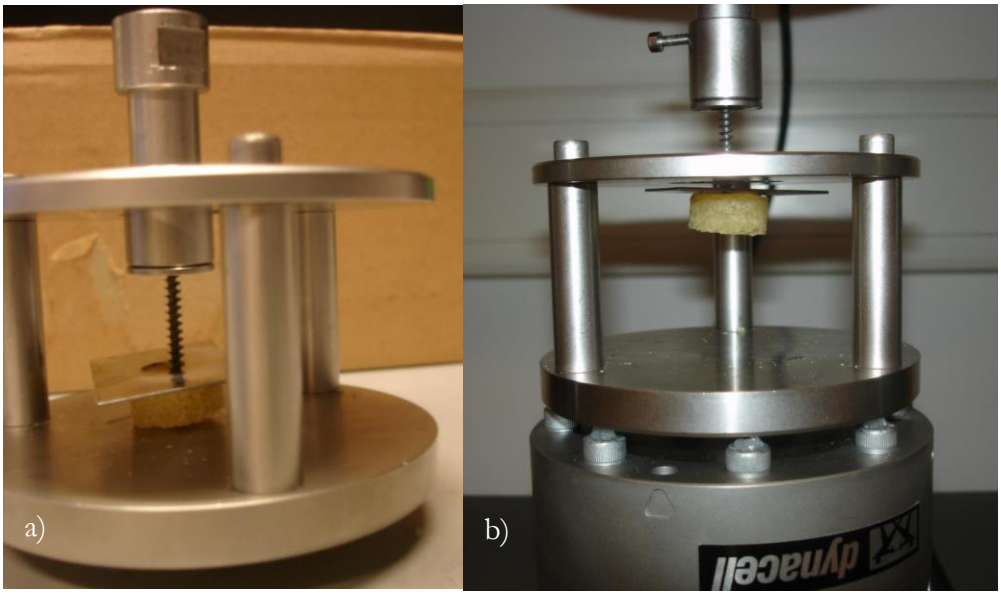

Figure 5.8: a) Assembly before mounting the different parts in the Instron machine and b) assembly just before testing in machine

The screw pull-out has been setup with a displacement of 5mm.min^{-1} as done in previous studies (Seebeck *et al.*, 2004, Stadelmann *et al.*, 2010) and recorded at a sampling frequency of 100Hz.

5.1.6. Results

Figure 5.9 shows the resultant graph. The maximum load obtained was 118.29N with a stiffness in the pseudo-elastic region of 228 N.mm^{-1}.

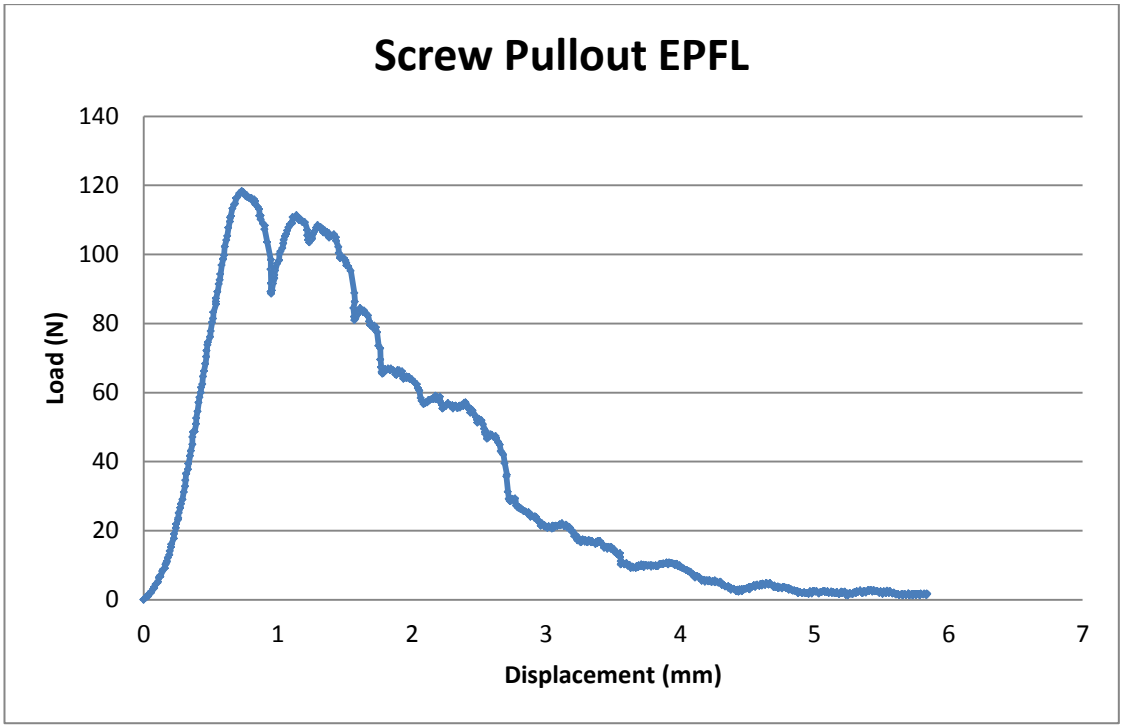

Figure.5.9: Graph result from screw pull-out test

Figure 5.10 shows the top edge of the sample at the end of the pull-out test.

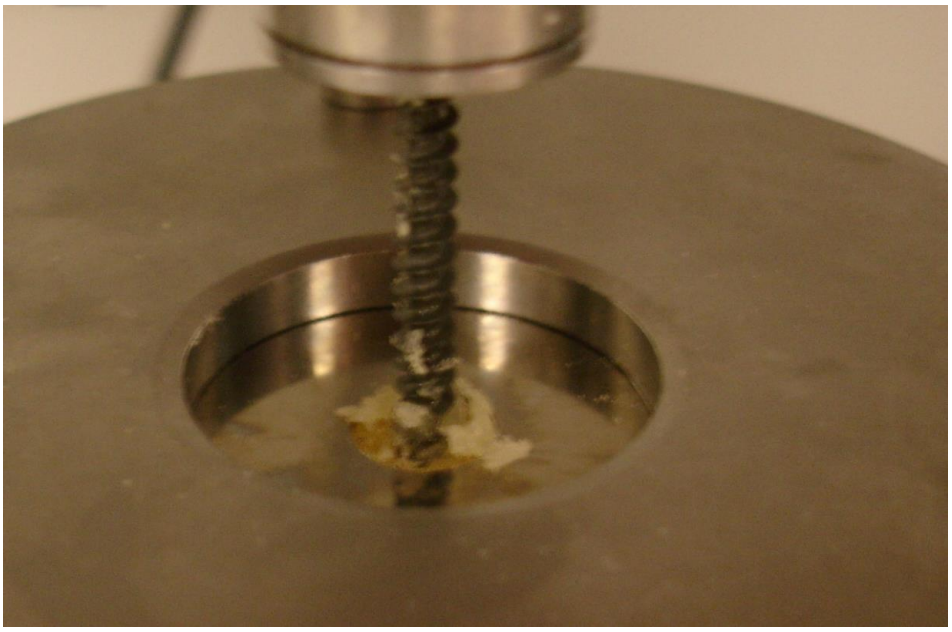

Figure 5.10: Zoom on the screw that has been pull-out from the bone.

Figure 5.10 show pieces of bone torn off from the sample inside the screw thread at the end of the screw pull-out test.

5.2. Model creation from real bone study

All results issued from any Finite Element (FE) software need validation (Dobson *et al*., 2005). This section describes the creation of the model that will replicate the mechanical test. The aim of the simulation was to validate the results generated by FE techniques.

During the mechanical test, the bone sample has been scanned using a micro-computed tomography (µCT) machine at two different stages:

1) Initially without the screw, in order to have the bone sample without any damage.
2) Then after the screw was inserted into the bone, as the screw is made of titanium which creates noise during the scan, the images generated were too poor to create a model from them but could still give the exact position of the screw into the bone.

In this case, it was then necessary to model the bone on its own and then to insert the screw in the same way as the mechanical test.

The entire process can be split into 10 stages that are represented in figure 5.11.

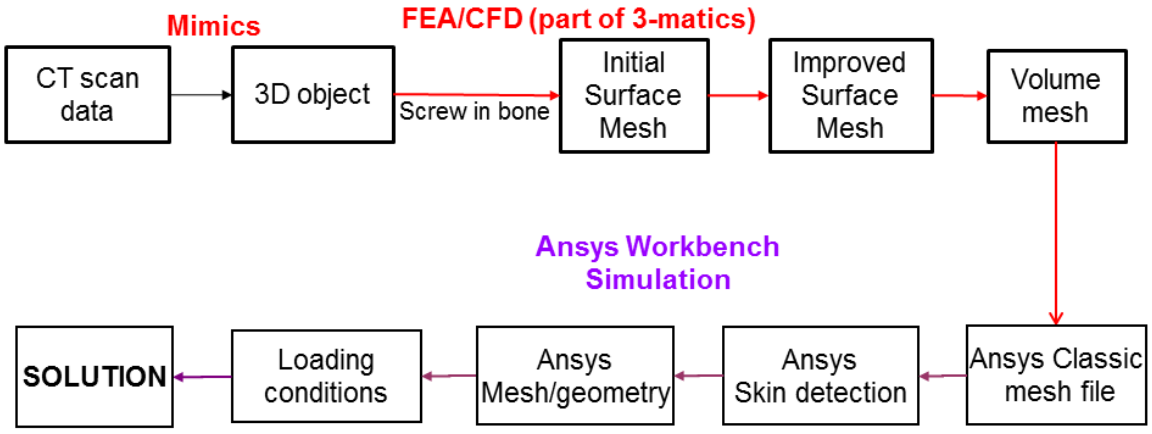

Figure 5.11: From µCT to FE model with Mimics package and Ansys®Workbench.

Modelling screw pull-out into existing scan data is challenging as it is necessary to:

- Maintain mechanical integrity while optimising computational requirement e.g. smoothing surface to reduce number of elements
- Create an accurate volume fraction e.g. thresholding, 3D calculation effect
- Transfer from one software to another e.g. Mimics to Ansys® Workbench
- Manage the modelling of the screw/bone interface

5.2.1. Computational issues

The studies with simplified bone models in 2D and 3D were carried first on a computer with Intel® Core™ 2 Quad CPU Q6600 @ 2.40GHz with 2.98GB of RAM and then on a computer with AMD Phenom™ II X4 940 Processor @ 3.00GHz with 8.00GB RAM. A new computer was acquired as the computational requirements for the model creation from real bone data were more important. This computer is a HPC with 2 processors E5640 @2.40GHz

and with 48GB of RAM. Even with this investment, a limitation appeared inside Ansys® when the models are exported internally to the Static Structural section from the Finite Element Modeler section, where skins are added to the models. This transfer is fully autonomous and the user has no control. This limitation appeared to be linked with the size of the models as the error messages appeared with models with over 1 million elements. It was therefore decided to aim for models with less than 1 million elements.

5.2.2. From images to volume mesh

The results from these scans are layers of images, evaluating the structures with grey values, see Figure 5.12. In this study, the Mimics package software has been used to be able to create the models from these images for the simulation.

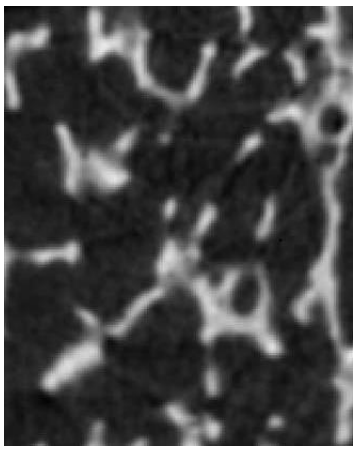

Figure 5.12: Example of cancellous bone image from µCT

5.2.3. Thresholding

This was done in parallel to test the process, to emphasise that different bone samples have been used. Preliminary testing of the procedure was needed before actually carrying out the mechanical test with human bone.

The resultant images from the μCT machine represent the structure using the grey scale value, based on density, of the pixels. It was necessary to differentiate the grey values defining the bone: this process is called thresholding.

There is no "standard" method for thresholding, the Mimics software offers with predefined thresholds sets. In this study, the first analysis was to compare the effect in bone volume fraction (BV/TV) obtained from taking the following Mimics preset threshold values: Bone, spongial bone (adult) and compact bone (adult).

The threshold unit used here is the Hounsfield unit. Table 5.1 shows the influence of the threshold on the bone volumes and surfaces and figure 5.13 illustrates this.

Table 5.1: 3D objects obtained with 3 different predefined threshold sets

Predefined threshold sets	Bone	Spongial Bone	Compact Bone
Predefined thresholds values	Min: 226 Max: 3024	Min: 148 Max: 661	Min: 662 Max: 1988
3D volumes obtained with high quality rendering	Volume: 755.76 mm^3 Surface: 5864.57 mm^2 Number triangles: 2974624 Number points: 1479954	Volume: 652.89 mm^3 Surface: 8571.00 mm^2 Number triangles: 4118624 Number points: 2045044	Volume: 556.67 mm^3 Surface: 5713.13 mm^2 Number triangles: 2891300 Number points: 1435720
Volume ratio (volume base cylinder=1994.20)	38%	33%	28%

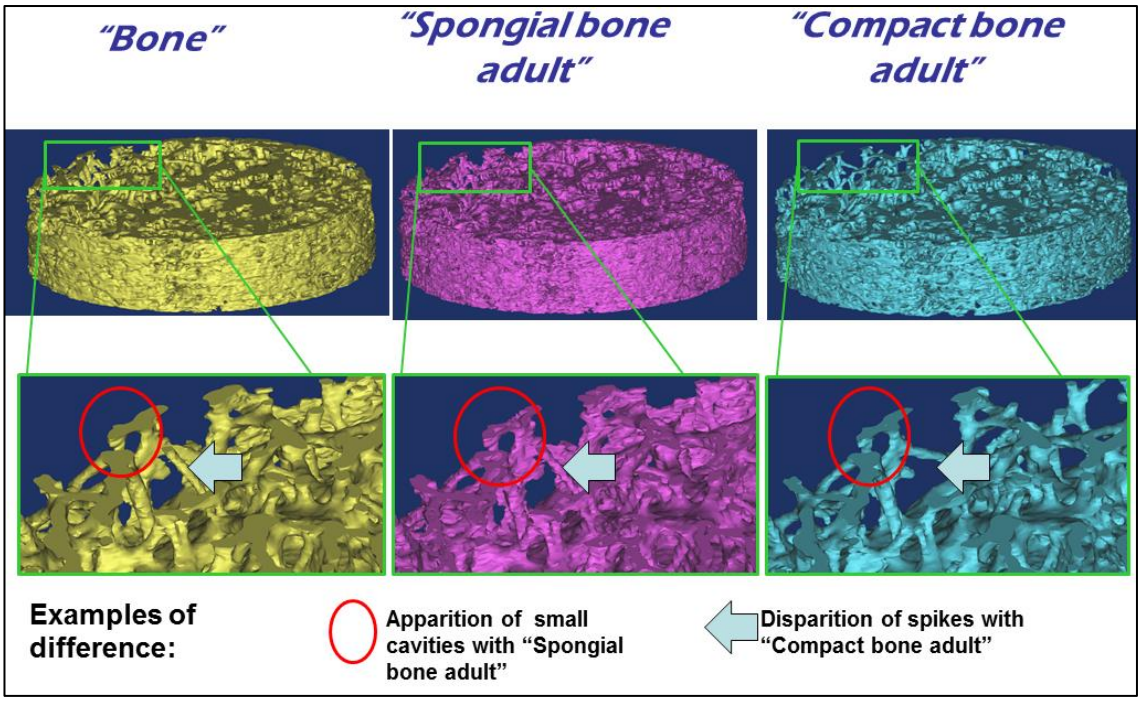

Figure 5.13: 3D representations of the same bone images with the different predefined threshold sets

It appears clearly that the structures have significant differences (volumes, surfaces and structures) using these predefined threshold sets. These predefined threshold sets differ significantly from one another and have been created by the software as a baseline for using CT. They have been applied here to µCT with only cancellous bone, which is different from the general CT cases in which an area of the body with many different tissues distinct from one another other is scanned.

Another study (Hara *et al*., 2002), compared smaller variations of the threshold. Their results showed that in the case of bones with a BV/TV <0.15, rod-like, a variation of 0.5% in threshold value could lead to a change of 5% in BV/TV with a change of 9% in maximum stiffness. In the case of bones with a BV/TV>0.3, plate-like, a variation of 0.5% in threshold value could lead to a change of 2% in BV/TV with a change of 3% in maximum stiffness. From these

results they could conclude that the threshold value has more influence on rod-like bone due to higher surface area/volume ratio.

There are many techniques available to use for thresholding. Four of them have been considered for the study. A review of three of the principal techniques has been made by Kim *et al* (2007): Global threshold, adaptive threshold and matched threshold. A much older one called half maximum height (HMH) has been developed by Ulrich *et al*. (1980).

The global threshold consists to take a global value for threshold "based on the histogram distribution of the 65,536 graylevel values in the 3D image of each specimen" figure 5.14 (Kim *et al*., 2007)

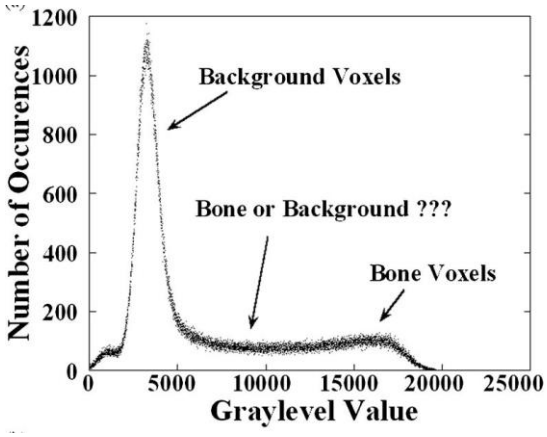

Figure 5.14: "Histogram of a typical 16-bit 3d µCT image of bovine trabecular bone. The left peak represents background voxels, whereas the right peak represents bone voxels. The voxels in between are ambiguous as they may represent bone or background voxels" (Kim* et al*., 2007)

The adaptive threshold involves selecting a number of different threshold values, calculating the volume of the resulting 3D body and finding the threshold value at which this changes significantly, figure 5.15.

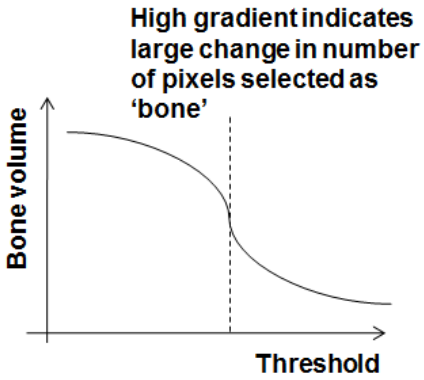

Figure 5.15: Bone volume by threshold values representing the adaptive threshold technique.

The matched global technique consists of determining experimentally the bone volume of the specimen and finding a threshold value that gives a 3D volume with the same bone volume. The measurement of the bone volume can be difficult. Archimedes' principle was considered to find the volume but it would imply to clean and dry the bone which would affect the bone's original mechanical property.

The last technique reviewed is the Half Maximum Height (HMH), which consists in taking a row of pixels crossing the boundary between two materials and use the mean value as the threshold.

Few studies have been done to compare all these techniques. Kim *et al*., (2007) compared the adaptive thresholding, global thresholding and matched global to bone volume fraction from Archimedes principle. The outcome was that although there are small differences in the architecture, the bone volume fractions were relatively consistent as was the apparent modulus. In another study, Coleman and Colbert (2007) compared the HMH and visual inspection technique using a microscope to measure specific distances for comparison and they councluded that the HMH technique is more accurate than the visual boundaries.

Another point of concern is the resolution of the voxels from the µCT scans. Yeni *et al* (2005) investigated "the effect of µCT voxel size on the finite

element model accuracy for human cancellous bone". For that purpose, they tested 3 voxel sizes (21, 50 and 110μm) and found that the bone volume fraction did not differ considerably but the modulus changed significantly only in the 110μm case. The resolution that has been used for the study is 18μm which is therefore not affecting any property.

5.2.4. 3D volume calculation

Post thresholding procedures can affect the volume fraction and microarchitecture of the bone. A study made by Leung *et al*. (2007) analyses the smoothing effect in micro FE modelling of a cancellous bone analogue material (aluminium foam). They have been studying the effect of the mesh creation and smoothing (degree of surface smoothing, this may include replacing elements with sharp corners etc.). The outcome from their study was that the selection of thresholding mainly affects the accuracy of the apparent modulus followed by mesh density and smoothing.

One post-thresholding stage that does not have literature is the effect of the 3D calculation. This can be explained by the fact that most of these studies concern the bone on its own. First of all, the bone samples are generally small and easier computationally, FE simulations with one body (no contacts) can accept many more elements. Therefore, it is assumed that they can accept one element per voxel, which corresponds to the optimal quality 3D volume calculation.

A small study of that effect has been done from the piece of bone that has been mechanically tested. In the study, from the same threshold setting, 3D volume calculations have been made with different predefined settings: optimal and low.

The 3D object obtained with optimal volume calculation had:

- Surfaces elements 13,289,090
- Volume of 565.49 mm^3

- Surface of 9,414.65 mm^2

The 3D object obtained with low volume calculation had:

- Surfaces elements 1,205,628
- Volume of 1275.70 mm^3
- Surface of 9,769.45 mm^2

The 3D objects obtained are different despite using the same images and threshold sets. The optimal one creates an element for each voxel, therefore it is assumed to be the closest to reality while the low quality is already smoothing and inflating the object. The main differences concern the volume (double) and the number of elements (10 times less).

Thus, it would not be feasible for our case study to use optimal 3D volume calculation because it would generate an assembly with too many elements for the computer abilities available as explained in section 5.2.1. Also, the thresholding issues appear now relatively minor compared to this effect, not taking into account the smoothing effects that are necessary to export the model from Mimics into Ansys® for FEA in order to obtain sliding contacts.

Thus, the final process decided at this stage was to use thresholding sets using visual inspection (which actually correspond to the "bone" predefined set). From the mask obtained with the thresholds, the optimal 3D calculation is used to create the reference 3D object. The reference 3D object is used as in the matched thresholding technique as a reference for the volume in the best case. Due to the need of restricting the number of elements, the original mask was then eroded to anticipate the inflation generated by the medium quality volume calculation, so that the final 3D object has the same volume as the reference one.

5.2.5. Screw positioning

For our study, it was important to position the screw in its exact position and orientation, the µCT scan of the bone with the screw inserted was used to

create a 3D object following the same techniques. This model showed noises but was good enough to be used as a reference for the positioning of the screw. The screw was positioned using reference points on the surfaces of the bone. These reference points could be spikes or plates that are easily recognisable in both 3D models. In this case, three points at the top and bottom surfaces of the bone were selected. The distances and the angles of these points to the tip of the screw on one side and the middle of the top part of the screw on the other side were measured and the screw was moved in a way that these distances and angles were matching, figure 5.16.

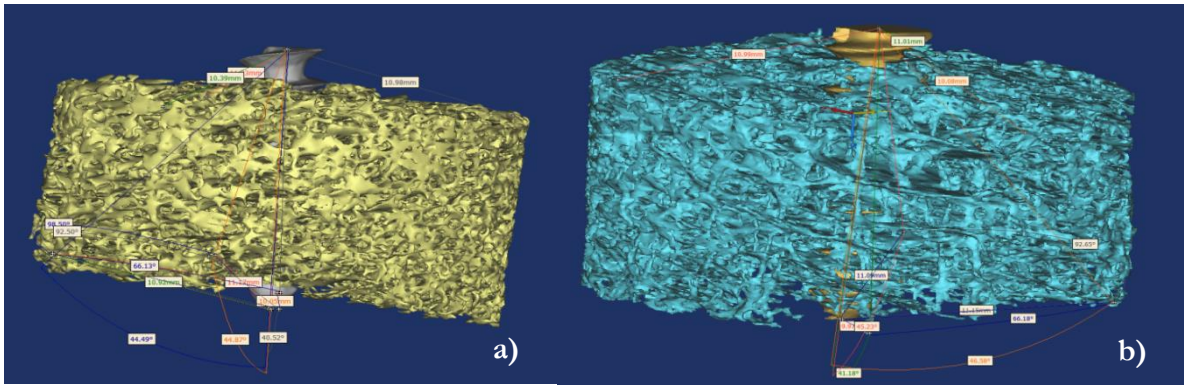

Figure 5.16: a) creation of the model with screw manually inserted and b) 3D object from the µCT scan of the bone with screw used as a reference.

The instructions for the improvement of the meshes generated and for the treatment of the meshed assembly (bone with screw) from surface meshes to volume meshes were carried out in 3-Matics and are detailed in Appendix C.

5.3. Simplification/reduction of real bone model and results with a continuum study

The previous section showed that the creation of the entire bone with the screw generated a model with a huge number of elements. As explained in section 5.2.1, it was not possible to deal with a model with over 1 million

elements. The idea in this section is to show that the whole piece of bone was not entirely necessary in order to have relatively accurate results. Also, the original boundary conditions, i.e. a plate fixed holding the bone with screw going through the plate and moving vertically, are giving complexity to the simulation due to numerous contact areas and bodies involved, i.e. 3 bodies: plate, bone and screw and 2 contacts, between the plate and the bone and between the bone and the screw.

Another simplification process was studied as well, this process was to change the cancellous bone, away from the screw by a continuum, figure 5.17.

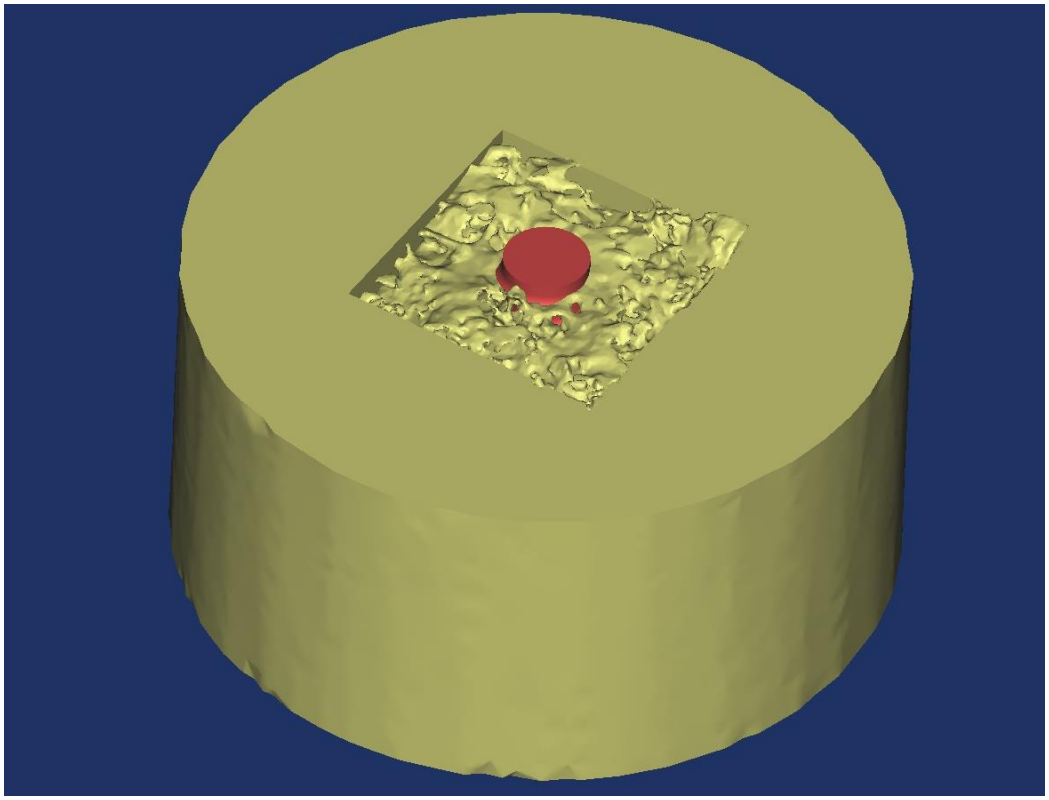

Figure 5.17: simplification process where cancellous bone away from screw contact is replaced by continuum.

The main problem of this model was the complexity of creation. The time required for the model creation was doubled due to the need to firstly deal with the cancellous bone needed, then to join it with the continuum and finally to add the screw. This process involved more contacts management and also the continuum part and the cancellous bone would need to have 2 different material

properties and therefore creation of 2 different bodies which prolonged the process. Due to the complexity generated, this idea was not pursued.

5.3.1. Hypothesis

A reference model with the same external dimension and same boundary conditions has been created in order to test the different size options for the bone model and to test simplifications of the boundary conditions. This reference model was an exact replica of the mechanical test except that cancellous bone was continuum in this case: the bone has the same size, the screw is centred and a plate with a hole of 9mm is fixed while the screw is displaced vertically (figure 5.18).

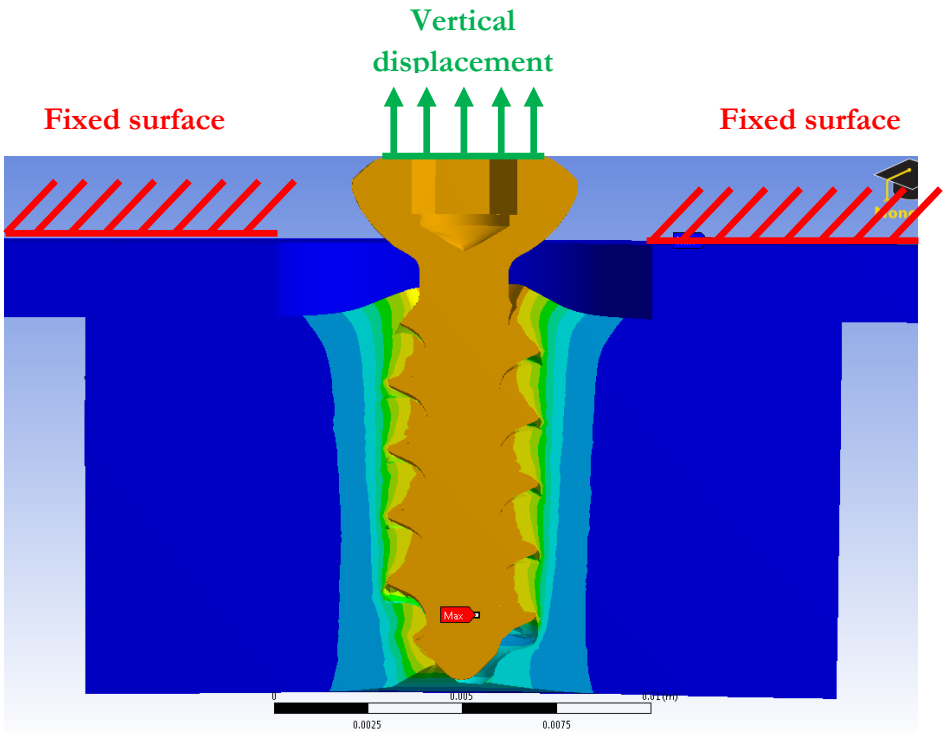

Figure 5.18: Front deformation view sliced of continuum model representing the mechanical test.

5.3.1.1. Boundary conditions

One way to simplify the model is to simplify the boundary conditions. The main idea in this section was to remove the top plate by fixing strategic parts of the bone. This action reduced the model to two bodies, with only one contact area between the screw and the bone.

From the reference model, it appeared that very small displacement and stress occurred on the outer part of the bone during the simulation. Therefore the idea was to define parts of the bone as fixed support. Also the bone size was reduced as well and for technical reasons, the bone sample forms a rectangular parallelepiped shape. Four hypotheses came out for the fixed support (figure 5.19):

- The top edges of the sample
- Specific points on the top surfaces
- The lateral edges of the sample
- The lateral faces of the sample

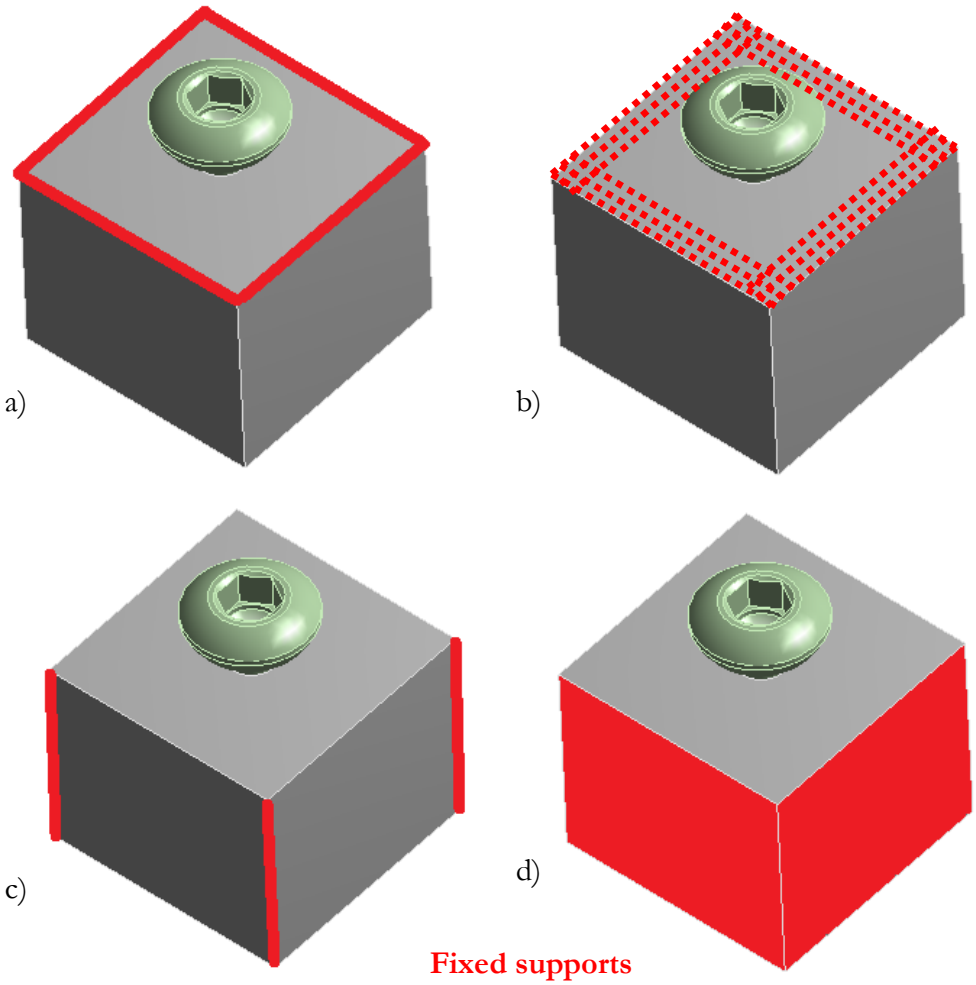

Figure 5.19: Different boundary conditions tested. Four hypotheses to represent the fixed supports represented (in red): a) top edges, b) points from the top surface, c) lateral edges and d) lateral faces.

Finally the four cases detailed were compared with the reference model and also with a model with same dimensions, 12x12x10mm, with a washer on top similar as the one used in the reference model, in order to compare the influence of the bone size reduction.

5.3.1.2. Bone sample dimension

The other part for the simplification of the model concerns the reduction of the bone sample size. In this case, there are two options available: reducing the depth and/or the width.

In the case of the depth of the bone, it has been seen previously that pull-out force was proportional to the length of screw thread involved in the bone. Therefore, each depth will be compensated by the factor of the length involved in the bone. In this case, 5 depths have been compared: 10mm, 8mm, 6mm, 4mm and 2mm. The bone sample has a rectangular parallelepiped shape with dimension 12mm x12mm x depth (10mm, 8mm, 6mm, 4mm or 2mm).

Concerning the width, seven cases with a depth of 4mm have been compared. The first case is a cylinder of 20mm diameter (as the bone sample) with 4mm depth. The other six cases have a rectangular parallelepiped shape with dimensions (all in mm): 15 x15x4, 14 x14 x4, 12 x12 x4, 10x10x4, 8x8x4 and 6x6x4.

The same boundary conditions and material properties used in the 2D and 3D simplified models have been applied to all the models.

5.3.2. Results

5.3.2.1. Boundary conditions

The results for the simulations comparing different boundary conditions are shown in figure 5.20 and table 5.2. The strength values in the table 5.2 correspond to the yield values measured in the screw pull-out curves.

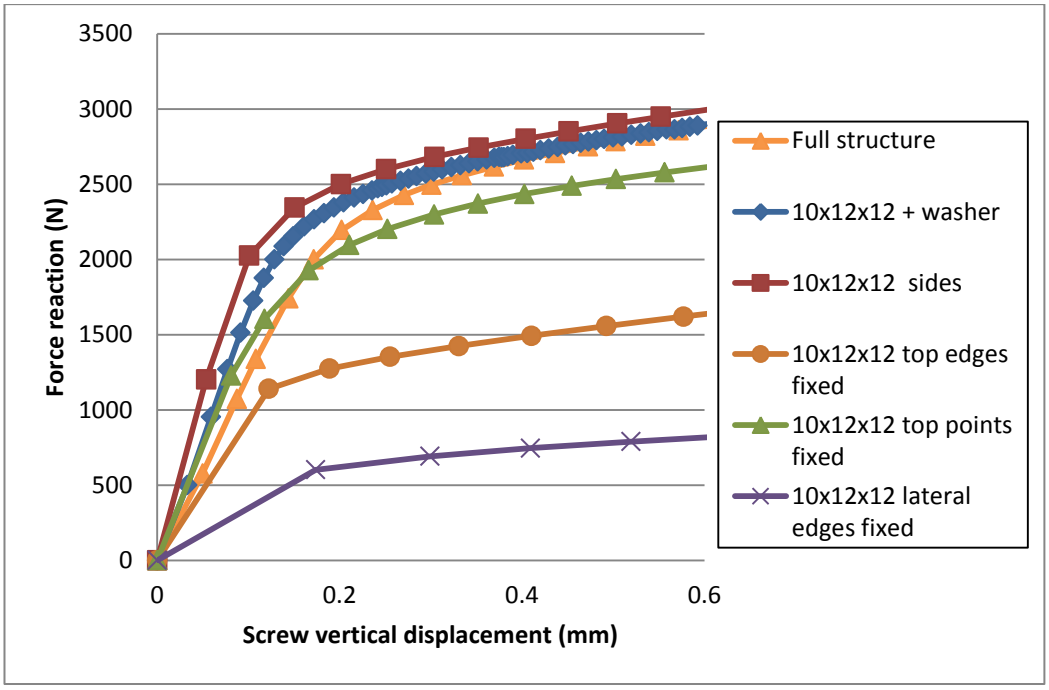

Figure 5.20: Screw pull-out result comparisons with depth compensation with different sample size and boundary conditions

Table 5.2: Summary table of results from screw pull-out result comparisons with depth compensation with different sample size and boundary conditions

Model	Stiffness (N.mm^{-1})	Yield strength (N)
Full structure	11654	2001
10x12x12 + washer	15556	2001
10x12x12 sides	20063	2026
10x12x12 top edges fixed	9315	1140
10x12x12 top points fixed	15140	1229
10x12x12 lateral edges fixed	3463	602

At first sight, it appears that the model with lateral edges fixed gave the results with most differences from the full structure in terms of stiffness and strength.

As expected, the model with the washer and the bone size reduction gave the closest results to the full structure. This model was used to control how the bone size reduction affects the results. In this case, it doesn't affect the strength

but makes the screw pull-out slightly stiffer. It was preferred not to use this model cannot in practice for the simulation as it would generate three bodies and two different contacts.

If the stiffness is compared, it appears that models with top edges fixed and top points fixed give results in the same range but meanwhile the strength halved. These boundary conditions could have been used eventually but a problem appeared when applied to cancellous bone models. Unlike these continuum models, cancellous bone models have a complex architecture leading to cases without clearly defined top flat surfaces and in some of the cases encountered, the fixed supports are clearly unbalanced (sides with few fixed support and sides with many).

The last boundary condition model with sides fixed shows a very similar strength with the full model, with a screw pull-out nearly twice stiffer. When it is compared with the model with washer and bone size reduction it appeared that the results were similar. This set up of boundary conditions offers then a results in the same range as expected from the full model but with 1 body and 1 contact less and there is no problem to apply it to more complex architecture.

5.3.2.2. Bone sample dimension

This section shows the results from different simulations tested on the effects of the bone sample size with a continuum representation for the screw pull-out.

5.3.2.3. Depth of the bone

The results from the depth of bone study are shown in figure 5.21 and table 5.3. The different depths are 10, 8, 6, 4, 2mm and the base is a square with dimensions 12x12mm. The force reaction from the screw pull-out test has been shown previously to be directly proportional to the screw length involved in the bone (Brown *et al*., 2011, Tenser *et al*., 1996). Therefore, here the results in each

case have been compensated to take into account the screw length involved. For example, results obtained with bone model 2x12x12mm were multiplied by 5, in order to be compared with the full structure that has a depth of 10mm.

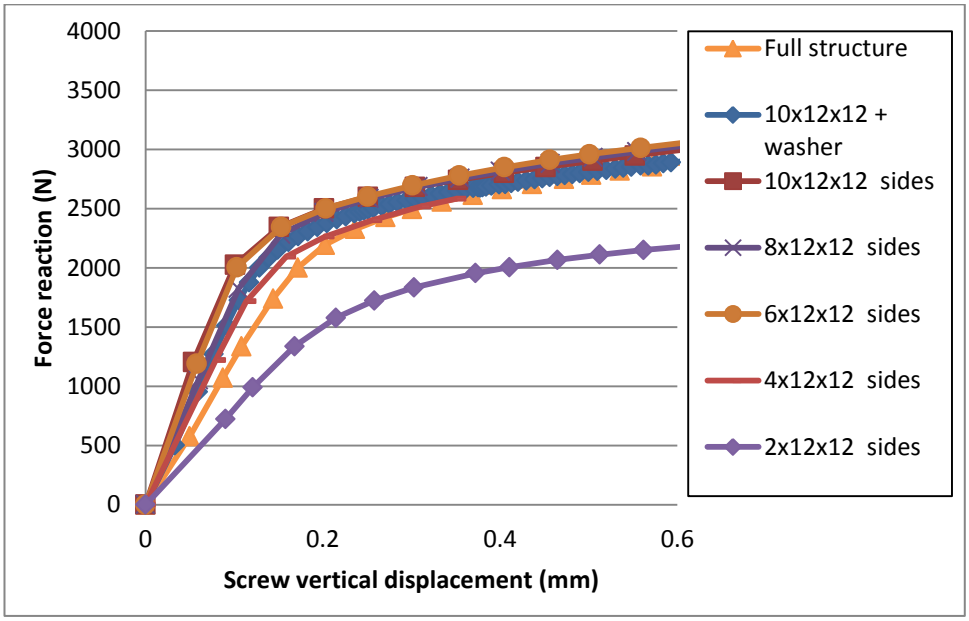

Figure 5.21: Screw pull-out result comparisons with depth compensation with different sample size and boundary conditions.

Table 5.3: Summary table of results from screw pull-out result comparisons with depth compensation with different sample size and boundary conditions.

Model	Stiffness (N.mm^{-1})	strength (N)
Full structure	11654	2001
10x12x12 + washer	15556	2001
10x12x12 sides	20070	2026
8x12x12 sides	17426	1826
6x12x12 sides	19473	2005
4x12x12 sides	13217	2095
2x12x12 sides	7949	1337

The results in all cases except 2x12x12mm show results in the same range with the compensation. It has been decided that it is necessary to use the full depth for comparison with the mechanical test in order to avoid potential

mistakes from natural heterogeneity of the bone sample tested. It has been decided as well that for other studies, a model with a depth of 4mm is sufficient for obtaining results.

5.3.2.4. Width

Different cases have been modelled in order to study the width influence on results. One case was with a cylinder bone with 20mm diameter, as the whole bone diameter. The other different widths are squared with 15, 14, 12, 10, 8 and 6mm sides. The depth is always 4mm for all the models. Figure 5.22 and table 5.4 show the results from the width study.

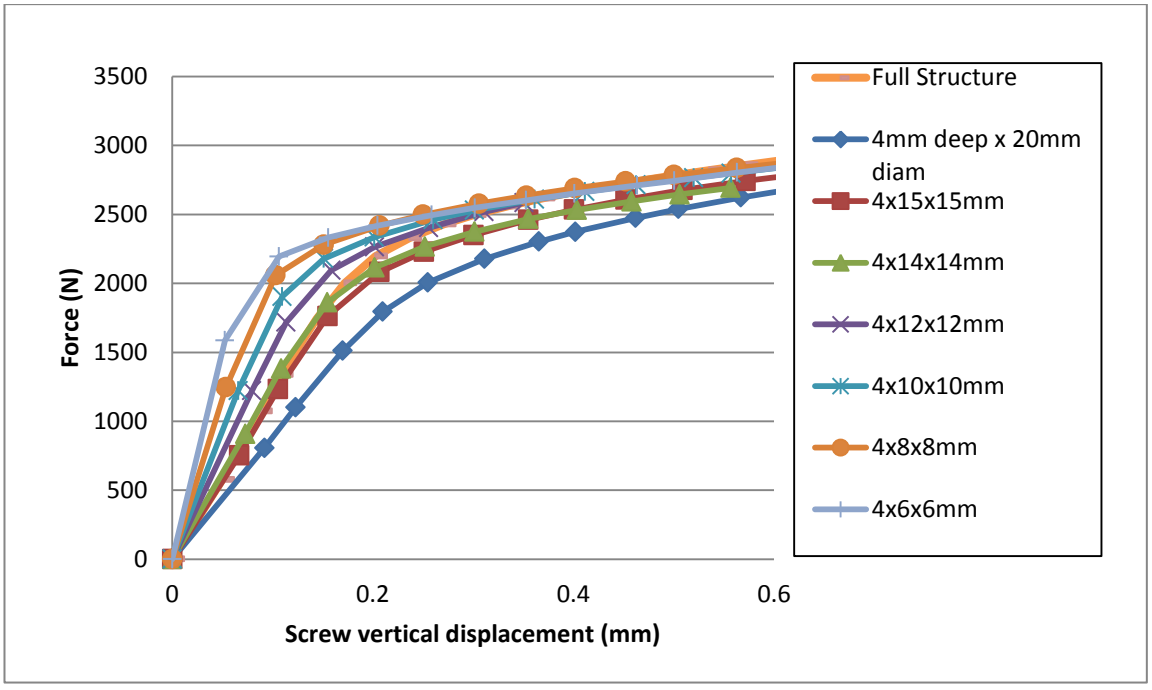

Figure 5.22: Screw pull-out result comparisons with models with different width.

Table 5.4: Summary table of results from screw pull-out result comparisons with models with different width.

Model	Stiffness (N.mm^{-1})	strength (N)
Full structure	11654	2001
4mm deep x 20mm diam.	8545	1794
4x15x15mm	11375	1762
4x14x14mm	12035	1862
4x12x12m	15126	1718
4x10x10mm	17359	1904
4x8x8mm	20007	2059
4x6x6mm	20611	2194

The results from the cylindrical model gave the lowest stiffness and strength as expected as there was the longest distance between the fixed edge and the screw centre. It was then possible to observe circles of influences while looking at the deformation which showed that most deformations were within a radius of 4mm from the screw centre. The other results show that a shorter width of the based square gives stiffer and stronger results. Computationally, small bone sample are easier to manage and for accuracy of results, it seems that a square with a side of 15mm gave closer results. In this situation, it was decided to select a compromise size which is 12x12mm based square.

5.3.3. Conclusion

The aim of this part was to prove that it was possible to simplify the modelling process while obtaining FE results in a similar range as the target model results. An objective of 2 bodies with less than 1 million elements was chosen for FE models as explained in section 5.2.1.

Therefore, in order to validate the model, the dimensions used were 10x12x12mm, which represents the full depth and a square around the centre of the screw of 12mm^2. It is important to consider the full depth as it is likely that the well-known intra-specimen variability could happen vertically and therefore the compensation would be biased.

Meanwhile it is also completely legitimate to use smaller samples in order to test different factors like screw design, influence of bone density and bone augmentation. Therefore, in these cases, a bone sample of 4x12x12mm was used.

5.4. Full contact

The creation of the model with full depth and contact and a square base of 12x12mm was made using Mimics package following the description described previously. The final model had 632,272 elements. The element type was linear as tetrahedrons with 4 nodes. Figure 5.23 shows a picture of the model sliced in the middle vertically.

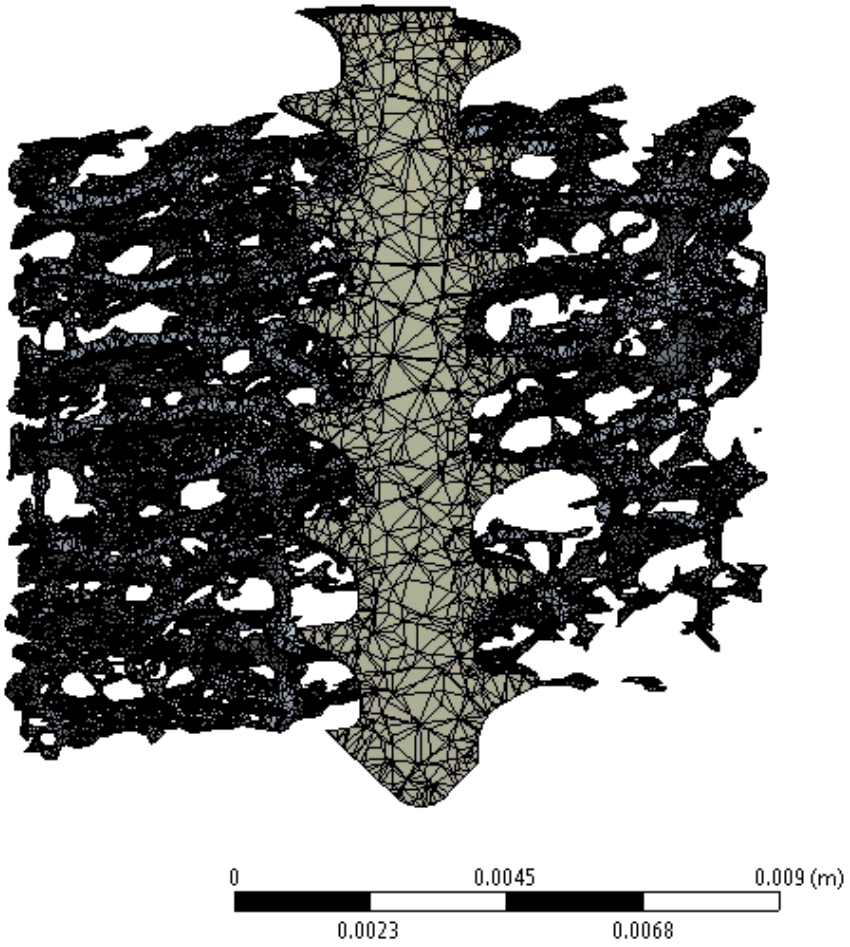

Figure 5.23: Sliced view of the meshes of model with all the contacts.

This model creation was challenging as many stages needed manual interventions as explained in previous part. It takes approximately 3 weeks to create such a model and to import it into Ansys® Workbench.

The boundary conditions were set up with a selection of all the vertexes from the lateral sides and with a displacement of 1mm applied at the top of the screw as illustrated in figure 5.24.

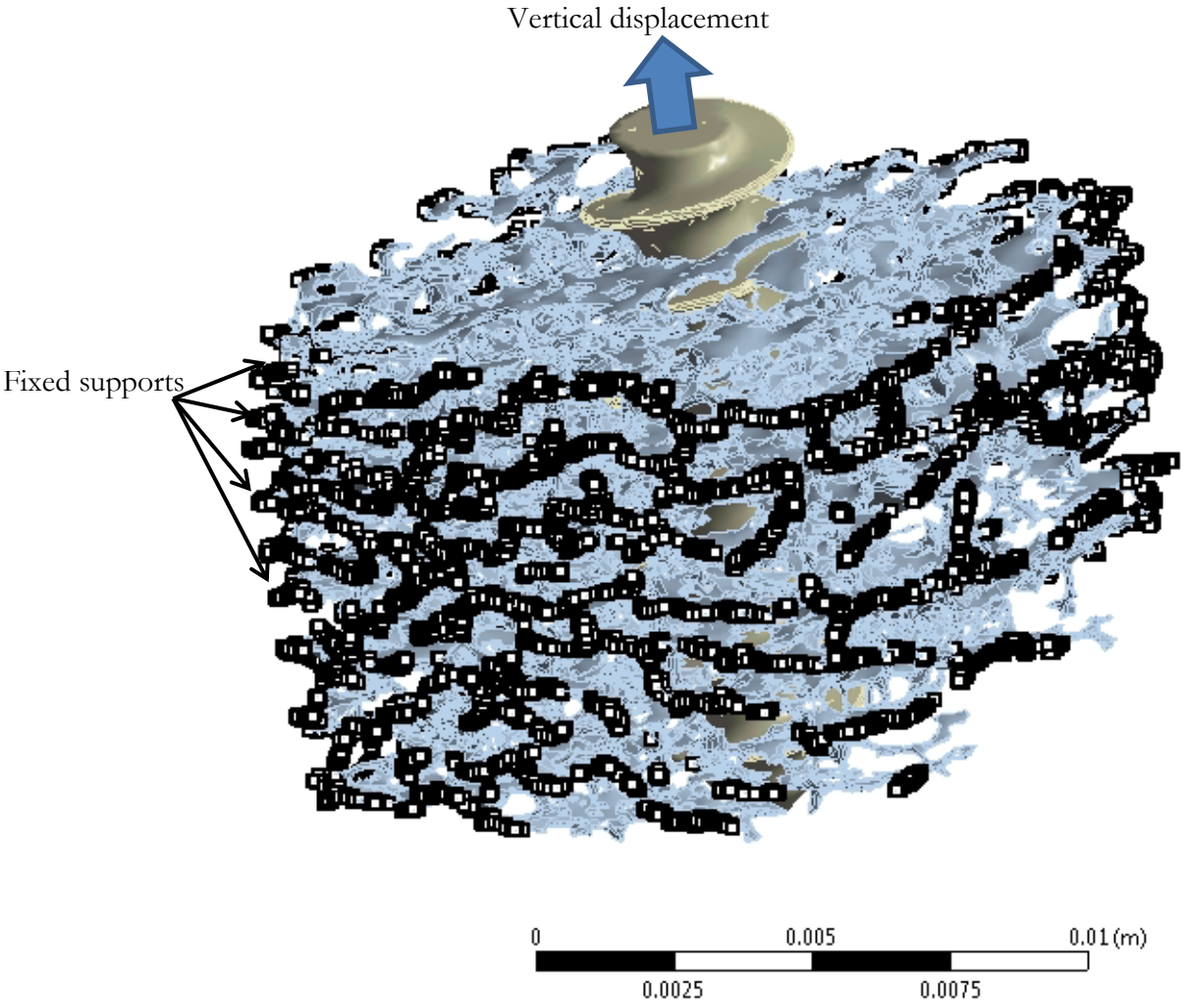

Figure 5.24: representation of the boundary conditions with model

The remaining variables are contact definitions (formulations and frictional coefficient) and the material properties for the cancellous bone.

5.4.1. Contact definitions and influence

Even though it is admitted to use a friction coefficient of 0.3 for the bone implant interface (Chen *et al.*, 2009). Four different friction coefficients have been tested in this simulation: 0.1, 0.3, 0.5 and bonded. In this study, the same material properties as in the previous chapter have been used and the bone sample had dimension 12x12x4mm. The results are shown in figure 5.25.

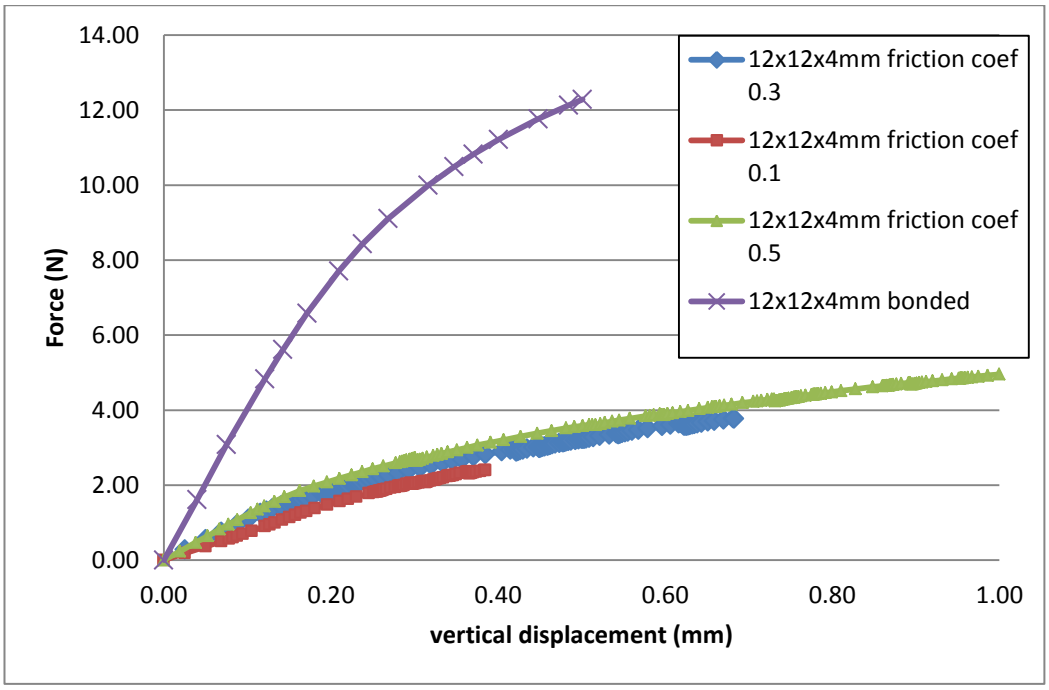

Figure 5.25: Comparison of friction coefficient in screw pull-out simulations

The main result from this study was that a simulation with bonded contact gave much stiffer and stronger results than the simulation with a friction coefficient between 0.1 and 0.5. Also, the differences between results with friction coefficient are relatively negligible to the range of magnitude expected for the validation of FE from the mechanical test. Indeed, simplifications of the model have been applied on the structure and the boundary conditions. Therefore, to conclude this study, it is important to define the contact as frictional rather than bonded and then as done by others (Chen *et al.*, 2009b;

Hou *et al.*, 2004), it has been decided to use a friction coefficient of 0.3 in all the following cases.

Concerning the contact definition in FE, it has been shown in chapter 3 from Simpson study (2005) that there are negligible differences from the use of different formulations for the penetration prevention and if the contact stiffness was between 0.1 and 1 it does not affect the results of the simulation.

5.4.2. Influence of the material property

As seen in chapter 2, cancellous bone structure and mechanical properties vary widely. Therefore many studies use different values for the cancellous bone's Young's Modulus and theoretically it is accepted that it varies from very low in the case of extreme osteoporosis of cancellous bone to 20GPa (Jansen *et al.*, 2009; Currey, 2002; Rincon Kohli, 2003). Similarly, the cancellous bone Yield point value varies up to 190 MPa (Gibson and Ashby, 1987) or 247 MPa (Currey, 2002).

In this part, values from the range used in the literature have been tested in order to find the best matching values. The main challenge with this method is time management and data management. Each of the following trials lasted over a week on the HPC computer with 2 processors E5640 @ 2.40GHz with 48GB RAM and generating files potentially over 500GB. In the previous simulations, the material properties for cancellous bone were Young's Modulus of 2.2GPa and plastic behaviour defined as bilinear hardening model with a yield stress of 35MPa and a tangent modulus of 22MPa (i.e. 1%) (Brown *et al.*, 2011). The results obtained with this set-up are shown in figure 5.25. The mechanical test results, which follows (figure 5.26), presents an offset that removes the beginning of the curve until the system reached the elastic range in order to have more comparable results.

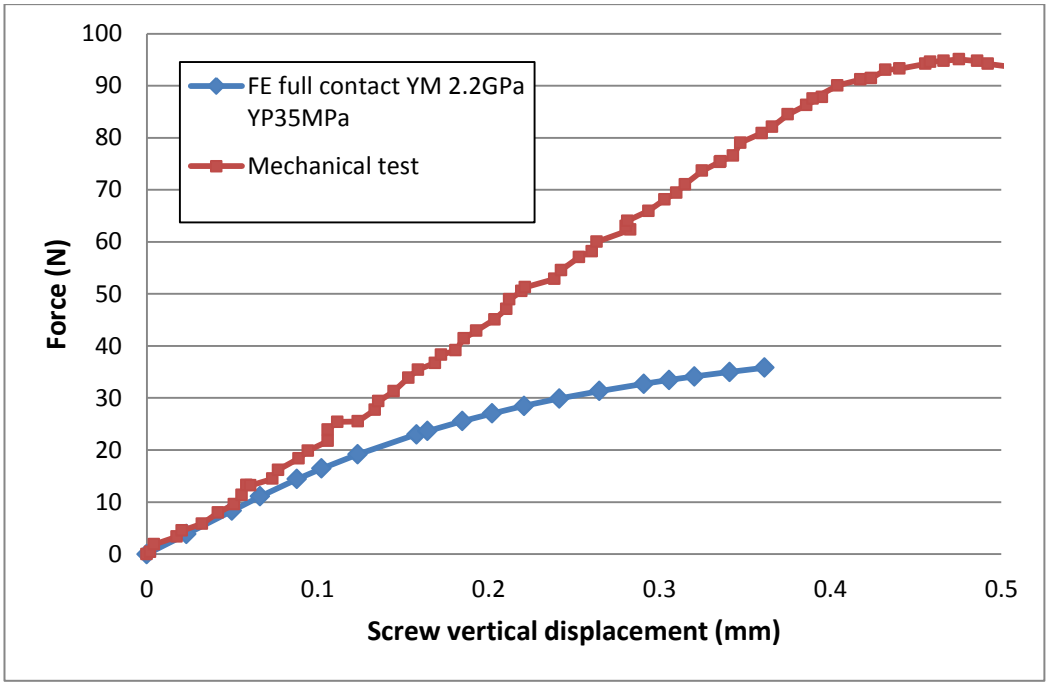

Figure 5.26: Comparison between mechanical results and FE results with Young Modulus of 2.2GPa and yield point of 35MPa.

The results are diverging at an early stage. Therefore the next trial is with the same Young Modulus and with a yield point of 110 MPa. In all these different trials the tangent modulus remains with the same percentage, i.e. 1%, as it is considered that elements would break beyond this point. Moreover, it is complex computationally to obtain results further the yield point as the bone is physically breaking. The results from this new attempt are shown in figure 5.27.

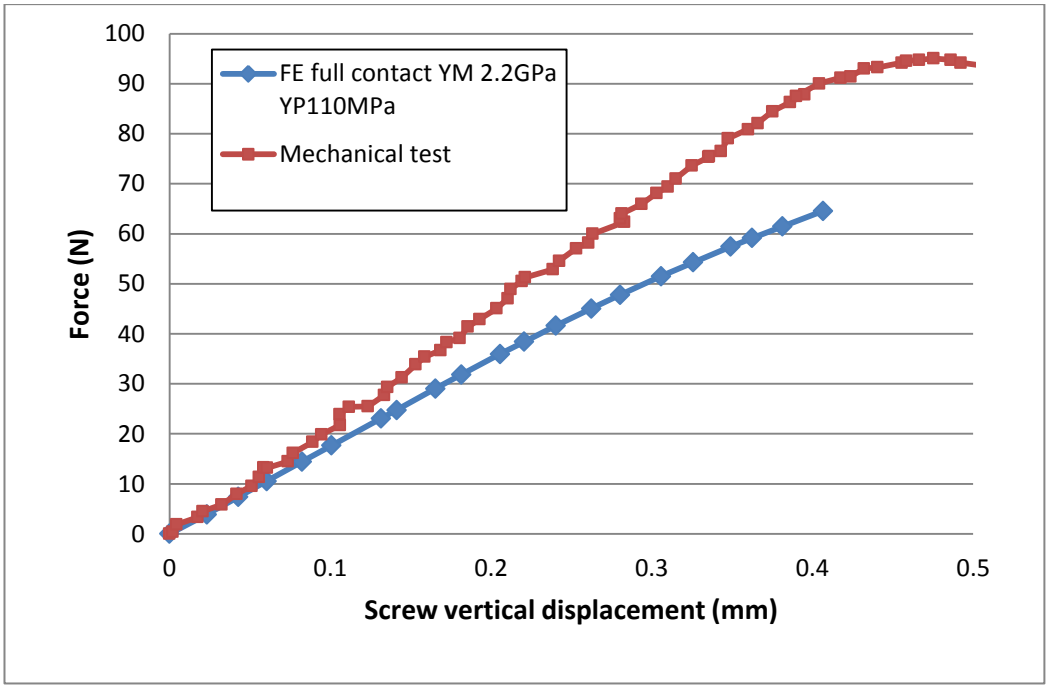

Figure 5.27: Comparison between mechanical results and FE results with Young Modulus of 2.2GPa and yield point of 110MPa.

The results are still diverging and the next trial is with a slightly increase of the Young Modulus to 3GPa and with a new yield point of 140 MPa. The results from this new attempt are shown in figure 5.28.

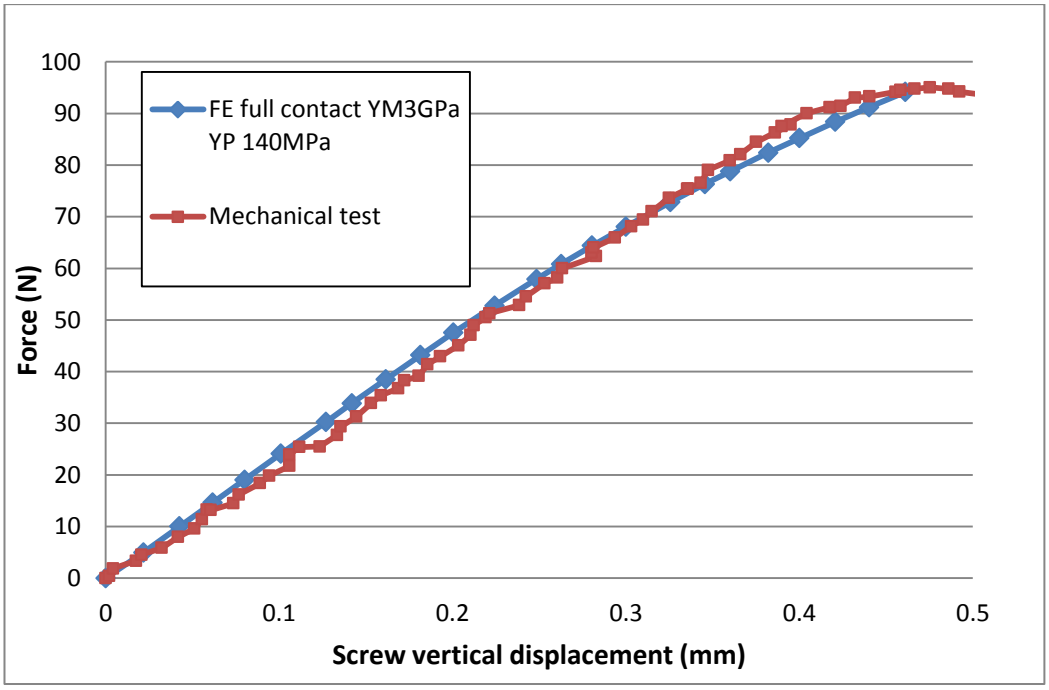

Figure 5.28: Comparison between mechanical results and FE results with Young Modulus of 3GPa and yield point of 140MPa.

The stiffness obtained for the FE simulation is 220N.mm^{-1} while it is 228N.mm^{-1} for the mechanical test. The FE simulation stopped just before the failure point due to the high distortion generated in elements as explained previously. The approximation of the stiffness from the FE simulation is less than 4% which is satisfactory regarding all the modelling constraints applied. Therefore, it is possible to conclude that FE simulations under these conditions are giving relatively accurate results concerning screw pull-out tests.

5.5. Conclusion

The aim of this chapter was to obtain a feasible way for validation of results produced with FE simulation. This stage was very important in order to give credibility to the results obtained in 2D and 3D with simplified models of cancellous bone and also for all the other simulations that have been or will be based on this research. RP appeared not to be ideal and therefore all efforts have been put on a comparison with a mechanical screw pull-out test from a

cancellous bone sample from a cadaver. The main challenge was to find a suitable process in order to generate a model based on the mechanical test. A few software packages were compared and due to the complexity of the cancellous bone structure and the requirements needed for this process, companies' experts were solicited and challenged to achieve this goal as the boundaries of these packages and computer power requirements were pushed. The process finally obtained for the creation of models based on the mechanical test is finally requiring a combination of Mimics and Ansys® software packages jointed installed on computers with special requirements.

Finally, the efforts for this process showed first that FE simulations are giving realistic results as they matched the mechanical test. Then, this new process offered many new possibilities that have never done before: to create FE screw pull-out simulations from human cadaver cancellous bone like to study screw position and type influence, augmentation and also other parameters all of them in real bone.

6. Chapter 6 – Screw position and type influence in real bone

This chapter shows a study of the influence of screw initial position in real bone with 2 types of screw. The first section focuses on the contact areas of different positions and the second section relates to the volume fraction influence.

6.1. Screw- bone contact area variation

Two types of screw with the same outer diameter of 4mm, a cancellous screw and a cortical screw, were moved in a bone sample. The designs are detailed in figure 6.1.

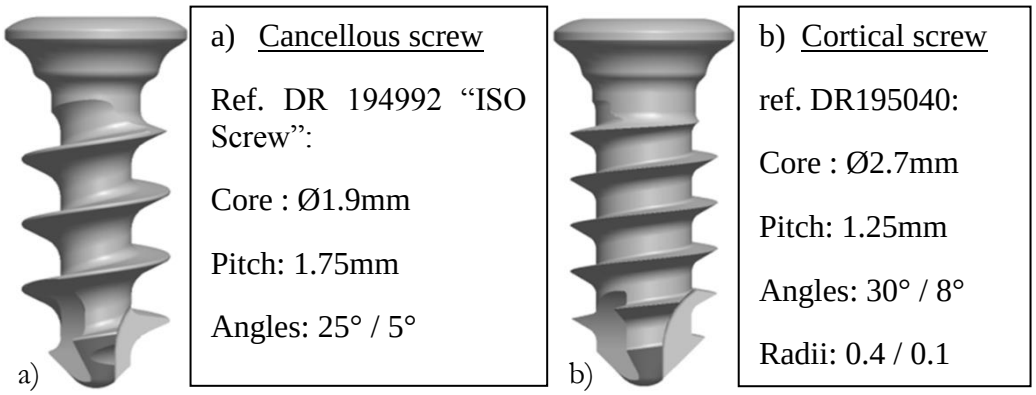

Figure 6.1: a) Cancellous and b) cortical screw details.

The bone sample was created from the bone sample in section 5.1. The top and bottom parts of the bone were chopped in order to have a bone model with 20mm diameter and 4mm depth, as explained in chapter 5. A number of positions of screw in bone were investigated along 2 perpendicular axes X and Y every 0.4mm (figure 6.2).

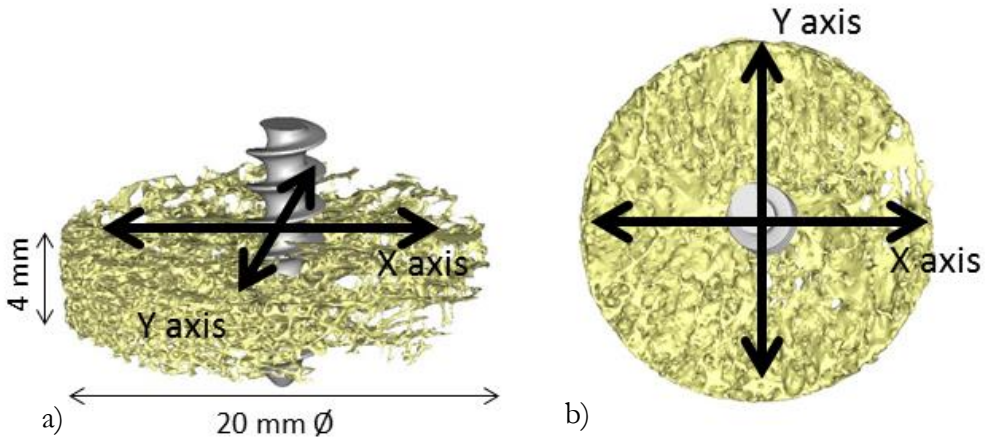

Figure 6.2: a) Isometric and b) top views of the screw and the bone showing the axis along which the screw has been moved in 0.4mm increments

The model can be used to investigate parameters and one measurable parameter that was readily available was contact area (figure 6.3)

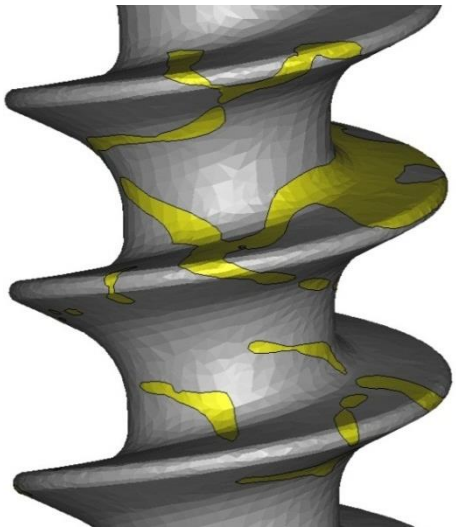

Figure 6.3: Front view of contact area (yellow) on cancellous screw in a bone with 11.6% apparent density

As cancellous and cortical screws have different designs and therefore different external surface areas. The contact area values measured were divided by the contact area of 4mm length of screws in order to base the comparison on unit values for all positions along each axis. The values are represented on figure 6.4 where on each bar chart:

- The red bars show the percentage of cancellous screw contact area as a percentage of the maximum potential for each position.
- The blue bars show the percentage of cancellous screw contact area as a percentage of the maximum potential for each position.

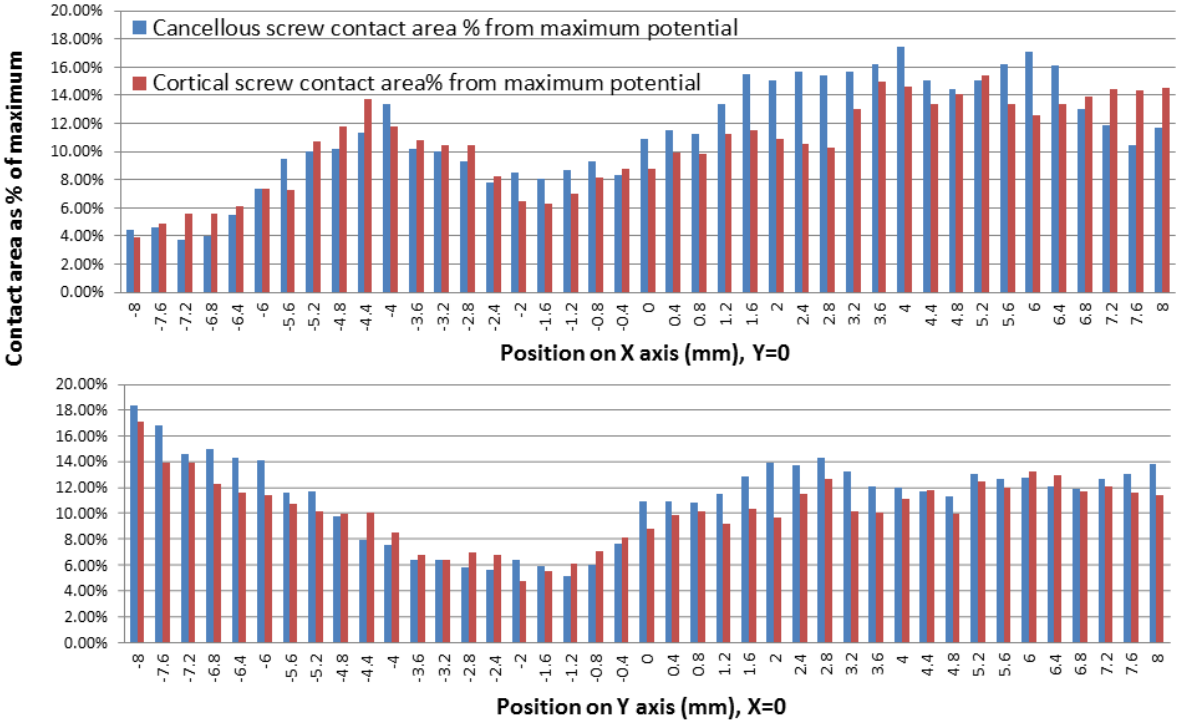

Figure 6.4: Contact area as a percentage of maximum for cancellous and cortical screws on each position.

Table 6.1: Statistics for 4mm depth of bone

Contact area (mm^2)	Cancellous screw	Cortical screw
Mean	7.18	7.36
Standard deviation	2.29	2.05

As FE simulations are highly time consuming, it was decided to undertake a spot check of extreme value cases with four cases. These four cases were required to be at an adequate distance from the sides of the entire bone sample, as it was necessary to have 12x12x4mm around the screw centre to create a bone model with dimensions large enough for the screw pull-out, in the conditions studied in chapter 5.

The four cases selected were:

- Case A (X=3.6mm, Y=0): both contact areas over 14% of the maximum potential area with the minimum difference between the two.
- Case B (X=0, Y=-1.6mm): both contact areas under 6% of the maximum potential area with the minimum difference between the two.
- Case C (X=0, Y=-4.4mm): maximum contact area difference between cancellous screw contact area and cortical screw contact area.
- Case D (X= 2.4mm, Y=0): maximum contact area difference between cortical screw contact area and cancellous screw contact area.

Figure 6.5 shows the positions selected in the entire bone sample with the cancellous screw. For each simulation, the bone sample was cropped to the dimension 12x12x4mm around the screw (figure 6.6). The boundary conditions and material properties were chosen as in Brown *et al.* (2011) study and as detailed in chapter 5.

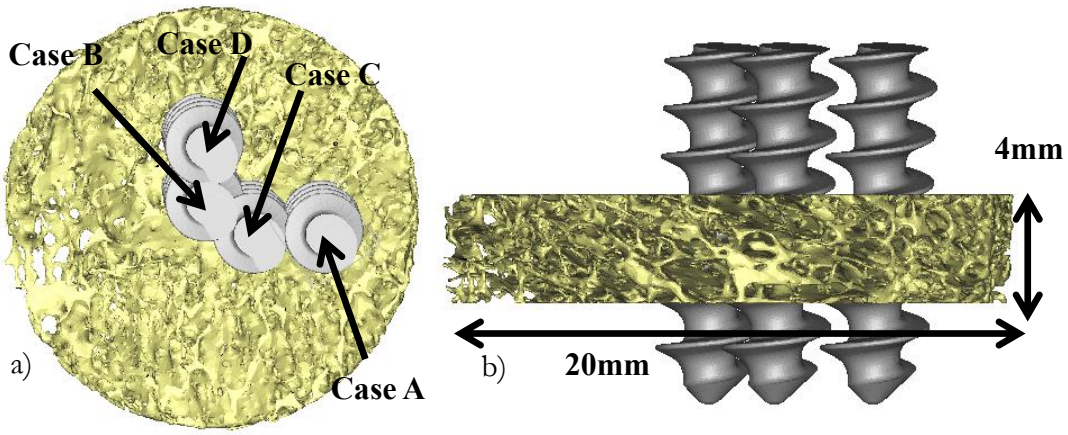

Figure 6.5: a) Top and b) front view of the selected cases in the bone sample.

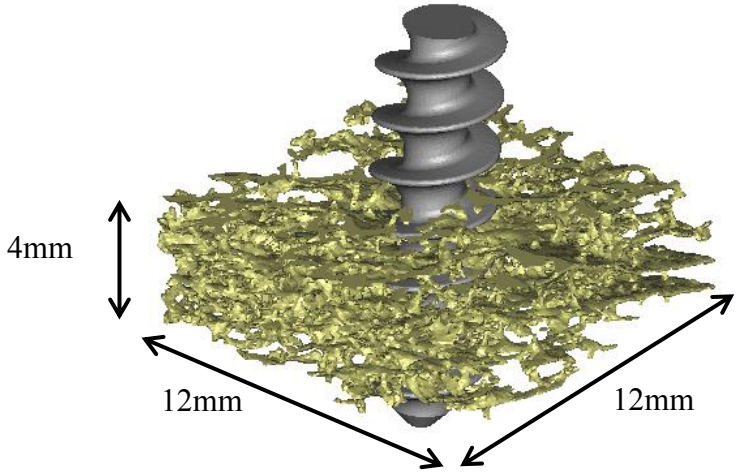

Figure 6.6: Example of model size

Two other cases from the same bone sample were added to this study:

- Case E: similar contact area (cancellous screw 8.3% and cortical screw 8.5%)
- Case F: similar contact area (cancellous screw 13.1% and cortical screw 12.6%)

It was possible to obtain specific data concerning each bone case with the use of ImageJ free software (Abramoff *et al*., 2004) combined with the plugin BoneJ (Doube *et al.*, 2010). Figure 6.7 showed the thickness measurement for the case D.

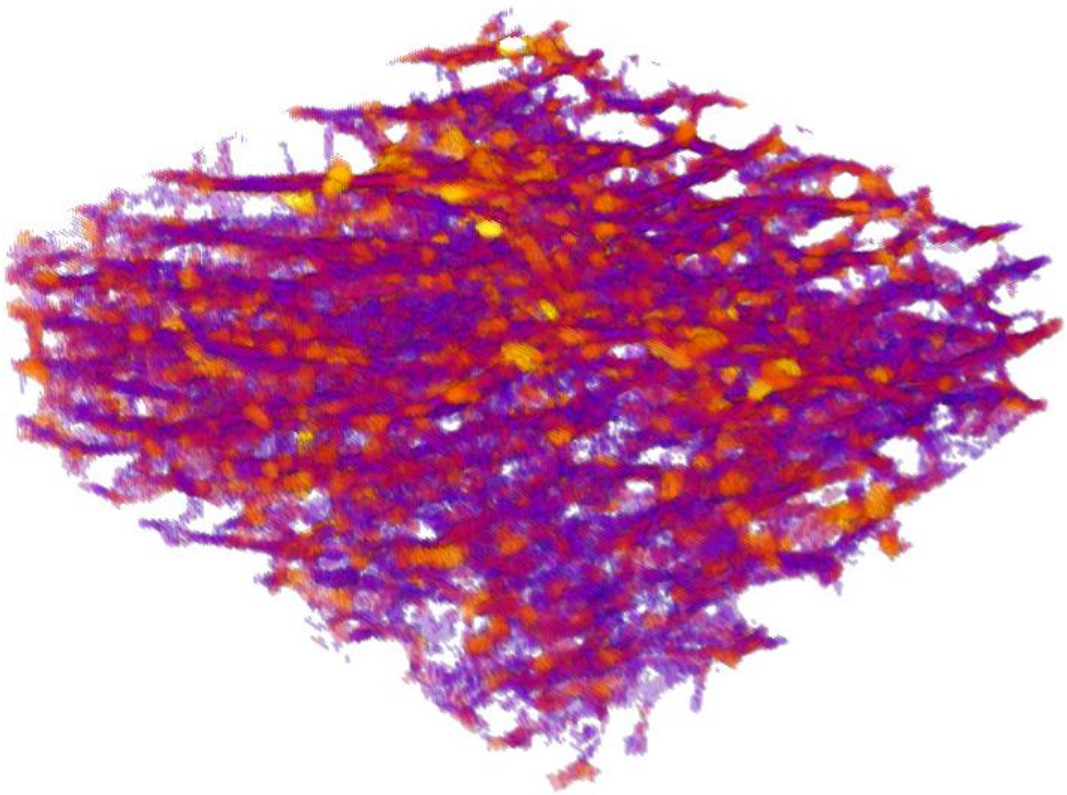

Figure 6.7: Strut thickness measurement for case D using ImageJ/BoneJ – Yellow for larger struts and blue for smaller struts.

The selected data were:

- **Trabecular thickness** (Tb.Th) (mean, standard deviation and maximum) and **trabecular spacing** (Tb.Sp) using Dougherty and Kunzelmann (2007) method.
- **Bone volume** (BV), **total volume** (TV) and **volume fraction** (BV/TV)
- **Structure model index** (SMI) using Hildebrand and Ruegsegger (1997) method with 2 voxels for resampling. The results to define cancellous bone structures are comprised between 0 and 3 where 0 means a plate structure and 3 means a rod structure = 0; rod = 3
- **Degree of anisotropy** (DA) is calculated from the formulae: $DA = 1 - \frac{\text{Short axis}}{\text{Long axis}}$, so the results should be comprised between 0 and 1 where 0 means isotropic and 1 means anisotropic bone.

Table 6.2 shows the organised data. It appeared that there was no major structural difference between each bone sample apart from the volume fraction, as they all had similars Tb.Th and DA and a SMI for a rod like structure.

Table 6.2: Data for each cancellous bone case

Bone sample	Mimics BV/TV (%)	Tb.Th Mean (mm)	Tb.Th Std Dev (mm)	Tb.Th Max (mm)	Tb.Sp Mean (mm)	Tb.Sp Std Dev (mm)	BV (mm^3)	TV (mm^3)	BV/TV (%)	SMI	DA
Case A	12.1%	0.152	0.049	0.427	0.903	0.323	72.4	590.6	12.3%	2.52	0.69
Case B	10.7%	0.147	0.048	0.374	0.977	0.366	62. 2	590.6	10.5%	2.64	0.66
Case C	11.6%	0.150	0.048	0.374	0.985	0.426	66.8	588.7	11.4%	2.60	0.67
Case D	11.9%	0.151	0.049	0.427	0.925	0.325	68.9	588.8	11.7%	2.53	0.72
Case E	9.5%	0.144	0.046	0.395	0.99	0.344	56.2	591.6	9.5%	2.83	0.61
Case F	12.6%	0.158	0.054	0.518	0.921	0.346	72.1	572.3	12.6%	2.40	0.71

A screw pull-out simulation was undertaken for each cancellous bone case with the 2 types of screw. A plot of stiffness against contact area (figure 6.8) showed generally increasing stiffness with increasing contact area between screw and bone.

Stiffness was chosen to be the indicator in these studies due to computing limitation. Stiffness could be obtained from a very small screw vertical displacement while strength needed more displacement and often elements would get too distorted before reaching that point. Many studies supported the relationship between stiffness and strength (Fyhrie and Vashishth, 2000, Yeni and Fyhrie, 2001, Yeni *et al.*, 2003) and so a study for all the cases reaching strength was carried out in appendix E.

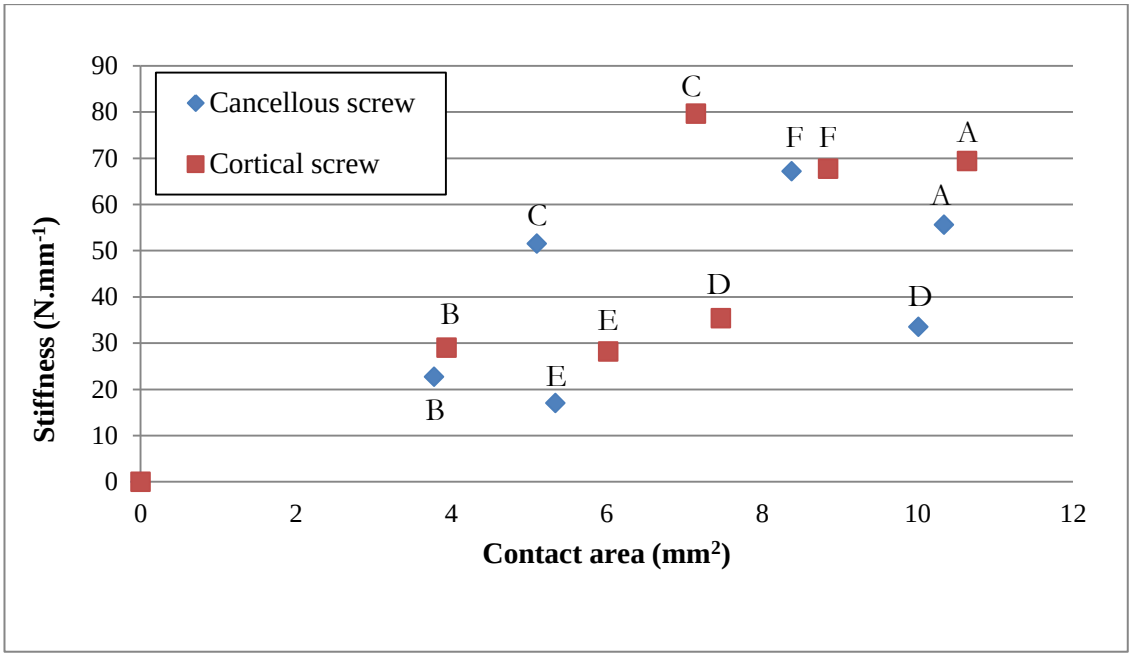

Figure 6.8: Stiffness by contact area

So far, the entire contact area was taken into consideration, and practically only the surface contact on the upper part of the screw was resisting during the pull-out. Therefore, the contact area elements were exported separately to the FE software Ansys® APDL. It was then possible to obtain a list of the nodes with their coordinates and also a list of all the elements with their related nodes (figure 6.9). Thus it was possible to calculate the normal for each element.

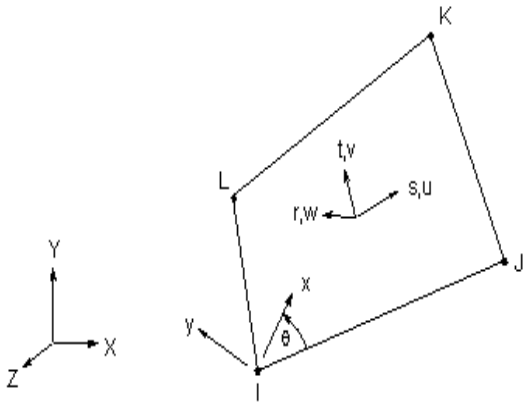

Figure 6.9: Illustration of the composition of an element

Each normal was given a coefficient according to the area of the surface element and classified in one of the three categories according to the normal angle with the horizontal. A representation of the categories was sketched on figure 6.10:

- Resisting contact: normal to contact >10° - Blue
- Frictional contact: -10°< normal to contact<10° - Green
- Non resisting contact: normal to contact < -10° - Red

The angle value of 10° has been arbitrarily chosen to ensure the selection of the root of the thread as a separate category.

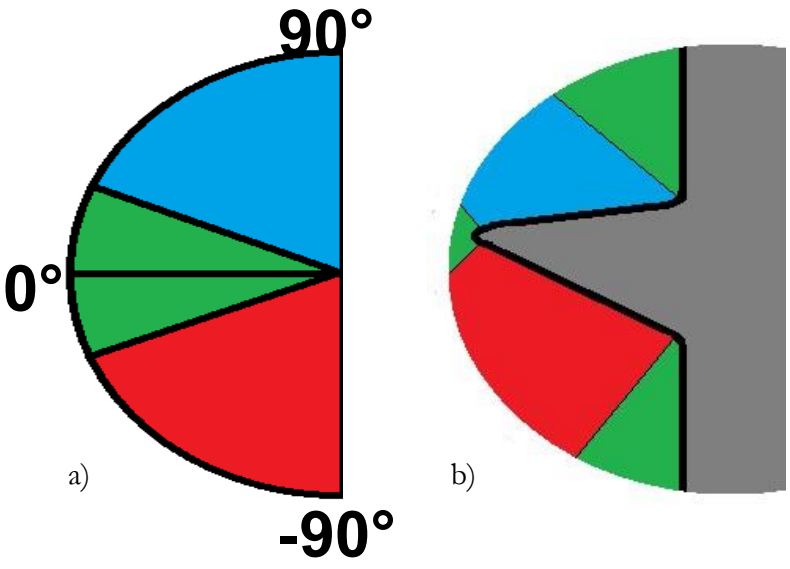

Figure 6.10: a) Normal to contact categories representation and b) Normal to contact categories representation on a screw thread

A plot of the pull-out stiffness against the upper resisting surface contact area also supported that generally increasing stiffness was induced with generally increasing contact area between screw and bone (figure 6.11)

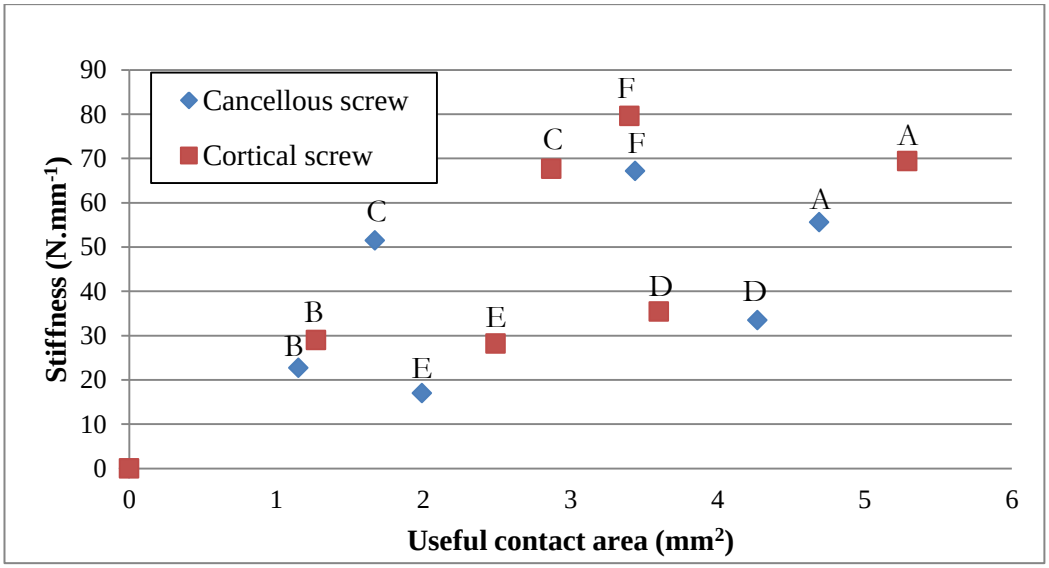

Figure 6.11: Stiffness by resisting contact area

No significant improvements appeared in the results of useful contact area from the results from total contact area. Part of the variability in the relationship between stiffness and contact area might be explained by local variations as illustrated by the exceptional cases in figure 6.12. Therefore, it was possible to conclude that contact area is not a precise predictor of stiffness

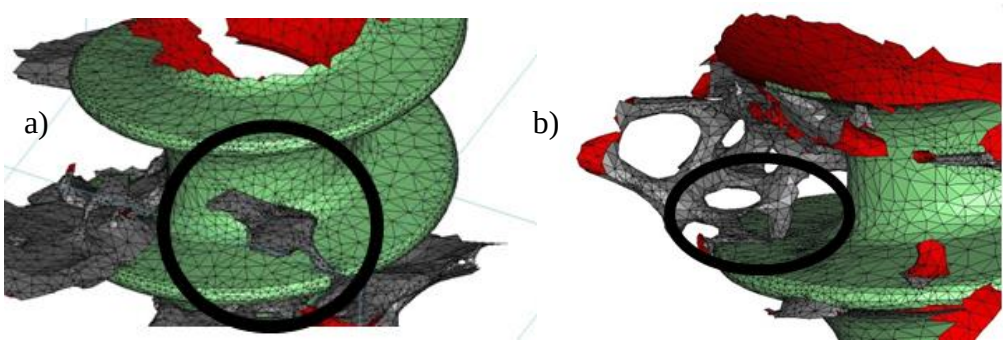

Figure 6.12: Examples of large contact with weak structure a) and small contact with strong structure b)

The actual contact area as a percentage of the maximum potential contact area varies from 3.7% to 18.3% for the cancellous screw and from 3.9% to 17.1% for the cortical screw depending on bone apparent density. So whatever

the screw design, the bone structure variability makes the contact area vary significantly.

Finally, when the screw performances were compared by cancellous bone cases as plotted in figure 6.13.

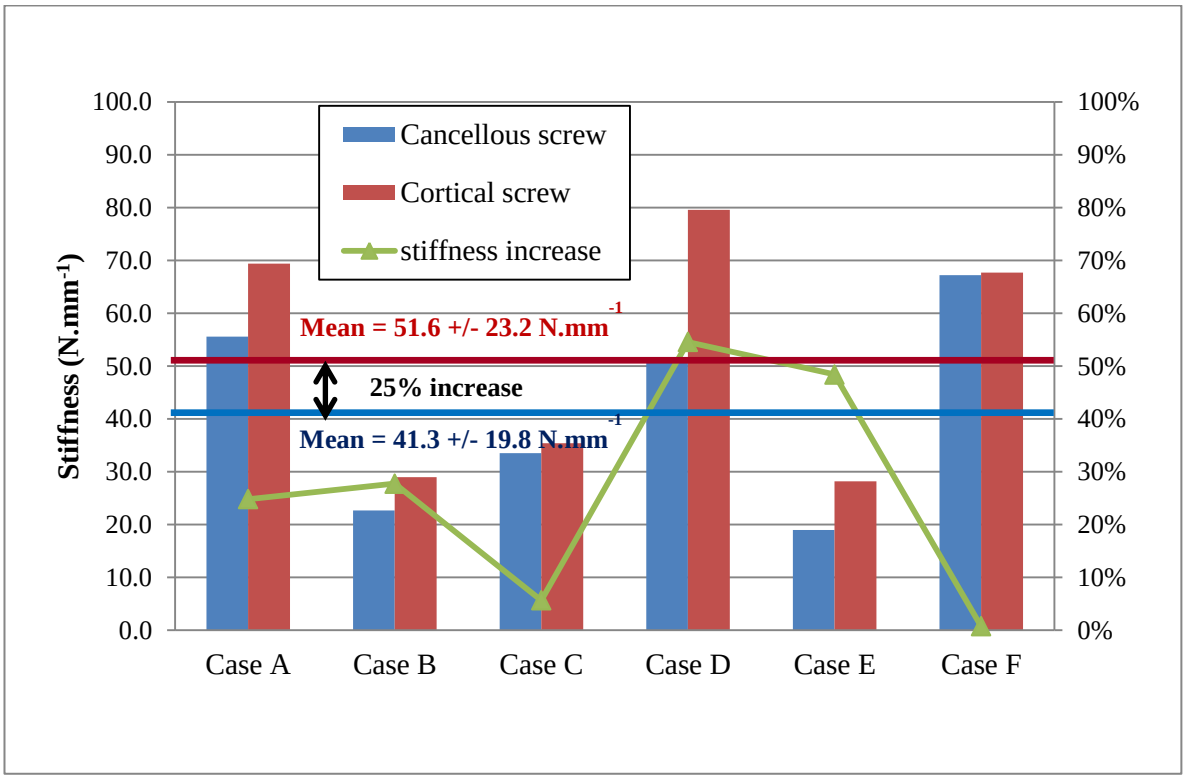

Figure 6.13: Stiffness by position in the bone sample and by screw

It appeared that in all the selected cases, a cortical screw gives higher stiffness than a cancellous screw and overall, the mean results of cortical screws are 25% stiffer from the mean results of cancellous screws.

6.2. Bone volume fraction influence

Throughout these studies, the bone apparent density has been systematically calculated from the cropped bone sample: 12x12x4mm (figure 6.6). It was necessary to calculate the bone apparent density for each cropped sample due to the well-known intra-specimen bone variation (Keaveny and Yeh, 2002).

It was evident that a bone sample with similar bone volume fraction could give very different contact areas. For example case A had a bone volume fraction of 12.1% and a contact area of 10.34mm^2, while case D had a bone volume fraction of 11.9% and a contact area of 5.10mm^2. This difference was observable (figure 6.14), in case a) the screw part in the bone was hardly visible while in case b) the screw could be observed.

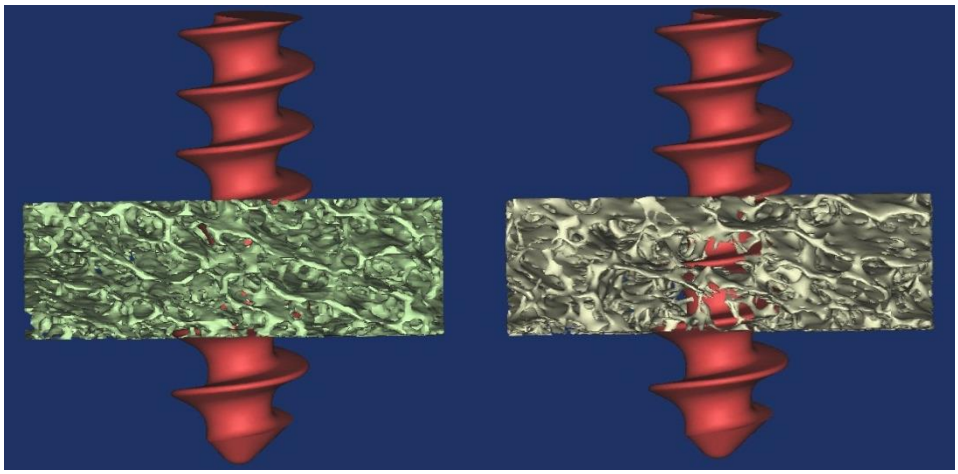

Figure 6.14: a) Cancellous screw in case A and b) Cancellous screw in case D.

It has been therefore decided to look at the volume fraction just around the screw and it has been called the local volume fraction. The local volume fraction was taken as the volume fraction of the piece of bone immediately around the screw (4x4x4mm) (figure 6.15) and the overall volume fraction was of the sample (12x12x4mm). A cube of 4mm sides was chosen because the screw outer diameters were 4mm.

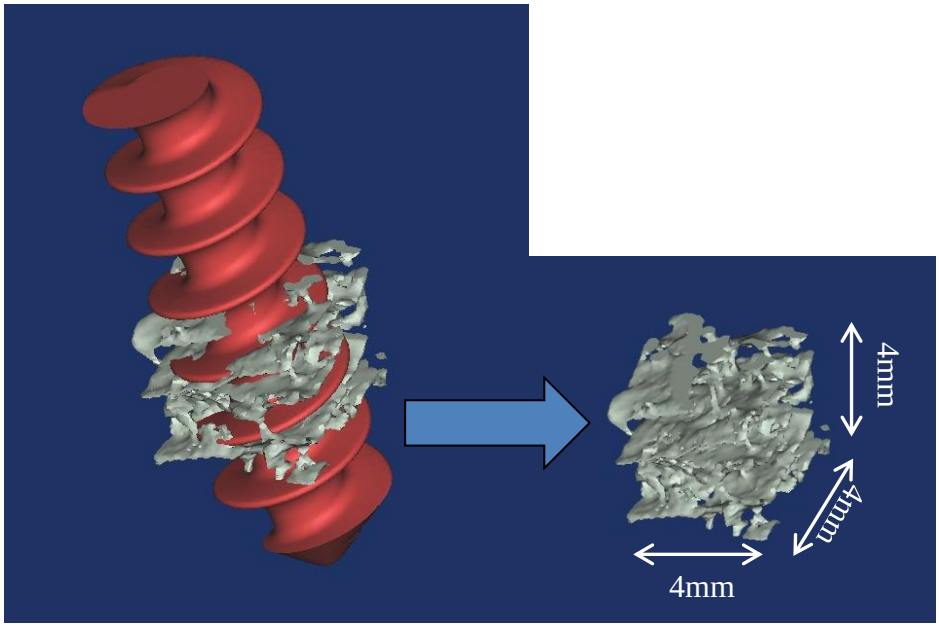

Figure 6.15: Illustration of the local volume fraction

Stiffness pull-out was then plotted against the overall volume fraction and local volume fraction, with results compared on 2 graphs (figure 6.16).

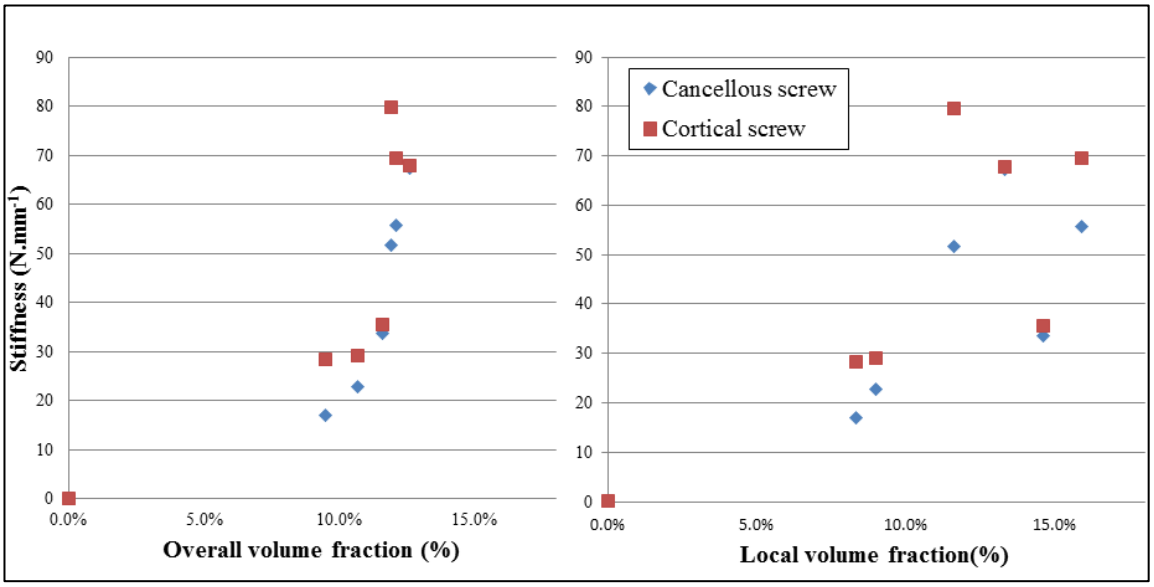

Figure 6.16: comparison of relation between stiffness and a) overall volume fraction and b) local volume fraction.

From this comparison, it was observed that stiffness by overall volume fraction seemed to have a power law relationship. New models were created

with volume fraction of 6.7%, 15%, 17.5% and 20%. These models were created from the cancellous bone sample case E and artificially inflated and eroded using functions available in Mimics. Pull-out simulations were undertaken with cancellous and cortical screws and the results are displayed in figure 6.17.

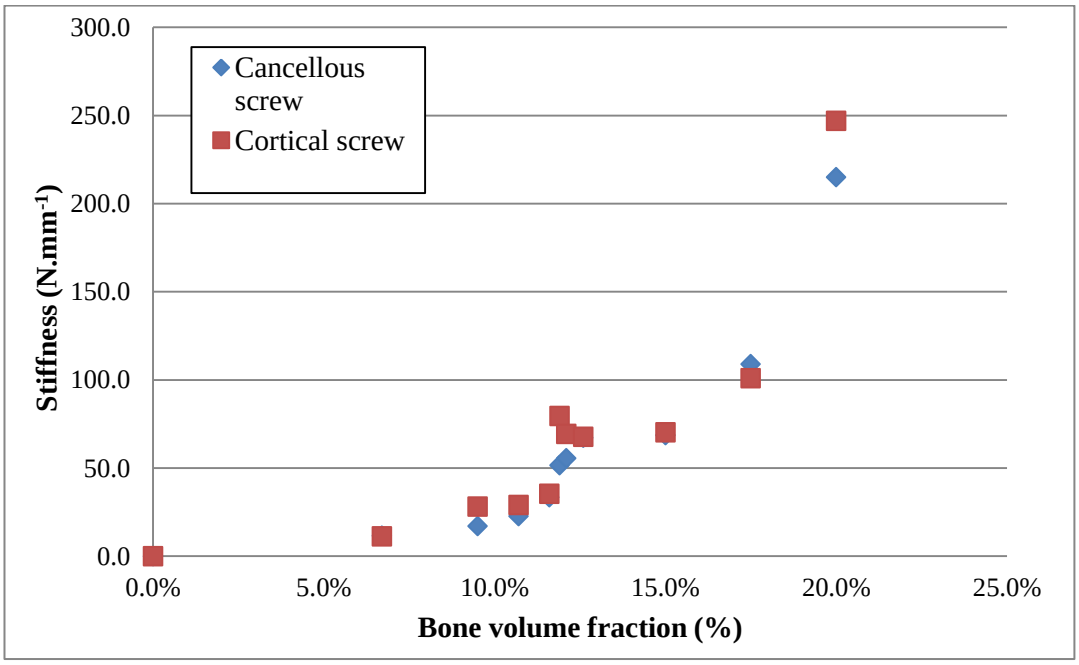

Figure 6.17: Stiffness against apparent density with new values from

A model with a volume fraction of 100% (continuum) was developed and added to the others plotted this time on a $\log_{10}$-$\log_{10}$ scale (figure 6.18).

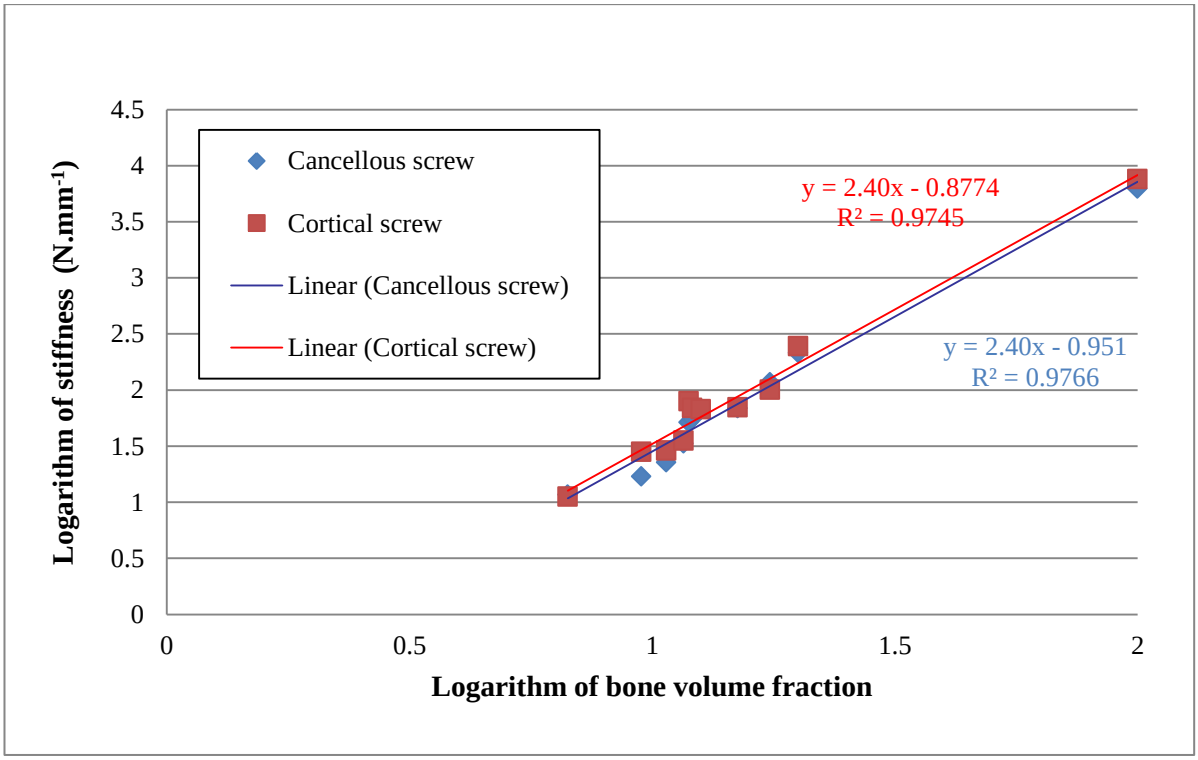

Figure 6.18: Screw pull-out stiffness by volume fraction density for cancellous and cortical screw on a log-log scale

For each screw, a power law relationship was able to describe the correlation between stiffness and bone volume fraction. This phenomenon was already observed in order to relate yield stress to apparent density in tension or compression tests on cancellous bone by Morgan and Keaveny (2001).

For the cancellous screw:

$$\text{Log}_{10}\ \text{Stiffness} = 2.40 \times \text{Log}_{10}\ \text{Volume fraction (\%)} - 0.951$$

$$\text{Stiffness} = 10^{-0.951} \times \text{Volume fraction (\%)}^{2.40}$$

$$\text{Stiffness} = 0.112 \times \text{Volume fraction (\%)}^{2.40}$$

For the cortical screw:

$$\text{Log}_{10}\ \text{Stiffness} = 2.40 \times \text{Log}_{10}\ \text{Volume fraction (\%)} - 0.877$$

$$\text{Stiffness} = 10^{-0.877} \times \text{Volume fraction (\%)}^{2.40}$$

$$\text{Stiffness} = 0.133 \times \text{Volume fraction (\%)}^{2.40}$$

A summary of all the results obtained in this study is available in appendix F.

In conclusion, all cases studied showed that cortical screws gave better stiffness than cancellous screws. No correlation was found between the stiffness and the contact area, useful contact area, or bone volume fraction. A highly probable correlation, with coefficients of determination R^2 superior to 0.97, between stiffness and bone volume fraction was found for both types of screws. This correlation shows that a small variation of volume fraction could significantly alter the stiffness. The correlation formula confirmed the fact that cortical screws established better stiffness than cancellous screw in any bone through a higher coefficient.

7. Chapter 7 – Augmentation study

This chapter details a study on the influence of bone augmentation on screw pull-out. The first section describes briefly a study carried out by Stryker, prior to this PhD project, on screw pull-out from augmented and non-augmented cancellous bone in cadavers as background to the model here. The second section explains the modelling based on the process from chapter 5 except that software limitations appeared requiring many manual inputs. The third section explains the simplification made which allowed the creation of further simulations. The results from these simulations are shown in the final section.

7.1. Cadaver study

This study was carried out by Stryker prior to the beginning of this PhD project; the results are presented in figure 7.1 and one of the reasons of this research project was to explain the findings. This augmentation study aimed to show the effect of bone augmentation on screw pull-out. The principle was to take two equivalent bone samples from each cadaver. For example, the first bone sample could be from the head of the right femur and then, the second bone sample would be from the head of the left femur.

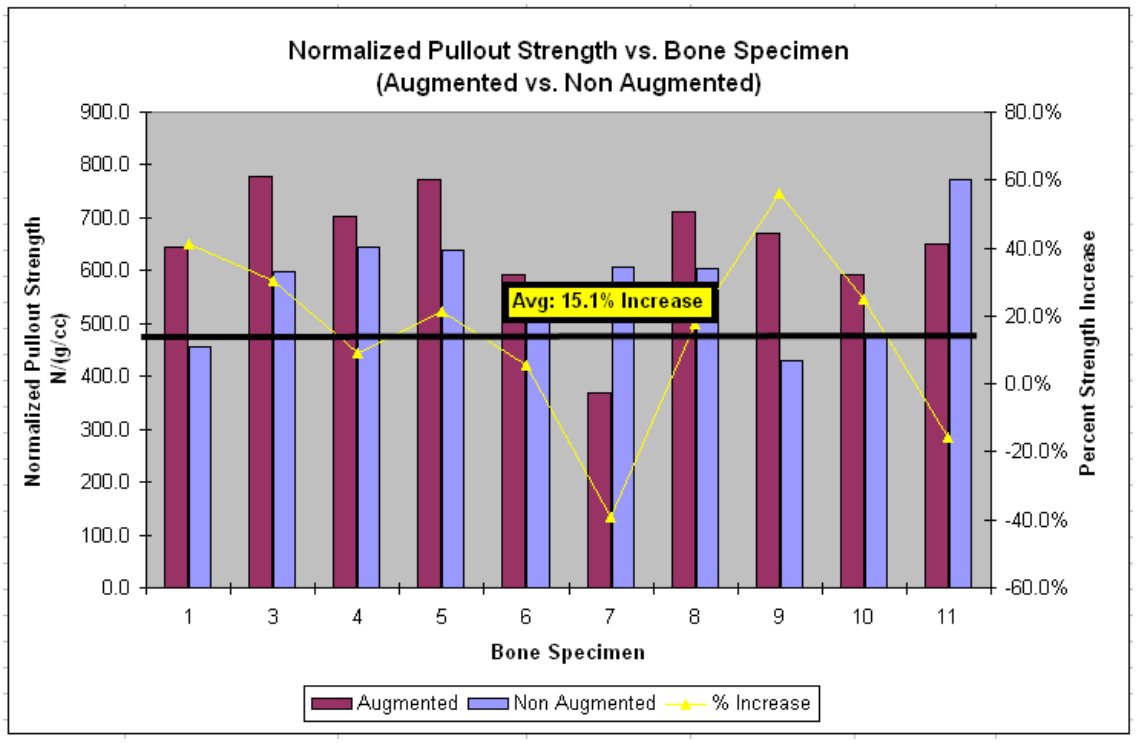

Figure 7.1: Cadaver study of screw pull-out from augmented and non-augmented cancellous bone (Stryker Osteosynthesis)

The results of this study are shown in figure 7.1 and although showing an average increase of 15.1% for the normalised strength for the cases with augmented bone, it appeared unexpectedly that 2 out 11 (bone specimen 7 and 11) showed better results without augmentation. There is also an animal study (Larsson *et al.*, 2012) obtaining similar results.

7.2. FE models

This section is about the initial modelling process for bone augmentation. This first model was more complex than previous studies, with 3 bodies and 3 types of contacts, and was used for comparison with the model which was simplified (2 bodies, 1 contact).

7.2.1. First result

Initially a cylinder of diameter 2.7mm was inserted in the bone model from case E (Volume fraction 9.5%). The modelling process was supposed to be similar as case E in chapter 6, except the method for the insertion of cement needed modification. Mimics became a limiting factor when modelling 3 bodies together. The previous modelling process was not fully automated and for the case of 3 bodies, it was not possible to insert and remove surfaces automatically. In this case, it was necessary to make the 3 bodies intersect and remove unwanted surfaces from final assembly, classifying the other surfaces according to the category they belonged. In this case, there were 6 categories of surface: bone, screw, cement, interface of the bone and the screw, interface of the bone and the cement and interface of the cement and the screw. Only after selecting and classifying the relevant categories of surfaces, it was possible to continue the process described in chapter 6. The model created (figure 7.2) was made of 3 bodies: screw, bone and cement and the different surfaces of contacts were defined.

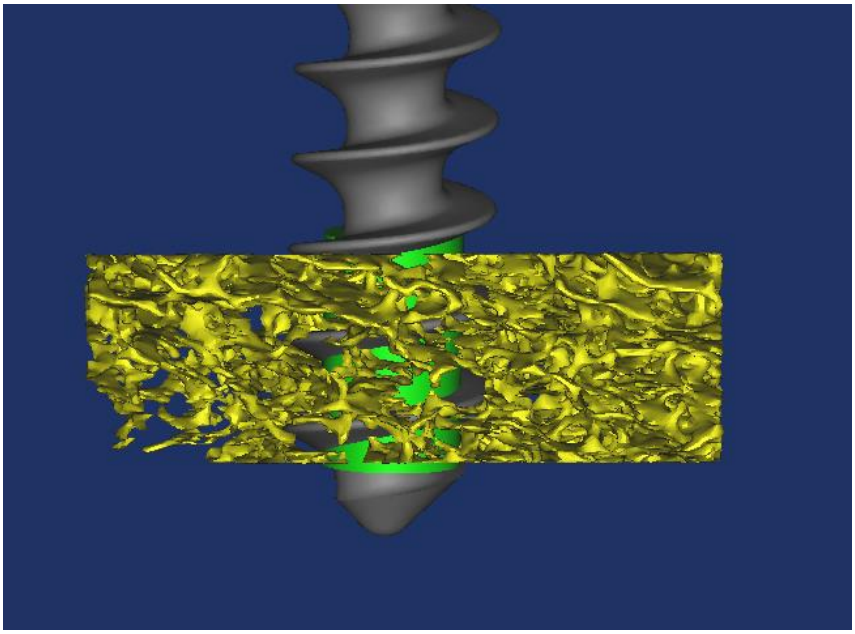

Figure 7.2: Cancellous bone Case E augmented (yellow) with 2.7mm diameter cement (green) and cancellous screw (grey).

As explained in chapter 3 and 4, the number of contacts was challenging for running simulations. This case with 3 categories of contacts was even more challenging and it took over 4 weeks in order to create this model. The results are compared with case E non-augmented and with cancellous screw in figure 7.3.

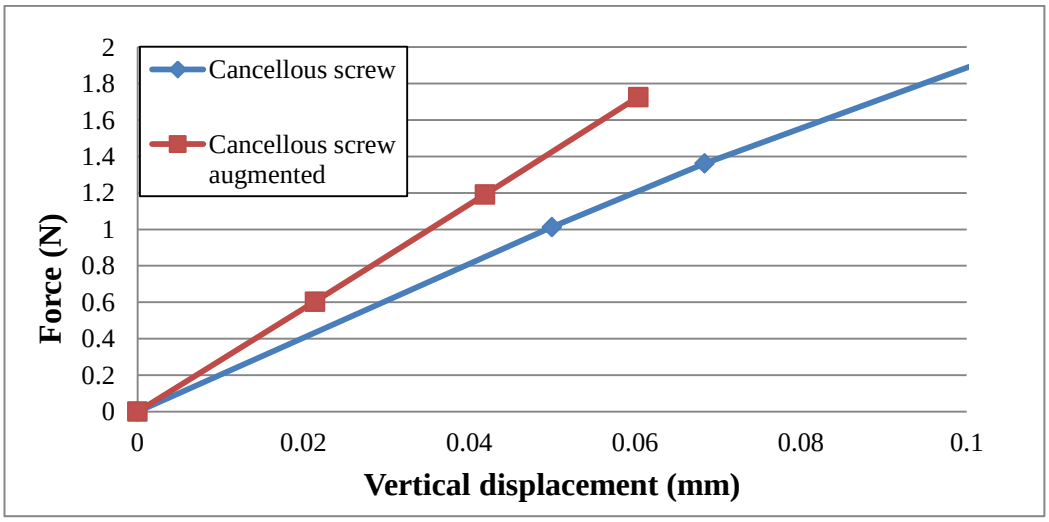

Figure 7.3: Stiffness comparison between cancellous screw with and without augmentation in case E

The stiffness measured for the augmented case was 28.6N.mm^{-1} and 19.0 N.mm^{-1} without augmentation. In this case, the augmentation increased the screw pull-out stiffness by 51%. These results were then compared to the previous case from chapter 6 in figure 7.4.

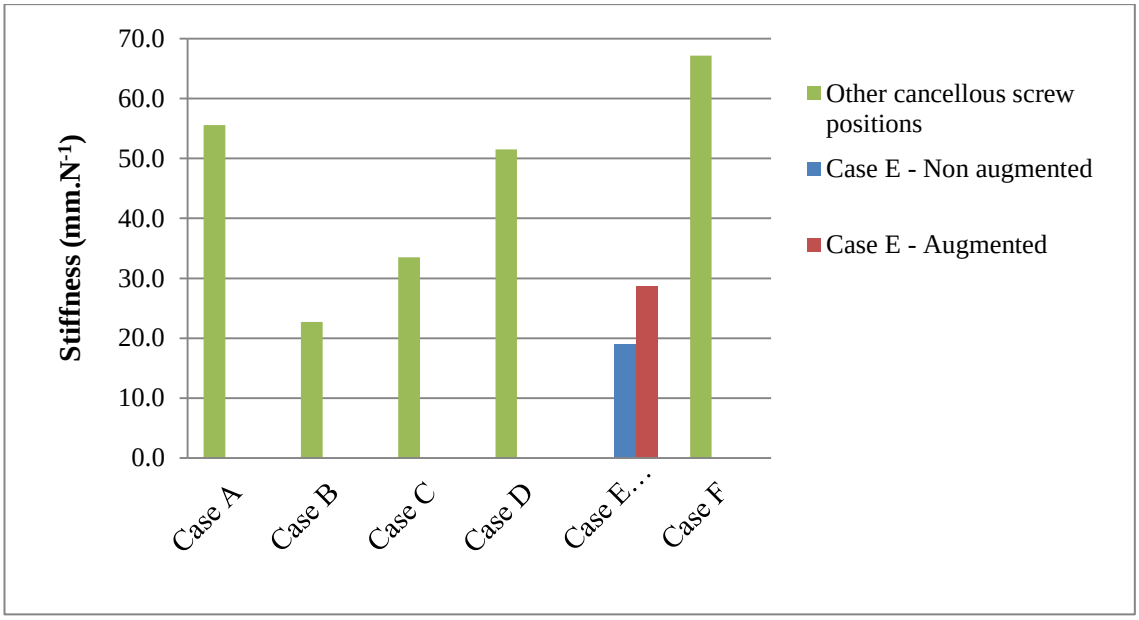

Figure 7.4: Comparison of case E augmented and non-augmented with previous cases non-augmented

This result shows that the screw pull-out of a cancellous screw is 51% stiffer with bone augmentation in the same conditions. However, as seen in chapter 6, cancellous screw pull-out stiffness can be significantly greater as a result of a small change in initial position and here case E - augmented has still a lower stiffness than cases A, C, D and F. This result can already explain the results obtained by Stryker on screw pull-out on augmented and non-augmented cancellous bone where augmented cases are giving lower results than non-augmented.

7.2.2. Simplification

Significant challenges were faced with this augmented model such as creation of the model with Mimics, mesh quality and number of contacts in Ansys®. Therefore simplification through assimilation of the cement as part of the bone as sketched in figure 7.5 was carried out. This simplification was made as the cement was considered as calcium phosphate cement and when crystallised, it became hydroxyapatite which is the principal mineral component of bone. Also as described in section 3.1.1, the cancellous bone was defined

using a Young's Modulus of 2.2GPa (Rincon Kohli, 2003) with a yield stress of 35MPa and the cement was modelled with calcium phosphate cement's properties with Young's modulus of 1.52GPa and a yield stress of 16.3MPa (Ikenaga *et al.*, 1998; Brown *et al.*, 2011). The simplification principle was to consider that these properties could be assimilate as similar in comparison to the material properties of the titanium alloy screw (Young's modulus of 114GPa).

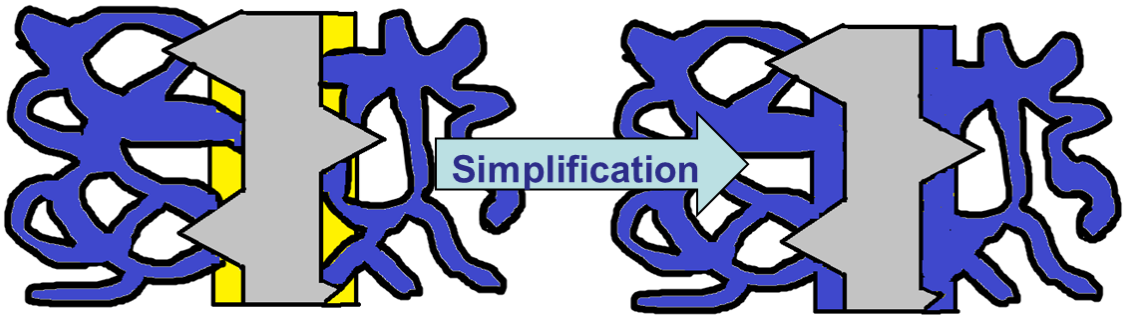

Figure 7.5: Sketches representing the simplification process for augmented case: cancellous bone in blue, cement in yellow and screw in grey.

The model boundary conditions, material properties and contact definitions before and after simplification are given in table 7.1:

Table 7.1: Details of modelling before and after simplification for augmented cases.

	Boundary conditions	**Material properties**	**Contacts**
Before simplification	Fixed on the sides Vertical displacement of 0.3mm on top of the screw	Bone: Young Modulus: 2.2GPa Yield Point: 35MPa Cement: Young Modulus: 1.5GPa Yield Point: 16.3MPa Titanium: Young Modulus: 114GPa	Cement/Bone: bonded Cement/Screw: frictional (0.3) Bone/Screw: frictional (0.3)
After simplification	Fixed on the sides Vertical displacement of 0.3mm on top of the screw	Bone and cement (as one body): Young Modulus: 2.2GPa Yield Point: 35MPa Titanium: Young Modulus: 114GPa	Bone/Screw: frictional (0.3)

A simplified model was created from the augmented case modelled and the comparison showed a close agreement for pull-out stiffness with the non-simplified model: 32.8N.mm^{-1} before and 32.3N.mm^{-1} after simplification.

7.2.3. Model tested

With the simplification it was then possible to create four models (figure 7.6): 3 with the cancellous screw and 1 with the cortical screw. Only one case of augmentation was created with the cortical screw as the cortical screw had a core diameter of 2.7mm and the cement diameters were chosen to be: 2.3mm, 2.7mm and 3.2mm.

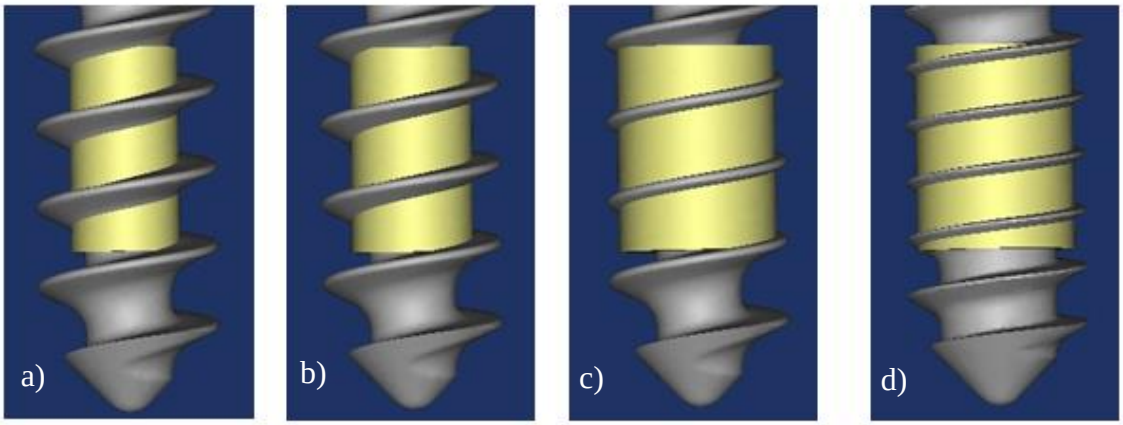

Figure 7.6: a) 2.4mmØ cement with cancellous screw, b) 2.7mmØ cement with cancellous screw, c) 3.5mmØ cement with cancellous screw and d) 3.5mmØ cement with cortical screw

These four models were tested in 3 different cancellous bone samples with volume fraction: 6.7%, 9.5% and 12.1%. The sample with volume fraction of 6.7% is the cancellous bone model that has been software-eroded in order to reach a very low value of volume fraction and the 2 other samples were case E (9.5%) and case A (12.1%) from the screw position influence study in chapter 5.

7.3. Results and conclusion

The results of the different cases studied are shown on the figure 7.7.

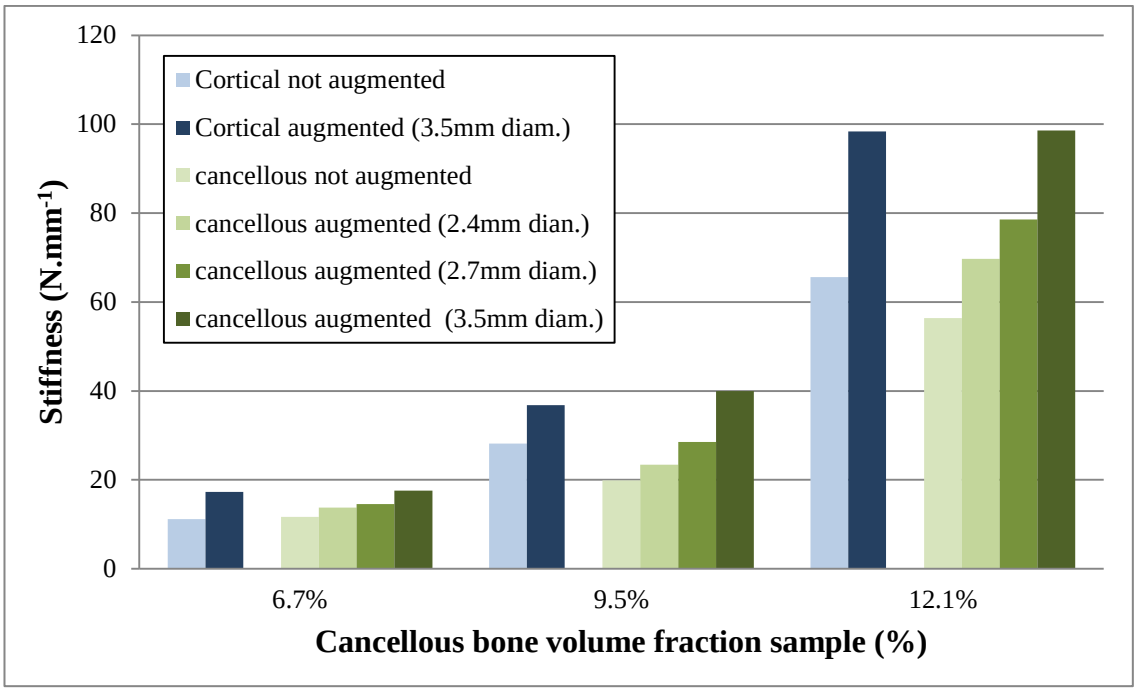

Figure 7.7: Summary results from augmented cases studied

The results were grouped by bone cases. Cortical screw results were presented in blue and cancellous screw results in green. For each bone case and screw, it appeared that bone augmentation each time improved the stiffness.

The diameter size of cement was significant as the larger the cement diameter the better the stiffness for the cancellous screw. Also when comparing cortical and cancellous screws with the same diameter of augmentation (3.5mm diameter), the results were similar, with the first time cancellous screw giving slightly better results:

- $17.3 N.mm^{-1}$ for cortical screw augmented and $17.6 N.mm^{-1}$ for the cancellous screw in the case with 6.5% volume fraction.
- $36.8 N.mm^{-1}$ for cortical screw augmented and $40.0 N.mm^{-1}$ for the cancellous screw in the case with 9.5% volume fraction.

- 98.4N.mm^{-1} for cortical screw augmented and 98.6N.mm^{-1} for the cancellous screw in the case with 12.1% volume fraction.

The diameter of cement were not corresponding to similar volume of cement as the volume of cement necessary to have 3.5mm diameter with the cortical screw represents 12.6mm^3 and for the cancellous screw it represents 20.8mm^3. The volume of cement necessary to have 2.7mm and 2.4mm with cancellous screws were respectively 7.4mm^3 and 3.7mm^3. Therefore, it was not possible to make a comparison in terms of volume of cement.

Finally the results showed each time a significant improvement of stiffness with augmentation but when compared with the effect of volume variation inside the bone sample (Cases A and E) it appeared that the improvement of stiffness from augmentation might not cover the loss in stiffness from a small change in bone structure. Therefore, the two cases of non-augmented bones that gave better results than augmented from the Stryker study were possibly due to the intra specimen variation of volume fraction.

8. Chapter 8 – Parametric study of screw characteristics

This chapter presents studies related to the screw type. As previously detailed cortical screws gave better results than cancellous screws within cancellous bone models, each screw design parameter was studied independently. The simulations were carried out first in the case of bone sample E with 9.5% volume fraction and then in the simplified bone, as designed in chapter 3, with the same volume fraction and dimensions. This parametric study aimed to show the relevance of each parameter and also to test if the results in the simplified bone model showed the same tendency.

8.1. Predrill with cancellous screw

This predrill study was about the effect of a predrill of 2.7mm diameter on the screw pull-out. This predrill dimension was chosen according to Stryker recommendations for a screw of 4mm diameter and applied to the model from the bone sample E and to the simplified model with same volume fraction.

8.1.1. Real bone model (volume fraction 9.5%)

The model with predrill was represented in figure 8.1.

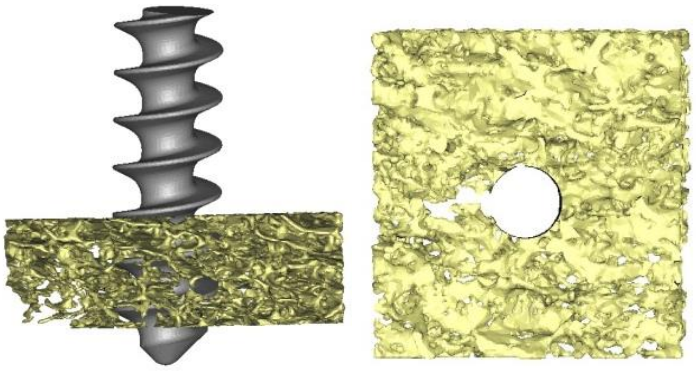

Figure 8.1: Cancellous bone with predrill model from real bone

The model without predrill had a contact area of 5.34mm^2 and the one with predrill had a contact area of 2.55mm^2, which meant that the contact area was 2.1 times larger without predrilling.

Figure 8.2 shows the results from the pull-out simulation.

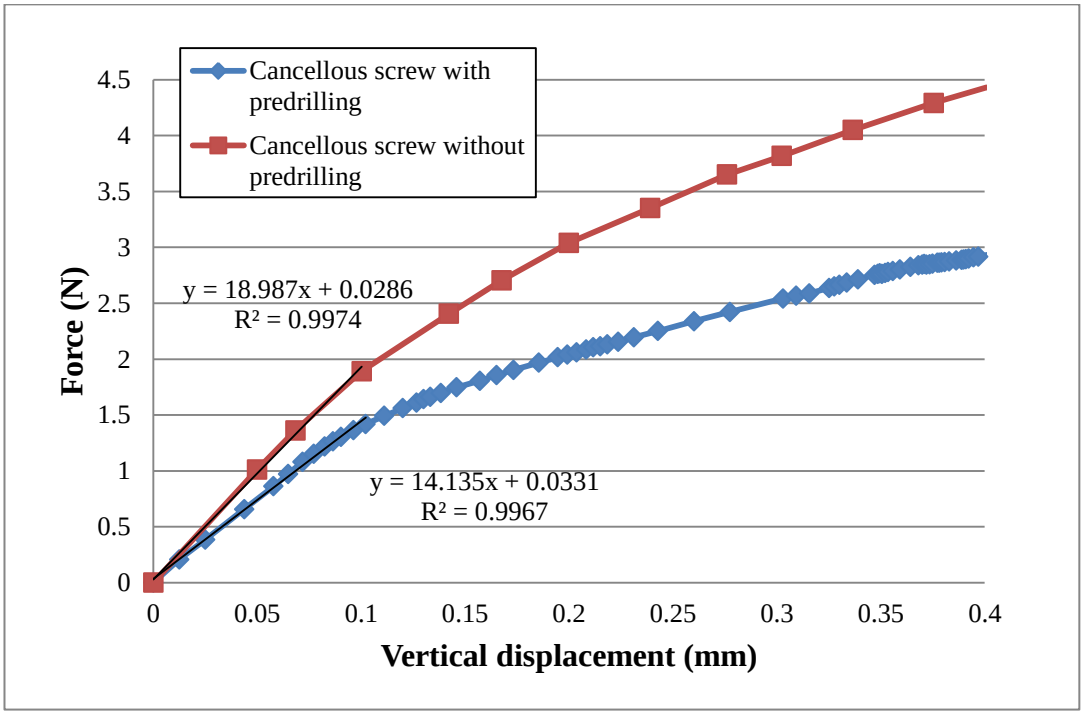

Figure 8.2: Screw pull-out comparison from real bone model with and without predrill.

The screw pull-out results were 32% stiffer without predrilling. Predrill following Stryker's recommendation for a 4mm cancellous screw can be hypothesised to weakening the pull-out.

8.1.2. Simplified bone model (volume fraction 9.5%)

The same simulation was carried out with a simplified bone model, made following the principle of spherical holes from chapter 3 and with the same bone volume fraction (9.5%). The model is presented in figure 8.3.

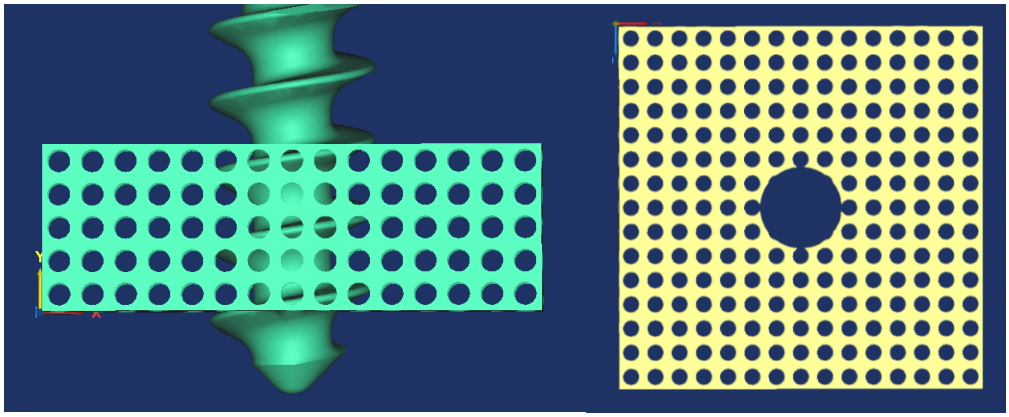

Figure 8.3: Cancellous bone with predrill model from simplified bone

The model without predrill had a contact area of 10.61mm^2 and the one with predrill had a contact area of 6.19mm^2 which meant that the contact area was 1.7 times larger without predrilling. In this case, the contact areas were more important with simplified bone model than from the real bone model and in both cases, the predrill reduced significantly the contact between screw and bone.

Figure 8.4 shows the results from the pull-out simulation.

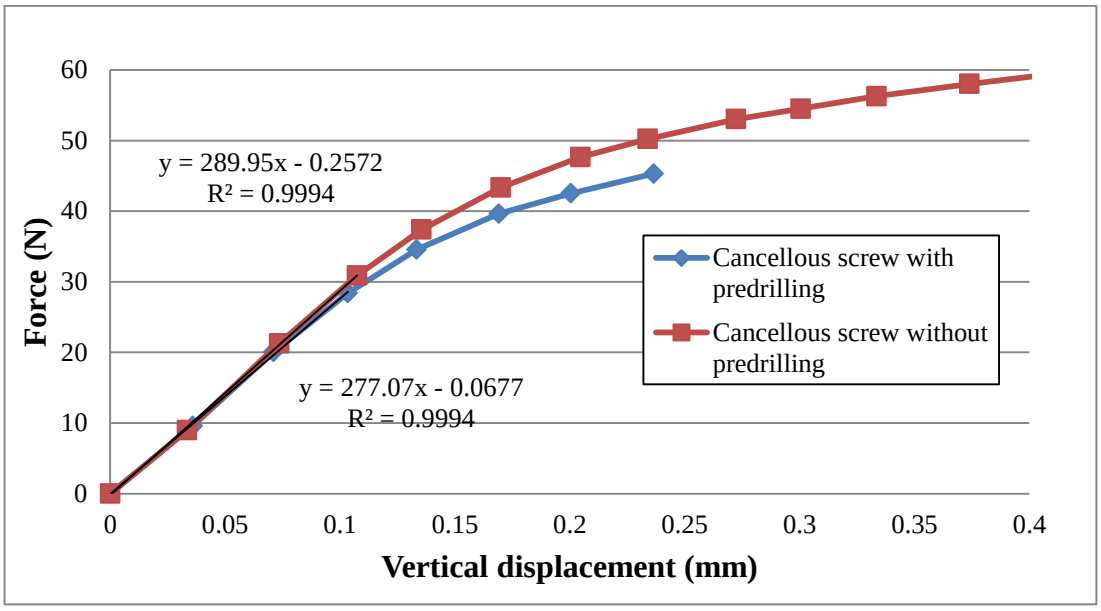

Figure 8.4: Screw pull-out comparison from simplified bone model with and without predrill.

In this case with simplified bone, the screw pull-out results were 5% stiffer without predrilling.

8.1.3. Conclusion for predrill

This study showed principally that predrills lower the stiffness. In the real bone case, the variation was significant (32%) while in the simplified bone case, this effect was not as important with 5% variation.

These results were not at all in the same order of values; in the real bone model the results were 19N.mm^{-1} and 14N.mm^{-1} and for the simplified bone, they were 290N.mm^{-1} and 277N.mm^{-1}. This study also showed that the results from the simplified bone model represented neither the order of values nor the variation due to predrill.

Chapter 5 detailed that contact area was not directly linked to stiffness and this predrill study confirmed it, as contact area difference was more important than the screw pull-out force difference in the real bone model, while this effect was not so significant with simplified bone model.

8.2. Variation of screw pitch for cancellous screw

The current study investigated the effect of reducing the screw pitch for the cancellous screw. The principle was to modify the cancellous screw design by reducing the pitch from 1.75mm to 1.25mm. This modification also implied a change in one of the radii. The fillet on the edge of the thread had to be changed from 0.8mm to 0.4mm radius as detailed in figure 8.5.

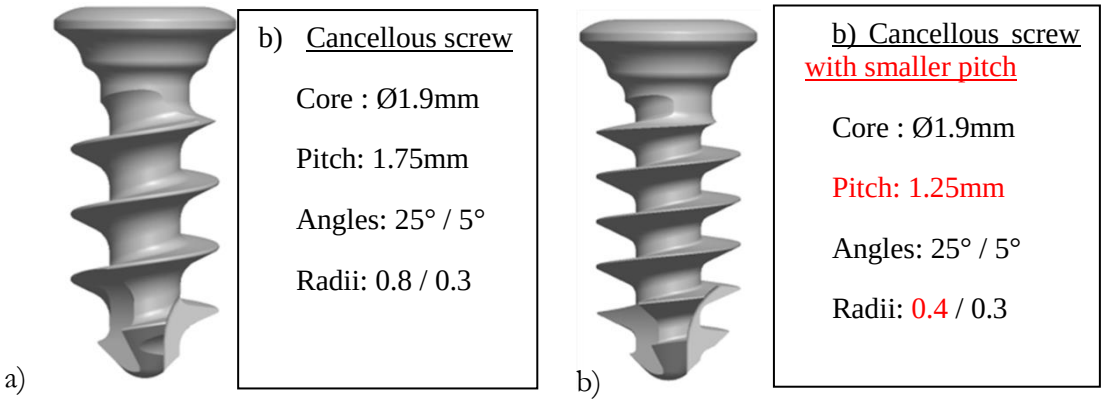

Figure 8.5: a) original cancellous screw and b) cancellous screw modification in red.

These two screws were used first in the real bone models in the same position for comparison and also in the simplified bone model with same volume fraction.

8.2.1. Real bone model (volume fraction 9.5%)

The force reaction during pull-out of the cancellous screw with smaller pitch was compared with the one from cancellous screw from both in bone model from case E (figure 8.6).

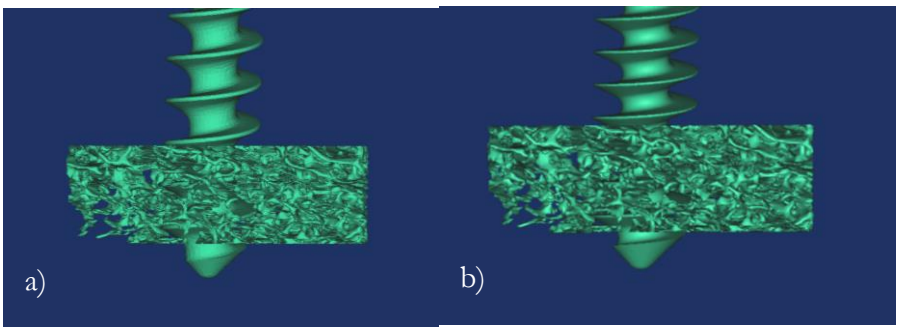

Figure 8.6: a) Cancellous screw and b) cancellous screw with smaller pitch in real bone model

The cancellous screw model had a total contact area of 5.34mm^2 and the one with smaller pitch a total contact area of 5.63mm^2. The difference of contact area is approximately 3%.

The pull-out results are given in figure 8.7.

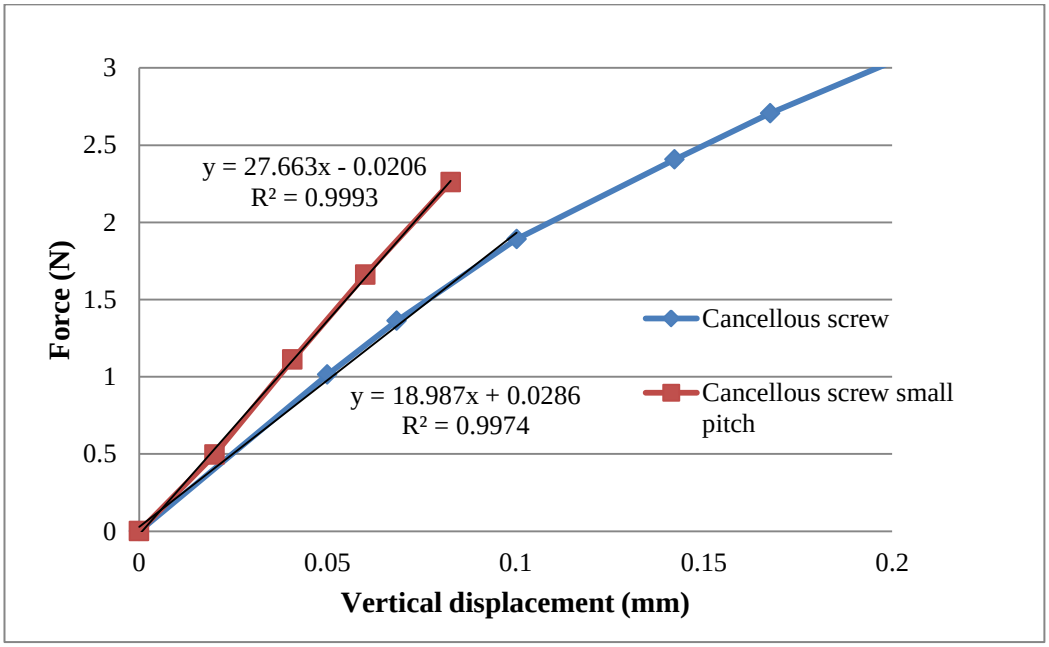

Figure 8.7: Pull-out comparison in real bone model between cancellous screw and cancellous screw with smaller pitch.

These simulations showed an improvement of 46% stiffness for the cancellous screw model with a smaller pitch, with 5% more contact area for that model. For this kind of bone architecture, it appeared that a smaller pitch would give an improvement for stiffness. This result also confirmed the fact that contact area and stiffness are not directly related, as marked variations in stiffness occur for a small variation in contact area.

8.2.2. Simplified bone model (volume fraction 9.5%)

The same simulation was compared with a simplified bone model as previously and the models are presented in figure 8.8.

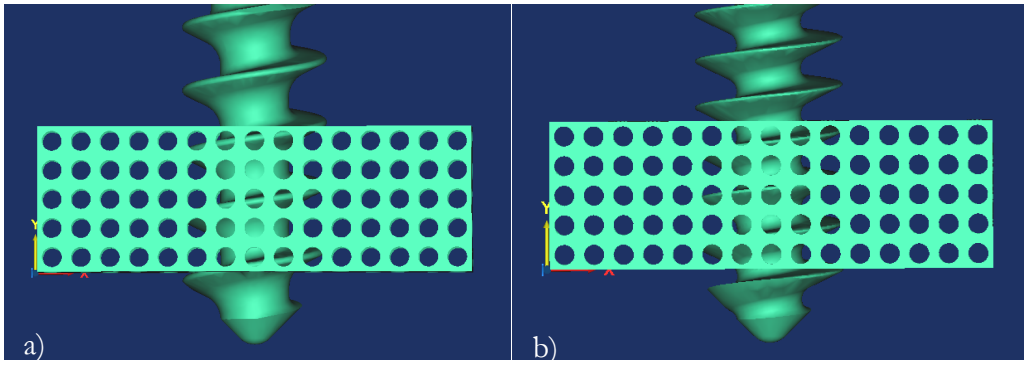

Figure 8.8: a) Cancellous screw and b) cancellous screw with smaller pitch in simplified bone model

In the case of the simplified bone model, the contact area for the cancellous screw was 10.61mm^2 and for the cancellous screw with smaller pitch 13.59mm^2. The pull-out results are shown in figure 8.9.

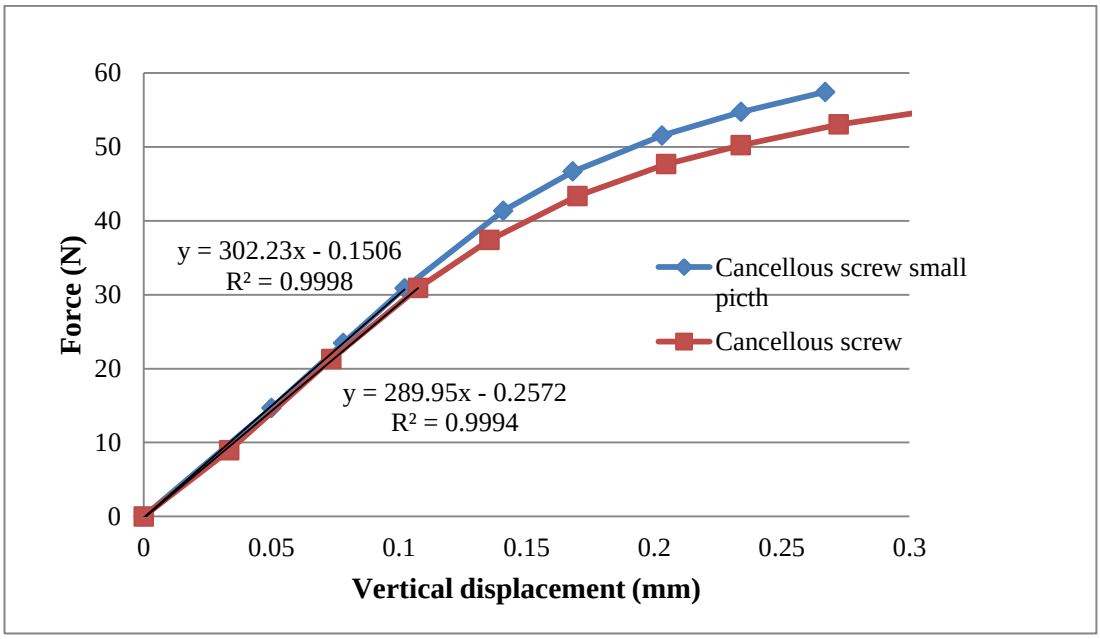

Figure 8.9: Pull-out comparison in simplified bone model between cancellous screw and cancellous screw with smaller pitch.

The results in this configuration were 4% stiffer for the cancellous screw with smaller pitch, which had 28% more contact area.

The results supported the tendency from the real bone model, i.e. increased stiffness. There was a significant difference between contact areas with the two types of screw in this simplified bone model while the contact areas in the real bone model were similar.

8.2.3. Conclusion for variation of cancellous screw pitch

This study showed mainly that a smaller pitch increased significantly the stiffness in the real bone model. The simplified model did not comply with behaviour as small stiffness variation was observed for overall very high stiffness values, 10 times stiffer than in the real bone model, which confirms the observation made in the section.

The contact area effect confirmed previous results, where no relation seemed to relate contacts and stiffness.

8.3. Variation of screw core diameter for cortical screw

This study was about the effect of reducing the core diameter for the cortical screw. The principle was to modify the cortical screw design by reducing the core diameter from 2.7mm to 1.9mm. This study was carried out because of the results showing that cortical screws gave better results than cancellous screw in cancellous bone. This modification is detailed in figure 8.10. These two screws were inserted in the two bone models for comparison.

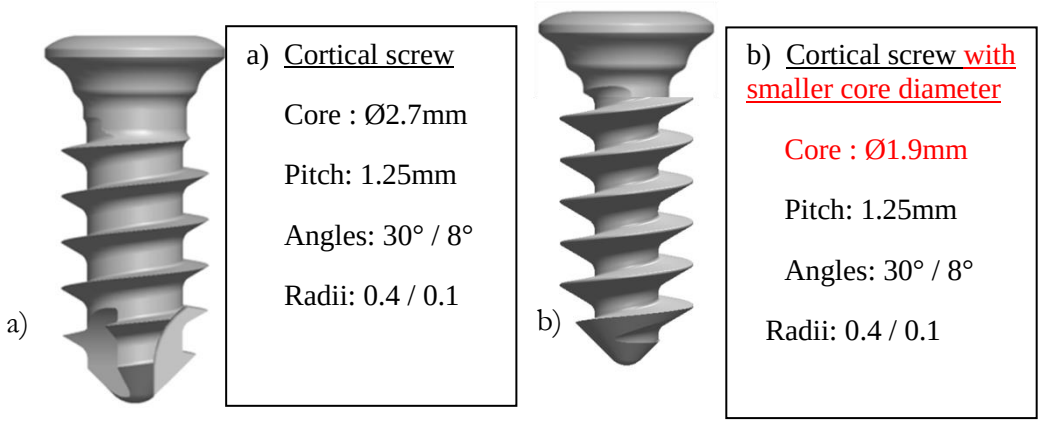

Figure 8.10: a) original cortical screw and b) modified cortical screw.

8.3.1. Real bone model (volume fraction 9.5%)

The force reaction during pull-out of the cortical screw with a smaller core diameter was compared with the one from the cortical screw from case E (figure 8.11).

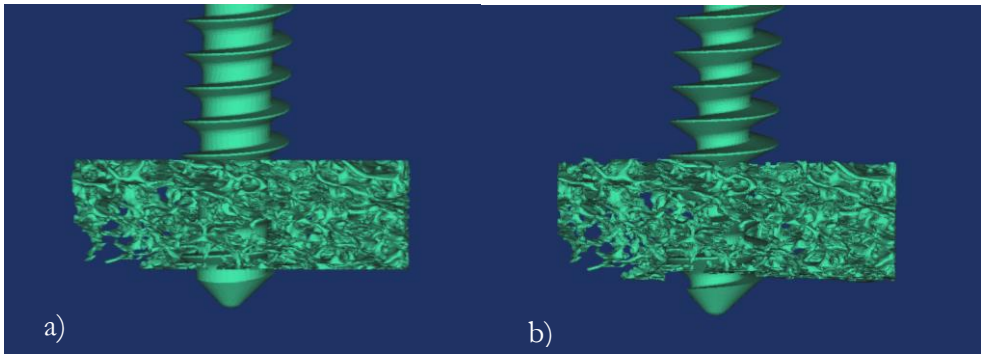

Figure 8.11: a) Cortical screw and b) cortical screw with smaller core diameter in real bone model

The model with the cortical screw had a contact area of 6.02mm^2 and the one with smaller core diameter a contact area of 5.55mm^2. The difference of contact area is approximately 8%.

The compared pull-out results are displayed in figure 8.12.

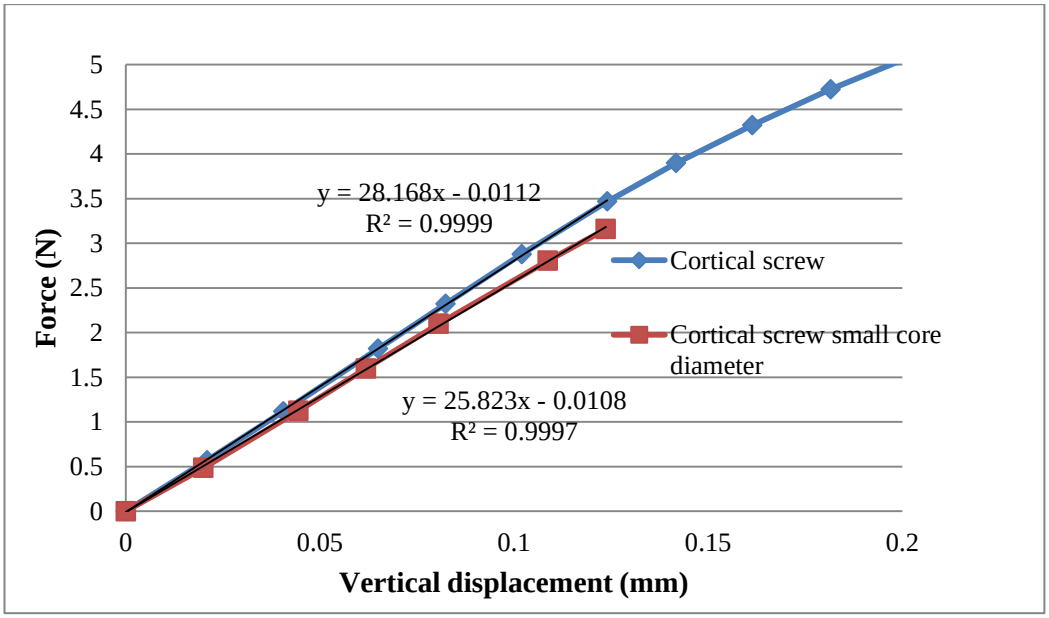

Figure 8.12: Pull-out comparison in real bone model between cortical screw and cortical screw with smaller core diameter.

These simulations showed an improvement of 10% stiffness for the cortical screw model with original core diameter for 8.5% more contact area for that model. This case suggested that the largest core diameter improved stiffness. It was also the only case showing potentially a relation between stiffness and contact area variation as both increased by similar ratio, i.e. 8.5% for contact areas and 10% for stiffness.

8.3.2. Simplified bone model (volume fraction 9.5%)

The same simulation was compared with a simplified bone model as previously discussed and the models are presented in figure 8.13.

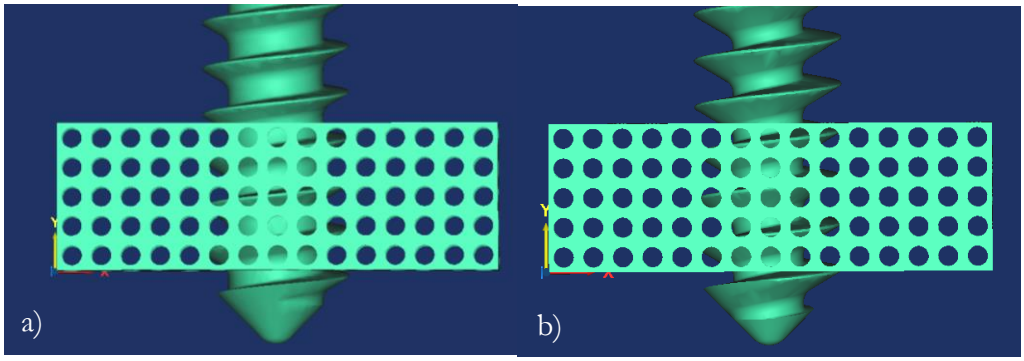

Figure 8.13: a) Cortical screw and b) cortical screw with smaller core diameter in simplified bone model

In the case of simplified bone model, the contact area for the cortical screw was 14.73mm^2 and for the cortical screw with smaller core diameter 13.40mm^2. The pull-out results are shown in figure 8.14.

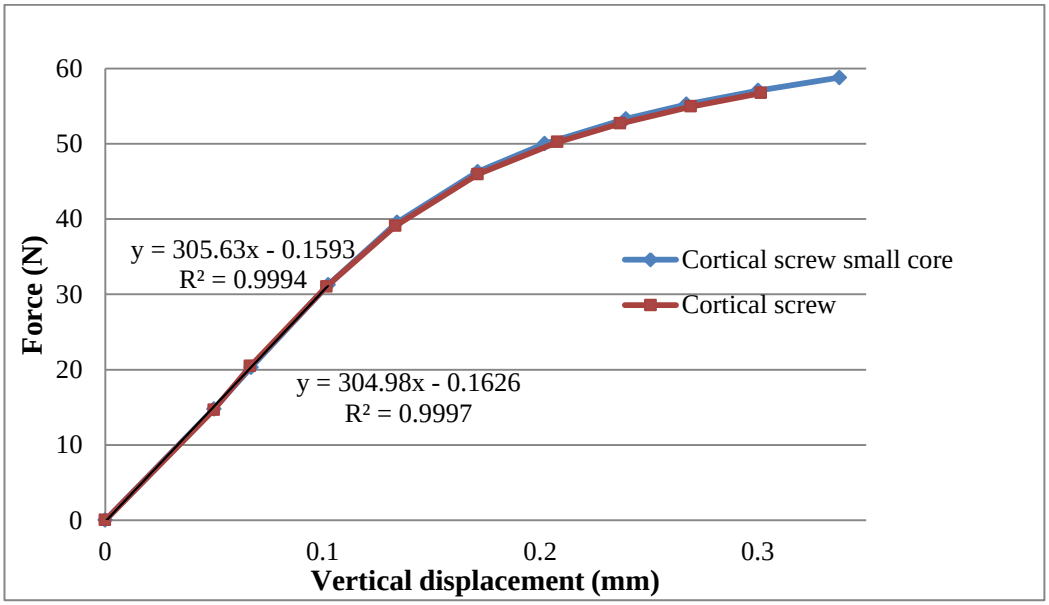

Figure 8.14: Pull-out comparison in simplified bone model between cortical screw and cortical screw with smaller core diameter.

The stiffness results from the pull-out simulation in this configuration were similar. Meanwhile, the model with larger core diameter had 9% more contact area. The slight increase of stiffness appearing in the real bone model, i.e. 10% stiffer for model with larger core diameter, did not appear in the simplified bone model.

8.3.3. Conclusion for variation of cortical screw core diameter

The main observation from this study was that a larger core diameter could increase the stiffness in the real bone model. The simplified model did not show similar behaviour, with practically no stiffness variation and again the results from simplified models gave very high stiffness values compare to the results from real bone models. The simplified bone model was again not representative of results from the real bone model. The contact area variations were similar to screw pull-out force in the real bone model case.

8.4. Thread angle influence

This study was made from the previous results by comparing the modified cancellous and cortical screws. The only differences between the modified screws were the thread angles and the radius of the tip of the thread (Figure 8.15).

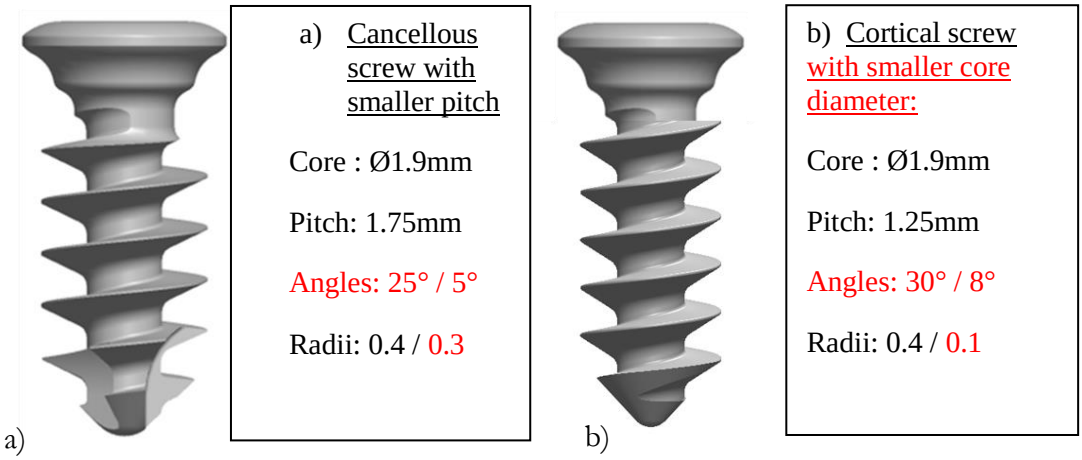

Figure 8.15: a) modified cancellous screw and b) modified cortical screw with differences highlighted in red.

8.4.1. Real bone model (volume fraction 9.5%)

The results in the real bone model were compared and showed that the model with the small core diameter cortical screw had contact area of 5.55mm^2 and the model with small pitch cancellous screw had contact area of 5.63mm^2. The pull-out results are plotted together in figure 8.16.

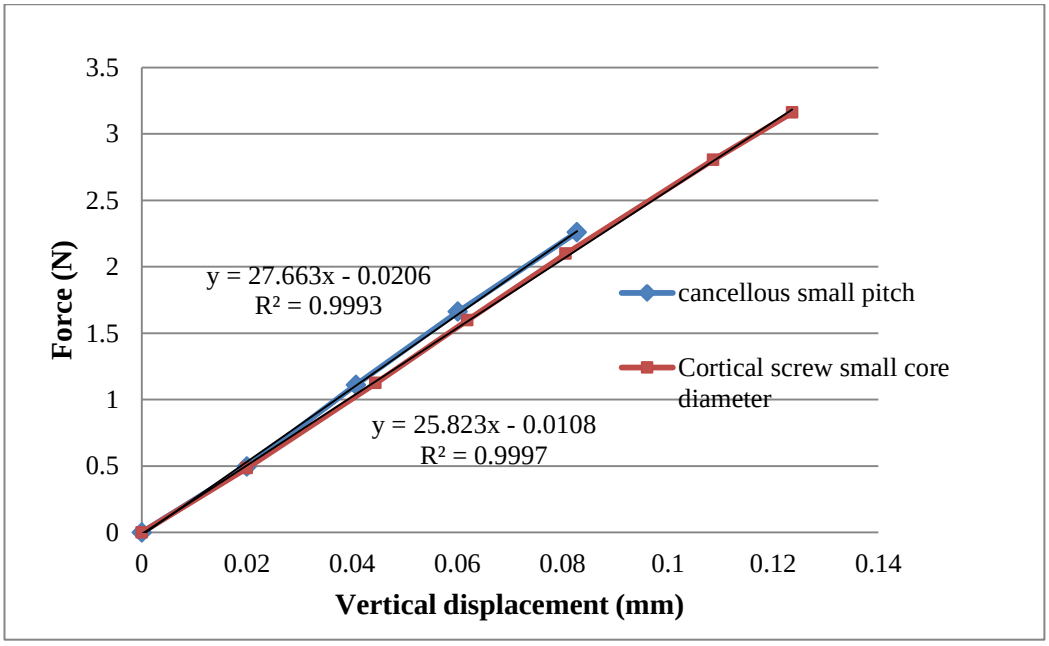

Figure 8.16: Pull-out comparison in real bone model between modified cancellous screw and modified cortical screw in order to study the thread angle influence.

These results showed a slight improvement with the model with cancellous thread angles being 7% stiffer than the model with cortical screw thread angles. These two models had similar contact area.

8.4.2. Simplified bone model (volume fraction 9.5%)

The contact area in the simplified bone model was 13.59mm^2 for the modified cancellous screw and 13.40mm^2 for the modified cortical screw. The results are shown in figure 8.17.

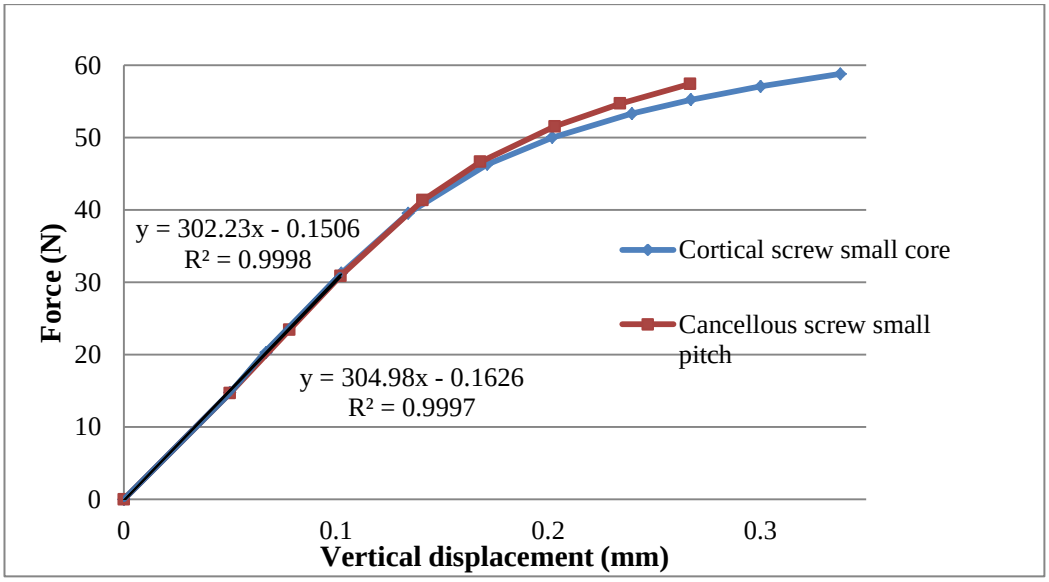

Figure 8.17: Pull-out comparison in simplified bone model between modified cancellous screw and modified cortical screw in order to study the thread angle influence.

Both contact area and stiffness were similar in the simplified bone model. The thread angle differences between the screws did not make significant difference for the screw pull-out simulations in simplified bone model.

8.4.3. Conclusion for variation of thread angles

This study showed that thread angles made a small difference in real bone model, i.e. the model with cancellous screw thread angles was 7% stiffer than the model with cortical screw thread angles.

The study also highlighted that contact areas were not a significant factor and again the simplified bone model was not representative.

8.5. Conclusions

This chapter presented studies related to the screw. Previously in chapter 6, cortical screws gave better results than cancellous screws in different cancellous bone models. In this chapter, each screw design parameter was studied independently and the results are summarised in table 8.1.

Table 8.1: Summary table of screw parameter study

Study	screw type	Predrill	Screw modifications	Screw/bone contact area (mm^2)	Stiffness results ($N.mm^{-1}$)	Influence
Predrill influence	cancellous	no	no	5.34	19.0	No predrill +35%
	cancellous	2.7mm ø	no	2.55	14.1	
Pitch influence	cancellous	no	no	5.34	19.0	Smaller thread +46%
	cancellous	no	Pitch 1.25mm	5.63	27.7	
Core diameter influence	cortical	no	no	6.02	28.3	Larger core diameter +10%
	cortical	no	core ø 1.9mm	5.55	25.8	
Influence of thread angles	cancellous	no	Pitch 1.25mm	5.63	27.7	smaller thread angles +7%
	cortical	no	core ø 1.9mm	5.55	25.8	

The predrill study showed that predrilling would weaken the structure and lower the stiffness in a screw pull-out, which corresponds to the second most significant factor.

Concerning the screw design, it was shown previously in chapter 6 that a cortical screw would give relative values as the cancellous screw. Each parameter was analysed independently and it appeared that the most important parameter was the thread pitch. A smaller pitch such as in the cortical screw would give an important improvement of the stiffness (+46%). The two other factors studied (core diameter and thread angle) showed stiffer results with a relatively lower influence: larger core diameter +10% and smaller thread angles

(from cancellous screw design) +7%. From this study, it seemed therefore that the theoretical best screws would be a cortical screw (diameter and pitch) with thread angles similar to the cancellous screw.

From an industrial point of view, there are 2 options: to create two screw models with the only difference being the thread angles (which in this specific case improved the fixation by 7%)

The simulations were carried out first in the real bone model and also in the simplified bone model. None of the results with the simplified bone model showed anything relevance to the real bone model. The simplified bone model showed in this study its limitation. The problem with any structured model is that there is no single weak point where the structure could start failing and the loads are shared in the structure. This explains as well the higher stiffness values measured each time with the simplified bone model compared to the values measured with the real bone model.

9. Chapter 9 – Conclusions and future work

9.1. Conclusions

This research has demonstrated the modelling of screw pull-out from different cancellous bone samples. The models are based on medical images and use the finite element method. Sliding contacts are an important part of the model.

The process adopted here can be extended to any modelling where implants are in contacts are in cancellous bone environments.

The modelling process was validated by comparison with a mechanical test, and the results generated from the simulation produced a good match to the mechanical test results.

From this modelling process it was possible to test different factors that could affect screw pull-out such as screw position, screw type, screw design, predrilling, and bone augmentation. These factors were tested on cancellous bone samples with a rod like architecture. This type of bone architecture corresponds to the weakest category of cancellous bone, the one that actually needs improvement the most.

From these investigations, the influence of the intra specimen variation of the cancellous bone appeared the most significant factor for screw pull-out, which means that a small variation in the screw position can lead to significantly different fixation stiffness. The small variations of screw positions observed were too small to consider that the surgeons could analyse the bone before screw insertion and therefore other improvement methods were considered. These include bone augmentation.

The study extended then to the influence of bone volume fraction on screw pull-out and a power law relationship was found showing that cortical

screws were giving as good or better stiffness results than cancellous screws in cancellous bone.

The study of bone augmentation showed it systematically improved the fixation stiffness for both types of screws tested and for all the different bone models tested. This analysis differs from the results from experimental studies and this difference was explained by the bone intra specimen variation. This variability is not manageable in experimental studies, but finite element simulations can readily detect these changes.

A comparison of the design features between cortical and cancellous screws showed that a smaller pitch was the most important factor for the improvement of the fixation. A larger core diameter and smaller thread angles also improved it, although to a lesser extent.

9.2. Future work

This study represents the preliminary studies for modelling improved screw fixation. The screw design features were tested on one bone sample and could be extended to other samples with different volume fractions. These tests were comparing the features between cancellous and cortical screw and the range of modification of these features could be wider in order to find the optimum pitch size, core diameter and thread angles.

The main outcome from this research was that cortical screws were giving as good or better stiffness results than cancellous screws in cancellous bone. A direct comparison of mechanical screw pull-out tests with both types of screws from a wide range of cancellous bone could confirm it.

Concerning the study on bone augmentation, it could be possible to extend the augmentation geometry. It appeared that a conical shape for the cement in simplified bone models was giving better results than a cylinder with the same diameter as the largest diameter of the cone. From the augmentation

study in real bone models, cement was systematically represented as a cylinder. Therefore, different shapes could be tested in the real bone models.

Contact studies showed that bonded contacts were creating highly significant improvement for the fixation which means that potentially a system that would bond the screw and the bone together would highly improve the fixation.

Finally, this modelling project opened many other possibilities of studies for any implant in cancellous bone environments such as anchors fixation, pedicle screws or intramedullary screws, and the bone augmentation results and screw design could be extended in these cases as well.

References

- Abramoff, M.D., Magalhaes, P.J., Ram, S.J., (2004). "Image Processing with ImageJ". Biophotonics International, 11(7), 36-42.

- Abshire, B.B., McLain, R.F., Valdevit, A., Kambic, H., (2001). Characteristics of pullout failure in conical and cylindrical pedicle screws after full insertion and back-out, The Spine Journal, 1, 408-414.

- Ahn, S.-H., Montero, M., Odell, D., Roundy, S., Wright, P.K. ,(2002). Anisotropic material properties of fused deposition modeling ABS, Rapid Prototyping, 8(4), 248-257.

- An, Y.H., Draughn, R.A., (2000). Mechanical testing of bone and the bone-implant interface. CRC PressI Llc.

- Asnis, S.E., Kyle, R.F., (1996). Cannulated Screw Fixation: Principles and Operative Techniques. Springer.

- Asnis, S.E., Ernberg, J.J., Bostrom, M.P., Wright, T.M., Harrington, R.M., Tencer, A., Peterson, M., (1996). Cancellous bone screw thread design and holding power. Journal of orthopaedic trauma, 10(7), 462-469.

- Augat, P., Rapp, S., Claes, L., (2002). A Modified Hip Screw Incorporating Injected Cement for the Fixation of Osteoporotic Trochanteric Fractures, Journal of Orthopaedic Trauma, 16(5), 311-316.

- Barucci, E.J., Gonzalez, M.H., Cooperman D.R., (1985). The effect of adjunctive methylmethcrylate on failures of fixation and function in patients with intertrochanteric fractures and osteoporosis, The Journal of Bone and Joint Surgery, 67(7), 1094-1107.

- Bayraktar, H.H., Keaveny, T.M., (2004). Mechanisms of uniformity of yield strains for trabecular bone. Journal of Biomechanics, 37(11), 1671-1678.

- Bayraktar, H.H., Morgan, E.F., Niebur, G.L., Morris, G.E., Wong, E.K., Keaveny, T.M., (2004). Comparison of the elastic and yield properties of human femoral trabecular and cortical bone tissue. Journal of Biomechanics, 37(1), 27-35.

- Bialoblocka-Juszczyk, E., Baleani, M., Cristofolini, L., Viceconti, M. (2008). Fracture properties of an acrylic bone cement. Acta of Bioengineering and Biomechanics, 10(1), 21-26.

- Bretton, E., (2008). Cortical Shell Evaluation in Bone Augmentation for enhanced Screws Fixation, Thesis submitted in partial fulfilment of requirements for a Masters Degree, EPFL, Lausanne, Switzerland.

- Bevill, G., Eswaran, S.K., Gupta, A., Papadopoulos, P., Keaveny, T.M., (2006). Influence of bone volume fraction and architecture on computed large-deformation failure mechanisms in human trabecular bone. Bone, 39(6), 1218-1225.

- Bevill, G., Easley, S.K., Keaveny, T.M., (2007). Side-artefact errors in yield strength and elastic modulus for human trabecular bone and their dependence on bone volume fraction and anatomic site. Journal of Biomechanics, 40(15), 3381-3388.

- Bevill, G., Eswaran, S.K., Farahmand, F., Keaveny, T.M., (2009). The influence of boundary conditions and loading mode on high-resolution finite element-computed trabecular tissue properties. Bone, 44(4), 573-578.

- Bevill, G.,. and Keaveny, T.M., (2009). Trabecular bone strength predictions using finite element analysis of micro-scale images at limited spatial resolution. Bone, 44(4), 579-584.

- Brown, G.A., McCarthy, T., Bourgeault, C.A., Callahan, D.J., (2000). Mechanical performance of standard and cannulated 4.0-mm cancellous bone screw. Journal of Orthopaedic Research, 18, 307-312.

- Brown, C.J., Sinclair, R.A., Day, A., Hess, B., Procter, P., (2011). An approximate model for cancellous bone screw fixation. Computer Methods in Biomechanics and Biomedical Engineering, 16(4), 443-450.

- Brown, C.J., Bennani, P., Hughes, C., Piper, A., Procter, P., (2012). Screw Augmentation using CaP Injectable Bone Cement, European Cells and Materials, 23(3), 17.

- Chapman, J.R., Harrington, R.M., Lee, K.M., Anderson, P.A., Tencer, A.F., Kowalski, D. (1996). Factors affecting the pullout strength of cancellous bone screws. Journal of Biomechanics Engineering, 118, 391-398.

- Chen, S.I., Lin, R.M., Chang, C.H., (2003). Biomechanical investigation of pedicle screw-vertebrae complex: a finite element approach using bonded and contact interface conditions, Medical Engineering & Physics, 25(4), 275-282.

- Chen, L.-H., Tai, C.-L., Lai, P.-L., Lee D.-M., Tsai, T.-T., Fu, T.-S., Niu, C.-C., Chen, W.-J., (2009a). Pull-out strength for cannulated pedicle screws with bone cement augmentation in severely osteoporotic bone: Influences of radial hole and pilot hole tapping, Clinical Biomechanics, 24(8), 613–618.

- Chen, T.-H., Lung C.-Y., Cheng, C.-K., (2009b). Biomechanical Comparison of A New Stemless Hip Prosthesis with Different Shapes-A Finite Element Analysis, Journal of Medical and Biological Engineering, 29(3), 108-113.

- Choueka, J., Koval, K.J., Kummer, F.J.,(1996). Cement augmentation of intertrochanteric fracture fixation: A cadaver comparison of 2 techniques, Acta orthopaedica Scandinavica, 67(2), 153-157.

- Chu, T.-M. G., Hollister, S.J., Halloran, J.W., Feinberg, S.E., Orton, D.G., (2002). Manufacturing and characterization of 3-D hydroxyapatite bone tissue engineering scaffolds, Annals of the New York Academy of Sciences, 961(1), 114-117.

- Coleman, M.N., Colbert, M.W., (2007). Technical note: CT thresholding protocols for taking measurements on three-dimensional models. American journal of physical anthropology, 133(1), 723-725.

- Collinge, C., Hartigan, B., Lautenschlager, E.P., (2006). Effects of surgical errors on small fragment screw fixation. Journal of orthopaedic trauma, 20(6), 410-413.

- Cosmi, F., Dreossi, D., (2006). Numerical and experimental structural analysis of trabecular architectures, Meccanica, 42, 85-93.

- Currey, J.D., (2002). Bones: structure and mechanics, Edition 2, Princeton University Press.

- Crum, M.S., Young, F.A.Jr., An, Y.H. (2000). Screw Pullout Test for Evaluating Mechanical Properties of Bone, Mechanical testing of bone and the bone-implant interface, 321-328.

- DeCoster, T.A., Heetderks, D.B., Downey, D.J., Ferries, J.S., Jones, W., (1990). Optimizing bone screw pullout force. Journal of Orthopaedic Trauma, 4(2), 169-174.

- Dobson, C.A., Sisias, G., Phillips, R., Fagan, M.J., Langton, C.M., (2006). Three dimensional stereolithography models of cancellous bone structures from microCT data: Testing and validation of finite element results. Proceedings of the Institution of Mechanical Engineers Part H. Journal of Engineering in Medicine, 220 (3), 481-484.

- Doube M., Kłosowski M.M., Arganda-Carreras I., Cordeliéres F., Dougherty R.P., Jackson J., Schmid B., Hutchinson J.R., Shefelbine S.J., (2010). BoneJ: free and extensible bone image analysis in ImageJ. Bone 47, 1076-1079.

- Dougherty R., Kunzelmann K., (2007). Computing local thickness of 3D structures with ImageJ. Microsc. Microanal, 13, 1678-1679.

- Ernberg, J.J., Asnis, S., (1996). Materials and Manufacturing of Orthopaedic Bone Screws, Cannulated screw fixations Principles and Operative Techniques, Asnis Kyle Editions, 1-14.

- Eswaran, S.K., Gupta, A., Keaveny, T.M., (2007). Locations of bone tissue at high risk of initial failure during compressive loading of the human vertebral body. Bone, 41(4), 733-739.

- Ferrara, L.A., Ryken, T.C., (2000). Screw Pullout Testing, Mechanical testing of bone and the bone-implant interface, edited by An, Y.H. and Draugh R.A., CRC press, 551-565.

- Flahiff, C.M., Gober, G.A., Nicholas, R.W., (1995). Pullout Strength of fixation screws from polymethylmethacrylate bone cement, Biomaterials, 16, 533-536

- Ford, C.M., Keaveny, T.M., (1996). The dependence of shear failure properties of trabecular bone on apparent density and trabecular orientation. Journal of Biomechanics, 29(10), 1309-1317.

- Fransen, P., (2007). Increasing pedicle screw anchoring in the osteoporotic spine by cement injection through the implant: Technical note and report of three cases, Journal of Neurosurgery Spine, 7, 366–369.

- Fyhrie, D.P., Vashishth, D., (2000). Bone stiffness predicts strength similarly for human vertebral cancellous bone in compression and for cortical bone in tension. Bone, 26(2), 169-173.

- Gefen, A., (2002a). Optimizing the biomechanical compatibility of orthopedic screws for bone fracture fixation, Medical Engineering & Physics, vol. 24(5), 337-347.

- Gefen, A., (2002b). Computational simulations of stress shielding and bone resorption around existing and computer-designed orthopaedic screws, Medical & Biological Engineering and Computing, 40, 311-322.

- Gibson, L.J., & Ashby, M.F., (1982). The mechanics of three-dimensional cellular materials. Proceedings of the Royal Society of London. A. Mathematical and Physical Sciences, 382(1782), 43-59.

- Gibson, L.J., (1985). The mechanical-behaviour of cancellous bone. Journal of Biomechanics, vol. 18, 317-328.

- Gibson, L., Ashby, M., (1987). Cancellous bone. Cellular Solids: Structure & Properties, 316-331.

- Gibson, L.J., Michael, J., Ashby, F., (1999). Cellular Solids: Structure and Properties, Edition 2, revised, Cambridge University Press.

- Gibson, L. J. (2005). Biomechanics of cellular solids. Journal of Biomechanics, 38(3), 377-399.

- Goldstein, S.A., Goulet, R., McCubbrey, D., (1993). Measurement and significance of three-dimensional architecture to the mechanical integrity of trabecular bone. Calcified Tissue International, 53, 127-133.

- Goulet, R.W., Goldstein, S.A., Ciarelli, M.J., Kuhn, J.L., Brown, M.B, Feldkamp, L.A., (1994). The relationship between the structural and orthogonal compressive properties of trabecular bone. Journal of Biomechanics, 27, 375-389.

- Haddock, S.M., Yeh, O.C., Mummameni, P.V., Rosenberg, W.S., Keaveny, T.M., (2004). Similarity in the fatigue behaviour of trabecular bone across site and species. Journal of Biomechanics, 37(2), 181-187.

- Hara, T., Tanck, E., Homminga, J., Huiskes, R., (2002). The influence of microcomputed tomography threshold variations on the assessment of structural and mechanical trabecular bone properties. Bone, 31(1), 107-109.

- Hasegawa, T., Inufusa, A., Imai, Y., Mikawa, Y., Lim, T.H., An, H.S., (2005). Hydroxyapatite-coating of pedicle screws improves resistance against pull-out force in the osteoporotic canine lumbar spine model: a pilot study, The Spine Journal, 5, 239–243.

- Hernandez, C.J., Keaveny, T.M., (2006). A biomechanical perspective on bone quality. Bone, 39(6), 1173-1181.

- Hildebrand, T., Rüegsegger, P., (1997). Quantification of bone microarchitecture with the structure model index. Computer Methods in Biomechanics and Bio Medical Engineering, 1(1), 15-23.

- Hodgskinson, R., Currey, J.D., (1990). The effect of variation in structure on the Young's modulus of cancellous bone: a comparison of human and non-human material. Proceedings of the Institution of Mechanical Engineers [H], 204, 115-121.

- Hou, S.M., Hsu, C.C., Wang, J.L., Chao, C.K., Lin J., (2004). Mechanical tests and finite element models for bone holding power of tibial locking screws. Clinical Biomechanics, 19, 738-745.

- Ikenaga, M., Hardouin, P., Lemaitre, J., Andrianjatovo, H., Flautre, B., (1998). Biomechanical characterisation of a biodegradable calcium phosphate hydraulic cement: a comparison with porous biphasic calcium phosphate ceramics. J. Biomed. Mater. Res., 40(1), 141-144.

- Janssen, D., Mann, K.A., Verdonschot, N., (2009). Finite element simulation of cement-bone interface micromechanics: A comparison to experimental results. Journal of Orthopaedic Research, 27(10), 1312-1318.

- Jones, J.R., Hench, L.L. (2003). Regeneration of trabecular bone using porous ceramics, Current Opinion in Solid State and Materials Science, Volume 7(4–5), 301-307.

- Jutley, R.S., Watson, M.A., Shepherd, D.E., Hukins, D.W., (2002). Finite element analysis of stress around a sternum screw used to prevent sternal dehiscence after heart surgery. Proceedings of the Institution of Mechanical Engineers, Part H: Journal of Engineering in Medicine, 216(5), 315-321.

• Kanis, J.A., Johnell, O., Oden, A., Jonsson, B., De Laet, D., Dawson, A., (2000). Risk of hip fracture according to the World Health Organization criteria for osteopenia and osteoporosis. Bone, 27(5), 585-590.

• Kapandji, I.A., (1988). Cuadernos de fisiología articular. Masson s.a., Barcelona.

• Keaveny, T.M., Borchers, R.E., Gibson, L.J., Hayes, W.C., (1993). Trabecular bone modulus and strength can depend on specimen geometry. Journal of Biomechanics, 26(8), 991-1000.

• Keaveny, T.M., Morgan, E. F., Niebur, G.L., & Yeh, O.C. (2001). Biomechanics of trabecular bone. Annual review of biomedical engineering, 3(1), 307-333.

• Keaveny, T.M., Yeh, O.C., (2002). Architecture and trabecular bone-toward an improved understanding of the biomechanical effects of age, sex and osteoporosis. Journal of Musculoskeletal and Neuronal Interactions, 2(3), 205-208.

• Kim, C.H., Zhang, H., Mikhail, G., von Stechow, D., Muller, R., Kim, H. S., and Guo, X. E., (2007). Effects of Thresholding Techniques on mu CT-Based Finite Element Models of Trabecular Bone, J. Biomechanical Engineering, 129, 481-487.

• Kissel, C.G., Friedersdorf, S.C., Foltz, D.S., Snoeyink, T., (2003). Comparison of Pullout Strength of Small-Diameter Cannulated and Solid-Core Screws, The Journal of Foot and Ankle Surgery, 42(6), 334–338.

• Kopperdahl, D.L., Keaveny, T.M., (1998). Yield strain behavior of trabecular bone. Journal of Biomechanics, 31(7), 601-608.

• Kopperdahl, D.L., Morgan, E.F., Keaveny, T.M., (2002). Quantitative computed tomography estimates of the mechanical properties of human vertebral trabecular bone. Journal of Orthopaedic Research, 20(4), 801-805.

- Kothari, M., Keaveny, T.M., Lin, J.C., Newitt, D.C., Majumbar, S., (1999). Measurement of intraspecimen variations in vertebral cancellous bone architecture. Bone, 25(2), 245-250.

- Larsson, S., Stadelmann, V.A., Arnoldi, J., Behrens, M., Hess, B., Procter, P., Murphy, M., Pioletti, D.P., (2012). Injectable calcium phosphate cement for augmentation around cancellous bone screws. In vivo biomechanical studies, Journal of Biomechanics, 45(7), 1156-1160.

- Leong, K.F., Cheah, C.M., Chua, C.K., (2003). Solid fabrication of three-dimensional scaffolds for engineering replacement tissues and organs, Biomaterials 23, 2363-2378.

- Leung, S.Y., Browne, M., New, A.M., (2008). Smooth surface micro finite element modelling of a cancellous bone analogue material. Proceedings of the Institution of Mechanical Engineers, Part H: Journal of Engineering in Medicine, 222(1), 145-149.

- Liu, X., S., Bevill, G., Keaveny, T.M., Sajda, P., Guo, X.E., (2009). Micromechanical analyses of vertebral trabecular bone based on individual trabeculae segmentation of plates and rods. Journal of Biomechanics, 42(3), 249-256.

- Martini, F., (2006). Anatomy and Physiology 6th edition (Englewood Cliffs, NJ: Prentice-Hall) chapter 6, 182-207.

- McDonnell, P., Liebschner, M.A.K., Wafa Tawackoli, Mc Hugh, P.E., (2009). Vibrational testing of trabecular bone architectures using rapid prototype models, Medical Engineering & Physics, 31, 108-115.

- McKoy, B.E., An, Y.H., (2000). An Injectable Cementing Screw for Fixation in Osteoporotic Bone, Journal of Biomedical Materials Research, 53(3), 216-220.

- Melchels, F.P., Feijen, J., Grijpma, D.W., (2010). A review on stereolithography and its applications in biomedical engineering. Biomaterials, 31(24), 6121-6130.

- Mittra, E., Rubin, C., Qin, Y.X., (2005). Interrelationship of trabecular mechanical and microstructural properties in sheep trabecular bone. Journal of biomechanics, 38(6), 1229-1237.

- Morgan, E.F., Bayraktar, H.H., Keaveny, T.M., 2003. Trabecular bone modulus–density relationships depend on anatomic site. Journal of Biomechanics, 36(7), 897-904.

- Morgan, E.F., Bayraktar, H.H., Yeh, O.C., Majumbar, S., Burghardt, A., Keaveny, T.M., (2004). Contribution of inter-site variations in architecture to trabecular bone apparent yield strains. Journal of Biomechanics, 37(9), 1413-1420.

- Morgan, E.F., Keaveny, T.M., (2001). Dependence of yield strain of human trabecular bone on anatomic site. Journal of Biomechanics, 34(5), 569-577.

- Oberg, E., Jones, F.D., Horton, H.L., (1987).Working strength of bolts. Ryffel HH, ed. Machinery's Handbook. New York: Industrial press, 1068-1069.

- Odgaard, A. (1997). Three-dimensional methods for quantification of cancellous bone architecture. Bone, 20(4).

- Parfitt, A.M., Drezner, M.K., Glorieux, F.H., Kanis, J.A., Malluche, H., Meunier, P.J., Susan M.O., Recker, R.R. (1987). Bone histomorphometry: standardization of nomenclature, symbols, and units: report of the ASBMR Histomorphometry Nomenclature Committee. Journal of bone and mineral research, 2(6), 595-610.

• Perren, S.M., Cordey, J., Baumgart, F., Rahn, B. A., Schatzker, J., (1992). Technical and biomechanical aspects of screws used for bone surgery. Int J Orthop Trauma, 2, 31-48.

• Procter, P., (2008-2012). A suggestion for why the pullout strength of screws varies, internal document, Private communication.

• Procter, P., (2012). Enhancing screw fixation in poor quality cancellous bone: Present and future options, European Cells and Materials, 23(3), 27.

• Quadrani, P., Pasini, A., Mattioli-Belmonte, M., Zannoni, C., Tampieri, A., Landi, E., Giantomassi, F., Natali, D., Casali, F., Biagini, G., Tomei-Minardi A., (2005). High-resolution 3D scaffold model for engineered tissue fabrication using a rapid prototyping technique, Medical & Biological Engineering & Computing 43, 196-199.

• Rice, J.C., Cowin, S.C., Bowman, J.A., (1988). On the dependence of the elasticity and strength of cancellous bone on apparent density. Journal of Biomechanics, 21, 155-168.

• Rincon Kohli, L., (2003). Identification of a multiaxial failure criterion for human trabecular bone. Faculté Sciences et Technique de l'Ingénieur, Institut de genie biomedical, section de genie mécanique, Lausanne, Switzerland, Ecole polytechnique Federale de Lausanne : PhD Thesis.

• Seebeck, J., Goldhahn, J., Morlock, M.M., Schneider, E., (2005). Mechanical Behaviour of screws in normal and osteoporotic bone, Osteoporosis international, 16(2), 107-111.

• Stadelmann, V.A., Bretton, E., Terrier, A., Procter, P., Pioletti, D.P., (2010). Calcium phosphate cement augmentation of cancellous bone screws can compensate for the absence of cortical fixation. Journal of biomechanics, 43(15), 2869-2874.

- Rüegsegger, P., Koller, B., Müller, R., (1996). A microtomographic system for the nondestructive evaluation of bone architecture. Calcified tissue international, 58(1), 24-29.

- Seideman, B.A., Asnis, S.E. (1996). Acetabular Reconstruction with Allografts Utilizing Cannulated Screws. In Cannulated Screw Fixation, 87-96, Springer New York.

- Shuib, S., Ridzwan, M.I.Z., Ibrahim, M.N.M., Tan, C.J., (2007), Analysis of Orthopedic Screws for Bone Fracture Fixations with Finite Element Method, Journal of Applied Sciences 7(13), 1748-1754.

- Simpson, D.J., (2005). A finite element strategy applied to intramedullary nailing of the proximal femur. Brunel University,London, U.K.: PhD Thesis.

- Snyder, B.D., Hayes, W.C., (1990). Multiaxial structure-property relations in trabecular bone. In: Biomechanics of diarthrodial joints, Springer Verlag, New York, 31-59.

- Stankewich, C.J., Swiontkowski, M.F., Tencer A.P., **(**1996). Augmentation of femoral neck fracture fixation with an injectable calcium phosphate bone mineral cement, Journal of Orthopaedic Research, 14(5), 786 – 793.

- Stoffel, K.K., Leys, T., Damen, N., Nicholls, R.L., Kuster, M.S., (2008). A new technique for cement augmentation of the sliding hip screw in proximal femur fractures, Clinical Biomechanics, 23, 45-51.

- Su, R., Campbell, G. M., Boyd, S.K., (2007). Establishment of an architecture-specific experimental validation approach for finite element modeling of bone by rapid prototyping and high resolution computed tomography, Medical Engineering & Physics 29, 480-490.

- Tencer, A.F., Asnis, S.E., Harrington, R.M., Chapman, J.R., (1996). Biomechanics of Cannulated and Noncannulated Screw, Cannulated screw fixations Principles and Operative Techniques, Asnis Kyle Editions, 15-40.

• Turner, C.H., Cowin., S.C., Rho, J.Y., Ashman, R.B., and Rice, J.C., (1990). The fabric dependence of the orthotropic elastic constants of cancellous bone. Journal of Biomechanics, 23, 549-561.

• Vichard, P., Gagneux, E. (1995). Il y a 100 ans: les premiers pas de l'ostéosynthèse des fractures. Histoire des sciences médicales, Tome XXIX.

• Weaver, J.K., Chalmers, J., (1966). Cancellous Bone: Its Strength and Changes with Aging and an Evaluation of Some Methods for Measuring Its Mineral Content: I. Age Changes in Cancellous Bone, J Bone Joint Surg Am 48, 289-299.

• Wermelin, K., Tengvall, P., Aspenberg, P., (2007). Surface-bound bisphonates enhance screw fixation in rats – increasing effect up to 8 weeks after insertion, Acta Orthopaedica, 78 (3), 385-392.

• Williams, J.M., Adewunmi, A., Schek, R.M., Flanagan, C.L., Krebsbach, P.H., Feinberg, S.E., Hollister, S.J., Das, S., (2005). Bone tissue engineering using polycaprolactone scaffolds fabricated via selective laser sintering, Biomaterials 26, 4817-4827.

• Williams, K.R., (2000). Finite Element Analysis for Evaluating Mechanical Properties of the Bone-Implant Interface, Mechanical testing of bone and the bone-implant interface, 567-580.

• Wimhurst, J.A., Brooks, R.A., Rushton, N., (2001). The effects of particulate bone cements at the bone-implant interface, the journal of bone and joint surgery, 588-592.

• Wirth, A.J., Mueller, T.L., Vereecken, W., Flaig, C., Arbenz, P., Müller, R., Van Lenthe, G.H., (2010). Mechanical competence of bone-implant systems can accurately be determined by image-based micro-finite element analyses. Archive of applied mechanics, 80(5), 513-525.

• Wirth, A.J., Goldhahn, J., Flaig, C., Arbenz, P., Müller, R., Van Lenthe, G.H., (2011). Implant stability is affected by local bone microstructural quality. Bone, 49(3), 473-478.

• Woo, D.G., Kim, C.H., Lim, D., Kim, H.S., (2010). Experimental and simulated studies on the plastic mechanical characteristics of osteoporotic vertebral trabecular bone, Current applied physics 10, 729-733.

• Woolf, A.D., Dixon, A.S.J., (1998). Osteoporosis: A Clinical Guide, Edition 2, Martin Dunitz.

• Wuisman, P.I.J.M., Van Dijk, M., Staal, H., Van Royen, B.J., (2000). Augmentation of (pedicle) screws with calcium apatite cement in patients with severe progressive osteoporotic spinal deformities: an innovative technique, Eur Spine J 9, 528–533.

• Ulrich, C.G., Binet, E.F., Sanecki, M.G., Kieffer, S.A., (1980). Quantitative assessment of the lumbar spinal canal by computed tomography. Radiology 134, 137-143.

• Yakacki, C.M., Poukalova, M., Guldberg, R.E., Lin, A., Gillogly, S., Gall, K., (2010). The effect of the trabecular microstructure on the pullout strength of suture anchors. Journal of biomechanics, 43(10), 1953-1959.

• Yeh, O.C., Keaveny, T.M., (1999). Biomechanical effects of intraspecimen variations in trabecular architecture: a three-dimensional finite element study. Bone, 25(2), 223-228.

• Yeni, Y.N., Fyhrie, D.P., (2001). Finite element calculated uniaxial apparent stiffness is a consistent predictor of uniaxial apparent strength in human vertebral cancellous bone tested with different boundary conditions. Journal of biomechanics, 34(12), 1649-1654.

• Yeni, Y.N., Hou, F.J., Ciarelli, T., Vashishth, D., Fyhrie, D.P., (2003). Trabecular shear stresses predict in vivo linear microcrack density but not diffuse damage in human vertebral cancellous bone. Annals of Biomedical Engineering, 31(6), 726-732.

• Yeni, Y.N., Christopherson, G.T., Neil Dong, X., Kim, D.G., Fyhrie, D.P., (2005). Effect of microcomputed tomography voxel size on the finite element model accuracy for human cancellous bone. Transactions of the ASME-K-Journal of Biomechanical Engineering, 127(1), 1-8.

• Zanetti, E.M., Salaorno, M., Grasso, G., Audenino, A.L., (2009). Parametric analysis of orthopedic screws in relation to bone density. The open medical informatics journal, 3, 19.

• Zhang, Q.H., Tan, S.H., Chou, S.M., (2004). Investigation of fixation screw pull-out strength on human spine, Journal of Biomechanics 37, 479-485.

Websites (Accessed 28th August 2012):

• http://www.osteosynthesis.stryker.com/medias/pdf/basicfragment_brochure_982183e4708.pdf
• http://www.utsouthwestern.edu/education/medical-school/departments/min-metab-center/research.html
• http://www.eng-tips.com/viewthread.cfm?qid=188553&page=6
• http://www.roymech.co.uk/Useful_Tables/Tribology/co_of_fricti.htm

Appendix A

Different models that could represent cancellous bone have been tried in order to make a selection. A comparison using models continuum, rods, cylinder holes and spherical holes was then established. These models have been created from models from literature, e.g. (Gibson, 2005, Melchels *et al.* 2010, Yeh and Keaveny, 1999).

Continuum model

The continuum model (see figure A.1) has been created not in order to be selected but in order to compare with the more complex models as the target of this study is to show the influence of the structure.

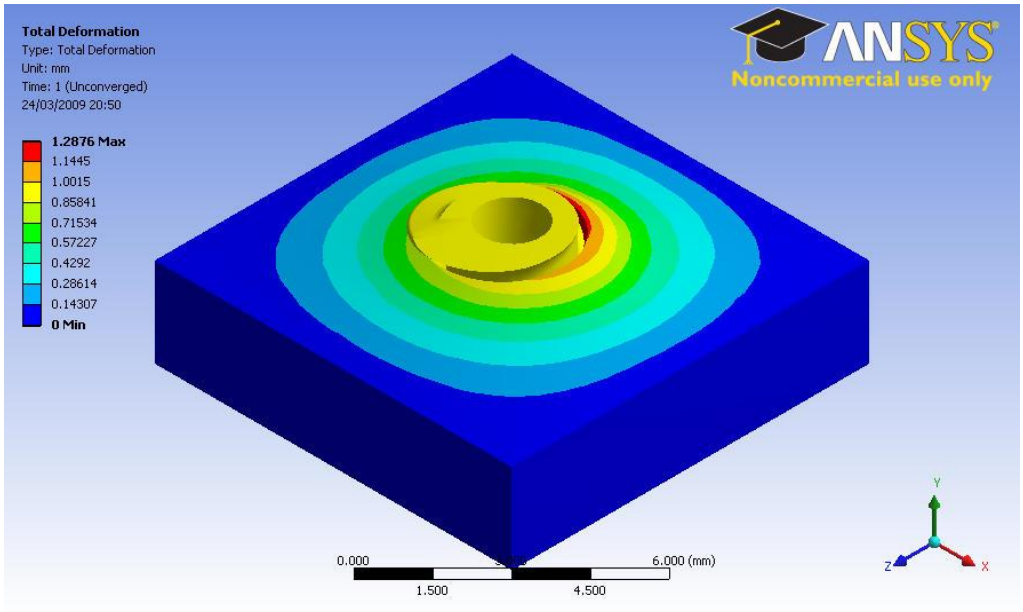

Figure A.1: General view of the continuum model

The vertical displacement has gone up to 0.88mm before computer model failure. Figures A.2 and A.3 show a split view of the total deformation of the structure with and without screw respectively.

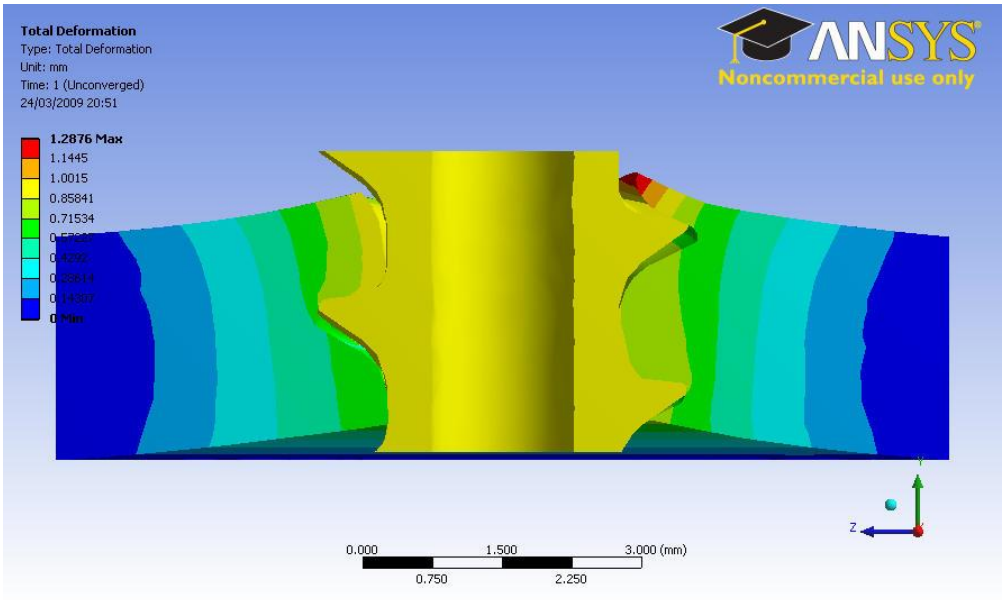

Figure A.2: Front section view of the continuum model total deformation

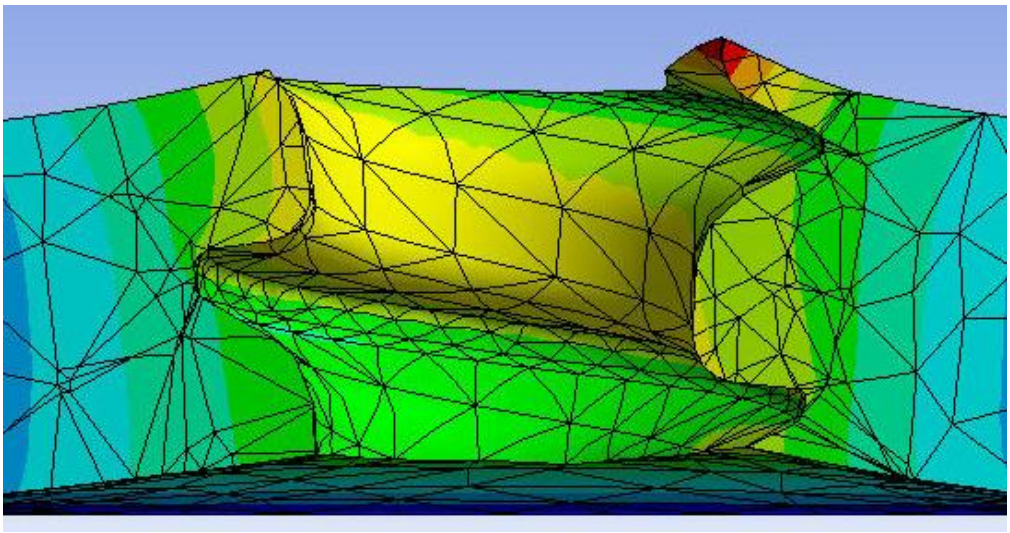

Figure A.3: Front section view of the continuum model total deformation with screw hidden

Rods cancellous bone model:

The rods cancellous bone model (figure A.4) has been created with cubic rods with a size of 0.1mm to create cells of 0.8mm. The screw vertical displacement stopped extremely early at 0.05mm before the simulation failed.

This model showed disadvantages due to the sharp edges (figure A.5 and A.6). These sharp edges implied extreme element distortion around them which led to model failure. To be able to run such a model, it would be necessary to create an extremely fine mesh which was over our computational ability to perform.

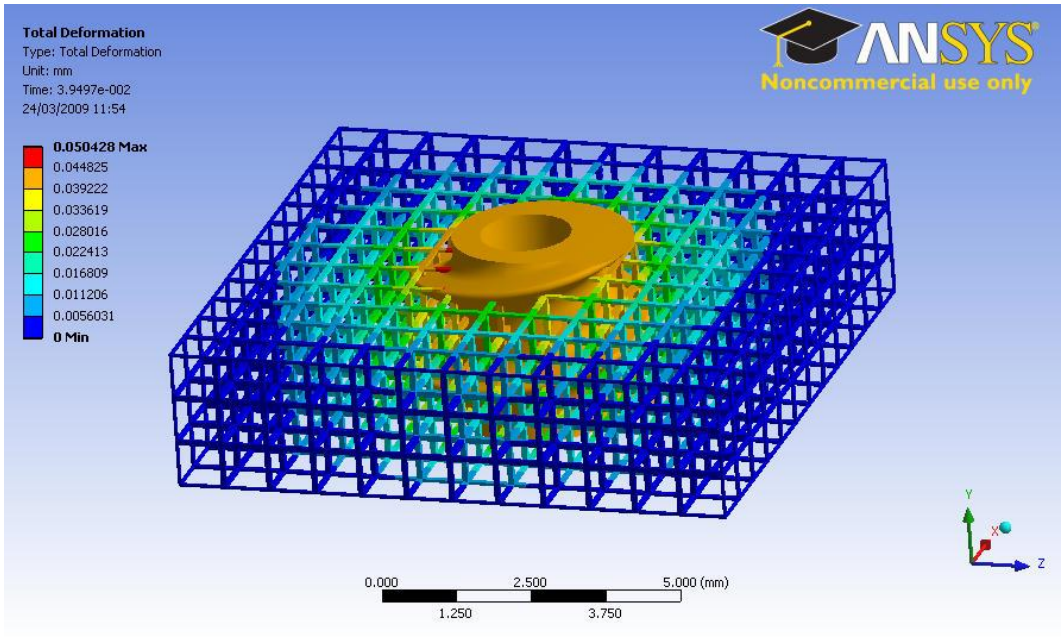

Figure A.4: Overall view of the rods cancellous bone model

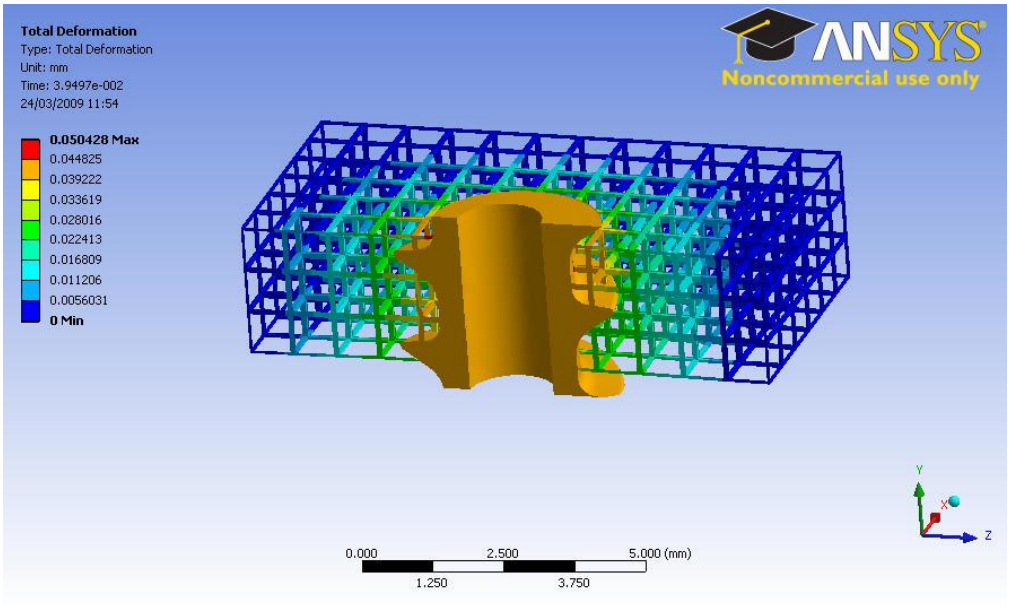

Figure A.5: Section view of the rods cancellous bone model result file for total deformation

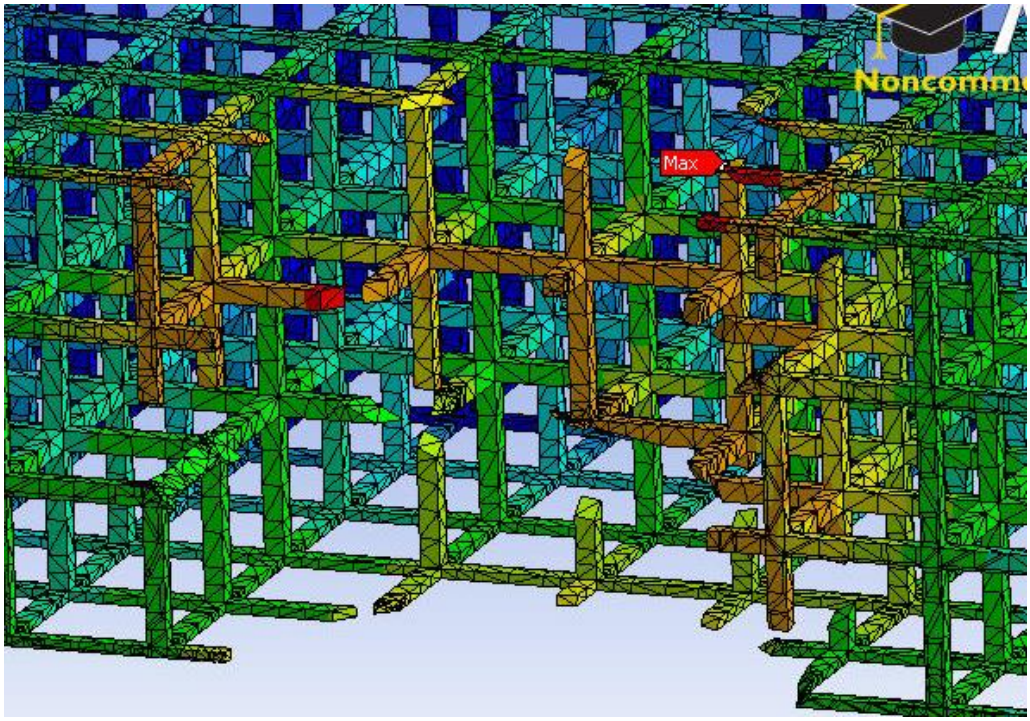

Figure A.6: Zoom on the contact area problems on the rods cancellous bone model total deformation result file with screw hidden

Cylinders holes cancellous bone model:

The cylinder holes model (figure A.7) has been created from continuum with cylinder holes of 0.7mm diameter in order to create cells of 0.8mm. The screw vertical displacement stopped at 0.31mm before computer system failure.

This model did not show any major disadvantage. The figures A.8 and A.9 showed the total deformation of the model. The major distortion was around the penetrating edge of the screw.

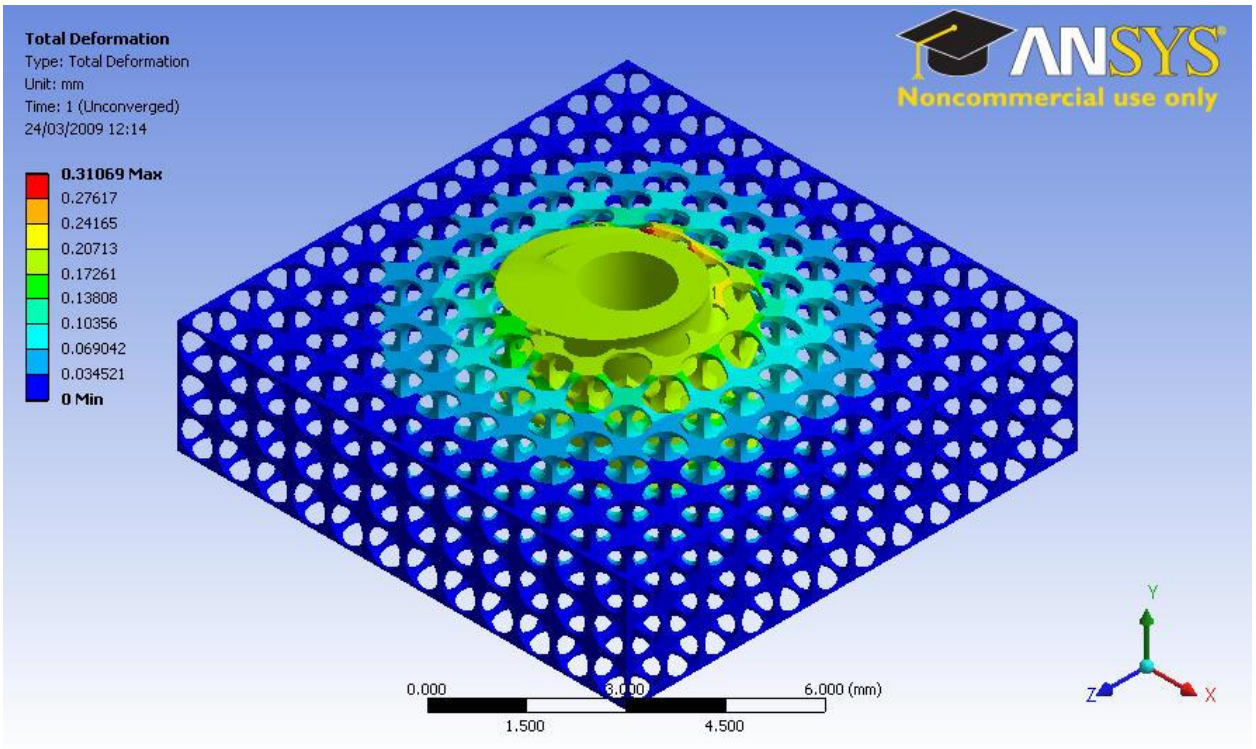

Figure A.7: Overall view of the model with cylinder holes

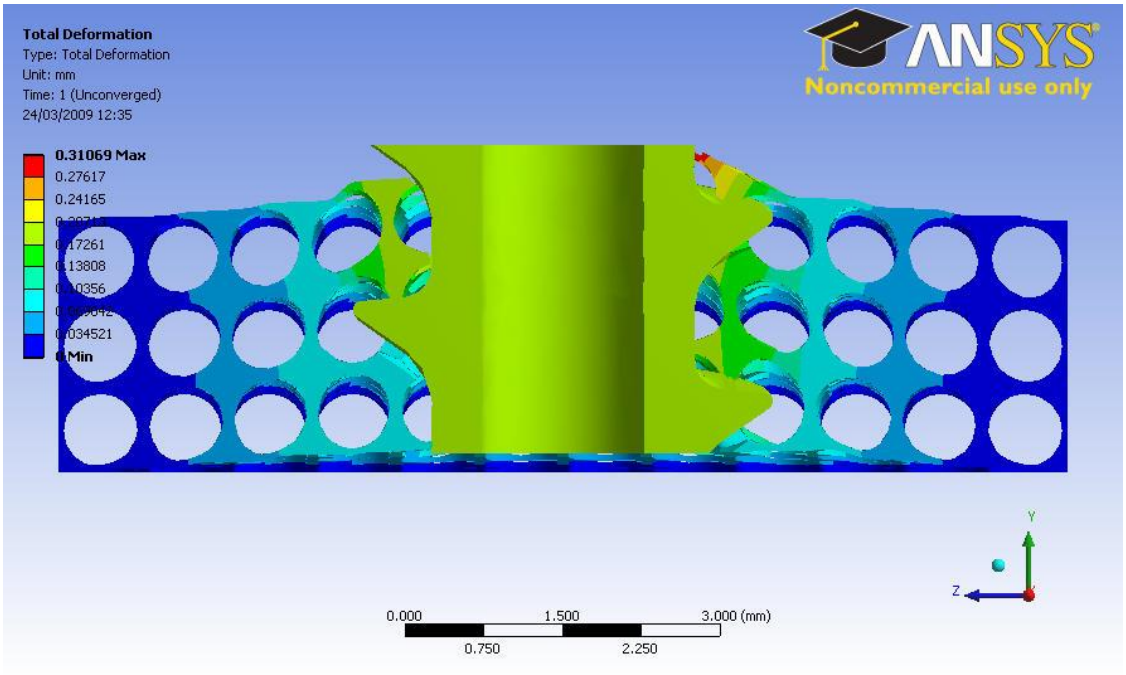

Figure A.8: Front section view of the total deformation of the cylinder holes model

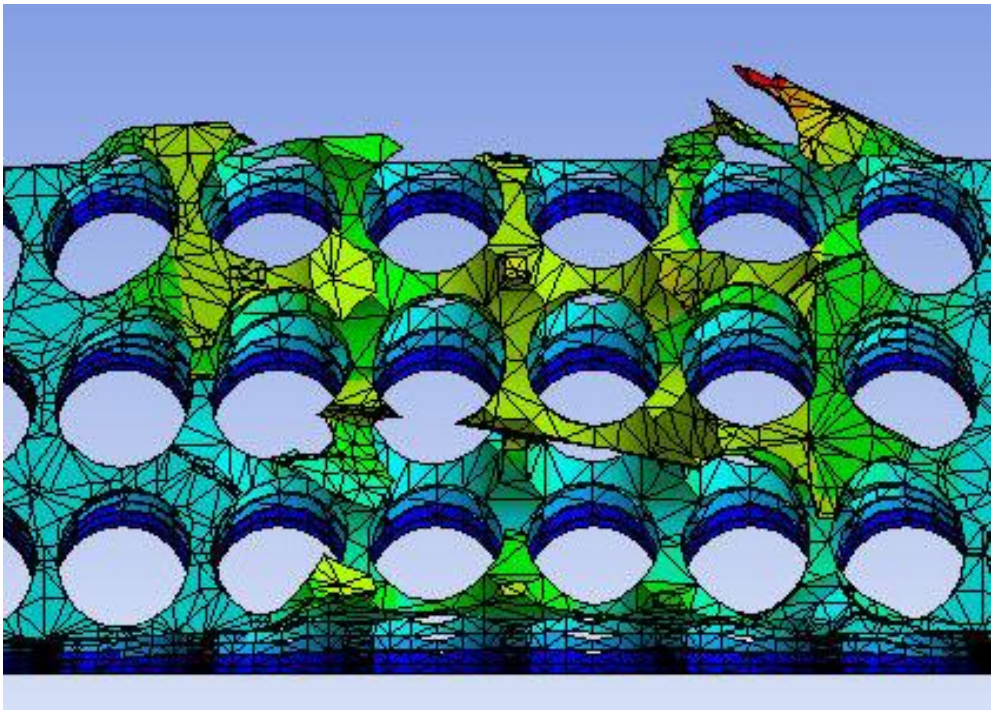

Figure A.9: Front section view of the total deformation of the cylinder holes model with screw hidden

Spherical holes cancellous bone model:

The spherical holes model (figure A.10) has been created from continuum with spherical holes of 1mm diameter in order to create cells of 0.8mm. The displacement stopped at 0.27mm.

This model did not show any major disadvantage. It offered the possibility to vary easily the volume density of the cancellous bone while varying the diameter of the spherical holes. The figures A.11 and A.12 showed the total deformation of the model. The major distortion was around the penetrating edge of the screw as well.

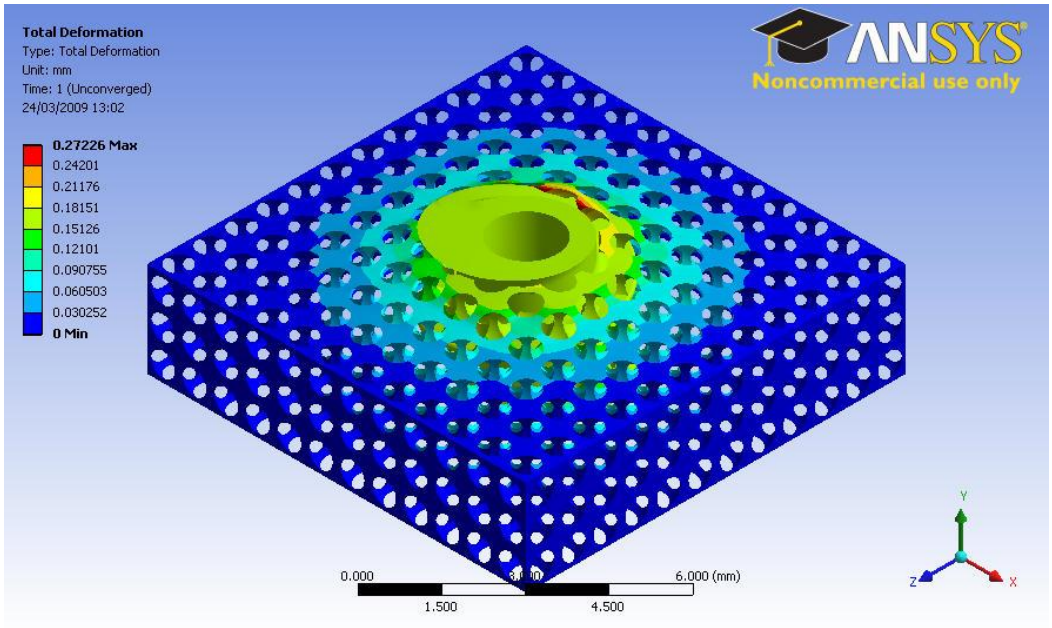

Figure A.10: Overall view of spherical holes model

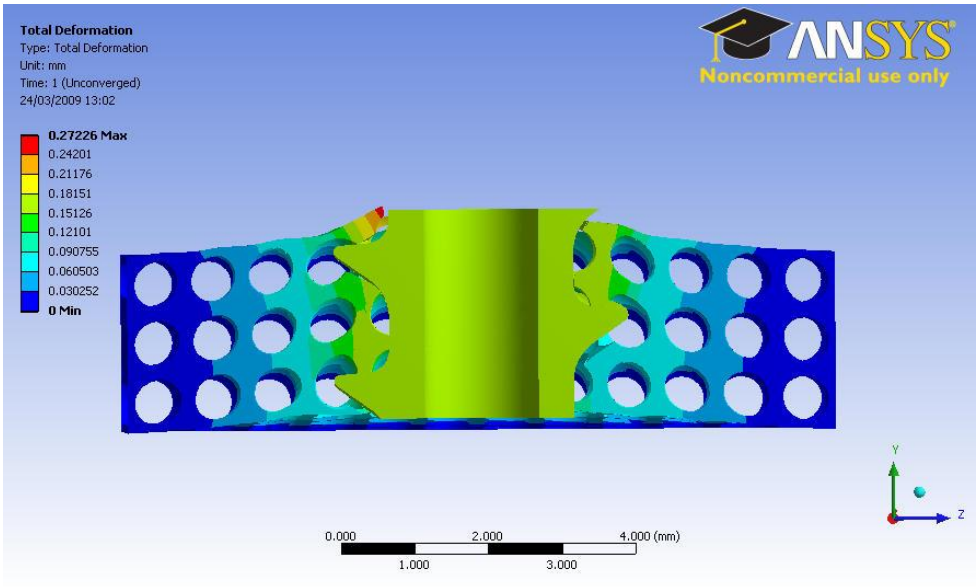

Figure A.11: front section view of the total deformation of the spherical holes model

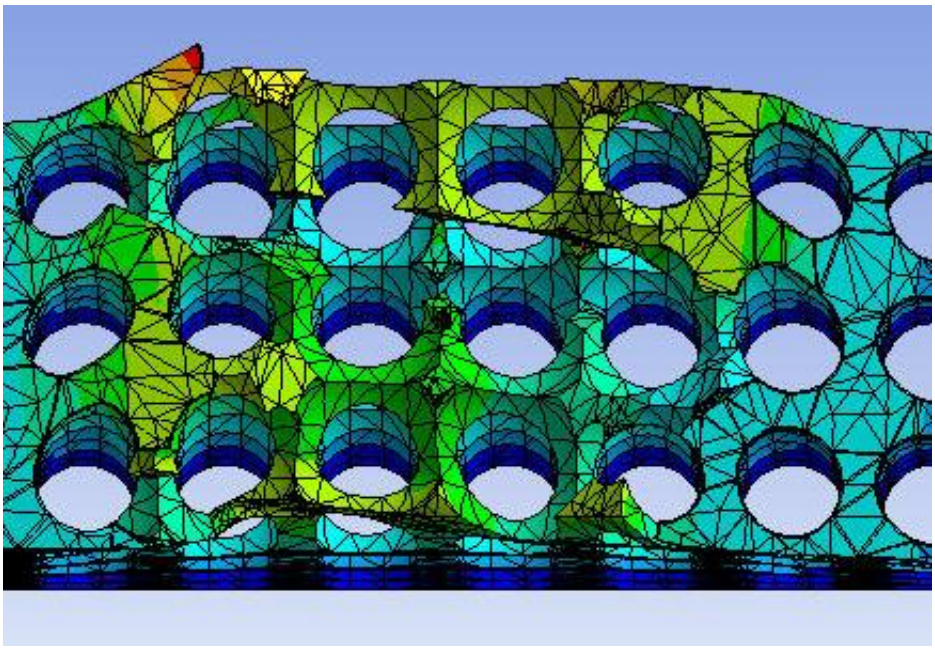

Figure A.12: section view of the total deformation of the spherical holes model with screw hidden

Finally it has been decided that the model with spherical holes would be the best models for the simulation, mostly due to the possibility to vary the bone apparent density by varying the diameter of the spherical holes.

Appendix B

Influence of the number of screw threads involved in the cancellous bone

A cancellous model with double length of screw involved from the simplified bone model with 15% apparent density was created (figure B.1). This simulation was undertaken in order to confirm that the screw pull-out force was proportional to the length of screw threads involved in the cancellous bone. Results were shown in figure B.2.

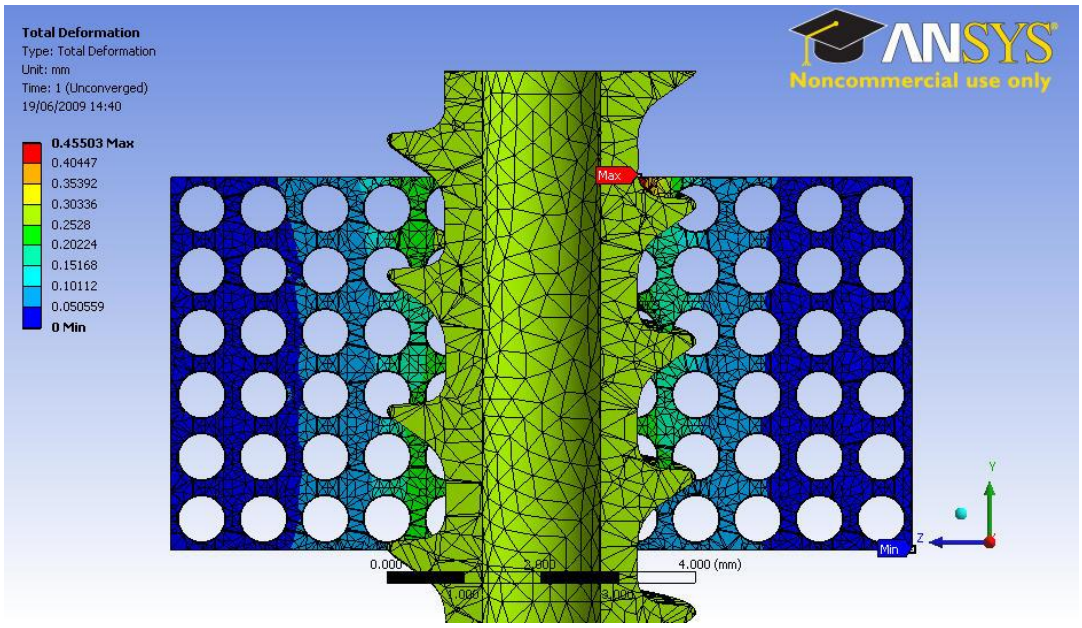

Figure B.1: front section view of total deformation of the double size model with cancellous bone 15%

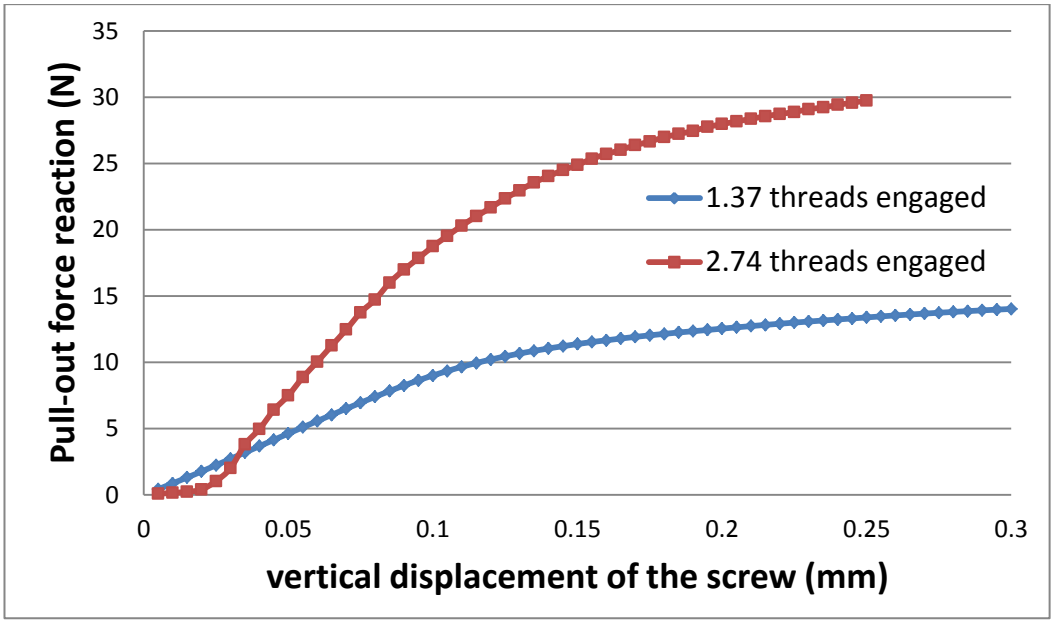

Figure B.2: Influence of the number of threads engaged in cancellous bone with 3D models with 15.0% apparent density

From the result, the first observation is that the pull-out force is proportional to the number of screw threads involved. Then, by comparison with the 2D models: 2D models screw pull out force was 230N (+/- 50) for 10mm of screw engaged in the cancellous bone. 3D models screw pull out force is 15N (+/- 1) for 2.40mm of screw engaged in the cancellous bone. By extrapolation, results from 3D models would be then a third from the results from the 2D models. Therefore it is possible to admit that they are in the same range. The difference could be explained by the simplification from the 2D models: screw not helicoidal and bone structure not in 3D.

N.B.: this phenomenon was observable only with regular structure. In the study with real bone models, the intra specimen variation made the results not proportional.

Appendix C

Process in 3-matics:

Instruction for the creation of cancellous bone models with screw inserted

Bone sample alone

Smooth

Smooth factor 0.7

Do not use compensation

Reduce triangles

Geometrical error 0.01

Flip Threshold angle 30

Ensure one shell

Mark shell, invert and delete other bits

Auto remesh

- Shape quality threshold 0.2 (then next time 0.3)
- Maximum geometrical error 0.02 (because small part and do not want triangles to be able to move very far)
- Do not control edge length
- Do not preserve surface contours

* using inspection to look at the number of triangles that have a shape quality of less than 0.2

Deal with intersecting and overlapping triangles

Delete intersecting triangles

Mark intersecting triangles (trial had 108)

select expand marked triangles and delete them

Mass hole filler

- Bad contour length of 5mm (or larger to ensure all are filled)

One was remaining so mark shell and invert again

Delete overlapping triangles

Mark overlapping triangles (trial had 8)

Select expand marked triangles and delete them

Mass hole filler as above

Second auto remesh

- Shape quality threshold to 0.3
- Maximum geometrical error 0.01
- Control edge length on, max edge length 0.3

Ensure one shell

Mark, invert and delete

Deal with intersecting and overlapping triangles

This time do not use hole filling as it may create more low quality triangles

Do it manually by marking, deleting and filling

Quality preserve reduce triangles

Use same parameters as automesh

Implanting Screw

*Can change the colour of the parts by selecting the surface and changing the colour in the lower menu. Cannot change internal colours of individual parts

** To ensure that the co-ordinate systems are the same go to edit update OCS to CS, method WCS

Auto Remesh

Remesh the screw to ensure that there are no local areas of high density mesh

- Shape quality threshold 0.3
- Max geometrical error 0.01
- Max edge length 0.2

Preserve surface contours

Create non-manifold assembly

Make sure screw is being inserted into the bone not other way round

Fix sharp triangles

- Mark and remove
- check filter distance and how this affects the geometry of the screw bone interface

Auto Remesh

Using the same shape quality thresholds as have been used on the 2 components previously

If they are different then for max geometrical error use the lowest of the two parts and for max edge length use the largest.

Deal with intersecting and overlapping triangles

Delete intersecting triangles

Mark intersecting triangles (trial had 2)

Select expand marked triangles and delete them

Delete overlapping triangles

Mark overlapping triangles (trial had 11)

Select expand marked triangles and delete them

If deleting wee bits make sure the interface belongs to the screw.

Checking for holes at the interface

Remeshing>Create non-manifold curves

Curve list. Non manifold curves-3

(3 is the number of surfaces that the edge belongs to. Normally this is 1 for a triangle on a surface but is more at the interface when surfaces are joining. All of these should be 'closed', if they are not there is a hole so fix it. Non-manifold curves-4 should be ok.)

Other holes not at the interface can be found by bad edges in the normal view.

Appendix D

3D models with 5.3% apparent density with a cancellous washer on top

A model with a washer on top was designed to prevent an early failure of the simulations due to the large distortion of the elements at the screw penetration edge (figure D.1). The washer had the same property as the cancellous bone. The first attempt was created with a washer with a thickness= 0.1mm.

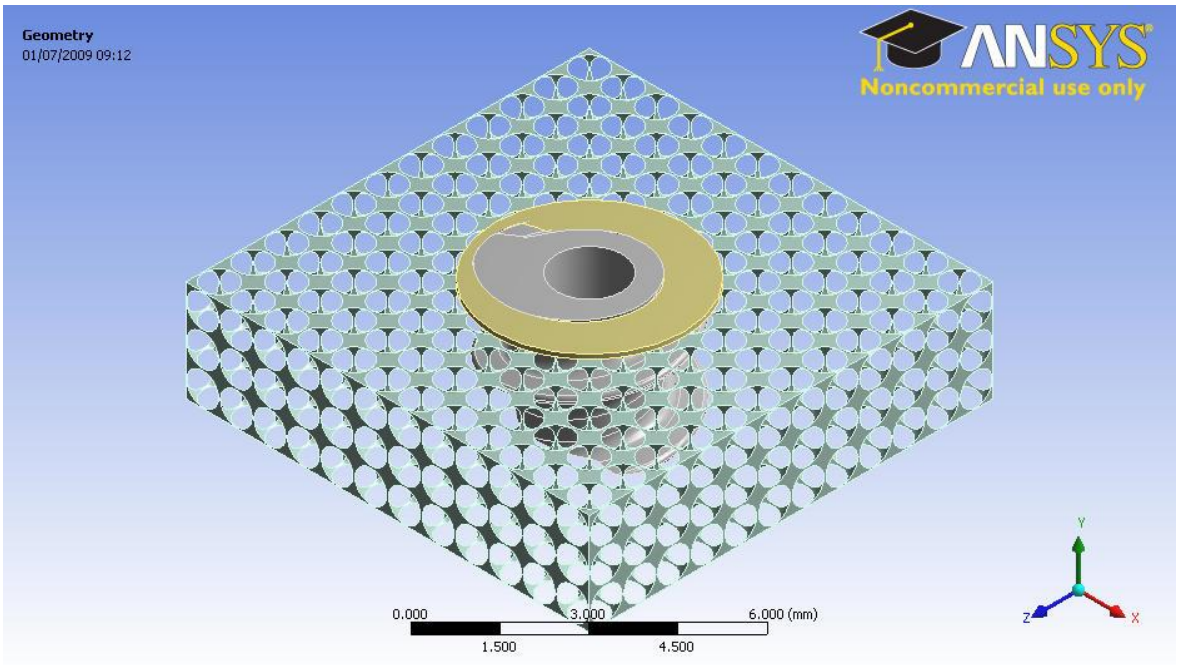

Figure D.1: 3D view of the model designed with a cancellous washer on top (cancellous bone with 5.3% apparent density)

The total deformation views were shown in figure D.2.

This trial was much faster computationally but at the same time, the washer affected significantly the results (figure 49) as the variability decreased (maximum difference up to 7%) and the pull-out force was more important, for example: 36% more for the case with washer for both positions 0.1

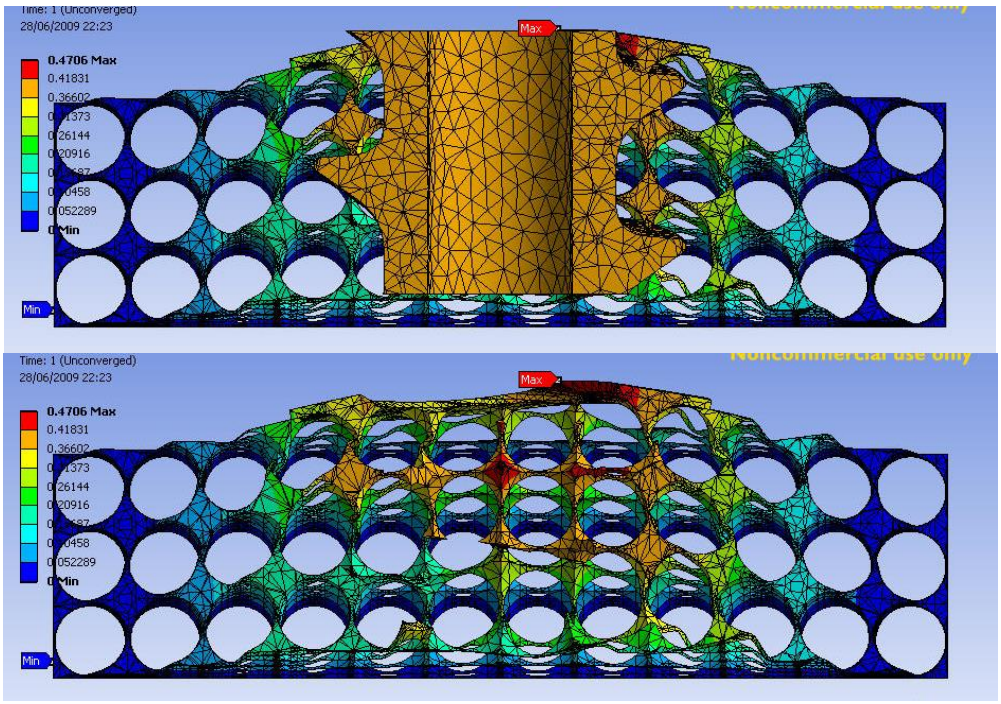

Figure D.2: Split views of deformation of the 3D models with 5.3% apparent density with (top) and without screw (hidden) (bottom) and washer 0.1mm thick

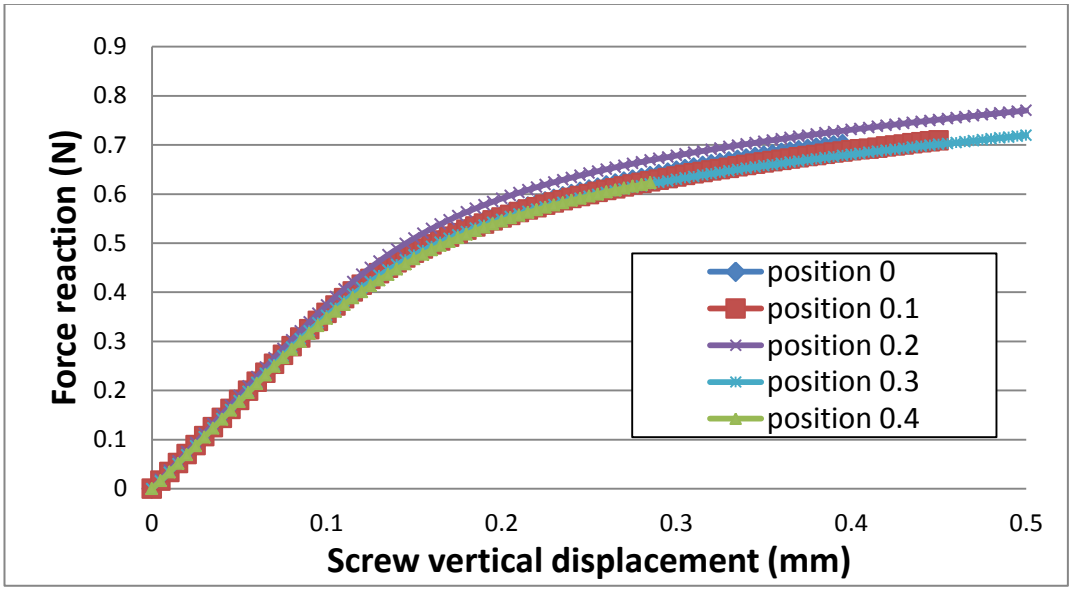

Figure D.3: Pull-out forces depending on the screw position for 3D models with 5.3% apparent density with a cancellous washer (0.1mm thickness)

Therefore another attempt was tried with a washer ten times thinner, a washer with a thickness of 0.01mm (figure D.4).

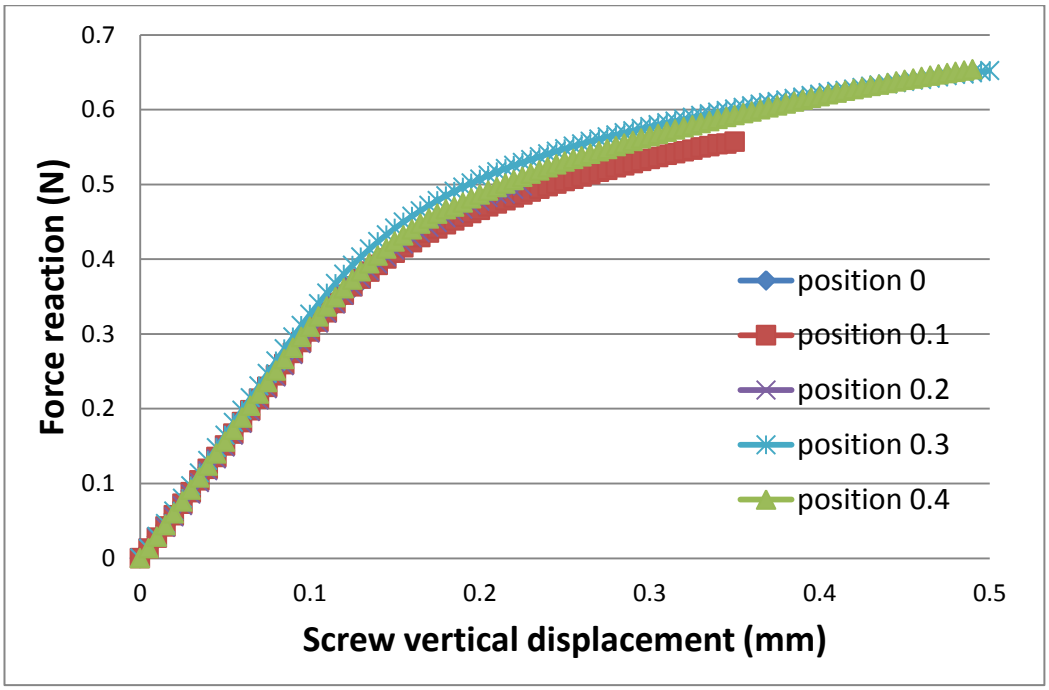

Figure D.4: Pull-out forces depending on the screw position for 3D models with 5.3% apparent density with a cancellous washer (0.01mm thickness)

The washer experiments were not successful because even with the thinner washer the results were still strongly affected to consider using a washer to simplify the computational issues.

Appendix E

Stiffness /strength correlation?

For each simulation that could reach the plasticity area, the stiffness was calculated as well as the Yield point.

A total of 15 simulations were available from:

- Cancellous screw pull-out from simplified bone study with apparent density (5.3%, 9.5%, 12.6% and 15%)
- Cancellous screw pull-out from simplified bone study with apparent density 9.5% with predrill, with augmentation and with smaller pitch
- Cancellous screw pull-out from 2 cases of real bone
- Cortical screw pull-out from simplified bone study with apparent density 9.5%, with smaller core diameter and from simplified bone with 12.6% apparent density
- Continuum bone.

Table E.1 Table of cases reaching strength. (SB: simplified bone model)

test/study	Stiffness ($N.mm^{-1}$)	Strength (N)	Ration: Stiffness/strength	
screw radial displacement 0.3 SB 5.3%	3.262	0.319	10.213	
screw radial displacement 0.4 SB 5.3%	2.775	0.260	10.674	
screw radial displacement 0.15 SB 5.3%	2.527	0.238	10.601	
screw radial displacement 0.1 SB 5.3%	2.415	0.220	10.982	
Continuum cancellous	6247.600	600.800	10.399	
SB 9.5% cancellous screw	289.950	30.893	9.386	
SB 9.5% cancellous screw predrill	277.070	28.406	9.754	
SB 9.5% cortical screw	305.630	31.040	9.846	
SB 12.6% cortical screw	564.230	61.894	9.116	
SB 9.5% cancellous screw augmented	310.930	33.867	9.181	
SB 9.5% cancellous screw small pitch	302.230	30.893	9.783	
SB 9.5% cortical screw small core	305.630	31.266	9.775	
Real bone case B cancellous screw	22.655	2.101	10.782	
Real bone case C cancellous screw	48.883	4.912	9.952	
SB 15% cancellous screw	90.000	9.001	9.999	
			10.029	Average
			0.572907538	SD

All these simulations covered a wide range of results.

The ratio of the stiffness by the Yield point was calculated for each of them:

- Average: 10.03
- Standard deviation: 0.57

When the bone was modelled with the same material property, it was observed that the Yield point and the stiffness were directly linked for a screw pull-out.

Appendix F

Table F.1: Summary result table from chapter 6

Case	screw type	bone volume fraction	Local volume fraction	Screw/bone contact area (mm^2)	Useful contact area (mm2)	% Useful contact	Stiffness results ($N.mm^{-1)}$
A	cancellous	12.1%	15.9%	10.34	4.69	45%	55.6
	cortical	12.1%	15.9%	10.64	5.29	50%	69.4
B	cancellous	10.7%	9.0%	3.78	1.15	30%	22.7
	cortical	10.7%	9.0%	3.94	1.27	32%	29.0
C	cancellous	11.6%	14.6%	10.01	4.27	43%	33.5
	cortical	11.6%	14.6%	7.47	3.6	26%	35.4
D	cancellous	11.9%	11.6%	5.1	1.67	33%	51.5
	cortical	11.9%	11.6%	7.15	3.4	48%	79.6
E	cancellous	9.5%	8.3%	5.34	1.99	37%	19.0
	cortical	9.5%	8.3%	6.02	2.49	41%	28.2
F	cancellous	12.6%	13.3%	8.38	3.44	41%	67.2
	cortical	12.6%	13.3%	8.85	2.87	32%	67.7